Novel insights into the localization and functions of tripartite motif-containing 22

Gayathri, Sivaramakrishnan

2008

Gayathri, S. (2008). Novel insights into the localization and functions of tripartite motif-containing 22. Doctoral thesis, Nanyang Technological University, Singapore.

https://hdl.handle.net/10356/14266

https://doi.org/10.32657/10356/14266

NANYANG TECHNOLOGICAL UNIVERSITY

NOVEL INSIGHTS INTO THE LOCALIZATION AND FUNCTIONS OF TRIPARTITE MOTIF-CONTAINING 22

GAYATHRI SIVARAMAKRISHNAN

SCHOOL OF BIOLOGICAL SCIENCES

2008

NOVEL INSIGHTS INTO THE LOCALIZATION AND FUNCTIONS OF TRIPARTITE MOTIF-CONTAINING 22

GAYATHRI SIVARAMAKRISHNAN

School of Biological Sciences

A thesis submitted to the Nanyang Technological University
in fulfillment of the requirement for the degree of
Doctor of Philosophy

2008

ACKNOWLEDGEMENTS

I would like to thank Nanyang Technological University for admitting me into the program, with financial support. I wish to express my sincerest gratitude to my supervisor Associate Professor Valerie Lin Chun Ling. She provided continuous guidance and support and has been extremely patient with me. Her uplifting words at all the right junctures made the Ph.D. experience a much better one. Of all that I have learnt from her as a scientist, her enthusiasm for scientific research and perseverance in pursuing an idea will undoubtedly stay with me for a long time to come. Thank you, Valerie, for being a great mentor and role model!

I humbly dedicate this thesis to my dear parents, Siva and Usha, my pillars of strength. Notwithstanding their lack of opportunity for higher education when they were younger, they recognized the importance of one, respected my decision to pursue a Ph.D, and have been extremely encouraging and supportive (and tolerant of my unpredictable mood swings towards the end of this project). Appa and Amma, all that I am now, I am because of you. Thank you very much! By being there for me when I needed them, comforting me, and for helping out at home in my absence, I am most grateful to my sisters, Geetha and Sandhya. My heartfelt appreciation and gratitude also goes out to my husband, Bhasker, for not only finding me attractive in my current form (an incomplete Ph.D, living miles away) but for also waiting for me, encouraging me and reminding me that the light at the end of the tunnel is near. Other members of my family (including my parents-in-law) have also contributed to the completion of this thesis by enquiring about its status (my grandmother, Ammamma, deserves special mention here for doing this almost every other day and reminding me that it does need to be completed soon!). I would like to thank them for their sincere good wishes.

I would also like to thank Prof. Alex Law and Prof. Lars Nordenskiöld for their continuous support throughout my candidature. This project was also possible because of the contributions, by way of invaluable expertise, insight and/or materials, of several faculty, staff and students at the School of Biological Sciences and other institutes in Singapore. I would particularly like to thank Dr. Li Hoi Yeung for providing us with

several plasmids (including the p80-coilin-EGFP plasmid created by Dr. Joseph Gall), Dr. Stephen Ogg (Institute of Medical Biology, Singapore) for helping us with the live-cell imaging study, Dr. Edward Manser (Institute of Molecular and Cellular Biology, Singapore) for the pXJ-FLAG vector, Dr. Thirumaran Thanabalu for his insight into the different residues that may be involved in the nuclear localization of TRIM22, Dr. Li Jingming for analysis of the TRIM22 promoter, Dr. Tan Nguan Soon for his insight on stable gene silencing and ready provision of materials required for this purpose, Mr. Kareem Mohideen Abdul and Dr. Ravikumar Manonmani for guiding me during the purification and refolding of TRIM22, Mr. Pritpal Singh S/O Gurmit Singh for assistance with live-cell imaging, and Ms. Geraldine Lee Cai Ling for assistance with flow cytometry analysis. I would also like to thank Dr. Suet Feung Ching (University of Cambridge), Dr. Bay Boon Huat (National University of Singapore), Dr. Ann Lee (National Cancer Center, Singapore), and Dr. Koh Cheng Gee for making several cell lines available to us.

It is difficult to overstate my appreciation to my past and present colleagues, who have provided tremendous support and friendship. I am grateful to Dr. Cao Shenglan, Dr. Zheng Zeyi, and Ms. Joyce Leo Ching-Li for patiently guiding me when I was a newbie and for encouraging me. Many thanks also to Ms. Smeeta Shrestha, Ms. Sun Yang, Ms. Tan Si Kee, Dr. Raj Mohan Raja Muthiah, Ms. Zhen Ling and Ms. Zheng Si Min who have helped me in the lab and with the TRIM22 project in one way or another.

My sanity at the work place can also be largely attributed to my friends in other labs within the school (Jui Gang, Yang Jie, Chian Feng, Li Fang, Jeyakumar, Krupakar, Elavazhagan, Rathi, Miao Huang, Shalini, Pritpal, Tuan Lin, and Yang Ye) who, by humoring me, having the occasional lunch or coffee with me or by simply giving me their broad smiles, made the last four years simply wonderful! To all my past educators (including A/Prof. Jeff Schwartz, A/Prof. Sarah Robertson, and Dr. Melinda Jasper at the University of Adelaide, South Australia) and other friends whom I have failed to mention due to space constraints, I thank you too, for being a part of my life and helping to mould me into what I am today.

TABLE OF CONTENTS

LIST OF PUBLICATIONS

Submitted manuscript

Sivaramakrishnan, G., Sun, Y., Tan, S.K., and Lin, V.C.L. Dynamic localization of Tripartite motif-containing 22 in nuclear and nucleolar bodies. Submitted to Biochemical and Biophysical Research Communications; awaiting decision.

Manuscript in preparation

Sivaramakrishnan, G., Rajmohan, R., Tan, S.K., and Lin, V.C.L. TRIM22's SPRY domain is essential for the formation of distinct TRIM22 nuclear bodies.

Meeting proceedings

Sivaramakrishnan, G., Sun, Y., Tan, S.K., and Lin, V.C.L. Tripartite motif-containing protein 22 nuclear bodies exhibit dynamic changes during cell cycle progression. Presented at the 2007 Annual meeting for the American Society for Cell biology, Washington DC, USA.

Sivaramakrishnan G., Sun, Y., Tan, S.K., and Lin, V.C.L. The progesterone-regulated protein TRIM22 forms nuclear and nucleolar bodies. Presented at the 2007 American Association for Cancer Research (AACR) Centennial Conference (Translational Cancer Medicine: Technologies to Treatment), Singapore. Abstract A26

Sivaramakrishnan G. and Lin, V.C.L. TRIM22 is localized as distinct nuclear bodies. Presented at the 2006 meeting on Dynamic Organization of Nuclear Function, Cold Spring Harbor Laboratory, Cold Spring Harbor, New York, USA. Abstract 166

LIST OF TABLES

LIST OF FIGURES

LIST OF ABBREVIATIONS

36B4	Human acidic ribosomal phosphoprotein
6xHis	Six repeats of the histidine residue
aa	Amino acid
AF	Activation function
ALV	Avian leukosis virus
Amp	Ampicillin
APL	Acute promyelocytic leukemia
AR	Androgen receptor
ARF	ADP ribosylation factor
ATF3	Activating transcription factor 3
ATRA	All-trans retinoic acid
bp	Base pair
BrdU	5-bromo-2'-deoxyuridine
CBP	cAMP response element binding (CREB) protein binding protein
CC	Coiled-coil
CDK	Cyclin dependent kinase
cDNA	Complementary DNA
CFP	Cyan fluorescent protein
CREB	cAMP response element binding (CREB)
Ct	Cycle threshold
DAPI	4',6-diamidino-2-phenylindole
DBD	DNA binding domain
DCC-FCS	Dextran-coated charcoal-fetal calf serum
DEPC	Diethylpyrocarbonate
DFC	Dense fibrillar center
DMEM	Dulbecco’s modified Eagle’s medium
DMSO	Dimethyl sulfoxide
DNA	Deoxyribonucleic acid
dNTP	Deoxyribonucleotide triphosphate

DPBS	Dulbecco's phosphate buffered saline
EBV	Epstein-Barr virus
ECL	Enhanced chemiluminescence
EDTA	Ethylenediaminetetraacetic acid
EGF	Epidermal growth factor
EGFR	Epidermal growth factor receptor
EMT	Epithelial-mesenchymal transition
ER	Estrogen receptor
ERα	Estrogen receptor subtype α
ERβ	Estrogen receptor subtype β
FC	Fibrillar center
FCS	Fetal calf serum
FLASH	FADD-like IL1β-converting enzyme-associated huge protein
FN3	Fibronectin III
Fv1	Friend virus susceptibility factor
GAPDH	Glyceraldehyde-3-phosphate
GC	Granular component
GFP	Green fluorescent protein
GR	Glucocorticoid receptor
HAT	Histone acetyltransferase
HDAC	Histone deacetylase
HECT	Homologous to E6AP Carboxy Terminus
HEPES	4-(2-hydroxyethyl) piperazine-1-ethanesulfonic acid
HFV	Human foamy virus
hr	Hour
HRE	Hormone response element
HRP	Horseradish peroxidase
HRT	Hormone replacement therapy
HSV-1	Herpes simplex virus-1
hTR	Human telomerase RNA
hTRIM5α	Human TRIM5α

IFN	Interferon
IgG	Immunoglobulin G
IPTG	Isopropyl-beta-D-thiogalactopyranoside
Kan	Kanamycin
kDa	Kilo Dalton
KSHV	Kaposi's sarcoma-associated herpes virus
LANA	Latency associated nuclear antigen
LB	Luria-Bertani (medium)
LBD	Ligand binding domain
LCMV	Lymphocytic choriomeningitis virus
LMP-1	Latent membrane protein-1
LTR	Long terminal repeat
MAPK	Mitogen activated protein kinase
MATH	Meprin and tumor necrosis factor receptor-associated homology domain
MAVS	Mitochondrial antiviral signaling protein
MEC	Mammary epithelial cells
MEF	Mouse embryonic fibroblasts
min	Minute
MLV	Murine leukemia virus
MPA	Medroxyprogesterone acetate
MR	Mineralocorticoid receptor
mRNA	Messenger RNA
MWCO	Molecular weight cut-off
NB	Nuclear body/bodies
NCBI	National Center for Biotechnology Information
NCC	National Cancer Centre
NCoR	Nuclear receptor corepressor
NFκB	Nuclear factor kappa B
NHL	NHL, NCL-1/HT2A/LIN-41 repeats
NLS	Nuclear localization signal
NoLS	Nucleolar localization signal

PBL	Peripheral blood leukocytes
PBS	Phosphate buffered saline
PCR	Polymerase chain reaction
PHD/BROMO	Plant homeodomain/BROMO
PI	Propidium iodide
PI3K	Phosphoinositide 3-kinase
PML	Promyleocytic leukemia
PMSF	Phenylmethylsulphonylfluoride
PPAR	Peroxisome proliferator activated receptor
PR	Progesterone receptor
PR-A	Progesterone receptor isoform A
pRb	Retinoblastoma protein
PR-B	Progesterone receptor isoform B
PRE	Progesterone response element
RAR	Retinoic acid receptor
RBCC	RING, B-box, and Coiled-coil domains
RD	Repressor domain
rDNA	Ribosomal DNA
Ref1	Restriction factor 1
RID	Receptor interacting domain
RIG-1	Retinoic-acid-inducible gene 1
RNA	Ribonucleic acid
RNP	Ribonuclear protein
rpm	Revolutions per minute
rRNA	Ribosomal RNA
rTRIM5α	Rhesus TRIM5α
RXR	Retinoid X receptor
SDS-PAGE	Sodium dodecyl sulfate-polyacrylamide gel electrophoresis
SEM	Standard error of the mean
SERM	Selective estrogen receptor (ER) modulator
SIP	SMN interacting protein

SMN	Survival motor neurons
SMRT	Silencing mediator of retinoic acid and thyroid hormone receptors
SnoRNP	Small nucleolar ribonuclear protein
SnRNA	Small nuclear RNA
SnRNP	Small nuclear ribonuclear protein
SPRY	SplA and ryanodine receptor
SRA	Steroid receptor RNA activator
SRAP	Steroid receptor activating protein
SRC-1	Steroid receptor coactivator-1
STAF50	Stimulated trans-acting factor of 50 kDa
SUMO	Small ubiquitin-related modifier
TEMED	N,N,N',N'- tetramethylethylendiamin
TJ	Tight junction
TMEM2	Transmembrane protein 2
TMG	Tri-methyl guanosine
TR	Tyroid hormone receptor
TRIM	Tripartite motif-containing
TRIM22	Tripartite motif-containing 22
Tris	2-amino-2-(hydroxymethyl)-1,3-propanediol
UBL	Ubiquitin-like
UV	Ultraviolet
VDR	Vitamin D receptor
VSV	Vesicular stomatitis virus
YFP	Yellow fluorescent protein

ABSTRACT

Tripartite motif-containing 22 (TRIM22) is an interferon (IFN)- and p53-inducible gene product previously shown to possess antiviral and growth inhibitory properties. Microarray analyses in progesterone receptor-positive and estrogen receptor-negative breast cancer cells (ABC28) revealed that progesterone dramatically enhances levels of the TRIM22 transcript. Since progesterone inhibits the growth of breast cancer cells, the aim of this study was to generate specific antibodies against TRIM22, to investigate TRIM22's function, and to investigate if TRIM22 mediated progesterone's growth-inhibitory effect in breast cancer cells.

Recombinant His-tagged TRIM22 protein was expressed from BL21(DE3) cells, purified under denaturing conditions and subsequently refolded to produce soluble protein. Mice were immunized with soluble TRIM22 protein to generate polyclonal antibodies. Use of these specific antibodies revealed that non-tumorigenic breast epithelial cells (MCF10A, MCF12A) expressed much greater levels of the endogenous TRIM22 protein compared to the tumorigenic breast epithelial cells (MCF7, T47D, ABC28). As expected from transcript data, progesterone and IFNs greatly enhanced TRIM22 protein levels. The TRIM22 antibodies were also used in immunofluorescence studies of the overexpressed and endogenous protein, which revealed that TRIM22 is a predominantly nuclear protein that is capable of localizing in distinct nuclear bodies (NB) and as a nucleoplasmic protein. Progesterone enhanced both these forms of the protein and, interestingly, also induced nucleolar bodies in ABC28 cells. Though TRIM22 also formed distinct NB in HeLa and MCF7 cells, IFNγ induced only nucleoplasmic TRIM22 and not NB in these

cells, suggesting that the forms and distribution of TRIM22 are regulated by specific cellular signals. To further test this notion, a cell synchronization study of HeLa cells stably expressing TRIM22-EGFP was performed. In these cells, TRIM22-EGFP formed NB in the G0/G1 phase but assumed a more speckled distribution in the S phase and became diffused in M phase cells. The speckled distribution of TRIM22 in the S phase was confirmed by the observation that endogenous TRIM22 also localized more diffusely in MCF7 cells arrested in the S phase by methotrexate.

In order to identify the determinants of TRIM22 NB formation and nuclear localization, TRIM22 deletion and mutation constructs were generated and the locations of the resultant proteins tested. The largest of the four domains in TRIM22, the C-terminal SPRY domain, was found to be critical for both nuclear localization and NB formation. Separately, the Cajal body signature protein p80-coilin and the nucleolar protein B23 were identified as interactors of TRIM22 within breast cancer cells. To clarify TRIM22's role in growth, the progression of cells through the cell cycle after TRIM22 overexpression and knockdown was analyzed. Consistent with a previous report that TRIM22 overexpression inhibited the growth of leukemic cells, in this study, TRIM22 overexpression enhanced the arrest of MCF7 cells in the G0/G1 phase while silencing TRIM22 in MCF12A cells enhanced the percentage of cells in the S phase of the cell cycle. Microarray analyses after silencing TRIM22 in progesterone-treated ABC28 cells and IFNγ-treated HeLa cells led to the identification of several common and signal-specific targets of TRIM22 such as Claudin-1.

This is the first demonstration of TRIM22's localization in the nucleus as two different forms depending on the amount of protein and the stimulus. In non-tumorigenic MCF12A cells that express large amounts of the TRIM22 protein and where TRIM22 is growth inhibitory, TRIM22 localizes as a nucleoplasmic protein and as NB. In HeLa cells where TRIM22 is greatly induced by IFNγ, the localization of the protein as a diffuse protein reflects the different dynamics of TRIM22 under the influence of IFNγ. Further biochemical characterization is required to investigate the possibility that this non-NB form is functional. While the significance of NB formation and nucleolar localization is not clear, our finding that TRIM22 is growth inhibitory in mammary epithelial cells suggests it is a putative tumor suppressor. Ongoing studies in the laboratory are aimed at identifying the genes and proteins involved in TRIM22's growth inhibitory properties in MCF12A cells and the mechanisms regulating TRIM22 NB formation in ABC28 cells and dispersal in IFNγ-treated cells. These studies will aid in understanding TRIM22's mechanisms of action in relation to antiviral activity and growth inhibition.

CHAPTER 1

INTRODUCTION

Introduction Summary

This introductory chapter has six sections. The first section will briefly introduce breast cancer and nuclear hormone receptors, their domain organization and mechanisms of action. Estrogen receptors (ER) and progesterone receptors (PR) and their ligands will then be discussed, with emphasis on the functions of progesterone and PR in the animal and in breast cancer cells. In addition, because the focus of this investigation is a member of the Tripartite motif-containing (TRIM) family of proteins, the domain organization, localization and functions of TRIM proteins will be summarized before launching into what is known about TRIM22/STAF50. Finally, as a prelude to a discussion of TRIM22's localization within the cell, the various subnuclear domains will be described and their interrelationships highlighted, where relevant.

1.1 Breast cancer and nuclear hormone receptors

1.1.1 Breast cancer

Breast cancer is second only to lung cancer as the leading cause of cancer-related deaths among women. In the US alone, statistics released by the American Cancer Society reported around 240,000 *new* invasive and in situ breast cancer patients and more than 40,000 deaths from breast cancer in 2007 (American Cancer Society, Breast Cancer Facts and Figures 2007-2008). In Singapore, breast cancer is the most prevalent cancer, with about 1000 *new* cases annually (Singapore Cancer Society data). There are several unmodifiable and modifiable risk factors for breast cancer. Some risk factors (early menarche, late menopause, obesity and hormone use) directly increase the cumulative exposure of breast tissue to the circulating ovarian hormones estrogen and progesterone. The period from 2000 – 2004 saw a decrease in the US breast cancer incidence rates, partly due to the decreased use of hormone replacement therapy (HRT) following publication of the Women's Health Initiative randomized trial that showed an increased risk for breast cancer in HRT patients (American Cancer Society, Rossouw et al., 2002). Breast cancer is usually treated by local and/or systemic therapy. Local therapy includes surgery and radiation therapy while systemic therapy includes chemotherapy and hormonal therapy.

In the normal adult mammary gland, cells positive for both the ER and the PR represent only about 7 - 10% of the luminal epithelial cell population. These receptors mediate the effects of estrogen and progesterone on development and differentiation of the mammary gland; estrogen/ER promotes the growth of ducts that invade the mammary fat pad while

progesterone/PR promotes the ductal side-branching and the development of acini at the end of the ducts that further develop to produce milk during lactation (Hewitt and Korach, 2000; Lydon et al., 1995; Ruan et al., 2005). ER-positive/PR-positive cells, though growth-arrested themselves due to the presence of inhibitory molecules such as p21 and p27 within these cells, express and secrete pro-proliferative molecules like Wnts and insulin-like growth factor-II, which stimulate the proliferation of nearby ER-negative/PR-negative progenitor or stem cells (Clarke, 2004; Haslam and Woodward, 2003; Kariagina et al., 2007). In contrast to the normal breast, around 70% of breast cancers are positive for both the ER and the PR at the time of diagnosis (Clarke, 2004; Mote et al., 2002). Although these tumors are less proliferative than ER-negative/PR-negative tumors, it is thought that ER-positive/PR-positive tumors may lose their innate growth-inhibitory mechanisms to become highly proliferating cells (Clarke, 2004). These cells are therefore routinely targeted in ER-positive/PR-positive breast cancer using receptor modulators, mostly against the ER, which would also result in reduced PR expression since the expression of PR is known to be under transcriptional control of ERα (Feng et al., 2007; Petz et al., 2002; Shang and Brown, 2002)

The selective ER modulator (SERM) tamoxifen is an example of an effective and relatively safe breast cancer therapeutic. Tamoxifen competes with endogenous estrogen preventing it from binding to ER (Jordan and Dowse, 1976). Unlike estrogen that exerts its proliferative effects by recruiting coactivators to target promoters, tamoxifen recruits corepressors to result in cytotoxic and cytostatic effects in target cells (Cameron et al., 2000; Shang and Brown, 2002). However, ER expression is not confined to the breast

and is also present in the bone and cardiovascular system, where estrogen has beneficial effects. The ability of tamoxifen to mimic estrogen's effects in these latter tissues largely minimizes the side-effects that would be present with the use of an ER-antagonist (Grey et al., 1995a; Grey et al., 1995b).

Resistance to endocrine therapy poses an additional challenge to the treatment of breast cancer. Almost all patients with advanced breast cancer who receive tamoxifen therapy eventually develop resistance to the therapy, due to reduced ERα expression (with a concomitant increase in expression of the epidermal growth factor receptor (EGFR)) or constitutive transcriptionally-active ER (Hoffmann and Sommer, 2005; Sluyser, 1994). This necessitates the use of further therapies targeting other molecules. The PR is targeted in addition to the ER in some advanced breast cancers, albeit only as a third- or fourth-line therapy because of the side effects of progestins (Klijn et al., 2000). Though not yet in clinical practice, androgen receptor (AR)-based therapies may also be useful since 25% of ER-negative breast cancers continue to express the AR and the growth-inhibitory effect of the progestin medroxyprogesterone acetate (MPA) in breast cancer cells was found to be partially dependent on the AR (Bentel et al., 1999; Birrell et al., 1998; Kuenen-Boumeester et al., 1996; Lea et al., 1989). Besides targeting nuclear hormone receptors, if the crucial downstream effectors of the mitogenic and growth-inhibitory effects of nuclear hormones are identified and characterized, targeting these molecules may provide several additional avenues for the treatment of breast cancer.

1.1.2 Nuclear receptors and their domain organization

Steroid hormones (such as estrogen and progesterone), thyroid hormones, retinoids, and vitamin D are small lipophilic molecules that have critical roles in multiple aspects of growth, differentiation, metabolism and reproduction, amongst other processes. Typically, they traverse the cell membrane and bind to cognate nuclear hormone receptors within the cell cytoplasm, resulting in the translocation of activated receptors into the nucleus for transcriptional regulation.

Nuclear receptors have a common modular structure typically consisting of five distinct regions: A, B, C, D and E regions. The N-terminal end has the highly variable A and B regions (which are collectively referred to as the A/B region), followed by the conserved zinc finger DNA binding domain (DBD; C region), a short D region and the less-conserved ligand binding domain (LBD; E region). In addition, ER and retinoic acid receptor (RAR) also contain the highly variable F region at their C-terminal ends, to enable them to distinguish ligands.

The A/B region is highly variable between the different nuclear receptors. In many of these receptors, region A encompasses the activation function (AF)-3 transactivation domain, which may be either present or absent in different nuclear receptor isoforms. For instance, PR-A lacks region A and hence the AF-3 domain, making it transcriptionally more dormant compared to PR-B, the longest PR isoform which contains the AF-3 domain (Sartorius et al., 1994b).

The DBD is the most conserved region, and is comprised of two zinc fingers. The coordination of zinc atoms by cysteine residues results in the formation of two loops, the first contributing to the “P box” and the second contributing to the “D box”. The P box residues allow the receptor to discriminate between similar hormone response elements (HRE) and are therefore critical for specificity. The D box residues form the dimerization interface and thereby determine the specificity for binding to nuclear receptors. The D region behaves as a flexible hinge between the DBD and LBD that allows the DBD to rotate. In many nuclear receptors, this region contains the nuclear localization signal (NLS) and may also contain residues critical for interaction with co-repressors. To the left of the DBD lies the AF-1 transactivation domain.

The LBD is a multifunctional domain that is primarily involved in recognizing and binding to ligands. However, it is also modulates homodimerization and heterodimerization, which is required for most of these hormones to bind to the HRE. In addition, this domain can mediate interactions with heat-shock proteins, which serve as molecular chaperones for nuclear receptors making them receptive to cognate ligands. The LBD encompasses the AF-2 domain allowing for ligand-dependent transcriptional activation of nuclear receptors.

1.1.3 Hormone response elements (HRE)

HRE are specific binding sites for hormone-receptor complexes. HREs tend to be located within the promoter of target genes of the hormone-receptor complex, although in some cases, they may be found several kilobases upstream of the transcriptional start site.

Comparisons of HRE sequences known to bind specific nuclear receptor complexes has revealed that the consensus HRE binding site is an inverted palindrome of two hexameric core repeats that are separated by three nucleotides. This structure binds to a dimerized hormone-receptor complex, which then regulates signal transduction. The class I receptors include the AR, PR, glucocorticoid receptor (GR), and mineralocorticoid receptor (MR), which bind to either 5'-AGAACANNNTGTTCT-3' (perfect palindrome class I HRE) or 5'-GGTACANNNTGTTCT-3' (consensus class I HRE) (where N can be any nucleotide) as homodimers (Beato et al., 1989; Cato et al., 1986; Nelson et al., 1999). To generate diversity, some of these receptors have non-palindromic HREs which consist of a second half-site that is inverted or repeated relative to the first while maintaining the three-nucleotide difference between the half sites (Glass, 1994).

The class II receptors include the ER, RAR, retinoid X receptor (RXR), vitamin D receptor (VDR), thyroid hormone receptor (TR), and peroxisome proliferator activated receptor (PPAR). These receptors, except homodimeric ER, recognize the 5'-AGGTCA(N_x)TGACCT-3' (consensus class II HRE perfect palindrome) as heterodimers (Klinge, 2001; Nelson et al., 1999). Besides inverting or repeating the second half-sites, the length of the spacer that separates the two half-sites also increases diversity among the HREs recognized by the class II receptors. Furthermore, nuclear receptors are able to distinguish between HREs via specific residues within their P or D boxes which come into contact with the core recognition motif within the HRE (Glass, 1994).

1.1.4 Mechanisms of nuclear receptor action

1.1.4.1 Pathways of nuclear receptor action

Nuclear receptors are transcription factors that are able to bind to DNA, either directly or indirectly, to regulate gene transcription. In the absence of ligand, the nuclear receptor exists as an intracellular protein that is incapable of binding to its cognate hormone because the hormone-binding cleft is collapsed (Gee and Katzenellenbogen, 2001). To expose the hormone-binding cleft, the inactive nuclear receptor must bind to a chaperone protein complex. The mature chaperone complex results from an ordered ATP-dependent assembly of chaperone proteins, such as heat-shock proteins (Hsp40, Hsp70 and Hsp90), p23, cyclophilins (Cyp40), immunophilins (FKBP52, FKBP51), and adaptor proteins (HOP) (Morimoto, 2002). Some of these proteins, such as Hsp70 and Hsp40, are important in the initial assembly but are not found in the mature complex (like Hsp90 and p23) (Morimoto, 2002). The mature complex binds to part of the LBD of the nuclear receptor, and this maintains the nuclear receptor in a ligand-responsive, but transcriptionally inactive, form. Binding of the cognate ligand to the exposed hormone-binding cleft in the LBD alters the conformation of the nuclear receptor, allowing it to dissociate from the chaperone complex. The ligand-bound nuclear receptor, now transcriptionally active, can bind to its specific HRE within seconds to regulate the general transcription machinery (including TATA-binding protein, TATA-binding protein associated factor, RNA polymerase II, and promoter-specific factors) in the promoters of target genes. Indeed, the addition of Hsp40, Hsp70, HOP, Hsp90, p23 and ATP were found to be adequate for immuno-isolated PR to bind to the progesterone response element (PRE) (Kosano et al., 1998).

The nuclear receptor only remains bound to the HRE transiently (five to ten minutes). When the level of steroid hormone drops, the ligand dissociates from the nuclear receptor, which then disassembles from the general transcription machinery. The chaperone proteins p23, and to a lesser extent Hsp90, have been implicated in promoting the rapid disassembly of the nuclear receptor. p23 inhibited binding of the TR/RXR heterodimer to the thyroid hormone response element and inhibited thyroid hormone-dependent transcription (Freeman and Yamamoto, 2002). After disassembly, Hsp90 and p23 are recycled while the released steroids are carried to the endoplasmic reticulum where they are metabolized and released from the cell via golgi vesicles.

In addition to binding directly to estrogen response element (ERE) and PRE, ER and PR may also stimulate gene transcription by binding to other transcription factors such as activator protein 1 (AP-1) and Sp1, which are able to bind to gene promoters. Cyclin D1 and PR are examples of genes regulated by ER despite the lack of canonical response elements for the ER (Castro-Rivera et al., 2001; Petz and Nardulli, 2000; Petz et al., 2002; Read et al., 1988; Sabbah et al., 1999). PR-binding consensus sequences or PRE are also absent in a large fraction of progesterone-regulated genes, implying there may be more genes that might be direct targets of the progesterone/PR complex despite lacking the canonical PRE (Richer et al., 2002).

There is also evidence that steroid receptors can signal from non-cognate ligands. This has been demonstrated for the PR, which mediated the effect of the neurotransmitter dopamine in rat sexual behaviour, and the AR, which mediated the effect of the progestin

MPA in human breast cancer cells (Bentel et al., 1999; Birrell et al., 1998; Mani et al., 1994). These non-cognate ligands do not bind to the steroid receptors but they may facilitate the activation of these receptors via effects on coactivators. As will be described later, coactivators enhance the effect of steroid hormone receptors. A ligand-independent role for ER was demonstrated when the steroid receptor coactivator (SRC-1) could phosphorylate ER at the AF-3 region (Tremblay et al., 1999). ER could also be indirectly activated by SRC-1 in a ligand-independent manner via a direct interaction between SRC-1 and cyclin D1 (Zwijsen et al., 1998; Zwijsen et al., 1997).

1.1.4.2 Nuclear receptor coactivators

Coactivators are molecules that bridge the nuclear receptors to the general transcription machinery. A number of nuclear receptor coactivators have been identified since the initial identification of SRC-1 by yeast-two-hybrid using PR as bait. These include two other SRC members, SRC-2 and SRC-3, PPARγ coactivator 1 (PGC1), p300/CREB binding protein (CBP), ACTR, and steroid receptor activator protein (SRAP), amongst many others (Chen et al., 1997; Kawashima et al., 2003; Robyr et al., 2000). In SRC proteins, the central regions containing multiple LXXLL motifs (where L refers to a leucine residue and X to any amino acid; also known as NR boxes) mediate their interactions with nuclear receptors at their AF-2 domains (Heery et al., 1997; Onate et al., 1998; Voegel et al., 1998). Likewise, p300/CBP interacts with nuclear receptors in a ligand-dependent and AF-2 domain-dependent manner (Shiama, 1997).

SRC-1 is a common coactivator for ligand-bound nuclear receptors; it not only stabilizes the pre-initiation complex at the promoter, but is also capable of utilizing its inherent histone acetyltransferase (HAT) activity to remodel the chromatin such that RNA polymerase II and other transcription machinery may gain access and transcription may proceed (Liu et al., 1999; Spencer et al., 1997). The interaction of SRC-1 with p300/CBP was found to be crucial for the ability of the latter to facilitate transcriptional activation mediated by TR/RXR (Li et al., 2000). p300/CBP can coactivate a large variety of transcription factors (including nuclear factor kappa B (NF-κB), AP-1, Jun, STATs, and Fos), and can therefore potentially integrate multiple signaling pathways in the cell (Shiama, 1997). As SRC-1 and SRC-3 can also serve as coactivators for other transcription factors (such as p53 and serum response factor), these factors may integrate different cellular functions (Kim et al., 1998; Lee et al., 1999). Interestingly, nucleic acids may also act as coactivators, as shown by the steroid receptor RNA activator (SRA), a RNA molecule that can transactivate steroid hormone receptors via their AF-3 domains (Lanz et al., 1999).

1.1.4.3 Nuclear receptor corepressors

Corepressors can bind to transcriptional activators, particularly the class II steroid receptors, and inhibit the formation of transcriptionally active complexes. Excellent examples are the nuclear receptor corepressor (NCoR) and the silencing mediator of retinoic acid and thyroid hormone receptors (SMRT) (Chen and Evans, 1995; Horlein et al., 1995). These molecules are related structurally and functionally and contain three repressor domains (RD1, RD2, and RD3) interspersed in the first half of the protein. The

RD domains either directly interact with histone deacetylases (HDAC) or indirectly through their interaction with another protein mSin3A (Heinzel et al., 1997; Huang et al., 2000; Nagy et al., 1997). The C-terminal end of NCoR and SMRT contain two nuclear receptor interacting domains (RID) containing the LXX(I/H)IXXX(I/L) (where L refers to a leucine residue, X to any amino acid, I to an isoleucine residue, and H to a histidine residue; also called CoRNR boxes) motif (Hu and Lazar, 1999; Perissi et al., 1999). The longer extension of the alpha helix formed by the NH_2-terminal of CoRNR boxes in corepressors appears to be required for their binding to unliganded nuclear receptors (Perissi et al., 1999). The interaction is reversible. In the presence of ligand, the AF-2 domain of the nuclear receptor triggers the release of corepressors from the LBD, enabling the binding of coactivators like p300/CBP and transcriptional activation.

NCoR and SMRT are not specific for nuclear receptors. They may also be recruited by other transcription factors like serum response factor, AP-1 and NFκB (Lee et al., 2000). By recruiting HDACs, these corepressor proteins deacetylate histone proteins causing chromatin compaction and transcriptional repression (Aranda and Pascual, 2001). In turn, NCoR and SMRT are regulated by cell signaling pathways which can alter their expression levels, subcellular localizations and association with other proteins (Hong and Privalsky, 2000; Zhang et al., 1998). For instance, the phosphorylation of SMRT by the mitogen activated protein kinase (MAPK) cascade modifies its localization and reduces its affinity for transcription factors (Hong and Privalsky, 2000). This compromises SMRT's ability to function as a corepressor.

1.1.4.4 Non-genomic pathways

Consistent with the time required for transcription and translation of target genes, the classical actions of steroid receptors are delayed by several minutes to hours. However, it is becoming increasingly evident that steroid receptors are capable of rapid non-genomic effects via signaling pathways originating from cytoplasmic or membrane-associated versions of these receptors. Treatment of breast cancer cells with progestin resulted in a rapid, though transient, activation of MAPK, phosphoinositide 3-kinase (PI3K), and p60-Src kinase (Boonyaratanakornkit et al., 2001; Migliaccio et al., 1998; Saitoh et al., 2005; Shupnik, 2004). Unlike PR which is predominantly cytoplasmic, ER is a predominantly nuclear protein. Only cytoplasmic ER was capable of anti-apoptotic actions dependent on the Src/Shc/ERK signaling pathway in a range of cells (Kousteni et al., 2001). Estrogen/ER activation of MAPKs may explain why aromatase inhibitors (which inhibit estrogen expression) are more effective than SERMs (which inhibit ER transcriptional activity in the nucleus) in treating breast cancer (Gee et al., 2001; Wilson et al., 2006).

1.2 The estrogen receptor and estrogen

1.2.1 Estrogen receptor subtypes

The human ER is a well-characterized class III nuclear receptor that binds to estrogens. ER has two subtypes, ERα and ERβ, which are transcribed from genes on different chromosomes. The human *ERα* gene, present on chromosome 6 (6q25.1), codes for a 595 aa protein that has been greatly investigated in terms of its role in breast cancer. The *ERβ* gene maps to chromosome 14 (14q22-24) and codes for a 530 aa protein. Both ERα and ERβ comprise the six distinct regions described in **section 1.1.2**. They are most similar in

their DBD regions (97% homologous), have identical P boxes and therefore bind to EREs with similar affinities (Enmark and Gustafsson, 1999). Both subtypes are 55% homologous in their LBD and are able to bind to the endogenous estrogen and 17β-estradiol, with varying affinities for other natural compounds (Enmark and Gustafsson, 1999). The other regions have less than 30% homology.

The ERα and ERβ subtypes are co-expressed in the bone, thyroid, adrenals, lung, epididymis and various regions of the brain (Couse and Korach, 1999). ERα is expressed predominantly in the uterus, mammary gland, pituitary, liver, kidney, heart and skeletal muscle while ERβ is expressed predominantly in the ovary and prostate, with detectable levels in the mammary gland (Couse and Korach, 1999). The finding that 17β-estradiol-liganded ERα activates transcription while 17β-estradiol-liganded ERβ inhibits transcription suggests that co-expression of both subtypes and the formation of heterodimers can result in a functional modulation of ERα's effects by ERβ (Pettersson et al., 2000; Pettersson et al., 1997).

1.2.2 Functions of estrogen receptors and estrogen

The estrogen/ER complex is important in triggering cell signaling cascades including those involved in cell proliferation and differentiation. Studies in ERα knock-out mice suggest that ER is involved in the development and function of the female reproductive system. ERα and ERβ receptors are also present in a wide range of non-reproductive tissues pointing to roles for the estrogen/ER complex in the physiology, maintenance and health of these tissues. Estrogen has important protective functions in the cardiovascular

system, bone and the brain, which are important motivations for the administration of estrogens to post-menopausal women as part of HRT (Couse and Korach, 1999). Estrogens have also been implicated in the progression of breast and endometrial cancers, consistent with their mitogenic effects in these tissues (Aupperlee and Haslam, 2007; Couse and Korach, 1999; Lydon et al., 1995).

1.3 The progesterone receptor and progesterone

1.3.1 Progesterone receptor isoforms

PR are ligand-activated transcription factors belonging to Class III of the nuclear receptor superfamily. The PR has three isoforms: A, B, and C. All three isoforms are products of the same gene located on chromosome 11 q22-34 but from different transcription and translation start sites (Conneely et al., 1987; Kastner et al., 1990; Kraus et al., 1993). PR-B is the longest, with an additional 164 aa sequence at the N-terminus, and has a molecular weight of 116 kDa (Conneely et al., 1987; Kastner et al., 1990; Kraus et al., 1993; Sartorius et al., 1994b). The additional N-terminal sequence corresponds to the A/B region containing the AF-3 domain. PR-A and PR-C are N-terminally truncated proteins of 94 kDa and 64 kDa respectively, which are translated from internal translation start sites (Kraus et al., 1993; Sartorius et al., 1994b; Wei et al., 1996). PR-B is more transcriptionally active than PR-A, a property attributed to the AF-3 domain in PR-B that PR-A lacks (Sartorius et al., 1994b). PR-C lacks transcriptional activity presumably because, in addition to lacking the AF-3 and AF-1 domains, it also lacks part of the DBD (Wei et al., 1996; Wei et al., 1997). Nevertheless, PR-C is functional as it can enhance

PR activity in breast cancer cells or inhibit PR-B activity in the uterus (Condon et al., 2006; Wei et al., 1996).

PR is expressed in the female reproductive tissues that are responsive to progesterone such as the uterus, ovary, breast and vaginal tissue (Batra and Iosif, 1985; Lydon et al., 1995; Mulac-Jericevic et al., 2000). PR has also been found in parts of the brain and the testes (Kato et al., 1978; MacLusky and McEwen, 1980; Terner, 1977). PR-positive cells in normal breast tissue and endometrial tissue generally co-express both PR-A and PR-B, consistent with the demonstrated physiological relevance of both isoforms in these tissues (Lydon et al., 1995; Mote et al., 1999; Mote et al., 2002; Mulac-Jericevic et al., 2000). In certain physiological states, such as during pregnancy or in the event of cancer, there is a shift in isoform expression (Arnett-Mansfield et al., 2001; Aupperlee et al., 2005; Mote et al., 2002).

PR expression depends on the activity of estrogen/ER, and in most target tissues, estrogen increases while progesterone decreases PR expression (Leavitt et al., 1977; Leavitt et al., 1974; Nardulli et al., 1988; Petz and Nardulli, 2000; Petz et al., 2002; Read et al., 1988). However, the effect of estrogen/ER on PR expression can be isoform-specific. For instance, in the mammary glands of adult ovariectomized mice, estrogen treatment stimulated PR-A, but not PR-B, expression (Aupperlee and Haslam, 2007). In contrast, progesterone treatment enhanced PR-B expression but inhibited the estrogen-induced increase in PR-A expression.

1.3.2 Functions of progesterone receptors and progesterone in the animal

Experiments with PR and ER "knockout" mice have demonstrated that PR is essential for ovulation, uterine development, implantation, lobular-alveolar development of the mammary gland and the sexual behavioral response (Hewitt and Korach, 2000; Lydon et al., 1995; Ruan et al., 2005). While both PR isoforms were important in ovulation, PR-A was required for implantation during pregnancy (Mulac-Jericevic et al., 2000). With regards to mammary gland development, combined estrogen and progesterone treatment led to normal ductal branching and proliferation in mice lacking PR-A, suggesting PR-B was adequate for normal proliferation and differentiation of the mammary epithelium (Mulac-Jericevic et al., 2000). However, a recent study in adult ovariectomized mice treated with estrogen and/or progesterone revealed that PR-A is the first isoform to be expressed coincident with the branching of ducts. Ductal branching was mediated by the proliferation of both the PR-A-positive and PR-A-negative cells, and not just the former, which stained poorly for the proliferation marker 5-bromo-2'-deoxyuridine (BrdU) (Aupperlee and Haslam, 2007; Aupperlee et al., 2005). The observation that many of the proliferating cells in the ducts or the alveoli did not express PR suggests that, at least in the virgin adult gland, the majority of PR-positive cells may signal to the PR-negative cells via paracrine mechanisms to induce cell proliferation. In the pregnant and lactating mammary glands, however, the formation of alveoli coincided with high PR-B expression. PR-B-positive cells stained well with BrdU, implying that alveologenesis is likely to be due to the proliferation of PR-B-positive cells (Aupperlee et al., 2005).

The PR isoforms also appear to have different roles in the uterus. In uterine epithelial cells where estrogen induces proliferation, progesterone is a potent antagonist as shown by extensive proliferation of the luminal and glandular epithelia in the uteri of mice lacking both PR isoforms (Lydon et al., 1995). In mice lacking PR-A, not only was this anti-proliferative effect of progesterone absent, but progesterone, presumably now acting through PR-B, enhanced the estrogen-induced proliferation of uterine epithelium (Mulac-Jericevic et al., 2000). These results support an inhibitory role for PR-A and a proliferative role for PR-B in uterine epithelium.

The shift towards the PR-B isoform during pregnancy-associated mammary epithelial cell (MEC) proliferation is inconsistent with the finding that, compared to normal breast tissue, tissues from patients with ductal carcinoma *in situ* and invasive breast cancer have greater PR-A levels (Graham et al., 1995; Mote et al., 2002). Likewise, the shift to a PR-A predominance in about half of the endometrial tumor tissues analyzed (which tended to be more aggressive) is inconsistent with an inhibitory role for PR-A in uterine tissue (Arnett-Mansfield et al., 2001). The reason(s) for these seemingly opposite effects of PR-A in normal and cancerous tissues is not clear but may be explained by deregulated signaling in the absence of PR-B. Evidence for deregulated signaling comes from the results of expression analyses in progesterone-treated breast cancer cells, which revealed that only a small subset of genes are common targets of both isoforms and that PR-A up-regulated genes rather than having an inhibitory effect on gene expression (Richer et al., 2002).

1.3.3 Functions of progesterone receptor and progesterone in breast cancer cells

Progesterone is synthesized mainly in the ovary and its function is mediated primarily via its cognate receptors, PR-A and PR-B. Thus, the functions of progesterone are closely intertwined with the functions of these receptors. In the breast, progesterone has been described as a mitogen. In the endometrium, the ability of progesterone to counteract the proliferative effects of estrogen has led to the administration of both hormones, as opposed to just estrogen, to menopausal patients during HRT. While combination therapy is effective in reducing the risk for endometrial cancer, results from the clinic suggest progestins can enhance the risk for breast cancer over and above that imparted by estrogen alone (Rossouw et al., 2002; Santen, 2003).

Numerous studies have been carried out in breast cancer cells in an attempt to delineate the signaling pathways downstream of progesterone/PR. Cell lines typically studied include MDA-MB-231 (ER-negative, PR-negative), MCF7 (ER-positive, PR-positive; where PR expression depends on ER activity), T47D (ER-positive, PR-positive; where PR expression is independent of ER activity) or clonal derivatives of these cell-lines artificially expressing PR (Lin et al., 1999; Sartorius et al., 1994a; Skildum et al., 2005; Sumida et al., 2004). Results from these studies do not conclusively show that progesterone promotes MEC growth (Clarke and Sutherland, 1990; Groshong et al., 1997; Lin et al., 1999; Musgrove et al., 1998; Skildum et al., 2005; Sumida et al., 2004; Sutherland et al., 1988). For instance, a study in modified T47D cells negative for ER and stably expressing either wild-type PR-B (T47D-YB) or a transcriptionally inactive PR-B mutant showed that the progestin R5020 could induce the proliferation of both cell types

(Skildum et al., 2005). However, only wild-type PR-B could enhance the expression of cyclin D1, cyclin E and cyclin dependent kinases (CDK) coincident with S phase progression. Though this implicates PR-B's transcriptional activity in the proliferative response, the non-genomic effect of PR-B via the MAPK cascade was also found to be important in the proliferative response since MCF7 cells expressing a mutant PR-B that was incapable of MAPK signaling failed to proliferate in the presence of progestin (Skildum et al., 2005). In another report, progestins inhibited proliferation and retarded T47D-YB cells in the late G1 phase after an initial proliferative burst lasting 48 hours (Groshong et al., 1997). Growth inhibition was prolonged in these cells, coincident with a reduction in the levels of cyclins and an increase in levels of CDK inhibitors, indicating a biphasic effect of progestins on breast cancer cells.

In other studies using MDA-MB-231 derivatives that express just the PR, progesterone inhibited cell growth (Lin et al., 2001; Lin et al., 2000; Lin et al., 1999; Lin et al., 2003; Sumida et al., 2004). In one such derivative, the ABC28 cell line, growth inhibition was associated with an up-regulation of the growth inhibitor $p21^{CIP1/WAF-1}$ and reductions in levels of cyclins A, B1 and D1, and phosphorylated p42/44 MAPK (Lin et al., 2003). Furthermore, progesterone greatly increased the presence and numbers of stress fibers and focal adhesions, consistent with these cells being considerably more flattened and well-spread (Lin et al., 2000). Progesterone also increased the attachment of ABC28 cells to the extracellular matrix proteins laminin and fibronectin, a finding that supported their reduced tumorigenicity in SCID mice (Lin et al., 2001). Interestingly, an independent study found that the poor ability of progestin-treated T47D cells to invade the fibroblast

layer in migration assays was enhanced upon PR-A expression (McGowan et al., 2004). Not only is this congruent with findings of greater PR-A levels in invasive mammary tumor tissues, but it implies PR-B may inhibit metastasis of progesterone-treated breast cancer cells. Thus, progesterone can exert growth inhibitory and anti-metastatic effects in the absence of estrogen and ER.

Focusing on the molecules downstream of progestins and PR is likely to clarify their effects in breast cancer cells. Microarray analyses of gene expression changes in hormone-treated ABC28 cells and in other breast cancer cells overexpressing PR have led to the identification of numerous downstream genes that are regulated by PR, with differences between receptor isoforms (Jacobsen et al., 2003; Jacobsen et al., 2005; Leo et al., 2005; Nagai et al., 2004; Wan and Nordeen, 2002). More than 200 genes that are involved in a myriad of pathways were found to be differentially regulated in ABC28 cells (Leo et al., 2005).

1.4 The TRIM/RBCC family of proteins

1.4.1 Domain organization of the TRIM family of proteins and functions of individual domains

The human genome has 64 genes that encode proteins belonging to the TRIM family (**Table 1.1**). This family is also referred to as the RBCC family since member proteins generally have a characteristic tripartite motif consisting of a **R**ING-finger domain, one or two **B**-box domains and a **C**oiled-**C**oil (CC) domain at the N-terminus (Reymond et al., 2001; Torok and Etkin, 2001). Proteins lacking the RING domain or both the RING

and B-box domains have also been classified by others to be TRIM proteins (Nisole et al., 2005). These have been included in **Table 1.1**. TRIM34/IFP1 is also an exception since it has two RBCC/TRIM motifs in tandem (Orimo et al., 2000a). For the majority of TRIM proteins, the order and spacing of the RING, B-box and CC domains is highly conserved in human TRIMs and in TRIMs from other species This suggests a common basic function of the RBCC domain organization as an integrated structure rather than as individual modules (Reymond et al., 2001; Torok and Etkin, 2001).

1.4.1.1 RING-finger domain

The RING-finger domain is a zinc-coordinating domain of 40 to 60 amino acids that seems to be involved mainly in protein-protein interactions. This domain is defined by a regular arrangement of cysteine and histidine residues that bind two zinc atoms per molecule in a “cross-brace” pattern. The “cross-brace” pattern is a result of one zinc atom being coordinated by the cysteine residues in positions 1, 2, 5, 6 and the second zinc atom by cysteine or histidine residues in position 3, 4, 7, 8. Of the two main subtypes of RING domains, H2 or C2, TRIM proteins have the C2 subtype. In the C2 subtype, the zinc atom is coordinated by a cysteine residue in the fifth coordination site. The RING domain is not restricted to the TRIM family and can be found in a range of proteins with broad biological functions, including members of the inhibitor of apoptosis (IAP) family of proteins and transcription factors like BRCA1 (Casey, 1997; Verhagen et al., 2001; Yang and Li, 2000). RING finger domains typically function as E3 ubiquitin ligases in regulating protein stability via the ubiquitination pathway. The role of the RING finger domain in E3 ligase activity will be discussed later in **section 1.4.3.2**.

Numerous studies have shown the importance of the RING domain. TRIM19/Promyelocytic leukemia (PML) protein is a nuclear protein which usually exists in distinct bodies called PML bodies. These bodies are crucial for PML's growth suppressive and apoptotic effects (Borden et al., 1997; Fagioli et al., 1998; Mu et al., 1994). In acute promyelocytic leukemia (APL), a chromosomal translocation event between chromosome 15 and 17 results in a fusion (PML-RARα) of the N-terminal RBCC domains of PML with RARα (Kastner et al., 1992; Rowley et al., 1977). Unlike full length PML, PML-RARα localizes as diffuse nuclear speckles, is associated with a failure in promyelocytic differentiation and results in cell transformation and APL (Kastner et al., 1992). The differentiation agent all-trans retinoic acid (ATRA), via a caspase 3-mediated cleavage of PML-RARα, induces a complete remission in APL patients, coincident with the re-formation of distinct PML bodies (Nervi et al., 1998; Warrell et al., 1991). Interestingly, mutations in the RING finger domain have also been found to alter the subcellular localization of PML from punctuate nuclear bodies (NB) to the diffuse and speckled nuclear staining reminiscent of the localization of PML-RARα in APL (Borden et al., 1995; Kastner et al., 1992). These mutations were capable of inhibiting PML's growth suppressive and apoptotic effects (Borden et al., 1997; Fagioli et al., 1998). The inability of RING mutants to suppress growth is consistent with the finding that p53 interacts with PML within PML bodies, but not PML-RARα, and that the PML NB regulates the function of p53 (Fogal et al., 2000). Given that alterations in PML's B-box and CC domains also led to localization as a dispersed protein, it is likely that all three domains are required for NB formation and efficient growth suppressive effects (Fagioli et al., 1998).

Like PML, the Ret finger protein (TRIM27/RFP) has roles in apoptosis for which an intact RBCC motif is necessary (Dho and Kwon, 2003). The RFP/ret oncogene is also the result of a translocation event between the 5' half (containing the RING finger motif) of the *Rfp* gene and the 5' truncated *ret* receptor tyrosine kinase gene (Takahashi and Cooper, 1987; Takahashi et al., 1988). The ability of this fusion protein to transform mouse embryonic fibroblasts (MEF) was inhibited when cysteine or histidine residues (Cys-16, Cys-31, or His-33) in the RING finger domain were substituted (with Phe-16, Phe-31, or Asn-33 respectively), implying that the RING domain is critical for the transforming ability of RFP/ret (Hasegawa et al., 1996).

1.4.1.2 B-box domain

The B-box domain is another zinc-binding motif, but one that is found exclusively in TRIM proteins (Torok and Etkin, 2001). TRIM proteins can have either one or two B-box domains (termed the B-box1 and B-box2 domains). If only one B-box domain is present (in the case of 49 out of the 68 TRIM proteins), this is the B-box2 domain; otherwise both B-box1 and B-box2 are present with B-box2 found about ten amino acids after B-box1. Some TRIM proteins do not have the RING and B-box domains (TRIMs 58 and 65) but have been listed as TRIM proteins perhaps due to the presence of the CC and SPRY domains (Nisole et al., 2005). There is little sequence similarity between the two B-box domains except for the presence of eight cysteine and histidine residues in B-box1, making it slightly larger than the seven cysteine/histidine residue-containing B-box2. Recent high resolution analyses of the structures of the B-box1 and B-box2 domains from TRIM18/MID1 revealed that both domains were capable of binding two zinc atoms in a

"cross-brace" pattern like in the RING finger domain (Massiah et al., 2007; Massiah et al., 2006). In contrast, the B-box2 domain from the Xenopus protein Xnf7, which was the very first to be characterized, was found to bind only one zinc atom (Borden et al., 1993). Analyses of the B-box domains in MID1, PML, and Xnf7 reveal that these domains are largely unstructured in the absence of metal ions (Borden et al., 1996; Borden et al., 1993; Massiah et al., 2007; Massiah et al., 2006).

The function(s) of the B-box domains have not been characterized as well as those for the RING finger domain. For the large part, B-box domains also appear to be important in protein-protein interactions. In MID1, a phosphoprotein, deletion experiments revealed B-box1 mediates MID1's interaction with Alpha 4 (α4), a regulatory subunit of the major serine/threonine phosphatase PP2A (Inui et al., 1998; Murata et al., 1997; Short et al., 2002; Trockenbacher et al., 2001). Massiah et al. subseqently showed that MID1's B-box1 domain does have a potential binding site for α4 (Massiah et al., 2006). MID1's interaction with α4 was necessary for recruitment of α4 into microtubules, where MID1 typically localizes (Cainarca et al., 1999; Liu et al., 2001; Schweiger et al., 1999; Short et al., 2002). Notably, the presence of large amounts of α4 not only mislocalized MID1 away from microtubules into the cytosol as clumps but also resulted in the dephosphorylation of MID1 without affecting its expression level (Liu et al., 2001). The B-box domains of MID1 are therefore important for interaction with α4-containing phosphatases such as PPA2, which in turn are likely to affect the location and functions of both MID1 and PPA2.

Table 1.1 The tripartite motif-containing (TRIM) protein family. Modified from Reymond et al. (2001)
[a]TRIM IDs of published TRIM proteins and [b]synonyms (and/or commonly used names). GLFND is also included in the table due to the inclusion of other proteins lacking RING domains (TRIMs 51, 58, 65, 66) as TRIM proteins by Nisole et al. (2005)
[c]The domains present: R, RING finger; B1, B-box1; B2, B-box2; CC, Coiled-coil; COS, COS box motif; FN3, fibronectin III; SPRY, SplA and ryanodine receptor/B30.2; NHL, NCL-1/HT2A/LIN-41 repeats; ARF, ADP ribosylation factor; PHD/BROMO, plant homeodomain/BROMO; FIL, filamin.
[d]The number of alternatively spliced forms is indicated.
[e]Ability to dimerize or multimerize
[f]Known function(s) of the protein. Where relevant, the virus against which the TRIM protein shows antiviral or proviral activity is indicated within brackets. Where relevant, the substrate which is the target of the TRIM protein's E3 ubiquitin ligase activity is indicated within brackets.
[g]Localization pattern of the protein within the cell: C, cytoplasmic; N, nuclear
[h]References from which data was obtained. For well-characterized proteins, a review is referenced.
[*]TRIM5α shows species specificity. Human TRIM5α restricts SIV and MLV but rhesus TRIM5α restricts HIV-1.

Name[a]	Synonym[b]	Domains[c]	Isoforms[d]	Self-interacting[e]	Cellular function[f]	Cellular localization[g]	References[h]
TRIM1	MID2	R B1 B2 CC COS FN3 SPRY		Yes	Antiviral activity (N-MLV), development	Filamentous (C)	Buchner et al., 1999; Short et al., 2002; Yap et al., 2004; Zhang et al., 2006
TRIM2	NARF	R B2 CC NHL			Response to seizure-related neural activities	Diffuse (C)	Ohkawa et al., 2001
TRIM3	BERP	R B2 CC NHL		Yes	Modulation of neurite outgrowth in PC12 cells	Diffuse, bodies (C)	El-Husseini and Vincent, 1999
TRIM4	RNF87	R B2 CC SPRY				Speckles (C)	Reymond et al., 2001
TRIM5[*]	RNF88	R B2 CC SPRY	6	Yes	(α isoform) antiviral activity (SIV, MLV, EIAV), E3 ligase activity (self)	Speckles (C)	Nisole et al., 2005; Stremlau et al., 2004; Yamauchi et al., 2008
TRIM6		R B2 CC SPRY		Yes		Speckles (C)	Reymond et al., 2001
TRIM7	GNIP	R B2 CC	4		Activation of glycogenin self-glucosylation	Diffuse (N and C)	Reymond et al., 2001; Skurat et al., 2002
TRIM8	GERP	R B1 B2 CC		Yes	Inhibition of SOCS-1 dependent IFNγ-mediated transcription, E3 ligase activity (SOCS-1)	Speckles (N)	Reymond et al., 2001; Toniato et al., 2002; Vincent et al., 2000
TRIM9	SPRING	R B1 B2 CC COS FN3 SPRY	3	Yes	Modulation of Ca^{2+}-dependent synaptic vesicle exocytosis	Filamentous (C)	Berti et al., 2002; Li et al., 2001
TRIM10	HERF1	R B2 CC SPRY	2	Yes	Erythroid differentiation and maturation	Aggregates (C)	Harada et al., 1999
TRIM11	BIA1	R B2 CC SPRY		Yes	E3 ligase activity (TRIM5α), proviral and antiviral (MLV, HIV), neuroprotection	Diffuse, speckles (N, C)	Niikura et al., 2003; Uchil et al., 2008
TRIM13	LEU5	R B2 CC	2		E3 ligase activity (self, CD3-δ)	Speckles (C)	Kapanadze et al., 1998; Lerner et al., 2007
TRIM14	Pub	B2 CC SPRY	2		Inhibition of Pu.1 transcriptional activity	Speckles (C)	Hirose et al., 2003
TRIM15	RNF93	R B2 CC SPRY	2		Antiviral activity (MLV)	Bodies (C)	Reymond et al., 2001; Uchil et al., 2008

Name[a]	Synonym[b]	Domains[c]	Isoforms[d]	Self-interacting[e]	Cellular function[f]	Cellular localization[g]	References[h]
TRIM16	EBBP	B2 CC SPRY			Regulation of keratinocyte differentiation		Beer et al., 2002
TRIM17	TERF	R B2 CC SPRY					Ogawa et al., 1998; Ogawa et al., 2000
TRIM18	MID1	R B1 B2 CC COS FN3 SPRY	2	Yes	Regulation of microtubule dynamics	Filamentous (C)	Cainarca et al., 1999; Short and Cox, 2006; Trockenbacher et al., 2001
TRIM19	PML	R B1 B2 CC	7	Yes	Apoptosis, senescence, antiviral activity (VSV, influenza A, HSV-1, HIV-1, MLV, HFV, Ebola virus, Rabies virus)	Bodies (N)	Everett and Chelbi-Alix, 2007; Jensen et al., 2001; Nisole et al., 2005
TRIM20	MEFV/PYRIN	B2 CC (?COS) SPRY	2	Yes	Innate immune response, Apoptosis	MEFV (filamentous), MEFV_d2 (N)	Chae et al., 2006; Mansfield et al., 2001; Papin et al., 2000
TRIM21	SSA/RO	R B2 CC SPRY	2		T-cell activation, E3 ligase activity (self, TRIM5α)	Diffuse, speckles (C)	Rhodes and Trowsdale, 2007; Yamauchi et al., 2008
TRIM22	STAF50	R B2 CC SPRY		Yes	Antiviral activity (HIV-1), leukemic cell differentiation	Diffuse, speckles (C)	Obad et al., 2004; Obad et al., 2007a, 2007b; Tissot and Mechti, 1995; Tissot et al., 1996
TRIM23	ARD1	R B1 B2 CC ARF	3	Yes	GTPase, vesicular transport	Speckles (N and C)	Vitale et al., 1996; Vitale et al., 2000
TRIM24	TIF1α	R B1 B2 CC PHD/BROMO			Epigenetic control of transcription, liver-specific tumor suppressor, binds to AF-2 domain of nuclear receptors	Speckles (C)	Khetchoumian et al., 2007; Laz et al., 2007
TRIM25	EFP	R B1 B2 CC SPRY			Antiviral (VSV, MLV) and proviral (HIV) activity, cell cycle regulation, E3 ligase activity (RIG-1, 14-3-3σ)	Diffuse, aggregates (C)	Gack et al., 2007; Urano et al., 2002
TRIM26	AFP	R B2 CC SPRY	2			Diffuse (C)	Reymond et al., 2001
TRIM27	RFP	R B2 CC SPRY	2		Gene silencing by stabilizing EID-1, an inhibitor of histone acetylation, apoptosis	Diffuse, speckles (N and/or C)	Cao et al., 1997; Dho and Kwon, 2003; Krutzfeldt et al., 2005
TRIM28	TIF1β/KRIP-1	R B1 B2 CC PHD/BROMO		Yes	Epigenetic control of transcription	Chromatin domains (N)	Kim et al., 1996; Moosmann et al., 1996
TRIM29	ATDC	B1 B2 CC (?COS)	2	Yes	Complementation of radiosensitivity in an AT cell line	Filamentous (C)	Brzoska et al., 1995
TRIM31	RING	R B2 CC	2			Diffuse (N and C)	Reymond et al., 2001
TRIM32	HT2A	R B2 CC NHL			Antiviral activity (HIV-1, HIV-2, EIAV), murine TRIM32 in apoptosis, E3 ligase activity (self, Piasy)	Diffuse, speckles (C)	Albor et al., 2006; Fridell et al., 1995; Horn et al., 2004
TRIM33	TIF1γ	R B1 B2 CC PHD/BROMO	1- 5	Yes	Control of transcription		Venturini et al., 1999
TRIM34	IFP1	R B2 CC R B2 CC SPRY	3	Yes	Antiviral activity (HIV-2, EIAV), interferon response		Li et al., 2007a; Orimo et al., 2000a
TRIM35	MAIR/HLS5	R B2 CC		Yes	Apoptosis, erythroid differentiation	Bodies (N and C)	Kimura et al., 2003; Lalonde et al., 2004
TRIM36	HAPRIN	R B1 B2 CC COS FN3 SPRY		Yes	Involvement in acrosome reaction	Filamentous (C)	Balint et al., 2004; Short and Cox, 2006
TRIM37	MUL	R B2 CC			Peroxisomal protein	Bodies (C)	Avela et al., 2000; Kallijarvi et al., 2002

Name[a]	Synonym[b]	Domains[c]	Isoforms[d]	Self-interacting[e]	Cellular function[f]	Cellular localization[g]	References[h]
TRIM38	RNF15	R B2 CC SPRY					Reymond et al., 2001
TRIM39	TFP	R B2 CC SPRY	2		Cell signaling mediated by cGMP-dependent protein kinase 1	Speckles (N)	Orimo et al., 2000b; Roberts et al., 2007
TRIM40	RNF35	R B2 CC					Reymond et al., 2001
TRIM41	RINCK	R B2 CC SPRY	3		E3 ligase activity (PKC)	Speckles (N and C)	Chen et al., 2007; Tanaka et al., 2005
TRIM42		R B1 B2 CC COS FN3					Reymond et al., 2001; Short and Cox, 2006
TRIM43		R B2 CC SPRY					Reymond et al., 2001
TRIM44	DIPB/MC7	B2 CC					Boutou et al., 2001
TRIM45	RNF99	R B1 B2 CC FIL			Control of transcription	Diffuse (N and C)	Wang et al., 2004
TRIM46	TRIFIC	R B2 CC COS FN3 SPRY				Filamentous (C)	Short and Cox, 2006
TRIM47	GOA	R B2 CC SPRY				(N)	Vandeputte et al., 2001
TRIM48	RNF101	R B2 CC SPRY					Nisole et al., 2005
TRIM49	RNF18	R B2 CC SPRY					Yoshikawa et al., 2000
TRIM50		R B2 CC (SPRY)					Nisole et al., 2005
TRIM51	SPRYD5	CC SPRY					Nisole et al., 2005
TRIM52	RNF102	R B2 CC					Nisole et al., 2005
TRIM53							Nisole et al., 2005
TRIM54	MuRF-3	R B2 CC COS ARF	2		Microtubule stability/Myogenic differentiation	Myofibrils	Gregorio et al., 2005; Short and Cox, 2006; Spencer et al., 2000
TRIM55	MuRF-2	R B2 CC COS ARF	2		Critical for maintenance of sarcomeric M-line region	Myofibrils/(N)	Short and Cox, 2006; Spencer et al., 2000
TRIM56	RNF109	R B1 B2					Nisole et al., 2005
TRIM57	TRIM59/MRF1	R B2 CC					Chang et al., 2002
TRIM58	BIA2	CC SPRY					Nisole et al., 2005
TRIM60	RNF129	R B2 CC SPRY					Nisole et al., 2005
TRIM61	(prediction only)	R B2 CC SPRY					Nisole et al., 2005
TRIM62		R B2 CC SPRY					Nisole et al., 2005
TRIM63	MuRF-1	R B2 CC COS ARF	1		Myogenic differentiation, muscle-specific E3 ligase activity (Titin)	Myofibrils/(N)/perinuclear envelope	Bodine et al., 2001; Short and Cox, 2006
TRIM64	(prediction only)	R B2 CC SPRY					Nisole et al., 2005
TRIM65		CC SPRY					Nisole et al., 2005
TRIM66	TIF1δ	B1 B2	2	Yes	Transcriptional repressor in spermatids	Bodies (N)	Khetchoumian et al., 2004
TRIM67	TNL	R B1 B2 CC COS FN3 SPRY				Filamentous (C)	Short and Cox, 2006
TRIM69	RNF36/TRIF				Apoptosis	Speckles (N)	Shyu et al., 2003
	GLFND	CC COS FN3 SPRY		Yes	Microtubule organization and stability	Filamentous (C)	Manabe et al., 2002; Short and Cox, 2006

Table 1.2 Tripartite motif-containing (TRIM) protein family members in other species. TRIM proteins that are not present in humans.
[a]TRIM IDs and [b]synonyms (commonly used names).
[c]The domains present: R, RING finger; B1, B-box1; B2, B-box2; CC, Coiled-coil; SPRY, SplA and ryanodine receptor/B30.2; NHL, NCL-1/HT2A/LIN-41 repeats; PHD/BROMO, plant homeodomain/BROMO
[d]Ability to dimerize or multimerize
[e]Known function(s) of the protein. Where relevant, the virus against which the TRIM protein shows anti-viral activity is indicated within brackets. Where relevant, the substrate which is the target of the TRIM protein's E3 ubiquitin ligase activity is indicated within brackets.
[f]Localization pattern of the protein within the cell: C, cytoplasmic; N, nuclear
[g]References from which this data was obtained.

Name[a]	Synonym[b]	Domains[c]	Species	Self-interacting[d]	Cellular function[e]	Cellular localization[f]	References[g]
Trim12		R B2 CC	*M. musculus*	Yes		Diffuse, speckles (C)	Reymond et al., 2001
Trim30	Rpt1	R B2 CC SPRY	*M. musculus*	Yes	Antiviral activity (HIV-1)	Speckles (N and C)	Patarca et al., 1988; Reymond et al., 2001
	LIN-41	R B1 B2 CC NHL	*C. elegans*		Heterochronic phenotype	Diffuse (C)	Slack et al., 2000
	NCL-1	B1 B2 CC NHL	*C. elegans*			Diffuse (C)	Frank and Roth, 1998
	eRBCC	R B2 CC SPRY	*A. japonica*		Eel adaptation from freshwater to seawater, E3 ligase activity (substrate not known)	(N)	Miyamoto et al., 2002
	Xnf7	R B2 CC SPRY	*X. laevis*	Yes	Pre-mRNA maturation	(N)	Beenders et al., 2007; Borden et al., 1993
Trim33	Ecto	R B1 B2 CC PHD/BROMO	*X. laevis*		E3 ligase activity (Smad4), development	(N)	Dupont et al., 2005
	Brat	R B1 B2 CC NHL	*D. melanogaster*		Cell growth and rRNA synthesis		Arama et al., 2000

B-box domains are also important for the formation of distinct PML NB. Mutations in PML's B-box domains disrupted NB formation despite PML still being able to homodimerize (Borden et al., 1996). This is consistent with the finding that the B-box domains of PML cooperate with its RING finger domain in inducing growth suppression (Fagioli et al., 1998). In TRIM5α, the B-box2 domain enhances the affinity of the protein for the human immunodeficiency virus (HIV-1) capsid protein, even though the SPRY domain is the region that interacts with the capsid protein (Li et al., 2007b). In the case of Xnf7, a nuclear protein, the B-box2 domain was found to be critical for the association of Xnf7 homotrimers with chromosomal loops (Beenders et al., 2007). B-box domains can also modulate self-interaction, as shown for TRIM27/RFP (Cao et al., 1997).

1.4.1.3 Coiled-coil (CC) domain

The CC domain follows the B-box2 domain in all TRIM proteins having both these domains (Reymond et al., 2001; Torok and Etkin, 2001). The coiled coil is a bundle of α-helices that are further wound into a super-helix (Lupas, 1996). It is the main structural element of fibrous proteins like keratin and fibrinogen. The primary sequence for the CC domain is not conserved between the TRIM proteins, except for the presence of hydrophobic leucine residues which give the domain its characteristic packing system (Lupas, 1996). Consistent with the known ability of coiled coils to mediate protein oligomerization, CC domains have been shown to be necessary for the homomultimerization of the RFP and MID1 proteins (Cainarca et al., 1999; Cao et al., 1997). An elaborate study by Reymond et al. identified numerous other TRIM proteins (TRIMs 6, 8, 11, 23, 28, 29, and 30) that were able to self-associate via their CC domains

(Reymond et al., 2001). Isolated CC domains from some of these proteins were sufficient for self-association and the formation of higher molecular weight complexes (Reymond et al., 2001). However, there are instances where even the presence of the CC domain results in the protein localizing diffusely within the cell with no evidence of multimerization (TRIMs 2, 7, and 45) (**Table 1.1**), or when CC domains, such as the one in TRIM5α and TRIM33/TIF1β, lack the inherent ability to multimerize and require other regions of the protein for this function (Javanbakht et al., 2006; Peng et al., 2000).

Multimerization and formation of higher order structures is important for the localization and function of numerous TRIM proteins. For instance, Xenopus TRIM Xnf7 could not associate with transcriptional units in the maturing oocyte in the absence of its CC domain, which prevented its trimerization (Beenders et al., 2007). In the case of PML, the CC domain is essential for multimerization as well as the complete growth suppressive effects of PML (Fagioli et al., 1998; Kastner et al., 1992). The CC domain in TRIM5α, though not important for localization of the protein in the cytoplasm, mediated binding to capsid protein and was required for retrovirus restriction (Javanbakht et al., 2006). The CC domain of RFP is required for interaction with the PML and Enhancer of polycomb proteins (Cao et al., 1998; Shimono et al., 2000).

1.4.1.4 C-terminal domains: COS and SPRY/B30.2 domains

The RING, B-box and CC domains are usually followed by one or two well-defined C-terminal domains of variable length and composition. These C-terminal domains include the **p**lant **h**omeo**d**omain (PHD)-BROMO domain, **N**CL-1/**H**T2A/**L**IN-41 repeat (NHL)

domain, **A**DP-**r**ibosylation **f**actor (ARF) domain, **F**ibro**n**ectin **III** (FN3) domain, **Sp**lA and **ry**anodine receptor (SPRY)/B30.2/RFP-like domain and the **m**eprin **a**nd **t**umor necrosis factor receptor-associated **h**omology domain (MATH) (Reymond et al., 2001). PHD/BROMO domains, found in TIF1α, β, γ proteins (TRIMs 24, 28, and 33), are characteristic motifs in proteins known to function at the chromatin level (Aasland et al., 1995; Khetchoumian et al., 2004; Kim et al., 1996; Le Douarin et al., 1996; Moosmann et al., 1996). NHL repeats are found in at least three TRIM proteins. In TRIM3/BERP, six NHL repeats are organized to form the β-propeller domain, which has been found to interact with myosin V and α-actin, suggesting a possible involvement in cargo transport and/or anchoring (El-Husseini and Vincent, 1999).

Short and Cox recently identified a new 67 aa motif, the "COS box", in the C-terminus adjacent to the CC domain that is largely responsible for the association of TRIM proteins with microtubules (Short and Cox, 2006). The COS box is present in as many as ten TRIM proteins, which have one of three distinct C-terminal domain arrangements. Class I subfamily proteins include MID1, TRIM1/MID2, TRIM9/SPRING, TRIM36/HAPRIN, TRIM46/TRIFIC and TRIM67/TNL, all of which have a COS box next to a FN3 domain and then a SPRY domain. Class II subfamily proteins, the muscle-specific MuRF proteins (TRIMs 63, 54, and 54), have a COS box next to an acid-rich region. There is experimental data available for Class I and Class II proteins showing that they do localize in a filamentous fashion to microtubules (**Table 1.1**). TRIM42, the only member of the Class III subfamily, has a COS box followed only by a FN3 domain but it has not been characterized in detail. TRIM20/PYRIN and TRIM29/ATDC have also been

reported to form filamentous structures but were excluded from the study by Short and Cox due to the absence of the RING finger domain in these proteins (Brzoska et al., 1995; Short and Cox, 2006). Likewise, another protein homologous to MID1, GLFND, which lacks the RING and B-box domains but has the CC, FN3, and SPRY domains and not yet been listed as a TRIM protein, was found to contain the COS box (Manabe et al., 2002; Short and Cox, 2006). GLFND also associates with microtubules after cytokinesis and was found to affect microtubule stability and organization (Manabe et al., 2002). The presence of the COS box in seemingly all microtubule-associated proteins is consistent with data showing that disruption of the COS box abrogated association with microtubules while addition of this motif redirected TRIM37/MUL, a non-microtubule protein, to microtubules (Short and Cox, 2006).

Despite the Short and Cox study showing the necessity of the COS box in microtubule association, it is also evident that the CC domain can influence the ability of the COS box to bind microtubules. Homodimerization mediated by the CC domain was found to mediate the association of some Class I and II proteins with microtubules (Centner et al., 2001; Reymond et al., 2001; Short and Cox, 2006; Short et al., 2002). Removal of the CC domain, but not the COS box, in GLFND reduced its affinity for microtubules and resulted is a less filamentous pattern of expression (Manabe et al., 2002). In addition, this mutant of GLFND suffered in its ability to stabilize microtubules after nocodazole treatment, suggesting that GLFND has to be able to dimerize in order to function.

The SPRY domain, which is also frequently referred to as the B30.2 domain since it is related to the B30.2 domain found in butyrophilin, is one of the most common domains in the C-terminal of TRIM proteins. Its function is not well understood and proteins containing the SPRY domains cover a wide range of functions including RNA metabolism (hnRNPs), intracellular calcium release (RyR receptors), immunity to retroviruses (TRIM5α), ubiquitin protein ligase activity (MID1, TRIM25/EFP) and regulation of cytokine signaling (SOCS) (Rhodes and Trowsdale, 2007). The SPRY domain is more variable, much unlike the rigid tripartite motif in the N-terminal region of TRIM proteins. In particular, the amino acid variability in the hydrophilic regions of different SPRY domains and the inherent flexibility found in certain regions of the SPRY domain suggest that the SPRY domains of TRIM proteins can greatly affect the conformation of the protein (Woo et al., 2006; Yao et al., 2006). This in turn may determine specificity of protein interactions and affect protein localization and function besides the common roles of TRIM proteins in antiviral activity and/or protein ubiquitination that appear to be dictated by the conserved tripartite motif.

The specific functions of several different TRIM proteins have been reported to be dependent on the SPRY domain. Human TRIM5α's (hTRIM5α) SPRY domain determines the specificity and strength of antiretroviral activity since single amino acid changes within this region were adequate to enhance the potency of the molecule against HIV-1 to the extent observed with rhesus TRIM5α (rTRIM5α) (Ohkura et al., 2006; Stremlau et al., 2005). The SPRY domain of TRIM21/SSA/RO was found to be necessary for regulation of IgG function (Ohkura et al., 2006; Rhodes and Trowsdale,

2007). Patients with mutations in the SPRY domain of MID1 have Opitz syndrome, which manifests as developmental disorders. These mutations, when artificially introduced into the MID1 protein, resulted in a diminished affinity for microtubules even though the proteins could self-associate and form high molecular weight complexes (Cainarca et al., 1999).

1.4.2 Localization of TRIM proteins in mammalian cells

The CC domain in TRIM proteins has been shown to be the domain predominantly responsible for protein multimerization. Studies with MID1, MID2, PML, RFP and MuRF-1 and others show that these multimerizing proteins localize to specific compartments within the cell (Buchner et al., 1999; Cao et al., 1997; Centner et al., 2001; Dyck et al., 1994; Reymond et al., 2001; Schweiger et al., 1999; Zhong et al., 2000a). Because of their inherent ability to multimerize, cytoplasmic TRIMs would often be found as filaments (TRIMs 1, 9, 18, 20, 36, 46, and 67), cytoplasmic bodies (TRIMs 4, 5, 6, 9, 10, 12, 14, 21, 23, 26, 27, 30, and 32) or as a ribbon-like structure (TRIMs 2 and 29). Nuclear TRIMs were found to localize as NB (TRIMs 8, 19, 30, and 32) or nuclear sticks (TRIM6). The locations of the different TRIM proteins in humans and other species have been summarized in **Tables 1.1** and **1.2**.

In many instances, besides locating to a specific compartment within the cell, TRIM proteins identify the cell compartment such that in the absence of the protein, the cell compartment no longer exists or, even if it does, does not function as it should. An excellent example is the PML body (reviewed in detail in **section 1.6.3**). A crucial

constituent of the PML body is PML, which can also exist as a nucleoplasmic protein (Muller et al., 1998). PML can only form bodies in the presence of the small ubiquitin-related modifier (SUMO) (Muller et al., 1998; Shen et al., 2006; Zhong et al., 2000a). The presence of sumoylated PML within PML bodies was critical for the localization and function of the apoptotic protein Daxx (Ishov et al., 1999; Zhong et al., 2000c).

1.4.3 Functions of TRIM proteins

TRIM proteins have different functions, such as in growth and differentiation, transcriptional control, antiviral activity and protein ubiquitination (**Table 1.1**)**.** Of these functions, apoptotic effects, protein ubiquitination and antiviral activity are more common and may reflect conserved functions attributed to the RBCC domain. Protein ubiquitination seems to depend on the E3 ligase activity of the RING domain of some TRIM proteins. The conserved order and spacing of the RING, B-box and CC domains is likely to facilitate interaction with substrates. Antiviral function has not been attributed to any one particular domain but may require the E3 ligase activity of the RING domain. For instance, E3 ligase activity of the Estrogen-responsive finger protein (TRIM25/EFP) is required for ubiquitination and thence activity of the antiviral molecule retinoic-acid-inducible gene 1 (RIG-1) (Gack et al., 2007). The variable C-terminal region may regulate the specificity of interactions of TRIM proteins with other proteins, including substrates and viral proteins.

1.4.3.1 TRIM proteins in growth and differentiation

TRIM proteins have roles in differentiation, regulation of cell cycle progression and apoptosis. TRIM proteins involved in differentiation are TRIM10/HERF1 (in erythrocytes), TRIM16/EBBP (in keratinocytes), TRIM22/STAF50 (in leukemia cells), and TRIM35/HLS5 (in erythrocytes). TRIM19/PML, TRIM20/PYRIN, TRIM25/EFP, TRIM27/RFP, TRIM35/HLS5, and TRIM69/TRIF are involved in growth suppression and/or apoptosis.

PML is one of the better characterized TRIM proteins with initial studies showing its growth suppressive effects when overexpressed (Fagioli et al., 1998; Mu et al., 1994). In these studies, the RBCC motif was the minimum requirement for this activity. In support of this, colony formation assays in *non-haematopoietic* cell lines showed that both PML and PML-RARα inhibited cell growth (Alcalay et al., 1998; Fagioli et al., 1998). Mechanisms underlying PML-mediated growth suppression have been shown to be both dependent and independent of two well-known growth suppressors, the retinoblastoma protein (pRb) and p53, as well as other apoptotic proteins like Daxx.

PML binds to over 50 proteins, one of which is the non-phosphorylated form of pRb. PML-RARα is also able to bind to non-phosphorylated pRb since it has an intact RBCC motif which was found to be adequate for this interaction between PML and pRb (Alcalay et al., 1998). Non-phosphorylated pRb halts cell cycle progression from the G1 phase to the S phase by binding to the E2F family of transcription factors (Weinberg, 1995). The E2F transcription factors, whose products are important for cell cycle

progression, are only released when pRb is phosphorylated. While it is not known how exactly the binding of PML to pRb might regulate the latter's function, the growth suppressive effects of PML can also be independent of pRb since both PML and PML-RARα were both able to inhibit growth of *non-haematopoietic* cells in colony assays in the absence of endogenous pRb (Alcalay et al., 1998).

The C-terminal of PML, while not essential, may modify the strength and quality of its interaction with pRb. This is because PML isoform II, which has a different C-terminal end to that of PML isoform IV, had a weaker interaction with pRb compared to PML IV (Alcalay et al., 1998). Furthermore, even though both PML and PML-RARα were able bind to unphosphorylated pRb, the localization of pRb in PML bodies was disrupted by PML-RARα and only PML was capable of inhibiting pRb's transcriptional regulatory effects (Alcalay et al., 1998). This implies that the interaction of wild-type PML with pRb is of a different nature, perhaps one that influences the growth suppressive activities of either or both these proteins.

p53 is another protein found within the PML body that may mediate PML's apoptotic and growth suppressive effects. PML directly interacts with p53, colocalizes with p53 within PML bodies, and promotes p53 transactivation in a promoter-specific manner (Fogal et al., 2000). Acetylation of p53 within PML bodies in a manner requiring direct interaction between p53 and PML was found to be one mechanism by which PML could modulate p53's activity in response to the Ras oncoproteins (Pearson et al., 2000). Interestingly, p53 could interact with PML isoform IV but not with either PML III or PML-RARα,

indicating the importance for the C-terminal of PML in regulating p53 activity and thus an isoform specific ability of PML to regulate growth via p53 (Fogal et al., 2000).

PML may also enhance apoptosis in a p53-independent manner. In mice lacking endogenous PML, activated splenocytes were more resistant to Fas-induced apoptosis, a process independent of p53 (Wang et al., 1998). Fas activation induces apoptosis by triggering the caspase cascade of events that leads to the activation of the major apoptosis executioner caspase 3. Daxx was initially identified as an interactor of Fas (Pluta et al., 1998). Daxx also interacts with PML, though only with sumoylated PML within bodies (Ishov et al., 1999). The interaction between Daxx and PML in bodies enhanced Fas induced apoptosis in a caspase-dependent manner (Torii et al., 1999). Another study reported that PML was capable of inducing apoptosis in a caspase-independent manner since caspase 3 was not activated and caspase inhibitors could not reverse PML-induced apoptosis (Quignon et al., 1998).

1.4.3.2 TRIM proteins as E3 ubiquitin ligases

In eukaryotic cells, protein ubiquitination has roles in protein trafficking, transcriptional regulation, subcellular localization, and proteasome-mediated proteolysis. Protein ubiquitination involves tagging proteins with a 76 aa polypeptide ubiquitin (or smaller ubiquitin-like (UBL) modifiers, which together with ubiquitin will be referred to as UBL) in a multi-step process that utilizes three different classes of enzymes. The enzymes (E1, E2, and E3) and their interconnections are illustrated in **Figure 1.1**. Only a handful of E1 and E2 molecules have been identified, with these molecules being specific for the UBL

in question. However, E3 ligases bind directly to the specific substrate to enable transfer of the activated ubiquitin from E2 to the substrate. Therefore, it makes sense for there to be a variety of E3 ligases. E3 ligases belong to three different categories based on the catalytic domain mediating the transfer of the ubiquitin moiety. They can contain either the HECT- (Homologous to E6AP Carboxy Terminus), U-box-, or RING finger domains to catalyze the transfer of activated ubiquitin (Meroni and Diez-Roux, 2005). RING finger domain E3s can be further subclassified as either multiprotein complexes that have small RING finger proteins or single protein RING finger E3s where a RING finger domain exists within a single polypeptide stretch. As TRIM proteins have a RING finger domain, they are classified as 'single protein RING finger E3 ubiquitin ligases' (Meroni and Diez-Roux, 2005).

A number of TRIM proteins in humans and other species have E3 ligase activity. For instance, TRIM25/EFP ubiquitinates two different substrates. Ubiquitination of the cell cycle regulator 14-3-3σ by EFP resulted in the former's proteasome-mediated degradation while ubiquitination of the viral RNA receptor RIG-1 increased its antiviral effects and facilitated its binding to mitochondrial antiviral signaling protein (MAVS) (Gack et al., 2007; Urano et al., 2002). Both 14-3-3σ and RIG-1 interacted directly with EFP on different sites. 14-3-3σ bound to the B-box and CC domains while RIG-1 bound to the SPRY domain. Domain deletion experiments revealed that the ability of EFP to reduce 14-3-3σ levels and ubiquitinate RIG-1 required an intact RING finger domain. In the study investigating EFP's effects on 14-3-3σ, evidence for the E3 ligase activity of EFP's RING finger domain came from observations that EFP could interact with the

ubiquitin conjugating enzyme UbcH8 (an E2 enzyme) and that the presence of UbcH8 with full-length EFP, but not EFP lacking the RING domain, enhanced the degradation of 14-3-3σ (Urano et al., 2002).

EFP is overexpressed in breast cancers. Silencing EFP led to an accumulation of 14-3-3σ, consistent with the EFP's role in enhancing breast cancer cell proliferation via inhibition of 14-3-3σ (Urano et al., 2002). Ubiquitination of RIG-1 is required for the induction of IFNβ, a key antiviral molecule (Gack et al., 2007). In *Trim25*$^{-/-}$ MEF, IFNβ production was undetectable compared to in wild type MEF and this was consistent with greater viral infection rates in *Trim25*$^{-/-}$ MEF (Gack et al., 2007). TRIM18/MID1 is also capable of regulating levels of the microtubule associated phosphatase PPA2 via the ubiquitin system. MID1 interacted with PPA2's regulatory subunit α4 to target PP2A, but not α4, for degradation (Albor et al., 2006). As the domain(s) responsible for MID1's effect on PPA2 levels were not clarified in that study, it is not known if MID1 itself acts as an E3 ubiquitin ligase or if it elicits its destructive ability indirectly via other proteins.

Other TRIM proteins reported to have E3 ligase activities are TRIM5α, TRIM8/GERP, TRIM11/BIA1, TRIM13/LEU5, TRIM21/SSA/RO, TRIM32/HT2A, TRIM41/RINCK, and TRIM63/MuRF-1 (Albor et al., 2006; Bodine et al., 2001; Chen et al., 2007; Horn et al., 2004; Lerner et al., 2007; Niikura et al., 2003; Wada and Kamitani, 2006; Yamauchi et al., 2008) (**Table 1.1**). Some of these TRIM proteins are also able to self-ubiquitinate (TRIMs 13, 5α, and 21) and ubiquitinate other TRIM proteins (TRIM21).

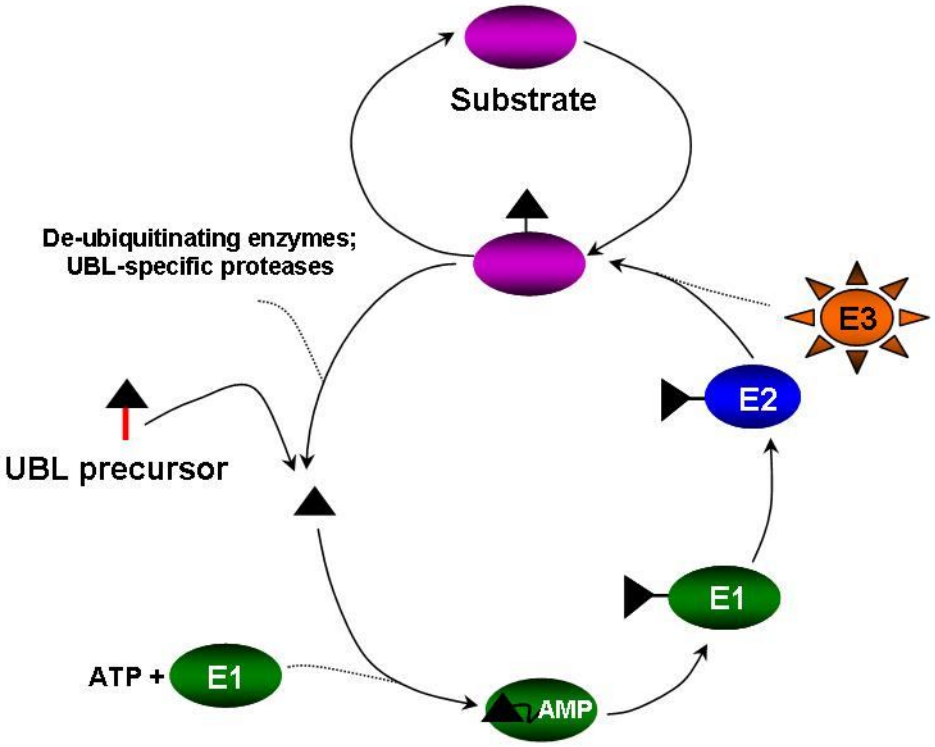

Figure 1.1 The generalized ubiquitin and ubiquitin-like (UBL) conjugation cycle.
After the UBL precursor is cleaved, the mature UBL (black) is adenylated and subsequently linked, via a high energy thioester bond, to an activating enzyme (E1). The activated UBL is transferred to a conjugating enzyme (E2). The UBL is attached, alone or with a UBL-protein ligase (E3), to an amino group of a substrate. This attachment is usually reversible and carried out by de-ubiquitinating enzymes and UBL-specific proteases. Modified from Schwartz and Hochstrasser (2003).

1.4.3.3 TRIM proteins in viral defense

Mammalian cells express different types of antiviral factors that target viruses at different stages of the infection process. For instance, APOBEC3G and ZAP bind to viral nucleic acids and trigger their modification or degradation resulting in viral instability (Gao et al., 2002; Harris et al., 2002; Zhang et al., 2003). Friend virus susceptibility factor (Fv1) and restriction factor 1 (Ref1) are able to bind to cytoplasmic retroviral capsid proteins, particularly those belonging to N and B-tropic murine leukemia viruses (N-MLV and B-MLV) (Kozak and Chakraborti, 1996; Stoye, 1998; Towers et al., 2000). While Fv1 and Ref1 are effective against a wide range of viruses, they are ineffective against primate lentiviruses, which can be restricted by TRIM5α in a similar fashion (Hatziioannou et al., 2004a; Hatziioannou et al., 2003; Hatziioannou et al., 2004b). Besides, TRIM5α, a number of other TRIM proteins are interferon (IFN)-inducible molecules, some with demonstrated antiviral properties (Bouazzaoui et al., 2006; Chelbi-Alix et al., 1998; Lavau et al., 1995; Li et al., 2007a; Obad et al., 2007b; Rajsbaum et al., 2008; Rhodes et al., 2002; Toniato et al., 2002).

TRIM5α

The *TRIM5* gene encodes six different isoforms, the largest and most well characterized of which is TRIM5α. TRIM5α localizes as cytoplasmic bodies and distinguishes itself from the other TRIM5 isoforms by the presence of a C-terminal SPRY domain. Stremlau et al. were the first to directly demonstrate the potent antiviral effect of rTRIM5α against the HIV-1 in cells of the Old World Monkey (Stremlau et al., 2004). As rTRIM5α could not restrict the simian immunodeficiency virus (SIV), it was considered to be species-

specific. Specifically, it was the capsid protein that contained the specificity determinant since rTRIM5α was unable to restrict HIV-1 when the HIV-1 capsid protein was replaced with the SIV-1 capsid protein (Stremlau et al., 2004). Substitution experiments further revealed that rTRIM5α, like Fv1 and Ref1, targets residue 110 on the HIV-1 capsid protein (Perron et al., 2004; Yap et al., 2004). Recognition of the capsid protein in the cytoplasm leads to its accelerated degradation (Campbell et al., 2008; Chatterji et al., 2006). Capsid protein within vesicles or other viral proteins like Gag and Pol were not affected by TRIM5α.

rTRIM5α's ability to distinguish HIV-1 from SIV-1 has been largely attributed to its SPRY domain. The rhesus TRIM5γ isoform, which lacks this domain but is otherwise identical to rTRIM5α, was not able to restrict HIV-1 (Stremlau et al., 2004). In addition, HIV-1, which was only modestly susceptible to hTRIM5α, could be greatly restricted in the presence of a chimeric hTRIM5α protein that had a rTRIM5α-derived SPRY domain (Stremlau et al., 2005). Within the SPRY domain, there are three regions that exhibit variability between the TRIM5α proteins (v1, v2 and v3) from different species. v1 (residues 286 – 371) was found to be most variable between the rTRIM5α and hTRIM5α proteins. A chimeric hTRIM5α containing the v1 region or residues 328 - 332 in the v1 region from rTRIM5α protein had effects comparable to that of wild-type rTRIM5α on HIV-1 infection (Stremlau et al., 2005). Notably, two amino acids within the v1 region of rTRIM5α were responsible for the rTRIM5α's potent antiviral effect against HIV-1.

Besides two critical residues in the SPRY domain, the RING finger and B-box2 domains are also likely to be important for retroviral restriction since substitutions of conserved residues in these domains reduced the antiviral effect of TRIM5α. (Li et al., 2007b; Stremlau et al., 2005). Avidity of TRIM5α for retroviral capsid protein also requires that the protein be able to trimerize. A linker region between the CC and SPRY domains was found to be important for TRIM5α trimerization since replacing a hydrophobic leucine residue in this region with a charged lysine severely attenuated the binding of mutant TRIM5α to capsid protein in a capsid binding assay (Javanbakht et al., 2006).

TRIM19/PML

PML is a direct target of both type 1 and 2 IFNs and the numbers of PML bodies increase upon IFN treatment (Chelbi-Alix et al., 1995; Heuser et al., 1998; Stadler et al., 1995). Overexpression of PML conferred resistance against infection by the vesicular stomatitis virus (VSV) while depletion of PML led to an increase in infectivity of herpes simplex type 1 (HSV-1) virus (Chelbi-Alix et al., 1998; Everett et al., 2006). Removal of PML's CC domain abrogated its antiviral effect (Chelbi-Alix et al., 1998). Nevertheless, the finding that resistance to virus in MEF is the same regardless of whether PML is present or absent suggests PML may be dispensable for protection against viruses in IFN-treated cells (Djavani et al., 2001; Lavau et al., 1995).

PML's mode of action is different from that of TRIM5α. In lymphocytic choriomeningitis virus (LCMV) and VSV-1 infection, PML reduces viral mRNA and protein synthesis (Chelbi-Alix et al., 1998; Djavani et al., 2001). PML was also reported

to repress transcription of the complex retrovirus human foamy virus (HFV) by binding to the viral transactivator and preventing its binding to viral DNA, though this finding was not supported by another study (Meiering and Linial, 2003; Regad et al., 2001).

Other TRIM proteins demonstrated to have antiviral effects are TRIM22/STAF50, TRIM25/EFP, TRIM32/HT2A, and TRIM34/IFP1. The ability of EFP to ubiquitinate the antiviral protein RIG-1 was described earlier in **section 1.4.3.2**. TRIM22's role as an antiviral protein will be discussed later in **section 1.5.7**. Recently, in a systematic analysis of the antiviral activities of 36 human TRIM proteins, Uchil et al. found that TRIM proteins can affect both the entry and/or release of HIV, MLV and/or the avian leukosis virus (ALV) (Uchil et al., 2008). Notably, while the predominant effect of TRIM proteins was antiviral in nature, some TRIM proteins could also enhance viral entry, viral release or viral protein transcription. For instance, TRIM11, by destabilizing the TRIM5α protein, could enhance the entry of N-MLV into HEK293 cells. However, TRIM11 also inhibited the release of MLV and HIV particles. As such, the mechanism by which TRIM proteins affect the viral life cycle can be complicated and a thorough investigation into the mechanism of action of each protein is required before it can be designated as an antiviral protein.

1.5 Tripartite motif-containing 22 (TRIM22)

1.5.1 Identification of TRIM22

TRIM22, also referred to as Stimulated Trans-acting Factor of 50 kDa (STAF50), is the focus of the present investigation. It was originally identified by Tissot and Mechti to be

downstream of IFN after differential screening of cDNA libraries from IFN-treated human lymphoblastoid Daudi cells (Tissot and Mechti, 1995). Other groups have since confirmed this IFN-induced up-regulation of the TRIM22 mRNA (Bouazzaoui et al., 2006; Gongora et al., 2000; Obad et al., 2004). Both type 1 (α and β) and type 2 (IFNγ) IFNs were able to induce the expression of the TRIM22 transcript, with IFNγ reported to be less effective (Tissot and Mechti, 1995). The induction of the TRIM22 RNA species was evident two hours after IFN α/β treatment and was not affected by cycloheximide treatment, indicating that TRIM22 is a primary target of IFNs.

The location of the TRIM22 gene locus in chromosome 11, position p15 was reported in two independent studies (Reymond et al., 2001; Tissot et al., 1996).

1.5.2 Sequence characteristics and domain organization of TRIM22

In the initial report of TRIM22, Tissot and Mechti identified the TRIM22 cDNA sequence to be 2811 bp long and one that encoded a 442 aa protein product (Tissot and Mechti, 1995). They also reported the presence of two different TRIM22 RNA species in different human tissues and suggested that a longer transcript may have been observed due to the presence of other potential polyadenylation signals in the 3' untranslated region of the TRIM22 transcript. However, the most recent entry for the TRIM22 mRNA sequence in the National Center for Biotechnology Information (NCBI) database describes a 3015 bp sequence made up of eight exons, including an open reading frame of 1497 bases that encodes a 498 aa protein product (**Figure 1.2**). *In vitro* transcription/translation of a 2.8 kb-insert containing phagemid using the reticulocyte

Figure 1.2 The TRIM22 mRNA sequence.
The TRIM22 mRNA sequence as described in the NCBI database (NM_006074.3) is a 3015 bp sequence that has eight exons (alternate blue and red lettering). A predicted open reading frame of 1497 bp (shown in **bold** lettering) encodes 498 aa. Two polyadenylation sites have been underlined.

lysate system led to the synthesis of a polypeptide having an apparent molecular mass of 54 kDa (Tissot and Mechti, 1995). In another study using rabbit polyclonal antibodies raised against TRIM22, a 58 kDa band that was enhanced in the presence of IFN α/β was detected (Gongora et al., 2000). However, the specificity of these antibodies was not investigated.

Analysis of the TRIM22 polypeptide sequence generated from the coding sequence revealed 44% and 41% similarity with the mouse Rpt-1 protein and the human TRIM21 protein, respectively (Tissot and Mechti, 1995). Two zinc finger motifs, one with a C3HC4 signature and another with a CHC3H2 signature, corresponding to the RING and B-box domains, were present. These motifs were separated by a 40 aa stretch rich in arginine (R) and lysine (L), which the authors termed the "intermediate motif" (Tissot and Mechti, 1995). They postulated that this basic motif may enhance the affinity of the protein for DNA. They also reported the presence of a central bipartite nuclear localization sequence (NLS) (from residues 253 – 271; KRSESWTLKKPKSVSKKLK). The involvement of this motif in nuclear localization has not been demonstrated experimentally. A comparison of 37 TRIM proteins further led to the identification of two other domains, the CC domain and SPRY domain, in the TRIM22 protein sequence (Reymond et al., 2001) (**Figure 1.3**).

1.5.3 Homology between TRIM22 and its paralogs

Reymond et al. found the *TRIM* genes to be generally dispersed throughout the genome, with the exception of two clusters located in the Human Leukocyte Antigen region

(Reymond et al., 2001). The first cluster was in 6p21-23 (*TRIMs 10, 15, 26, 27, and 31*). *TRIM22* was found in the second cluster at 11p15 with *TRIM34, TRIM5, TRIM6,* and *TRIM21*. The TRIM proteins in the second cluster share the same domain arrangement (RING, B-box2, CC, SPRY) and were found to have more homology with TRIM22 than the other TRIM proteins. Pair-wise alignments of TRIM22 with these paralogs revealed that the human TRIM34 protein variant 1 (488 aa) is the closest paralog and has 60.8% homology to TRIM22. TRIM22 has 57.2% homology to TRIM6 variant 1 (516 aa), 52.8% homology to TRIM5α (493 aa) and 41.9% homology to TRIM21 (475 aa). An alignment of TRIM22 with these proteins using the T-coffee software (Notredame et al., 2000) showed four stretches of higher dissimilarity (**Figure 1.3**). Two of these were found within the SPRY domain (from residues 373 – 399 and residues 425 – 432) and one to the left of the SPRY domain (from residues 324 – 342). The fourth dissimilar region was found within the RING domain (from residues 46 – 51).

1.5.4 TRIM22 expression level in different tissues

Three studies have investigated TRIM22 transcript expression in human tissues. Two of these used the TRIM22 coding sequence as probes to analyze TRIM22 mRNA expression by Northern blotting and reported an expression profile that is largely inconsistent with the results of the third and the most recent study where specific primers against TRIM22 allowed for the distinction between the TRIM22 and TRIM5α mRNAs (Sawyer et al., 2007). The older studies found high TRIM22 expression levels in peripheral blood leukocytes (PBL), the spleen, and the ovary but very low levels in other tissues (Gongora et al., 2000; Tissot and Mechti, 1995).

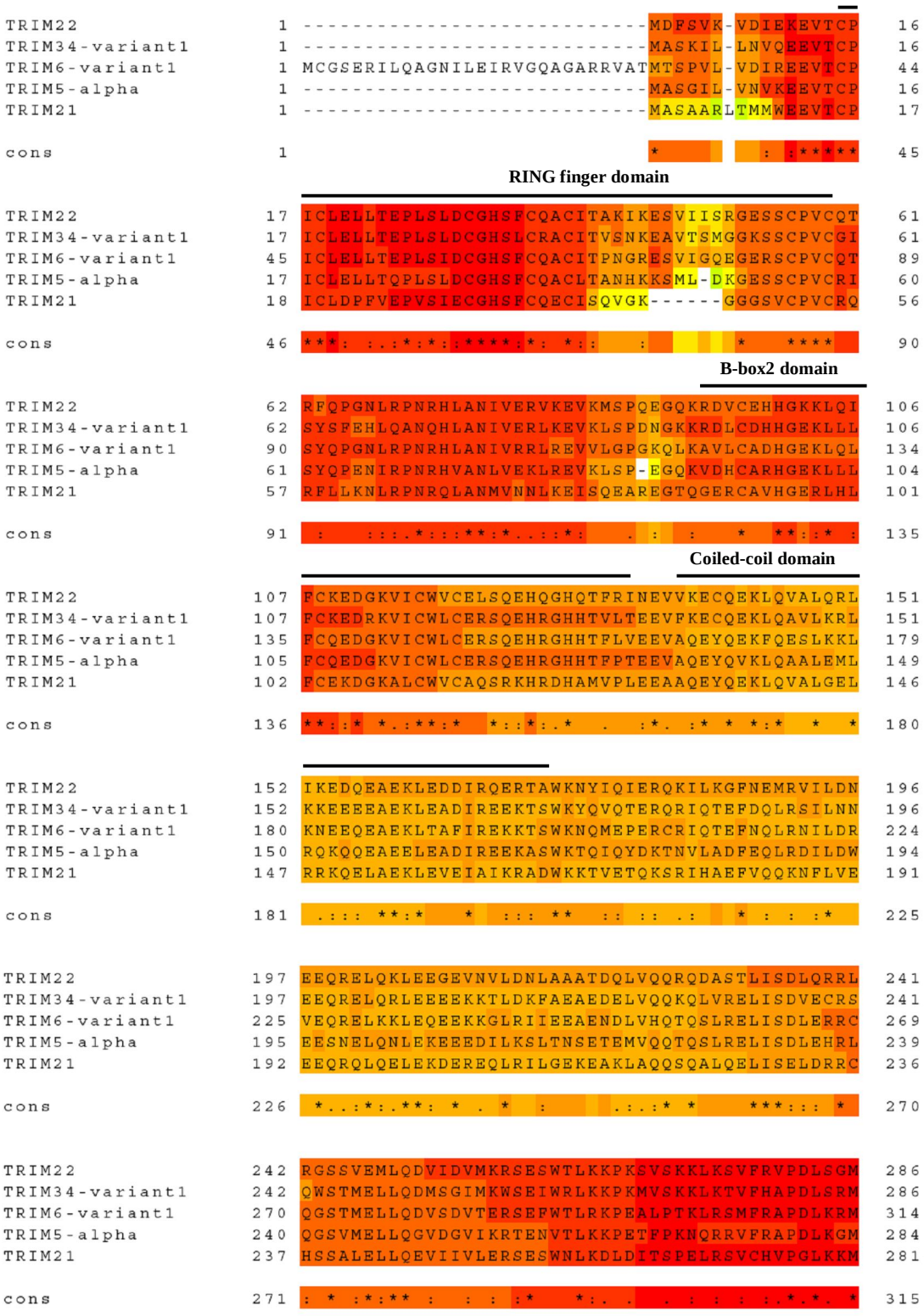
RING finger domain
B-box2 domain
Coiled-coil domain

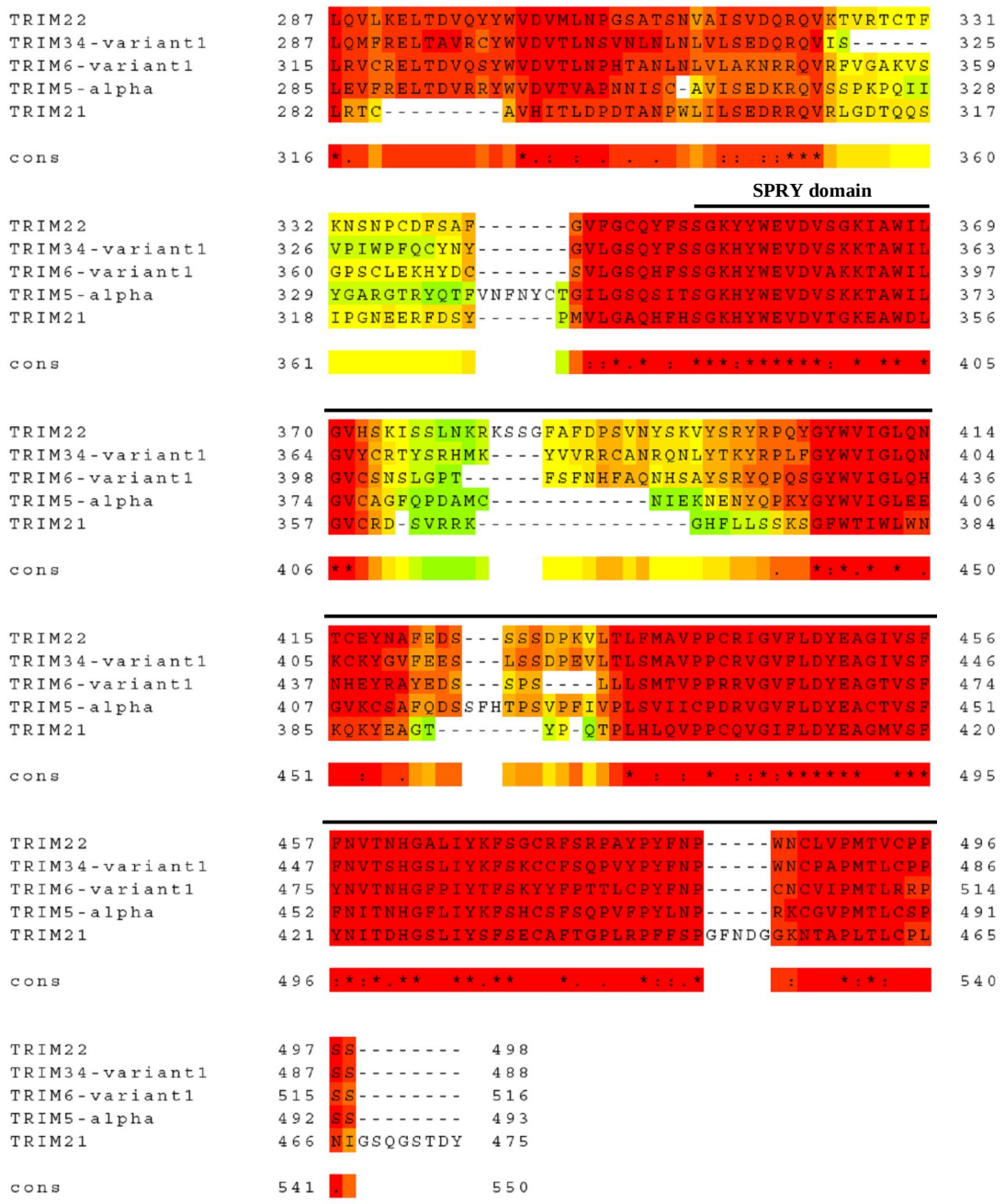

Figure 1.3 Alignment of TRIM22 sequence with those of its paralogs TRIMs 34, 6, 5*α*, and 21 to show regions of similarity.

Proteins arranged in order of decreasing homology to TRIM22. Bars are used to denote the regions encompassed by the different domains. Colors (BAD AVG GOOD) indicate the extent of homology. Consensus regions indicated with an asterisk (*). Protein IDs used for alignment were: TRIM22 (NP_006065), TRIM34-variant 1 (NP_067629), TRIM6-variant 1 (NP_001003818), TRIM5α (NP_149023), TRIM21 (NP_003132). T-coffee was used to generate the alignment (http://www.tcoffee.org/).

TRIM22 expression could not be detected in the mammary gland (Gongora et al., 2000). In the third and latest study, stimulated PBL, but not unstimulated PBL, expressed high levels of TRIM22 (Sawyer et al., 2007). TRIM22 mRNA expression levels were low in peripheral lymphoid organs (spleen) and the ovary and higher in the thymus. Of the other tissues, the colon, small intestine, skin, cerebellum, placenta, cartilage, pancreas, and testis expressed moderate TRIM22 levels while other organs expressed low or undetectable levels (Sawyer et al., 2007).

1.5.5 TRIM22 protein characteristics and cellular localization

An interaction mating analysis in yeasts initially revealed that TRIM22 does not form a homodimer (Reymond et al., 2001). Subsequently, a study in HeLa cells stably expressing FLAG-tagged TRIM22 showed that TRIM22, like its other paralogs TRIM34, TRIM6 and TRIM5α, forms trimers (Li et al., 2007a). The oligomerization of TRIM proteins was detected by cross-linking proteins with glutaraldehyde prior to SDS-PAGE analysis. TRIM22 also appears to be a very stable protein since a 7-hr cycloheximide treatment regimen did not reduce its levels (Li et al., 2007a). In contrast, TRIM5α and TRIM4 levels diminished rapidly after cycloheximide treatment.

Reymond et al. described EGFP-tagged TRIM22 to be a diffuse cytoplasmic protein that could also form cytoplasmic speckles in U20S (osteosarcoma cells), although, from the supplementary images available at http://www.tigem.it/TRIM/, some nuclear localization was evident (Reymond et al., 2001). In another study, the localization of exogenous human TRIM22 was investigated in HeLa cells co-expressing rhesus TRIM5α. While the

majority of TRIM22 localized in the cytoplasm, in some of these cells, TRIM22 and TRIM5α were partly localized in the nucleus (Li et al., 2007a). Despite the slight colocalization between these proteins, they did not interact directly in coimmunoprecipitation studies (Li et al., 2007a). It is to be noted that the coding sequence for TRIM22 used by Reymond et al. was shorter, resulting in a 442 aa protein that lacks four amino acids at positions 174 – 177 and differs at the C-terminal end by four point mutations when compared with the most recent sequence (which results in a 498 aa protein that is referred to as "full-length" in this study as it is the longest isoform identified) available in the NCBI database. In the present study, we present evidence that the complete TRIM22 sequence codes for an exclusively nuclear protein that also forms NB.

1.5.6 Post-translational modifications in TRIM22

Cells may regulate the abundance, location, and activity of proteins via post-translational modifications. These modifications, which include phosphorylation, acetylation, methylation, glycosylation, ubiquitination, sumoylation and ISGylation can be found either alone or in combination. The multiple modification of proteins is beneficial in allowing proteins to perform more than one function at any given time and may also result in additional functions due to cross-talk between modifications (Hunter, 2007). Thus far, the post-translational modification of TRIM22, by ubiquitination, sumoylation and ISGylation, has only been explored by Obad (Obad, 2007). All three of these processes involve the conjugation of a UBL (or ubiquitin itself) to the substrate after an enzymatic cascade involving three classes of enzymes (activation by E1, transfer onto

catalytic residue in E2, and conjugation to substrate aided by an E3 ligase). An isopeptide bond forms between a glycine residue at the C-terminal end of the UBL and the lysine residue of the substrate. In Obad's investigations, TRIM22 was co-expressed with ubiquitin, the UBLs SUMO or ISG15 in kidney epithelial cells and lysates analyzed by Western blotting (Obad, 2007).

1.5.6.1 Ubiquitination

The process of ubiquitination was reviewed in **section 1.4.3.2**. Like other TRIM proteins that have been found to function as E3 ligases, the presence of the RING finger domain in TRIM22 may likewise enable it to function as an E3 ubiquitin ligase. To be able to function as an E3 ubiquitin ligase, TRIM22 must be able to bind ubiquitin. In the presence of the proteasome inhibitor lactacystine, TRIM22 was found to be mono-or di-ubiquitinated (Obad, 2007). While this experiment confirms that TRIM22 is indeed ubiquitinated, it does not necessarily reflect the E3 ligase activity of TRIM22 since TRIM22 may have been the substrate for another E3 ligase, resulting in ubiquitinated TRIM22.

1.5.6.2 Sumoylation

Sumoylation, the addition of 10 kDa SUMO moiety in a reversible manner to proteins, has been found to be critical for the formation of TRIM19/PML NB and regulates the functions of numerous other proteins (Geiss-Friedlander and Melchior, 2007; Shen et al., 2006; Zhong et al., 2000b). Mapping the residues that accept SUMO in a few known proteins has enabled the identification of a consensus stretch ΨKxE (in which Ψ is an

aliphatic branched amino acid and x is any amino acid) (Geiss-Friedlander and Melchior, 2007). Three sites of high probability (lysines at positions 6, 153 and 265), fitting this consensus, were identified in TRIM22 using the SUMOplot analysis program (http://abgent.com/doc/sumoplot2). TRIM22-bound SUMO could not be detected in Obad's study even though TRIM22 levels were clearly higher in these cells compared to those not expressing SUMO (Obad, 2007). Indeed, there is evidence for protein stabilization via sumoylation (Desterro et al., 1998). It is possible that TRIM22 was sumoylated but the detection of TRIM22-bound SUMO was difficult due to the presence of only very small quantities of these conjugates within the cell.

1.5.6.3 ISGylation

ISG15 is an IFN-inducible UBL of 17 kDa that is rather understudied compared to ubiquitin and other UBL (Schwartz and Hochstrasser, 2003). ISG15 was recently found to mediate the autoISGylation of EFP, which itself can serve as an E3 ligase to ISGylate 14-3-3σ (Zou et al., 2007; Zou and Zhang, 2006). The co-expression of both ISG15 and TRIM22 resulted in an "ISGylation ladder" that was absent in cells overexpressing either of the two proteins (Obad, 2007). While this provides some evidence that ISG15 can bind to TRIM22, further experiments are clearly required to determine if TRIM22 serves as an ISG15 E3 ligase like EFP, or if it is just a substrate.

1.5.7 TRIM22's antiviral properties

TRIM22 is a target of IFN, a key antiviral agent that RNA viruses are particularly susceptible to (Barr et al., 2008; Bouazzaoui et al., 2006; Gongora et al., 2000; Katze et

al., 2002; Tissot and Mechti, 1995). Expression analyses have also shown TRIM22 to be up-regulated by different viral proteins. These include the Tat-1 protein from HIV-1, the latency associated nuclear antigen (LANA) protein from the Kaposi's sarcoma-associated herpes virus (KSHV), and latent membrane protein-1 (LMP-1) from Epstein-Barr virus (EBV) (Izmailova et al., 2003; Renne et al., 2001; Zhang et al., 2004).

Notably, transient expression of TRIM22 in 293T cells and human monocyte-derived macrophages prior to HIV infection reduced viral replication rates by as much as 50 – 90% (Bouazzaoui et al., 2006). TRIM22's mode of action is not entirely clear. TRIM22, like mouse Rpt-1 protein and the viral protein LANA, was able to inhibit transcription directed by the long terminal repeat (LTR) region from HIV (Patarca et al., 1988; Renne et al., 2001; Tissot and Mechti, 1995). A recent study also showed that expression of a 442 aa TRIM22 variant binds to and re-localizes, but does not alter the stability of, the HIV-1 Gag protein in a manner requiring two cysteine residues in the RING domain of the protein. In the presence of TRIM22, Gag failed to accumulate at punctate structures in the cell periphery and this was associated with poor release of virus particles (Barr et al., 2008). In consideration of Li et al.'s finding that TRIM22 could not bind pre-assembled HIV-1 capsid-nucleocapsid protein complexes in an *in vitro* assay, it is possible that TRIM22 binds to the Gag protein via another protein or that TRIM22 binds Gag proteins before these interact to prevent the formation of functional capsid-nucleocapsid complexes (Li et al., 2007a). In another study, fusion of TRIM22's tripartite motif to the C-terminal CypA domain sequence such that the TRIM22-CypA fusion protein could be targeted directly to HIV-1 capsids (an inherent property of the CypA domain that allows

the owl TRIMCypA protein to potently restrict SIV) in the mammalian cell did not alter its inability to restrict retrovirus (Zhang et al., 2006). The latter study should be interpreted with caution since replacement of the SPRY domain with the CypA domain may have greatly modified the three-dimensional structure, which in turn may have interfered with the TRIM22's antiviral effect, despite the presence of the RING domain which was found to be crucial for antiretroviral activity in the most recent study of the protein (Barr et al., 2008). As SPRY domains have been shown to be important in affording the ability to bind to viral proteins, the ability of full length 498 aa TRIM22 to restrict retroviruses should be investigated (Li et al., 2007b).

More evidence in support of TRIM22's antiviral role comes from a recent analysis of the *TRIM22* gene in primate genomes. In this study, the ratio of amino acid-altering base changes to "silent"/baseline changes in the *TRIM22* genes of 27 primate genomes was calculated and used as a measure of protein evolution. The *TRIM22* gene, like the *TRIM5* gene, was found to have evolved under episodic positive selection (Sawyer et al., 2007; Sawyer et al., 2005). The positive selection of the *TRIM22* gene was mutually exclusive to the selection of *TRIM5* gene and only one of these genes, not both, were positively selected in any given primate genome (Sawyer et al., 2007). Moreover, some species have retained only one gene; the *TRIM22* gene is absent in the cow genome which has an expanded cluster of the *TRIM5* gene while the dog genome has the *TRIM22* gene but not the *TRIM5* gene. In contrast, the *TRIM6* and *TRIM34* genes appear to be more static (Sawyer et al., 2007).

There is experimental data supporting the presence of retroviral recognition determinants within the CC and SPRY domains of TRIM5α (Javanbakht et al., 2006; Sawyer et al., 2005; Stremlau et al., 2005). TRIM22 may likewise harbor such determinants since alignment of TRIM22 protein sequences from primates revealed differences in nine residues (Sawyer et al., 2005). Three of these residues were present in the CC domain, two in the SPRY domain between residues 308 – 310 and a further four in the SPRY domain between residues 327 – 337. Interestingly, these latter four residues lie within a stretch of residues (from 324 – 342) that are highly dissimilar between TRIM22 and its paralogs (**Figure 1.3**), making them likely determinants in the recognition of viruses specifically targeted by TRIM22.

1.5.8 TRIM22's roles in growth and differentiation

Studies relating to TRIM22's cellular effects have focused predominantly on its role in leukemic cell differentiation since agents that lead to the differentiation of these cells also increase TRIM22 levels. p53 is a transcription factor that usually mediates cell cycle arrest and apoptosis but also induces differentiation of some tissues, including leukemic cells (Ko and Prives, 1996). Expression analysis of two leukemic cell lines (U-937 and K562) expressing a temperature-inducible p53 mutant revealed that TRIM22 is a direct downstream target of p53 in these cells (Obad et al., 2004). Consistent with TRIM22 being a direct target of the tumor suppressor p53, TRIM22 levels were increased in MCF7 cells exposed to ultraviolet (UV)-irradiation and in p53-positive B-lymphoblastoid cells (TK6) that were treated with genotoxic agents (UVB, adriamycin, MMS, cisplatin, camptothecin) (Amundson et al., 2005; Obad et al., 2004).

To elucidate the mechanism behind p53's effect on TRIM22, the TRIM22 promoter was searched for potential p53 binding sites. Analysis of the 394 bp proximal promoter region revealed no putative p53-binding sites but there was one such site in the first intron (Obad et al., 2004). This site was cloned into pGL3 downstream of the luciferase reporter gene to investigate its effect on SV40-driven luciferase expression. The p53 response element enhanced SV40-driven luciferase activity by 8-fold only in p53-expressing U-937 cells. A mutation incorporated into the response element abolished this enhancement indicating a specific effect of p53 on transcriptional induction of TRIM22. Furthermore, electromobility shift assays showed the response element sequence, but not the mutant sequence, could bind to the p53 protein. In cells lacking endogenous p53, such as in NB4 and HL60 cells, the p53 transactivator p73 could also enhance SV-40 driven luciferase expression. The ability of both p53 and p73 to bind to the p53 binding site found in the first intron of TRIM22 increases the repertoire of agents that could potentially enhance TRIM22 expression levels and the range of cells in which this increase may be elicited.

The role of TRIM22 in the cell is not clear. As a downstream target of p53, it is possible that TRIM22 is involved in apoptosis, cell cycle arrest or differentiation. Overexpression of TRIM22 in U-937 cells led to reduced clonogenic growth on soft agar to an extent comparable to the growth inhibition induced by $p21^{WAF1}$ (a CDK inhibitor) (Obad et al., 2004). However, whether this was due to necrosis or to apoptosis is not known. In her dissertation, Obad clarified that cell death induced by TRIM22 was unlikely to be mediated by caspase cleavage since a broad spectrum caspase inhibitor (z.vad.fmk) did not reverse cell death (Obad, 2007).

ATRA, an agent that induces differentiation in leukemic cells, was able to increase TRIM22 expression levels in NB4 and HL60 cells (Obad et al., 2004). When human bone marrow cells at various stages of differentiation were analyzed for TRIM22 expression, it was found that cells early in the maturation process such as CD34-positive progenitor cells, monocytes and early granulocytes had greater TRIM22 levels than more mature cells (Obad et al., 2007a). TRIM22 could not be detected in mature erythrocytes. When progenitor cells were induced to differentiate into erythrocytes, TRIM22 expression reduced during the maturation process. However, whether TRIM22 mediates differentiation in leukemic cells or if the reduction in TRIM22 levels is a by-product of the differentiation process needs to be ascertained.

Another clue to the function of TRIM22 comes from studies in T-cells, which express high levels of TRIM22 when not activated. One of the functions of IFN is to induce the activation of T-cells and to enhance the interaction of the T-cell receptor complex with the target cell that needs to be destroyed. As *TRIM22* is an IFN target gene with much sequence similarity to mouse Rpt-1, which is down-regulated during T-cell activation, TRIM22 levels were investigated in partially and fully activated T-cells (Gongora et al., 2000; Tissot and Mechti, 1995). There was a marked increase in TRIM22 expression during partial T-cell activation in one study but the two studies on this subject have both reported a reduction in TRIM22 levels in fully activated cells (Gongora et al., 2000; Obad et al., 2007b). This was consistent with the observation of a negative correlation between TRIM22 levels and the levels of CD25, a T-cell activation marker. As further experiments revealed that TRIM22 did not suppress the activity of the CD25 promoter,

the observed changes in TRIM22 levels may have been a result of the activation process (Obad et al., 2007b). While these studies support a differentiation-regulatory role for TRIM22, it should also be noted that the observed differences in TRIM22 expression levels in cells of the haematopoietic lineage may be a result of other cellular processes such as cell activation, proliferation, and/or survival.

1.6 Subnuclear domains and their functions

The localization of TRIM proteins was discussed in **section 1.4.2**. Since TRIM proteins have been found in different cell compartments as multimers, Reymond et al. suggested that one of the "functions" of TRIM proteins may be to identify cell compartments (Reymond et al., 2001). Several TRIM proteins are localized as either nuclear speckles (TRIM8/GERP and TRIM39) or NB (TRIM19/PML, TRIM66/TIF1δ, and TRIM69/TRIF). They can also be localized in both the nucleus and the cytoplasm depending on the cell type (TRIM27/RFP, TRIM35/HLS5). TRIM protein localization within the nucleus can also change depending on the stimulus; PML NB disperse in virus infected cells and RFP is sequestered into NB in the presence of PML (Cao et al., 1998; Everett and Chelbi-Alix, 2007). To facilitate a better understanding of NB and as a prelude to the discussion of TRIM22's localization within the cell, the following sections will discuss the different non-membranous subnuclear domains/organelles that exist within the interchromatin space. Subnuclear domains/organelles include the nucleolus, which is by far the largest of these structures, as well as smaller organelles such as Cajal bodies (CBs), Speckles, Cleavage bodies, Gems, PML bodies, and paraspeckles (Fox et al., 2002; Matera, 1999) (**Figure 1.4**). Apart from the nucleolus, the two more common

structures are PML bodies and CBs. These are heterogeneous bodies of 0.2 - 1 μm that contain a range of other proteins. Studies with NB have found them to be dynamic structures that interact with other nuclear structures in a cell-cycle dependent manner (Li et al., 2006; Schul et al., 1999). These interactions presumably facilitate the trafficking/shuttling of proteins leading to an intricate co-ordination of nuclear processes.

1.6.1 Nucleolus

The nucleolus is the site of ribosomal DNA (rDNA) transcription into pre-rRNA, pre-ribosomal RNA (rRNA) processing and modification and pre-ribosome assembly. It is compartmentalized into three morphologically distinct regions. At the ultrastructural level, the innermost fibrillar center (FC) is composed of one or more pale structures containing RNA polymerase 1 (Thiry and Lafontaine, 2005). The FC is surrounded by a dense fibrous layer containing fibrillarin, termed the dense fibrillar component (DFC). These layers are embedded within a single large nucleophosmin/B23-rich region called the granular component (GC).

Although the primary site of rDNA transcription has not been established, the presence of RNA polymerase 1, DNA topoisomerase, transcriptionally competant rDNA, transcription factors and some nascent pre-rRNA in the FC suggests rDNA is transcribed in this region or at the interface with the DFC. The DFC contains nascent pre-rRNAs as well as fibrillarin, a key component of the RNA modification apparatus, implicating the DFC region in pre-rRNA modification.

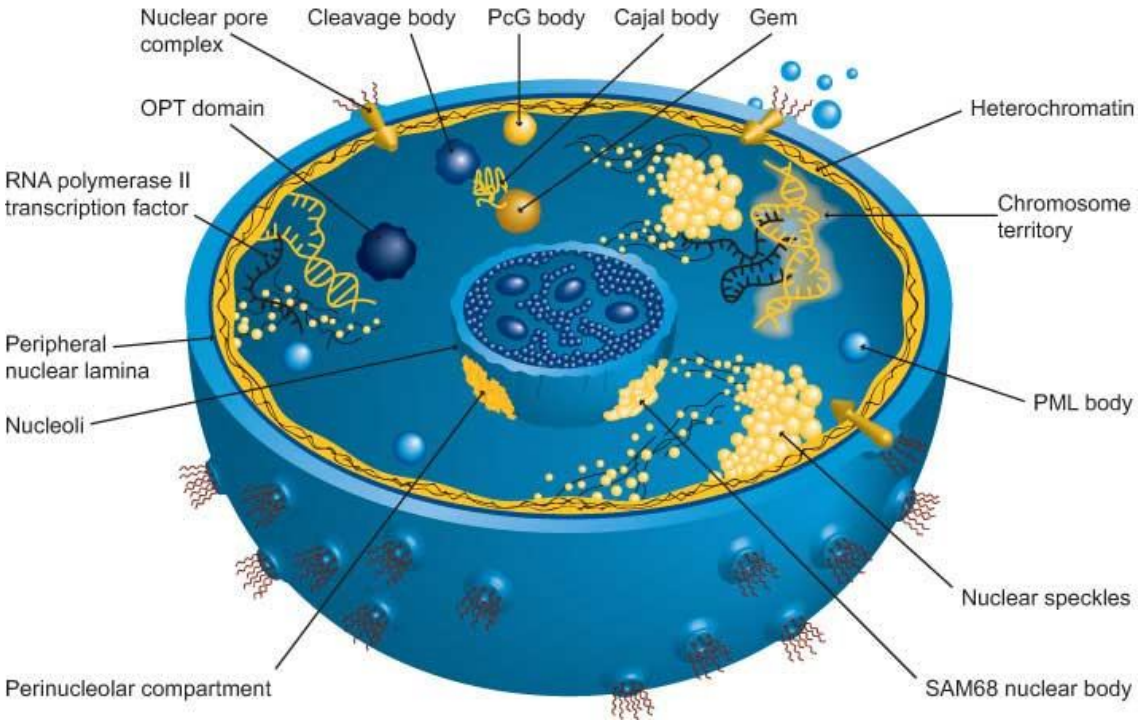

Figure 1.4 Subnuclear structures within the mammalian cell.
Image obtained from http://www.abcam.co.jp/ps/CMS/Images/Nuc_Domains-Claudie---johns.jpg

The GC accounts for a large mass of the nucleolus and contains pre-ribosomes at an advanced stage of maturation. The three-layer nucleolar structure may therefore reflect the maturation process of pre-ribosomes (Sirri et al., 2008; Thiry and Lafontaine, 2005). The role of B23 in ribosome biogenesis is not clear but there is some evidence that certain proteins, like the tumor suppressor ARF and C23/nucleolin, bind to B23 in order to enter and exit the nucleolus (Colombo et al., 2005; Enomoto et al., 2006; Li et al., 1996). The entry of ARF via B23 likely enables ARF to negatively regulate rRNA transcription within the nucleolus (Ayrault et al., 2006).

The functions of the nucleolus are likely to include those beyond a recognized central role in ribosome biogenesis. An analysis of the proteins identified in isolated HeLa nucleoli revealed that 5% of the proteins are involved in pre-mRNA processing, 3.5% in cell-cycle regulation, and 1% in DNA damage repair (Andersen et al., 2002; Scherl et al., 2002). Moreover, 30% of the identified nucleolar proteome consists of uncharacterized or novel proteins. The proteins found in the nucleolus may reflect a transient role for the nucleolus in processes that these proteins have been implicated in. Indeed, nucleolar proteins, regardless of their abundance within the nucleolus, appear to constantly exchange between the nucleoplasm and the nucleolus (Phair and Misteli, 2000). Another role for the nucleolus in the sequestration of proteins in order to modulate their activity within the nucleoplasm cannot be ruled out.

1.6.2 Cajal bodies

CBs (coiled bodies that were renamed in honor of their discoverer Ramón y Cajal) are 0.5 - 1 µm non-membranous NB that are capable of moving over large distances within the nucleus. Marked unambiguously by the presence of p80-coilin, CBs disassemble during mitosis, reassemble during the mid-G1 phase, are capable of fusing and separating, and are found next to nucleoli and within the nucleoplasm (Andrade et al., 1993; Platani et al., 2000). CBs are also enriched in at least 30 proteins belonging to several different classes, including ribonuclear proteins (RNP), nucleolar proteins, transcription factors and proteins involved in the regulation of the cell cycle (Cioce and Lamond, 2005). The localization of CB components within CBs is highly dependent on p80-coilin since deletion mutants of p80-coilin led to an aberrant localization of snRNPs and nucleolar antigens (Bohmann et al., 1995).

1.6.2.1 Role for CBs in biogenesis of snRNP

CBs are not static bodies serving merely as protein reservoirs. In fact, numerous CBs are dynamic and CB components are capable of exchanging rapidly with the surrounding nucleoplasm, nucleoli and with other NB (Dundr et al., 2004; Li et al., 2006). Several functions have been attributed to CBs, the most prominent of which is in the biogenesis of small nuclear and small nucleolar RNPs (snRNP and snoRNP respectively). snRNPs, when charged with modified small nuclear RNA (snRNA), are key components of the spliceosome, a structure that is involved in pre-mRNA splicing to form functional mRNA. snRNP biogenesis (the process of activating snRNP with snRNA) has both cytoplasmic and nuclear phases (Stanek and Neugebauer, 2006). At the start of the cycle,

snRNAs (U1, U2, U4, U5) are transcribed and processed by RNA polymerase II in the nucleoplasm before being exported to the cytoplasm. In the cytoplasm, snRNAs are surrounded by Sm protein rings and modified by the addition of the tri-methyl guanosine (TMG) cap at the 5' end before re-import back into the nucleus. Another snRNA, U6, is transcribed by RNA polymerase III and achieves a mono-methyl cap in the nucleoplasm. In the nucleus, U1, U2, U4 and U5 snRNAs translocate to CBs where specific nucleotides are modified (by methylation and pseudouridylation). In contrast, U6 snRNA is base-modified within the nucleolus before targeting to CBs. Within CBs, snRNAs are assembled with snRNPs to form mature U2, U4/U6, and U4/U6•U5 snRNPs, which then exit the CB and function as part of the spliceosome in splicing reactions.

There are several lines of evidence supporting the snRNP biogenesis pathway above. CBs are unlikely to be major sites of mRNA transcription despite containing RNA polymerase II subunits and nascent RNA polymerase II transcripts since they only label with tritiated Br-UTP after some time (Callan and Gall, 1991; Jordan et al., 1997; LaMorte et al., 1998). CBs also have a high concentration of the SMN, snRNP, Sm protein epitopes, and TMG (Dundr et al., 2004). Because snRNA bind to Sm proteins (whose assembly requires SMN) and TMG in the cytoplasm, the presence of these factors and absence of nascent snRNA within the CB indicates that CBs are more likely to contain mature snRNP (Matera, 1999). It has also been proposed that CBs may be involved in the regeneration of U4/U6 and U4/U6•U5 snRNP, which are destroyed during the splicing reaction. LSm and SART3 are proteins capable of re-annealing U4 and U6 snRNPs *in vitro* (Achsel et al., 1999; Bell et al., 2002). The presence of these factors in CBs, albeit

fleetingly, provides some evidence for the regenerative capability of CBs (Dundr et al., 2004).

1.6.2.2 Role for CBs in biogenesis of snoRNP

Like snRNP maturation, snoRNP maturation is also likely to take place in CBs. Fluorescently-tagged U3 and U8 snoRNA, which are involved in rRNA maturation, transiently localize in CBs before accumulating in nucleoli (Narayanan et al., 1999). Photobleaching microscopy also revealed that the dissociation kinetics of the snoRNP components fibrillarin and Nopp140 were comparable (Dundr et al., 2004). Fibrillarin is a likely methytransferase which associates with snoRNPs and is involved in rRNA modification while Nopp140 is a chaperone for the snoRNPs in their role in rRNA maturation. The similar dissociation times for these molecules implies that a mature U3 snoRNP is formed in CBs before it is targeted to the nucleolus (Dundr et al., 2004).

1.6.2.3 Role for CBs in transcriptional regulation from specific gene loci

CBs are also likely to be involved in the regulation of transcription from specific gene loci such as the snRNA gene loci and histone gene loci in interphase cells. The interactions between CBs, that can be surrounded by transcription foci, and these loci have been found to be significantly more frequent than would be expected if they randomly associated (Jordan et al., 1997). Frey et al. elegantly showed that CBs specifically associated with repetitive U2 snRNA-coding cDNA arrays only in the presence of nascent U snRNA transcripts and that the transcriptional status of the locus was a determinant of this association (Frey and Matera, 2001). Interestingly, in this study,

there was also some evidence for the participation of CBs in the early steps of snRNP and snoRNP biogenesis since PHAX, a protein involved in the export of snRNA and snoRNAs from the nucleus, localizes within CBs (Boulon et al., 2004; Frey and Matera, 2001).

One of the first few evidences for the role of CBs in the regulation of transcription from histone gene loci came from the finding that CBs contain U7 snRNP, a key component of the histone pre-mRNA 3' end processing machinery (Frey and Matera, 1995). CBs also associate transiently, but specifically, with the replication-dependent histone gene cluster (HIST2) in chromosome 1 and the pattern of association of CBs with HIST2 (an increase between mid-to-late G1 phase, high in S phase and basal levels in G2 phase) corresponds to changes in histone gene expression (Shopland et al., 2001). In addition, since sustained contact between motile CBs and HIST2 was not required for histone gene expression, CBs might signal to prolong histone gene expression while being available for transcription of other genes required in a metabolically active cell (Shopland et al., 2001). The link between CBs and histone biosynthesis, and perhaps other cell-proliferation related phenomena, may be NPAT, CDK2 and cyclin E. NPAT is a CDK2/cyclin-E binding protein that exists within CBs in a manner independent of its association with CDK2/cyclin-E (Cioce and Lamond, 2005; Zhao et al., 1998). CBs containing NPAT were found adjacent to histone gene clusters in chromosomes 6 (in both the G1 and S phases) and 1 (in S phase only) in human fibroblasts (Cioce and Lamond, 2005). The kinase activity of CDK2/cyclin E on NPAT appears to be important for histone gene expression since both a block in NPAT phosphorylation and its silencing led to reduced

histone biosynthesis (Cioce and Lamond, 2005; Su et al., 2004; Ye et al., 2003; Zhao et al., 2000).

1.6.2.4 Role for CBs in biogenesis of human telomerase

CBs may also be involved in the maturation of human telomerase RNA (hTR) and biogenesis of the telomerase RNP. hTR is used as a template by the telomerase reverse transcriptase (hTERT) (both are essential components of the human telomerase RNP) to synthesize telomeric DNA repeats at the ends of eukaryotic chromosomes. The continual synthesis of telomere regions in DNA by telomerase prevents telomeric attrition and enables the DNA to divide limitlessly. hTR have been shown to contain a short CB-specific localization motif also found in other small CB-specific guide RNAs (Jady et al., 2004). Fluorescence *in situ* hybridization experiments revealed that this motif was necessary for the accumulation of hTR within CBs, maximally during the S phase of the cell cycle when synthesis of telomeric DNA most likely occurs (Jady et al., 2004; Marcand et al., 2000). Evidence for the role of CBs in biogenesis of the telomerase RNP include the interaction of SMN, a key CB component, with telomerase RNP (Bachand et al., 2002) and the requirement for hTERT expression before hTR accumulates within CBs in cancer cells (Zhu et al., 2004). It is to be noted that the localization of hTR seems specific for cancer cells. Therefore, CBs may be acutely involved in inhibiting replicative senescence in these cells.

1.6.3 PML bodies

The functions of the TRIM protein PML in senescence, apoptosis and antiviral activity has been reviewed in the earlier sections. PML is a crucial constituent of PML bodies, which are also known as PML oncogenic domains (PODs), nuclear domain 10 (ND10), and Kr bodies. Typically, cells contain 1 – 30 PML bodies per nucleus depending on the cell type, phase of the cell cycle the cell is in and its differentiation stage. PML has seven major isoforms, all of which contain the RBCC tripartite motif but differ in their central or C-terminal regions due to alternative splicing (Bernardi and Pandolfi, 2007). All seven isoforms are capable of localizing in PML bodies together with other proteins like SUMO-1, p53, Sp100, Daxx, Sp140, CBP, BLM and pRb (Alcalay et al., 1998; Bloch et al., 1996; LaMorte et al., 1998; Muller et al., 1998; Zhong et al., 1999; Zhong et al., 2000a; Zhong et al., 2000c). In cells where the *PML* gene is disrupted, distinct NB are absent and the other components of PML bodies localize aberrantly (Ishov et al., 1999; Zhong et al., 2000a). However, PML is still normally localized in distinct NB when one of the other usual components of these bodies is absent (Ishov et al., 1999; Zhong et al., 1999). An exception may be SUMO-1, since it has been shown that SUMO-1 modification of the PML dimer is necessary for PML body formation (Muller and Dejean, 1999; Muller et al., 1998; Zhong et al., 2000a).

PML bodies are heterogeneous structures that have been implicated in various cellular processes. Many of the aforementioned PML body proteins reside only transiently within PML bodies. Some are transcription regulators (CBP, Sp1, PR, TIF1α and RXRα, p53, and pRb) that function with PML in transcriptional complexes/units (Boisvert et al.,

2001; Guiochon-Mantel et al., 1995; LaMorte et al., 1998; Yondola and Hearing, 2007). Like PML, they can localize in a diffuse manner within the nucleoplasm. As such, the actual function of the PML NB is still not clear.

Three different functions for the PML body have been proposed (Zhong et al., 2000b). The PML NB may serve as a depot to hold transcription factors and cofactors till they are required at sites of transcription. Some of these factors, such as p53, also acquire specific modifications within these bodies (Pearson et al., 2000). Additionally, the periphery of the PML body has also been shown to associate with newly synthesized RNA (Boisvert et al., 2000). This implies a role for the PML body in delineating regions of transcription within the nucleoplasm. The third proposed role for the PML NB is in the provision of a scaffold for the assembly of different protein complexes that may then go on to repress or activate transcription. The transactivation cofactor CBP is a dynamic component of PML bodies that forms complexes with a variety of transcription factors, including RARα/RXRα and p53 (Boisvert et al., 2001; Doucas et al., 1999; LaMorte et al., 1998). In the presence of retinoic acid, RARα/RXRα associates with CBP to activate transcription. Likewise, the tumor suppressor p53 forms a trimeric complex with PML and CBP (Pearson et al., 2000). The CBP-actylated-p53-PML complex was required for p53 to exert its apoptotic effect since fibroblasts lacking PML could not undergo apoptosis. Therefore, by associating with CBP and regulating its release from the PML body, the PML body can potentially modulate the activity of different CBP-containing transcription complexes (Doucas et al., 1999).

1.6.4 Gems

Nuclear foci containing the *survival motor neurons* (*SMN)* gene product SMN were originally called "gemini of coiled bodies" (or Gems) as they were found adjacent to CBs. However, these foci are completely coincident with CBs throughout interphase and maximally during the mid-S phase (Li et al., 2006). SMN is one component of a large protein complex containing SMN-interacting proteins (the SIP proteins) and Sm-core proteins (SmB, SmD1-3, SmE-G) (Gubitz et al., 2004). It plays an important role in the assembly of snRNPs in the cytoplasm, prior to their accumulation within CBs. Consistent with this, SMN is localized diffusely in the cytoplasm, where it associates with snRNPs (Massenet et al., 2002; Narayanan et al., 2004; Narayanan et al., 2002). The coincidence of gems with CBs may reflect a continued requirement of SMN during snRNP biogenesis, in the first instance during incorporation of snRNPs into CBs. Indeed, the interaction of SMN with p80-coilin was critical for the translocation of snRNP to CBs (Hebert et al., 2001). Mutations in or deletions of the *SMN1* gene result in the neurodegenerative disorder, spinal muscular atrophy (Lefebvre et al., 1995).

1.6.5 Cleavage bodies and DDX1 bodies

Cleavage bodies were identified as NB containing the cleavage stimulation factor CstF-64 and the cleavage and polyadenylation specificity factor (CPSF-100) (Schul et al., 1996). Cleavage bodies frequently associate with CBs in the nucleus and with bodies composed of the DEAD box protein DDX1, a putative RNA unwinding protein involved in RNA processing (Li et al., 2006; Schul et al., 1996). CBs, cleavage bodies and DDX1 bodies were maximally associated during the mid-S phase (Li et al., 2006). Interestingly,

unlike CBs, gems and DDX1 bodies, cleavage bodies formed long thin needlelike structures in cells treated with the actin polymerization inhibitor latrunculin B (Li et al., 2006). These needlelike structures were not associated with actin or laminins but colocalized with hyperphosphorylated RNA polymerase II (which is active during RNA elongation) and contained processed RNA. The significance of these associations and the function(s) of cleavage bodies are not clear. However, the lack of RNA and DNA in these bodies and the observation that they were not disrupted by transcriptional inhibitors, but were reduced in numbers by inhibitors of DNA replication, suggest a role for cleavage bodies as storage compartments for pre-assembled complexes important in DNA replication (Li et al., 2006). The close association of cleavage bodies with CBs at histone gene clusters, which are also maximally transcribed during the S phase, points to a role for cleavage bodies in the replication of histone genes (Schul et al., 1999).

1.6.6 Speckles / Interchromatin Granule Clusters

Speckles, or interchromatin granule clusters as they are sometimes referred to, are irregular punctuate subnuclear structures of variable size. Consistent with their proposed function as storage, assembly and/or modification compartments that can supply proteins to sites of transcription, speckles are enriched in pre-mRNA splicing factors and localize within the nucleoplasm and tend to be positioned around highly active transcription sites (Lamond and Spector, 2003). These factors, some of which contain a speckle-targeting signal, include snRNPs, spliceosome subunits, and other non-snRNP splicing factors involved in regulating the splicing machinery (such as kinases and phosphatases). Despite the presence of splicing factors, speckles are not considered to be splicing sites as active

genes localize at the periphery, rather than within, speckles. It is not clear if speckles contain nascent RNA, but if they do, then a direct role in pre-mRNA splicing reactions can be attributed to speckles (Lamond and Spector, 2003).

1.6.7 FLASH bodies

The FADD-like IL1β-converting enzyme-associated huge protein (FLASH) protein was initially discovered to be a component of the cytoplasmic death-inducing signaling complex that could interact with caspase 8 (Imai et al., 1999). Recently, other studies have found it to be a NB protein capable of colocalizing with both CBs and PML bodies (Barcaroli et al., 2006b; Milovic-Holm et al., 2007). The nuclear localization of FLASH was linked to the mitochondrial Fas effector response after the discovery that activation of the Fas/CD95 complex and caspase 8 resulted in the translocation of FLASH from NB to mitochondria (Milovic-Holm et al., 2007). The importance of FLASH NB in Fas-induced apoptosis was further established by showing that FLASH binds to caspase 8 (which is enriched in mitochondria). Fas-mediated apoptosis was also inhibited by down-regulating FLASH and by preventing its translocation from the nucleus into the cytoplasm (by using an inhibitor of the exporter Crm-1) (Milovic-Holm et al., 2007).

Although FLASH interacts with the well-established PML body component Sp100, not all PML bodies colocalized with FLASH bodies (Milovic-Holm et al., 2007). Similarly, while FLASH bodies were always colocalized with bodies formed by NPAT (a component of CBs), a small fraction of CBs failed to colocalize with FLASH bodies in the range of cells investigated (Barcaroli et al., 2006b). The formation of distinct NB by

FLASH also does not require either PML or p80-coilin since MEF lacking these proteins have FLASH bodies (Barcaroli et al., 2006b; Milovic-Holm et al., 2007). Despite the observation that some CBs failed to colocalize with FLASH, silencing FLASH expression resulted in aberrant distribution of CB components coincident with an S phase arrest (Barcaroli et al., 2006a; Barcaroli et al., 2006b). The S phase arrest is not surprising since FLASH is known to interact with histone gene promoter sequences and modulate histone gene transcription (Barcaroli et al., 2006a; Barcaroli et al., 2006b). FLASH may therefore provide a yet-unexplored but interesting link between CBs and PML bodies.

1.6.8 Others

There are numerous other subnuclear domains that have been described in interphase cells. These include the Oct1/PTF/transcription (OPT) domain, GATA-1 bodies, the Perinuclear compartment (PNC), polycomb-group proteins (PcG), hnRNP protein clusters, and heat-shock factor 1 (HSF1) foci (Matera, 1999). A notable characteristic of NB is their dynamism, the presence of common proteins within one or more of them and their ability to associate in a cell-cycle dependent manner with other NB or to specific nuclear regions.

1.7 Scope of study

Estrogen is a well-established breast mitogen and inhibitors of estrogen/ER action are effective as first-line therapies for breast cancer. In contrast, the role of progesterone in breast cancer is not clear and studies have reported its role in growth stimulation or inhibition depending on experimental conditions (Clarke and Sutherland, 1990; Groshong

et al., 1997; Lin et al., 1999; Musgrove et al., 1998; Skildum et al., 2005; Sumida et al., 2004; Sutherland et al., 1988). The generation of a breast cancer cell line expressing PR independently of ER (ABC28) has enabled a better understanding of progesterone's role without interference from estrogen/ER signaling pathways (Lin et al., 1999). Previous work in these cells has shown that progesterone regulates numerous genes, markedly inhibits cell growth and induces remarkable focal adhesions (Leo et al., 2005; Lin et al., 2000; Lin et al., 1999). TRIM22/STAF50, a relatively understudied TRIM protein implicated in growth inhibition, was identified to be one such progesterone-regulated target. Knowledge of TRIM22's cellular role(s) is likely to serve the broader aim of clarifying progesterone's role within breast cancer cells.

Hypothesis

TRIM22 exerts growth inhibitory effects in mammary epithelial cells and may mediate progesterone's growth-inhibitory effects in these cells.

Broad aim

To characterize the TRIM22 protein and to understand its role in the mammalian cell, particularly in mammary epithelial cells

Specific aims

1. To investigate the regulation of TRIM22 by progesterone and estrogen in breast cancer cells

2. To generate a polyclonal antibody specific for TRIM22 that will be initially required to confirm the regulation of TRIM22 at the protein level and which will be used to further understand the function of the protein
3. To investigate the contribution of the different domains to the localization of TRIM22
4. To identify the proteins that interact with TRIM22 in mammalian cells
5. To gain a better understanding of the function of TRIM22 and its downstream targets

CHAPTER 2

MATERIALS AND METHODS

2.1 Chemicals

Dextran, bovine serum albumin (BSA), human insulin, hydrocortisone, charcoal, propidium iodide, RNase A, pepstatin A, leupeptin, aprotinin, Tris base, ethylenediaminetetraacetic acid (EDTA), sodium vanadate, phenylmethylsulphonylfluoride (PMSF), β-mercapthoethanol, ethidium bromide, formaldehyde, diethylpyrocarbonate (DEPC), NaF, 4-(2-hydroxyethyl) piperazine-1-ethanesulfonic acid (HEPES), Tween 20, Urea, 17β-estradiol, progesterone, thymidine, L-arginine and L-cysteine were obtained from Sigma Chemical Co (St. Louis, MO, USA). NP-40 was purchased from USB Corp. (Cleveland, OH, USA). Proteinase K was purchased from Finnzymes (Espoo, Finland). Cholera toxin, triton-X-100, ethanol, isopropanol and methanol were from Merck KGaA (Darmstadt, Germany). Ultrapure agarose and phenol:chloroform:isoamyl-ethanol were obtained from Invitrogen Inc. (Carlsbad, CA, USA). Isopropyl-β-D-thiogalactopyranoside (IPTG) was obtained from Fermentas Inc. (Hanover, MD, USA). Redivue™ deoxycytidine 5'-[$^{\alpha\text{-}32}$P]-triphosphate (~3000 Ci/mmol) was obtained from Amersham Biosciences Inc. (Piscataway, NJ, USA). Epidermal growth factor (EGF) and IFNγ was purchased from ProSpec-Tany TechnoGene Ltd (Rehovot, Israel). IFNβ was obtained from Dr. Liu Ding Xiang (Nanyang Technological University, Singapore). Methotrexate was obtained from Dr. Alex Gong Xiandi (Nanyang Technological University, Singapore).

2.2 Cell lines

MCF7 cells, adherent mammary epithelial cells derived from the pleural effusion of a female human (Caucasian) with breast adenocarcinoma, were obtained from American

Type Culture Collection (Manassas, VA, USA) in 1995 at passage 147. T47D cells, adherent mammary epithelial cells derived from the pleural effusion of a female human with infiltrating ductal carcinoma (Keydar et al., 1979), were obtained from Dr. Suet Fueng Ching from the University of Cambridge (UK). Isolation and characterization of PR-transfected ABC28 cells have been described in detail previously (Lin et al., 1999). These cells were generated from a single MDA-MB-231 clone that was transfected with PR expression vectors hPR1 and hPR2, which contained the coding sequences for human PR-A and PR-B respectively, in the pSG5 plasmid (Kastner et al., 1990). ABC28 cells expressed ~660 fmol PR per mg protein as determined by enzyme immunoassay. Vector-transfected CTC15 cells expressed no PR and were used as a control cell line for studies using ABC28 cells (Lin et al., 1999). MDA-MB-231 cells are adherent mammary epithelial cells derived from the pleural effusion of female humans (Caucasian) with breast adenocarcinoma. COS-7 cells, adherent cells derived from the kidney of an African green monkey, and HeLa cells, adherent cervical epithelial cells derived from a human (Black) with cervical adenocarcinoma, were obtained from Dr. Koh Cheng Gee from Nanyang Technological University (Singapore). MCF10A cells, adherent mammary epithelial cells derived from a female human (Caucasian) with mammary fibrocystic disease, and MCF12A cells, spontaneously immortalized adherent luminal mammary epithelial cells derived from a female human (Caucasian), are ER-negative and PR-negative non-tumorigenic MEC lines (Kenny et al., 2007). MCF10A cells were obtained from Dr. Ann Lee from the National Cancer Centre (NCC; Singapore). MCF12A cells were obtained from Dr. Bay Boon Huat from the National University of Singapore.

2.3 Cell culture and treatments

Cells were routinely maintained in phenol-red containing Dulbecco's Modified Eagle Medium (DMEM) supplemented with 7.5% fetal calf serum (FCS), 2 mM L-glutamine and 40 μg/ml gentamycin. MCF12A cells were cultured in media also containing 2 μg/ml human insulin and 0.5 μg/ml hydrocortisone. MCF10A cells were cultured in MCF12A media also containing cholera toxin (0.1 μg/ml) and EGF (0.01 μg/ml). All hormone treatment experiments with cells were conducted using phenol red-free DMEM supplemented with 2 mM L-glutamine, 40 μg/ml gentamycin and 5% dextran-coated charcoal-treated FCS (DCC-FCS) (Test Medium). FCS was treated with dextran-coated charcoal to remove the endogenous steroid hormones that might interfere with and complicate the effects of progesterone and 17β-estradiol in this study. For all hormone treatment experiments, cells were grown in Test Medium for 48 hr before they were treated with 0.1 μM progesterone, 0.001 μM 17β-estradiol, or progesterone and 17β-estradiol from a 1000-fold stock in ethanol. This gave a final concentration of ethanol of 0.1%. Treatment controls received 0.1% ethanol only. HeLa and MCF7 cells were treated with either 250 IU/ml or 500 IU/ml of IFNβ or IFNγ for 24 or 48 hr in normal growth media.

To determine the effect of methotrexate on the distribution of endogenous TRIM22, MCF7 cells were grown on coverslips for 48 hr in normal growth media before treatment with 10 μM methotrexate in media containing 10% serum or just media for 48 hr. For the serum deprivation studies, MCF7 cells stably expressing TRIM22-EGFP (MCF7-TRIM22-EGFP) were plated in normal growth media before serum deprivation (0%

serum) or culture in 10% serum (10% serum control) for 72 hr. For the serum treatment studies, MCF7-TRIM22-EGFP cells were serum starved for 72 hr before being cultured in serum-free media (0% serum control) or in 10% serum-containing media (10% serum) for 24 hr.

All cell culture reagents were from Invitrogen Inc. FCS was from Hyclone (Logan, UT, USA) or Promocell GmbH (Heidelberg, Germany). All cell culture plastic-wares were purchased from Falcon (Becton Dickinson, San Jose, CA), NUNC (Nalge Nunc International, Rochester, NY, USA) or Corning (Corning Incorporated, NY, USA).

2.4 RNA extraction and analysis of purity and integrity

Total RNA was extracted using TRIzol reagent (Life Technologies, Inc., Gaithersburg, MD, USA). Briefly, cells were resuspended in TRIzol reagent and lysed by pipetting through a 1 ml eppendorf tip 20 times. RNA was double extracted into an aqueous phase using chloroform:isoamyl-ethanol (24:1) and phenol:chloroform:isoamyl-ethanol (50:24:1), then precipitated using isopropanol and washed with 70% ethanol in DEPC-treated sterile double-distilled water before resuspension in 0.2% DEPC-treated sterile double-distilled water. RNA was quantitated using a spectrophotometer (Beckman Coulter Inc., Fullerton, CA, USA) and purity determined by calculating the ratio of absorbances at 260 nm and 280 nm. An $Abs_{260\ nm}/Abs_{280\ nm}$ ratio greater than 1.8 was considered acceptable. To determine RNA integrity, 0.5 µg of total RNA was resolved on a 1% ethidium bromide-stained agarose gel and 28S to 18S band intensities compared.

RNA was deemed intact if the intensity of the 28S RNA species was at least as bright as or brighter than the intensity of the 18S RNA species.

2.5 PCR

2.5.1 cDNA synthesis

cDNA was synthesized from total RNA using random hexamers or oligo(dT) primers and SuperScript II ™ reverse transcriptase according to manufacturer's instructions (Invitrogen, Inc.). Briefly, 5 μg total RNA was incubated with 0.25 μg random primer in DEPC-treated sterile double-distilled water at 70ºC for 10 min. After the reaction was cooled on ice for 3 min, it was incubated with a mixture containing 5X first strand buffer, 0.01 mM dithiothreitol, and 0.4 mM dNTPs at 25 ºC for 10 min, then 42 ºC for 2 min before incubating with reverse transcriptase for 50 min. The reverse transcriptase was inactivated by heating at 72 ºC for 10 min.

2.5.2 Real-time PCR

Real-time PCR was performed using SYBR Green PCR reagents on an ABI Prism 7700 Sequence Detection System (Applied Biosystems Inc., Foster City, CA, USA) according to the manufacture's protocol. Primer sequences used in real-time PCR have been tabulated in **Table 2.1**. The lengths of PCR products ranged from 100 to 200 bp. PCR for each gene fragment was performed in triplicates and each primer set was repeated two to three times. To ensure PCR product specificity, melting curves were generated after amplification. The changes in fluorescence of the SYBR Green I dye in each cycle were monitored by ABI 7700 system, and the threshold cycle (Ct), which is defined as the

cycle number at which the amount of amplified target reaches a fixed threshold, was obtained for each gene. The relative amount of PCR products generated from each primer set was determined on the basis of the Ct value. The 36B4 transcript, coding for human acidic ribosomal phosphoprotein P0, was amplified as control to normalize the quantity of the cDNA sample used. The expression difference for each gene between ethanol (control) and hormone-treated samples was calculated by normalizing Ct values with 36B4 gene expression according to the formula: Relative expression = $2^{[[Ct(control)gene\ X - Ct(hormone)gene\ X] - [Ct(control)36B4 - Ct(hormone)36B4]]}$. The real-time PCR reagents and consumables were from Applied Biosystems, Inc.

2.5.3 Conventional PCR

Conventional PCR was used to amplify the 3' half of the TRIM22 transcript (using the TRIM22-3' primer set; **Table 2.1**) from ABC28, T47D, and HeLa cells. PCR products were resolved on 1% agarose gels before analysis by ethidium bromide incorporation. PCR reagents were from Fermentas, Inc.

2.6 Northern blotting analysis

15 µg of total RNA from ABC28 cells treated for 16 or 24 hr with 0.1% ethanol or 0.1 µM progesterone were resolved on a 1.5% formaldehyde-agarose gel. Gel-embedded RNA was checked for integrity by visualizing the 28S and 18S bands and then denatured by incubations in 1.5 M NaCl/0.5 M NaOH buffer followed by neutralizations in 1.5 M NaCl/0.5 M Tris-Cl (pH 7.0) buffer. RNA was transferred overnight onto optimized nylon membranes (Amersham Biosciences, Inc.) and covalently linked to the membrane

Table 2.1 Primers (5' → 3') used in the amplification of genes by PCR.

Gene	Primer sequences	Annealing temperature
TRIM22	Forward primer: GGATGCCAGCACGCTCATCTCAG	58°C
	Reverse primer: TTCAGCATCACGTCCACCCAGTAG	
TRIM22-3'	Forward primer: GAAGGTGAGGTGAATGTGCTG	58°C
	Reverse primer: CGGGGTACCTCAGGAGCTCGGTGGGCA	
TRIM22-North	Forward primer: ATGGATTTCTCAGTAAAGGTAG	60°C
	Reverse primer: TCACGAAGAGAAATATTGGCAGCC	
TRIM34	Forward primer: ACTCCAGGCAGTCCTCAAGA	58°C
	Reverse primer: TCCTCAGCCTCTGCAAACTT	
TRIM6	Forward primer: AGGGGTATGCAGCAATTCAC	58°C
	Reverse primer: CATGGAGAGAAGCAGGGAAG	
TRIM5	Forward primer: TGGCAGATTTTGAGCAACTG	58°C
	Reverse primer: TCCTTTTTATGACGCCATCC	
TRIM7	Forward primer: GTGGCACAGAAGCAGAATGA	60°C
	Reverse primer: AGAGACTGTGGTTGGCTTGG	
E2F7	Forward primer: GCTTGGACCCTGTTGCTCCT	60°C
	Reverse primer: CTGGCTTCAGGCTCTCCACA	
LSM14a	Forward primer: CCGTGGGAGTGACATTAAAGA	60°C
	Reverse primer: CTGACTGTATGTGGGCATCCT	
STEAP3	Forward primer: GGGAGTTCAGCTTCGTTCAG	60°C
	Reverse primer: TGGGAGGCAGGTAGAACTTG	
SARA2	Forward primer: TCTTGGATTGGATAATGCAGGAA	60°C
	Reverse primer: ACGTCATGCCAGCAATGG	
MAPK3	Forward primer: GCAGGACCTGATGGAGACTGAC	60°C
	Reverse primer: CCAGAATGCAGCCCACAGAC	
CSS2	Forward primer: GCTGAACTGGAACGCACGTA	60°C
	Reverse primer: CGGGATGGTGCTGGAATAC	
CLDN1	Forward primer: CCTATGACCCCAGTCAATGC	60°C
	Reverse primer: TCCCAGAAGGCAGAGAGAAG	
TMEM2	Forward primer: GCCTGTCGTCATGCTGGAGA	60°C
	Reverse primer: CCGCTGCAAATAGCCAAAGG	
ATF3	Forward primer: AAGAACGAGAAGCAGCATTTGAT	60°C
	Reverse primer: TTCTGAGCCCGGACAATACAC	
BNIP3L	Forward primer: GGACAGAGTAGTTCCAGAGGCAGTTC	60°C
	Reverse primer: GGTGTGCATTTCCACATCAAACAT	
ADAMTS8	Forward primer: TCCCCCCAAAAGTCAAATACAC	60°C
	Reverse primer: TGGATGATGTTGGTGGTTGCT	
RAFTLIN	Forward primer: ATGAAGGGCCCTGTCCAAGA	60°C
	Reverse primer: CAGGATTGGAGTGCCCAGTG	
36B4	Forward primer: GATTGGCTACCCAACTGTTGCA	58 – 60°C
	Reverse primer: CAGGGGCAGCAGCCACAAAGGC	

by UV. A TRIM22 single-stranded PCR product corresponding to 1 – 1056 bp of the coding sequence (obtained using the TRIM22-North primer set; **Table 2.1**) was labeled with dCTP-^{32}P by random priming reaction using the Redivue labeling kit (Amersham Biosciences, Inc.) and allowed to hybridize overnight to RNA at 42°C in pre-warmed ULTRAhyb buffer (Ambion, Inc., Austin, TX). The hybridized membrane was exposed to an X-ray film (Eastman Kodak Co., New Haven, CT) and developed using a phosphoimager (Molecular Imager FX, Biorad).

2.7 Chemical transformation of bacteria

5 – 10 µl of ligation reactions were transformed into Top10 chemically competent bacteria (Invitrogen, Inc.) by a standard protocol involving an initial incubation on ice for 30 min, heat-shock at 42ºC for 2 min before a further incubation on ice for 5 min. Transformed cells were allowed to recover in LB by shaking at 220 rpm at 37ºC for 1 hr before being spread on LB-ampicillin (LB-amp) (for pXJ-FLAG constructs) or LB-kanamycin (LB-kan) (for pEGFP-N1, pECFP-C1, pEYFP-C1, pET-24b+ constructs) agar plates. Plates were incubated at 37ºC overnight and plasmids in resistant colonies checked for inserts by restriction digestion and sequencing. Positive plasmids were extracted from cells using the HiSpeed Plasmid Midi/Maxi kits (Qiagen Inc, Valencia, CA, USA), and sterilized in 70% ethanol for use in mammalian cell transfection. Chemically competent BL21(DE3) cells used for the expression of TRIM22-$(His)_6$ from the pET-24b+ bacterial expression vector were a kind gift from Dr. Joe Yoon Ho Sup (Nanyang Technological University, Singapore).

2.8 Cloning of TRIM22 and mutants into expression vectors

The TRIM22 coding sequence and coding sequences of deletion and selected point mutants were amplified from RZPD clone TRIM22-pCMV-SPORT6 (IMAGE id: 5583800) using Pfu polymerase (Promega, Madison, USA) and specific primers (designed against the TRIM22 sequence in MGC clone 44863 (IMAGE consortium ID: 5583800) available under the NCBI entry BC035582; synthesized by 1st Base, Singapore). Primer sequences have been tabulated in **Table 2.2** and **Table 2.3**. Amplified sequences were gel-extracted and subsequently digested with relevant restriction enzymes before purification. Target vectors were digested with appropriate restriction enzymes and gel-extracted before treatment with calf-intestinal phosphatase to minimize vector self-ligation. Amplified sequences were ligated to target vectors using T4 ligase by incubation at 16ºC overnight.

The 1497 bp TRIM22 amplicon was cloned into pEGFP-N1, pEYFP-C1, pXJ-FLAG, and pET-24b+ vectors. The TRIM22 mutants were cloned into the pXJ-FLAG vector (obtained from Dr. Edward Manser, Institute of Molecular and Cellular Biology, Singapore). The accuracy of the TRIM22 coding sequence and mutant sequences was checked by sequencing of entire inserts and the regions flanking these inserts to ensure tags were in-frame (Research Biolabs, Singapore and 1st Base, Singapore). Restriction enzymes, T4 ligase, calf-intestinal phosphatase and buffers used in cloning were obtained from New England Biolabs, Inc (Beverly, MA, USA). Gel extraction and purification of vectors and inserts were performed using kits (Qiagen, Inc.).

2.9 Expression, purification and refolding of full-length TRIM22

2.9.1 Expression and extraction of TRIM22-$(His)_6$

TRIM22-$(His)_6$ in a BL21(DE3) host was amplified in 50 ml of LB-kan by overnight incubation at 37°C with shaking at 220 rpm. 20 ml of overnight culture was inoculated into 1 L of LB-kan till $Abs_{600\ nm}$ was 0.2 $\pm$ 0.05 and incubated at 37ºC with shaking. Once $Abs_{600\ nm}$ was 0.5 $\pm$ 0.05, IPTG was added to a final concentration of 1 mM and bacteria cultured for 4 – 6 hr at 30ºC with shaking to induce expression of TRIM22-$(His)_6$. Bacteria were pelleted by centrifugation (4500 rpm, 20 min, 4ºC) and resuspended in 50 ml Tris-phosphate buffer (100 mM NaH_2PO_4, 10 mM Tris-Cl, pH 8.0) before lysis by sonication (26% amplitude, 2 sec pulse, 1 sec pause) on ice till the cell suspension became noticeably less turbid. Insoluble inclusion bodies were extracted from lysed material by centrifugation (8000 g, 10 min, 4ºC) and then subjected to 8 M urea solubilization by incubating in lysis buffer (8 M urea, 100 mM NaH_2PO_4, 10 mM Tris-Cl, pH 8.0) at 30ºC for 30 min. Solubilized TRIM22-$(His)_6$ was extracted by retaining the supernatant after centrifugation (18,000 rpm, 20 min, 4ºC) (referred to as an inclusion body preparation).

2.9.2 Purification of TRIM22-$(His)_6$

Ni-NTA agarose beads (Qiagen, Inc.) were set in pre-cleaned columns and equilibrated with lysis buffer twice before an overnight incubation with rotation at 4ºC with the inclusion body preparation. Beads were subsequently washed thrice with 8 M urea wash buffer (same constitution as lysis buffer except pH 6.3) before elution of bound protein with 8 M urea elution buffer (same constitution as lysis buffer except pH 4.5).

Table 2.2 Primers (5' → 3') used in the amplification of TRIM22 and deletion mutants.

[a]PCR products were cloned into different vectors at the indicated restriction sites.

[b]Restriction sites have been highlighted in **bold lettering**. Start and termination codons (where present) have been underlined. The Kozak sequence (cacc), flanking sequences (added to facilitate restriction digestion), and nucleotides added to bring the coding sequence in-frame are indicated in small lettering.

[c]TRIM22 in pET-24b+ was generated for the expression of TRIM22-$(His)_6$ in bacterial cells. All other constructs were expressed in mammalian cells.

[d]TRIM22 in pEGFP-N1 was generated for the expression of TRIM22-EGFP for overexpression and localization studies.

[e]TRIM22 in pEYFP-C1 was generated for the expression of EYFP-TRIM22 for localization.

[f]TRIM22 in pXJ-FLAG was generated for the expression of FLAG-TRIM22 for localization and coimmunoprecipitation studies.

[g]TRIM22 in pcDNA3.1Hyg was generated for the expression of TRIM22 without a tag

[h]TRIM22-ΔNLS was generated by two sequential cloning procedures, the TRIM22 coding sequence to the left of its putative NLS was cloned using primer set 1 and the TRIM22 coding sequence to the right of its NLS was cloned using primer set 2.

Insert	Target vector	Restriction sites[a]	Primer sequences[b]
TRIM22[c]	pET-24b+	Nde1, Xho1	Forward primer: ggaattc**CATATG**GATTTCTCAGTAAAGGTAG
			Reverse primer: ccg**CTCGAG**GGAGCTCGGTGGGCACAC
TRIM22[d]	pEGFP-N1	Nhe1, Xho1	Forward primer: cta**GCTAGC**caccATGGATTTCTCAGTAAAGGTA
			Reverse primer: ccg**CTCGAG**GGAGCTCGGTGGGCACAC
TRIM22[e]	pEYFP-C1	Xho1, Kpn1	Forward primer: ccg**CTCGAG**aaATGGATTTCTCAGTAAAGGTAG
			Reverse primer: ccg**GGTACC**TCAGGAGCTCGGTGGGCA
TRIM22[f]	pXJ-FLAG	Xho1, Xho1	Forward primer: ccg**CTCGAG**ATGGATTTCTCAGTAAAGGTAG
			Reverse primer: att**CTCGAG**TCAGGAGCTCGGTGGGCA
TRIM22[g]	pcDNA3.1Hyg	Xho1, Xho1	Forward primer: ccg**CTCGAG**ATGGATTTCTCAGTAAAGGTAG
			Reverse primer: att**CTCGAG**TCAGGAGCTCGGTGGGCA
TRIM22-SPRYΔ4	pXJ-FLAG	Xho1, Kpn1	Forward primer: ccg**CTCGAG**ATGGATTTCTCAGTAAAGGTAG
			Reverse primer: cgg**GGTACC**TCAGCACACAGTCATGGGGAC
TRIM22-SPRYΔ5	pXJ-FLAG	Xho1, Xma1	Forward primer: ccgCTCGAGATGGATTTCTCAGTAAAGGTAG
			Reverse primer: ggg**CCCGGG**TCACACAGTCATGGGGACTAGGCAGTTC
TRIM22-SPRYΔ9	pXJ-FLAG	Xho1, Kpn1	Forward primer: ccgCTCGAGATGGATTTCTCAGTAAAGGTAG
			Reverse primer: cgg**GGTACC**TCAGACTAGGCAGTTCCAAGGATT

Insert	Target vector	Restriction sites[a]	Primer sequences[b]
TRIM22-SPRYΔ14	pXJ-FLAG	Xho1, Kpn1	Forward primer: ccg**CTCGAG**ATGGATTTCTCAGTAAAGGTAG
			Reverse primer: cgg**GGTACC**TCAAGGATTGAAATACGGATAAGC
TRIM22-SPRYΔ19	pXJ-FLAG	Xho1, Kpn1	Forward primer: ccg**CTCGAG**ATGGATTTCTCAGTAAAGGTAG
			Reverse primer: cgg**GGTACC**TCAATAAGCAGGTCGAGAAAAGC
TRIM22-SPRYΔ29	pXJ-FLAG	Xho1, Kpn1	Forward primer: ccg**CTCGAG**ATGGATTTCTCAGTAAAGGTAG
			Reverse primer: cgg**GGTACC**TCAGAACTTGTAGATGAGTGCTCC
TRIM22-ΔSPRY	pXJ-FLAG	Xho1, Xho1	Forward primer: ccg**CTCGAG**ATGGATTTCTCAGTAAAGGTAG
			Reverse primer: ccg**CTCGAG**TCACGAAGAGAAATATTGGCAGCC
TRIM22-ΔSPRY/CC	pXJ-FLAG	Xho1, Kpn1	Forward primer: ccg**CTCGAG**ATGGATTTCTCAGTAAAGGTAG
			Reverse primer: ccg**CTCGAG**TCATTCCTTGACCACCTCGTT
TRIM22-ΔSPRY/CC/B2	pXJ-FLAG	Xho1, Kpn1	Forward primer: ccg**CTCGAG**ATGGATTTCTCAGTAAAGGTAG
			Reverse primer: ccg**CTCGAG**TCACCCCTCCTGTGGGCTCAT
TRIM22-ΔRING	pXJ-FLAG	Xho1, Kpn1	Forward primer: ccg**CTCGAG**ATGCAGCCTGGGAACCTCCGA
			Reverse primer: ccg**GGTACC**TCAGGAGCTCGGTGGGCA
TRIM22-ΔRING/B2	pXJ-FLAG	Xho1, Kpn1	Forward primer: ccg**CTCGAG**AACGAGGTGGTCAAGGAATG
			Reverse primer: ccg**GGTACC**TCAGGAGCTCGGTGGGCA
TRIM22-ΔRING/B2/CC	pXJ-FLAG	Xho1, Kpn1	Forward primer: ccg**CTCGAG**TGGAAGAATTATATCCAGATCG
			Reverse primer: ccg**GGTACC**TCAGGAGCTCGGTGGGCA
TRIM22-ΔRING/B2/CC/182	pXJ-FLAG	Xho1, Kpn1	Forward primer: ccg**CTCGAG**GGGAAATATTACTGGGAAGTAG
			Reverse primer: ccg**GGTACC**TCAGGAGCTCGGTGGGCA
TRIM22-ΔNLS[h]	pXJ-FLAG	HindIII, Xho1	Forward primer 1: ccc**AAGCTT**ATGGATTTCTCAGTAAAGGTA
(primer set 1 for left of NLS,			Reverse primer 1: ccg**CTCGAG**CATGACGTCAATCACATCCTG
primer set 2 for right of NLS)		Not1, Kpn1	Forward primer 2: aaggaaaaaa**GCGGCCGC**aAGTGTATTCCGAGTACCAGAT
			Reverse primer 2: ccg**GGTACC**TCAGGAGCTCGGTGGGCA

Table 2.3 Primers (5' → 3') used in the generation of FLAG-TRIM22 point mutants.

[a]Restriction sites have been highlighted in **bold lettering**. Termination codons have been underlined. Flanking sequences (added to facilitate restriction digestion) are indicated in small lettering. Mutated residues have been highlighted in **bold lettering and underlines**.
[b]TRIM22-C494A, TRIM22-C494E, TRIM22-V493A, TRIM22-V493A,C494A PCR products were generated using the forward primer ccg**CTCGAG**ATGGATTTCTCAGTAAAGGTAG and indicated reverse primers.
[c]TRIM22-V493L was generated by site-directed mutagenesis of FLAG-TRIM22 using sense and anti-sense primers.

Insert	Target vector	Restriction sites	Primer sequences[a]
TRIM22-C494A[b]	pXJ-FLAG	Xho1, Kpn1	Reverse primer: gg**GGTACC**TCAGGAGCTCGGTGGG**GC**CACAGTCATGGGGACTAGGCA
TRIM22-C494E[b]	pXJ-FLAG	Xho1, XmaI	Reverse primer: ggg**CCCGGG**TCAGGAGCTCGGTGG**CTC**CACAGTCATGGGGACTAG
TRIM22-V493A[b]	pXJ-FLAG	Xho1, Xma1	Reverse primer: ggg**CCCGGG**TCAGGAGCTCGGTGGGCAC**G**CAGTCATGGGGACTAGGCA
TRIM22-V494L[c]	pXJ-FLAG	Site-directed mutagenesis	Sense primer: CCTAGTCCCCATGACT**T**TGTGCCCACCGAGCTCC Antisense primer: GGAGCTCGGTGGGCACA**A**AGTCATGGGGACTAGG
TRIM22-V493A,C494A[b]	pXJ-FLAG	Xho1, Kpn1	Reverse primer: gg**GGTACC**TCAGGAGCTCGGTGGG**GC**C**G**CAGTCATGGGGACTAGGCAGT

Aliquots of uninduced culture, IPTG-induced culture, soluble and insoluble fractions of lysed bacteria, inclusion body preparation, flow-through, wash and elution fractions were resolved on SDS-PAGE gels and stained with Coomassie Blue to visualize size, quantity, purity and integrity of the induced protein (if present) in the different fractions.

2.9.3 Refolding of TRIM22-$(His)_6$

To shift the TRIM22-$(His)_6$ from a 8 M urea buffer into a reduced-urea buffer, a pulse-refolding protocol modified from that used by Hopfner et al. was employed (Hopfner et al., 1997). Purified TRIM22-$(His)_6$ was concentrated using a 10,000 MWCO Amicon® Ultra column (Millipore Corporation, Bedford, MA, USA). A protocol 200 µl of purified protein (6000 µg/ml) was added in 50 µl pulses to 20 ml cold refolding buffer (50 mM Tris-Cl, 20 mM $CaCl_2$, 5 mM EDTA, 0.5 M L-arginine, 0.5 mM L-cysteine, pH 7.5) and allowed to incubate with constant mixing (40 hr, 4ºC). To remove any precipitates that may have formed, buffer containing refolded protein was centrifuged (15,000 rpm, 30 min, 4ºC). Supernatant was then column-concentrated to yield refolded TRIM22-$(His)_6$ at a concentration of 1000 µg/ml.

2.10 Immunization of Balb/c mice and serum collection

Refolded TRIM22-$(His)_6$ was used as immunogen and injected into male BALB/C inbred mice. Mice were about seven weeks old at the time of first injection. 50 µg immunogen was prepared with Freund's Complete Adjuvant (Pierce Biotechnology, Inc.) at 1:1 ratio for the initial injection and with Freund's Incomplete Adjuvant (Pierce Biotechnology, Inc.) at 1:1 ratio for the subsequent booster injections. Mice were injected

intraperitoneally with 100 µl of immunogen/adjuvant mixture. Blood was withdrawn from the tail vein of mice (~100 µl) after administration of anesthesia (0.01% ketamine/0.001% xylazine in sterile water). Primary immunization was administered on Day 0 and boosters administered every 2 weeks. Sera were collected 10 days post-injection and tested by Western blotting for reactivity against immunogen and a progesterone-regulated band at 50 – 60 kDa. Together with the initial injection, each animal was boosted four times at 14-day intervals. 10 days after the final booster was administered, mice were subjected to cardiac puncture under anesthesia and bled dry. Mice were handled following the guidelines on the Care and Use of Animals for Scientific Purposes (2004) set by National Advisory Committee for Laboratory Animal Research (NACLAR) in Singapore.

2.11 Immunoblotting

2.11.1 Cell lysate preparation and protein quantitation

Cells were lysed with cold lysis buffer (50 mM HEPES, 150 mM NaCl, 1% triton X-100, 5 µg/ml pepstatin A, 5 µg/ml leupeptin, 2 µg/ml aprotinin, 1 mM PMSF, 100 mM sodium fluoride and 1 mM sodium vanadate, pH 7.5), and passed through a ½ cc syringe 15 times to facilitate extraction of all proteins. Lysate was cleared by centrifugation (10,700 rpm, 12 min, 4ºC) and protein quantitated using the BCA protein assay kit (Pierce Biotechnology, Inc., Rockford, IL, USA).

2.11.2 Western blotting analysis

10 - 40 μg of lysates were resolved by SDS-PAGE and transferred to nitrocellulose membranes using a wet-transfer system (Biorad-Laboratories, Inc, Hercules, CA, USA). Membranes were incubated with specific primary antibodies in 5% skimmed milk and then with corresponding HRP-conjugated secondary antibodies before detection with ECL reagent (Amersham Biosciences, Inc.). X-ray films (Eastman Kodak Co.) were used to capture luminescence.

The primary antibodies used for Western blotting were:

1. Mouse anti-His (27-4710-01): from Amersham Biosciences, Inc
2. Mouse anti-TRIM22 (this study)
3. Mouse anti-GAPDH (clone 6C5, 4300): from Ambion Biosciences, Inc.
4. Mouse anti-FLAG (F 1804): from Sigma-Aldrich, Inc (St. Louis, USA).
5. Rabbit anti-GFP (G 1544): from Sigma-Aldrich, Inc.
6. Mouse anti-B23 (clone FC82291, B 0556): from Sigma-Aldrich, Inc.
7. Rabbit anti-ATF3 (clone C-19, sc-188): from Santa Cruz Biotechnology, Inc.
8. Rabbit anti-Claudin-1 (clone JAY.8, 51-9000): from Zymed Laboratories, Inc (South San Francisco, CA, USA).

The secondary antibodies used for Western blotting were:

9. Anti-mouse-IgG-HRP (NA931V): from Amersham Biosciences, Inc.
10. Anti-rabbit-IgG-HRP (AP132P): from Chemicon International, Inc (Millipore Corporation).

2.12 Transfection into mammalian cell lines

2.12.1 siRNA transfection

Pre-designed control and TRIM22 siRNA (obtained from Ambion, Inc) were transfected into MCF12A, ABC28, and HeLa cells using Lipofectamine 2000 reagent (Invitrogen, Inc.) according to manufacturer's instructions. siRNA sequences have been tabulated in **Table 2.4**. ABC28 cells were plated in phenol red-free DMEM supplemented with 5% DCC-FCS and incubated at 37ºC for 48 hr prior to transfection. MCF12A and HeLa cells were plated in normal growth media supplemented with 7.5% FCS and incubated at 37ºC for 24 hr prior to transfection. For each well of a 6-well plate, 6 µl Lipofectamine 2000 reagent and 10 - 80 nM siRNA were added into a final 2 ml transfection medium volume and incubated for 8 hr before either a media change (MCF12A) or treatment with ethanol, progesterone or IFNγ, where relevant. Cells were harvested 24 - 72 hr after treatment.

2.12.2 Plasmid transfection

For localization and size determination of exogenous full-length TRIM22 and deletion mutants, cells were transiently transfected with sterilized constructs for 24 to 48 hr using Fugene 6 (Roche Diagnostics, Indianapolis, IN, USA) at a plasmid:reagent ratio of 1:3. For generation of MCF7 cells and HeLa cells stably expressing TRIM22-EGFP, cells were transfected with Lipofectamine reagent (Invitrogen, Inc.) and selected in 500 µg/ml (MCF7) or 400 µg/ml (HeLa) Geneticin (G418; Invitrogen, Inc.) containing complete DMEM 48 hr later. Clones exhibiting least morphological variability from parental cells were sorted by FACSorter (BD Biosciences, San Jose, CA, USA) to obtain cell populations enriched with TRIM22-EGFP expressing cells.

Table 2.4 Annealed sense and antisense siRNA sequences (5' → 3') used in silencing experiments.

[a]21-base long siRNA sequences were obtained from Ambion, Inc. Overhangs (small lettering) at the 3' ends were included during synthesis to facilitate silencing.

Name	Sequence[a]	siRNA ID	Position in TRIM22 mRNA sequence
TRIM22 siRNA 5	Sense: GGUCACCAAACAUUCCGCAtt Antisense: UGCGGAAUGUUUGGUGACCtt	107935	379 – 397 bp
TRIM22 siRNA 6	Sense: GGGUUCAAUGAAAUGAGAGtt Antisense: CUCUCAUUUCAUUGAACCCtt	107936	556 – 574 bp
TRIM22 siRNA 7	Sense: GGAAGGCACGAUUUCACUCtt Antisense: GAGUGAAAUCGUGCCUUCCtc	107937	2015 – 2033 bp

2.13 Immunofluorescence

Cells were fixed with 3.7% formaldehyde for 10 min and permeabilized with 0.2% triton-X-100 for 10 min. After washing with PBS, cells were blocked with 2% FCS/PBS for 1 hr, and incubated with primary antibodies in 2% FCS/PBS for 2 hr at 37ºC or overnight at 4ºC. Cells were subsequently incubated with secondary antibodies and 4',6-diamidino-2-phenylindole (DAPI) (0.1 µg/ml) (Invitrogen, Inc.) in 2% FCS/PBS for 2 hr at 37ºC before mounting on glass slides using anti-fade fluorescence mounting media (Invitrogen, Inc.).

The primary antibodies used for immunofluorescence were:

1. Mouse anti-TRIM22 (this study)
2. Rabbit anti-fibrillarin (H-140, sc-25397): from Santa Cruz Biotechnology, Inc. (Santa Cruz, CA, USA)
3. Mouse anti-p80-coilin (clone pδ, C 1862): from Sigma-Aldrich, Inc (St. Louis, USA).
4. Rabbit anti-p80-coilin (clone 204/10): from Dundee Cell Products (Dundee, Scotland, UK)
5. Mouse anti-FLAG (F 1804): from Sigma-Aldrich, Inc.
6. Rabbit anti-FLAG (F 7425) from Sigma-Aldrich, Inc.
7. Mouse anti-B23 (clone FC82291, B 0556): from Sigma-Aldrich, Inc.

The secondary antibodies used for immunofluorescence were:

8. Alexa Fluor 633 nm anti-mouse IgG (H+L) (A21050): from Invitrogen Molecular Probes (Carlsbad, CA, USA).

9. Alexa Fluor 488 nm anti-rabbit IgG (H+L) (A11034): from Invitrogen Molecular Probes.

2.14 Image acquisition and manipulation

2.14.1 Fluorescence microscopy

DAPI staining of nuclei, staining of TRIM22, fibrillarin, B23, p80-coilin and FLAG-tagged proteins were visualized by fluorescence microscopy using appropriate band-pass filters. All fluorescence images were acquired with an Olympus Manual Reflected Fluorescence System attached to an Olympus DP30BW Digital Camera (Olympus Singapore Pte Ltd, Singapore). Imaging was performed at RT using a 60X UPlanSApo oil objective (Olympus). Images were acquired as black and white TIFF files using DP Controller and color added using DP Manager (Olympus). Live cell imaging was performed by Dr. Stephen Ogg at the Institute of Medical Biology (Singapore).

2.14.2 Confocal microscopy

Laser scanning confocal microscopy was used for Z-stack analysis of the colocalization of endogenous p80-coilin with TRIM22-EGFP in MCF7 cells. Analysis was performed on a LSM6 Meta confocal microscope (Carl Ziess, Oberkochen, Germany) equipped with a digital imaging system.

2.15 Site-directed mutagenesis

FLAG-TRIM22's valine (V) at position 493 was mutated to a leucine (L) residue by site-directed mutagenesis using the Stratagene site-directed mutagenesis kit (Stratagene, La

Jolla, CA, USA) (**Table 2.3**). 10 ng of FLAG-TRIM22 was used as a template in a PCR with HPLC-purified sense and anti-sense primers, fresh dNTPs, reaction buffer and Pfu *Turbo* polymerase using the following cycling conditions: Initial denaturation at 95ºC for 2 min, 10 cycles of 95ºC for 50 sec, 70ºC for 50 sec, 68ºC for 5 min 46 sec followed by a further 10 cycles of 95ºC for 50 sec, 70ºC for 50 sec, 68ºC for 7 min 12 sec to amplify the plasmid incorporating the desired mutation. Methylated parental template DNA was digested for 1 hr at 37ºC by Dpn1 (10 units/µl) and 4 µl of resultant product transformed into Top10 bacteria. Transformed bacteria were spread on LB-amp plates and colonies screened to identify clones carrying the mutated plasmid.

2.16 Cell synchronization

HeLa cells stably expressing TRIM22-EGFP (HeLa-TRIM22-EGFP) were grown in 12-well dishes (flow cytometry), on glass coverslips (immunofluorescence) and in 60 mm dishes (Western blotting) in normal growth media. 24 hr later, cells were synchronized using the double thymidine block method modified from Pederson and Robbins and Li et al. (Li et al., 2006; Pederson and Robbins, 1971). Briefly, cells were exposed to 2.5 mM thymidine for 16 hr, then washed twice with sterile DPBS to remove thymidine and replenished with normal growth media for 12 hr. After this, thymidine was added for an additional 16 hr. Cells were harvested at 0 (immediately following removal of the second thymidine treatment), 3, 5, 8, and 14 hr for parallel flow cytometry, immunofluorescence and Western blotting analysis.

2.17 Flow cytometry

To determine the percentage of cells in each stage of the cell cycle, cells were stained with propidium iodide (Vindelov's cocktail containing 10 mM Tris-Cl, pH 8.8, 10 mM NaCl, 50 µg/ml propidium iodide, 10 µg/ml RNase A, 0.1% NP-40) and analyzed by flow cytometry (FACSCalibur using Cell Quest version, BD Biosciences) after gating to remove cell debris and aggregates.

2.18 Coimmunoprecipitation

To investigate the interaction of FLAG-tagged TRIM22 and its mutants with p80-coilin-EGFP and B23, MCF7 cells were plated in 10 cm dishes at a density of 5 x 10^5 cells. 24 hr later, cells were transfected with 5 µg p80-coilin-EGFP (a kind gift from Dr. Joseph Gall) and 3 µg pXJ-FLAG constructs using Fugene 6 at a plasmid: reagent ratio of 1:2 in antibiotic-free DMEM. 40 hr post-transfection, proteins were extracted as described above in **section 2.11.1**. 240 µg of lysates were incubated with 30 µl of anti-FLAG M2 affinity beads (A 2220) overnight with rotation, after which beads were pelleted by centrifugation (7,300 rpm, 1 min, 4ºC) and washed thrice with cold TBS buffer (150 mM NaCl, 50 mM Tris-HCl, pH 7.4). Beads were resuspended in an equal volume of 2X sample buffer, and boiled for 8 min before SDS-PAGE and Western blotting as described earlier in **section 2.11.2**.

2.19 Microarray expression analysis and verification

2.19.1 Sample preparation, hybridization, and scanning

Sample preparation

Microarray expression analysis was conducted in two sets each of ABC28 and HeLa cells. Each set consisted of samples transfected with control siRNA, TRIM22 siRNAs 6 or 7 for 8 hr prior to treatment. ABC28 cells were treated with progesterone (10 nM) and HeLa cells were treated with IFNγ (250 IU/ml). 48 hr later, RNA was extracted using TRIzol reagent as described in **Section 2.4** and subsequently purified using the RNeasy kit (Qiagen, Inc.). RNA purity ($Abs_{260\ nm}/Abs_{280\ nm}$) and quantity were determined rapidly and accurately using the Nano-Drop 1000A Spectrophotometer (NanoDrop Technologies, Wilmington, DE, USA). 0.5 µg of RNA was resolved on a 1% TBE-agarose gel to determine its integrity. 0.5 ug of intact RNA was amplified using the Illumina® TotalPrep RNA Amplification Kit according to manufacturer's instructions (Illumina, Inc., San Diego, CA, USA). Briefly, mRNA within total RNA was reverse transcribed with oligo(dT) primers bearing a T7 promoter using the reverse transcriptase Array-Script™. Array-Script™ is engineered to produce higher yields of virtually full-length cDNA compared to wild type enzymes, ensuring the production of reproducible microarray samples. The cDNA was subjected to second strand synthesis and purification to become a template for *in vitro* transcription with T7 RNA Polymerase. To maximize cRNA yield, Ambion's proprietary MEGAscript® *in vitro* transcription (IVT) technology along with biotin UTP (provided in the kit) was used to generate hundreds to thousands of biotinylated, antisense RNA copies of each mRNA (referred to as cRNA).

Hybridization and scanning

0.75 µg of biotinylated purified cRNA from each sample was hybridized with an array (containing around 22,000 transcript probes) in the Illumina Sentrix® BeadChip HumanRef-8 arrays (Illumina, Inc.) for 16 hr at 58ºC. Arrays were washed and subsequently incubated with buffer containing Streptavidine-Cy3 for 10 min at room temperature. Arrays were washed to remove excess Streptavidine-Cy3 before spin-drying and scanning using the Illumina® BeadArray Reader (Illumina, Inc.).

2.19.2 Data analysis

Data obtained from the Array Reader were analyzed using GeneSpring GX Software (Agilent Technologies, Inc.). Signal intensities between 50 and 21553 units were considered true signals. Signal intensities of genes were compared between control siRNA-transfected samples and TRIM22 siRNA 6- or 7- transfected samples.

2.19.3 Verification of microarray results

Real-time PCR

The RNA samples used for cRNA synthesis and microarray analysis were also subjected to reverse transcription and analyzed by real-time PCR as highlighted in **section 2.5**. The genes that were identified to be differentially regulated by at least 2 fold were analyzed in triplicate in both sets of samples using specific primers (**Table 2.1**). For every run, 36B4 levels were also analyzed to ensure amount of template in each sample within a set were similar.

Western blotting analysis

To confirm the regulation of selected genes at the protein level, lysates were collected at the 48 hr time-point. In addition to the samples collected for analysis of transcript expression (that is, treated control siRNA, TRIM22 siRNA 6 or TRIM22 siRNA 7 transfected samples), *untreated* control siRNA transfected cells were also collected to investigate the effect of progesterone and IFNγ treatment on the expression of these proteins in ABC28 and HeLa cells, respectively. The levels of TRIM22 were investigated as a positive control and the levels of GAPDH investigated as a loading control.

2.20 Statistical analysis

All quantitative data are expressed as mean. Comparisons were made by the Student's *t*-test (two-tailed, equal variance) and $P<0.05$ is considered significant.

CHAPTER 3

RESULTS

3.1 Hormonal regulation of TRIM22 transcript levels in breast cancer cells

3.1.1 Progesterone increases TRIM22 transcript levels rapidly and dramatically

Microarray analyses of progesterone-treated ABC28 cells revealed that progesterone treatment enhances TRIM22 transcript levels rapidly. Real-time PCR was performed using primers specific for TRIM22 and the housekeeper 36B4 to confirm the result obtained from the microarray analysis (**Table 2.1**; melting curves for TRIM22 and 36B4 shown in **Appendices Figure A1**). A time-dependent analysis revealed that the TRIM22 transcript was up-regulated as early as 3 hr by 6.5-fold in ABC28 cells but not in the vector-transfected control cells CTC15. At the 24-hr time point, TRIM22 transcript levels were increased by more than 25-fold (**Figure 3.1A**).

3.1.2 The extent of progesterone-induced up-regulation differs in ER-positive breast cancer cell lines

In MECs that have both the ER and PR, PR expression can be under the control of ER activity (MCF7 cells) or independent of ER activity (T47D cells) (Read et al., 1988; Wei et al., 1988). In progesterone-treated T47D cells, TRIM22 transcript levels were increased by more than 15-fold in three independent experiments (**Figure 3.1B**). In the MCF7 cell line, treatment with progesterone alone did not have an effect on TRIM22 transcript levels (**Figure 3.1C**). This is expected since it has been shown previously that, in the absence of estrogen, PR levels are low in MCF7 cells (Read et al., 1988). Together with the observation that progesterone could not increase TRIM22 levels in vector-transfected control CTC15 cells, this suggests TRIM22 is downstream of progesterone acting via the PR.

3.1.3 The TRIM22 transcript induced by progesterone and IFNγ contains the 3' end required for the expression of a 498 aa protein

The TRIM22 mRNA reported in earlier publications codes for a 442 aa TRIM22 protein. The more recent entries (NM_006074.3), including the cDNA clones provided by the Mammalian Gene Collection program (BC035582, BC022281), describe a sequence coding for a 498 aa TRIM22 protein. This longer coding sequence of 1497 bp has an additional 168 bp that the shorter variant lacks at its 3' end (**Table 3.1**). In order to test if this 168 bp sequence was present in the progesterone- and IFNγ-treated cells, RNA extracted from these cells was reverse-transcribed using oligo(dT) primers (T47D cells) or random hexamers (ABC28 and HeLa cells). Specific primers (TRIM22-3' primer set in **Table 2.1**) designed to amplify the 3' half of the TRIM22 mRNA including the 168 bp sequence yielded a 879 bp fragment from ABC28 and T47D cells treated with progesterone and HeLa cells treated with IFNγ that was undetectable in the ethanol-treated (control for progesterone) or untreated (control for IFNγ) samples (**Figure 3.1D, E**). Sequencing results confirmed that the PCR products belonged to TRIM22 but not to other paralogous TRIMs such as TRIM34 and TRIM6 that have high sequence similarity to TRIM22.

Further to this, a Northern blotting analysis was performed to investigate how many transcripts were present in ABC28 cells in the absence and presence of progesterone. A single-stranded TRIM22 sequence obtained after amplification using specific TRIM22 primers (TRIM22-North primer set in **Table 2.1**) was labeled with ^{32}P and used as a probe for this analysis. Only one transcript was up-regulated by progesterone in ABC28

cells (**Figure 3.1F**). A specific transcript in progesterone-treated T47D cells could not be detected by Northern blotting, likely due to the lower levels of the TRIM22 transcript in these cells. Nevertheless, from these results, it is clear that progesterone and IFNγ up-regulated the expression of TRIM22 mRNA that codes for a 498 aa protein.

3.1.4 17β-estradiol inhibits TRIM22 expression in breast cancer cells

The effect of 17β-estradiol on TRIM22 transcript expression was also investigated. In T47D cells, TRIM22 transcript levels were *reduced* by at least 2-fold upon 17β-estradiol treatment in all three experiments (**Figure 3.1B)**. In addition, in two out of the three experiments (experiments 2 and 3), 17β-estradiol was able to partially reverse the increase in TRIM22 expression induced by progesterone since cells treated with both hormones showed only a 5-fold up-regulation of TRIM22 transcript compared to the greater-than-15 fold up-regulation of TRIM22 observed in the presence of only progesterone (**Figure 3.1B**). However, as will be shown later, we found that 17β-estradiol does not modulate the level of the TRIM22 protein. In MCF7 cells, however, 17β-estradiol did not consistently reduce TRIM22 levels (**Figure 3.1C**).

These results suggest progesterone and 17β-estradiol can have different regulatory effects in breast cancer cells. The presence of ER may also modulate the effect of progesterone on TRIM22 levels as 24-hr progesterone treatment induced TRIM22 expression by approximately 25-fold in ER-negative ABC28 cells (**Figure 3.1A**) but could only up-regulate TRIM22 expression in ER-positive T47D cells by at most 20-fold (**Figure 3.1B**).

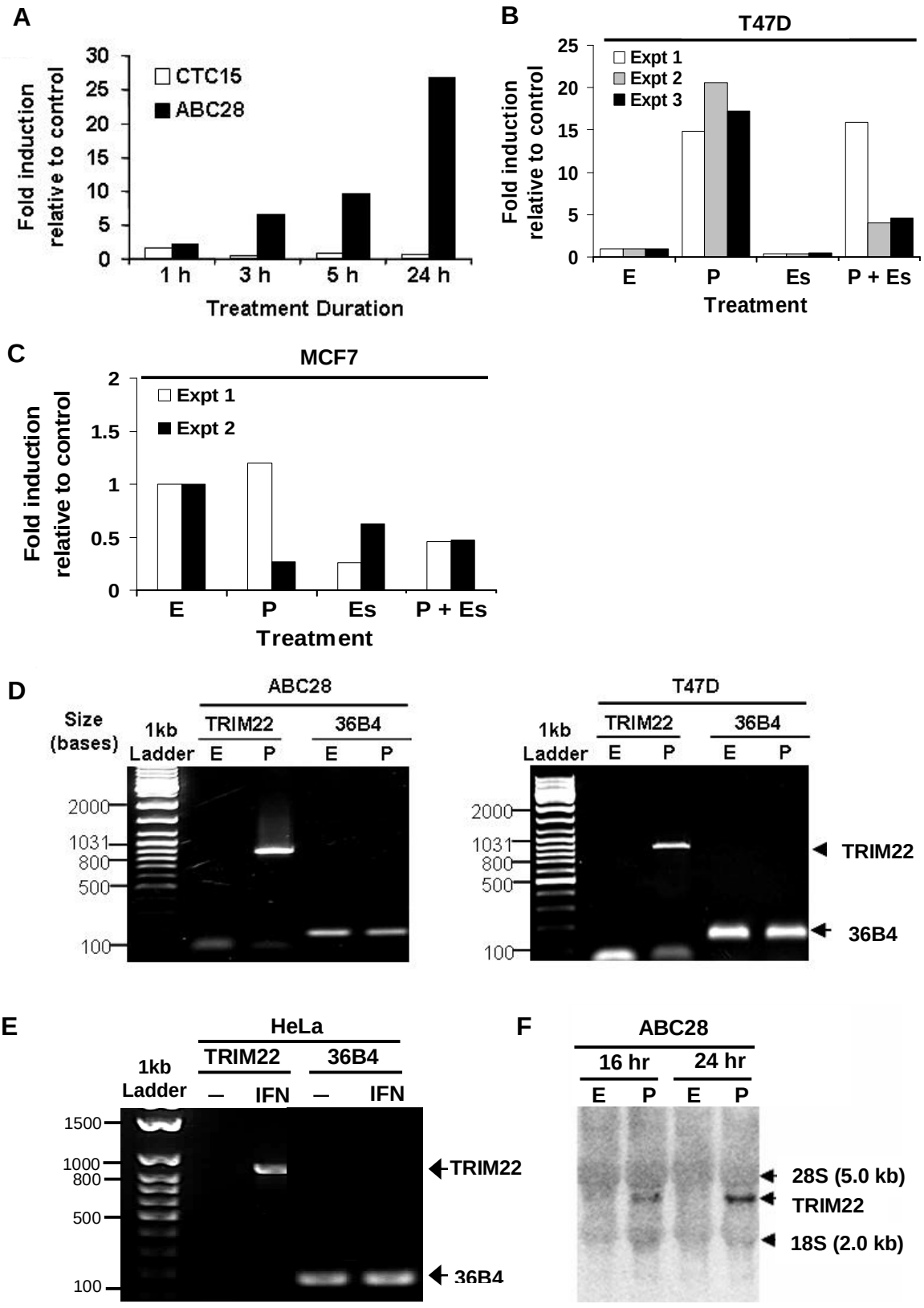
A
Fold induction relative to control
CTC15
ABC28
1 h
3 h
5 h
24 h
Treatment Duration
B
T47D
Expt 1
Expt 2
Expt 3
E
P
Es
P + Es
Treatment
C
MCF7
Expt 1
Expt 2
D
ABC28
T47D
Size (bases)
1kb Ladder
TRIM22
36B4
TRIM22
36B4
E
HeLa
IFN
F
ABC28
16 hr
24 hr
28S (5.0 kb)
18S (2.0 kb)

Figure 3.1 The TRIM22 transcript is up-regulated by progesterone and IFNγ.
(A) Progesterone up-regulated TRIM22 expression in ABC28 breast cancer cells. TRIM22 transcript expression levels were analyzed in CTC15 and ABC28 cells treated with ethanol or progesterone for 1, 3, 5, and 24 hr. **(B)** Progesterone up-regulated TRIM22 expression in breast cancer cells T47D. TRIM22 transcript expression levels were analyzed in T47D cells treated for 24 hr with ethanol (E), progesterone (P), 17β-estradiol (Es) or both hormones (P+Es). Results from three independent experiments (expt) are presented. **(C)** Progesterone did not alter TRIM22 expression in MCF7 breast cancer cells. TRIM22 transcript expression levels were analyzed in MCF7 cells treated for 24 hr with ethanol (E), progesterone (P), 17β-estradiol (Es) or both hormones (P+Es). Results from two independent experiments are presented. **(A - C)** Results are presented as fold changes after hormone treatment relative to ethanol-treated controls which was set at 1. **(D)** Progesterone-regulated TRIM22 mRNA contains the 3' coding sequence for the 498 aa TRIM22 protein. Total RNA from ABC28 and T47D cells treated with ethanol (E) or progesterone (P) was reverse-transcribed. Resulting cDNA was used as template to amplify the 3' half of the TRIM22 coding sequence and the housekeeping gene 36B4. The progesterone-regulated PCR product of 879 bp obtained with the TRIM22 primers was sequenced to confirm the TRIM22 identity. **(E)** IFNγ-regulated TRIM22 mRNA contains the 3' coding sequence for the 498 aa TRIM22 protein. Total RNA from HeLa cells left untreated or treated with IFNγ was reverse-transcribed and resulting cDNA analyzed as in **(D)**. **(D, E)** Results are representative of two independent experiments. **(F)** Progesterone up-regulated TRIM22 mRNA expression in ABC28 cells by Northern blotting analysis. 15 µg of total RNA from ABC28 cells treated with ethanol (E) or progesterone (P) for 16 or 24 hr was analyzed.

Table 3.1 TRIM22 nucleotide sequences available in the NCBI database and comparison of the resultant protein sequences with the sequence used in this study.
[a]When compared to the protein product from the entry used in this study (BC035582), several differences emerged. These differences have been highlighted as **deletions (x)**, **mutations**, or **additions**.

Nucleotide sequence accession	Coding sequence length (bp)	Resultant protein product[a] – differences from MGC clone BC035582 denoted (**deletions (x)**, **mutations**, additions highlighted)	Number of amino acids
BC035582, DQ894384, NM_006074.3	1497	MDFSVKVDIEKEVTCPICLELLTEPLSLDCGHSFCQACITAKIKESVIISRGESSCPVCQTRFQPGNLRPNRHLANIVERVKEVKMSP QEGQKRDVCEHHGKKLQIFCKEDGKVICWVCELSQEHQGHQTFRINEVVKECQEKLQVALQRLIKEDQEAEKLEDDIRQERTAW KNYIQIERQKILKGFNEMRVILDNEEQRELQKLEEGEVNVLDNLAAATDQLVQQRQDASTLISDLQRRLRGSSVEMLQDVIDVMK RSESWTLKKPKSVSKKLKSVFRVPDLSGMLQVLKELTDVQYYWVDVMLNPGSATSNVAISVDQRQVKTVRTCTFKNSNPCDFS AFGVFGCQYFSSGKYYWEVDVSGKIAWILGVHSKISSLNKRKSSGFAFDPSVNYSKVYSRYRPQYGYWVIGLQNTCEYNAFEDSS SSDPKVLTLFMAVPPCRIGVFLDYEAGIVSFFNVTNHGALIYKFSGCRFSRPAYPYFNPWNCLVPMTVCPPSS	498
BC022281	1497	MDFSVKVDIEKEVTCPICLELLTEPLSLDCGHSFCQACITAKIKESVIISRGESSCPVCQTRFQPGNLRPNRHLANIVERVKEVKMSP QEGQKRDVCEHHGKKLQIFCKEDGKVICWVCELSQEHQGHQTFRINEVVKECQEKLQVALQRLIKE**N**QEAEKLEDDIRQERTAW KNYIQIERQKILKGFNEMRVILDNEEQRELQKLEEGEVNVLDNLAAATDQLVQQRQDASTLISDLQRRLRGSSVEMLQDVIDVMK RSESWTLKKPKSVSKKLKSVFRVPDLSGMLQVLKELTDVQYYWVDVMLNPGSATSNVAISVDQRQVKTVRTCTFKNSNPCDFS AFGVFGCQYFSSGKYYWEVDVSGKIAWILGVHSKISSLNKRKSSGFAFDPSVNYSKVYSRYRPQYGYWVIGLQNTCEYNAFEDSS SSDPKVLTLFMAVPPCRIGVFLDYEAGIVSFFNVTNHGALIYKFSGCRFSRPAYPYFNPWNCLVPMTVCPPSS	498
NM_006074.2 X82200	1329	MDFSVKVDIEKEVTCPICLELLTEPLSLDCGHSFCQACITAKIKESVIISRGESSCPVCQTRFQPGNLRPNRHLANIVERVKEVKMSP QEGQKRDVCEHHGKKLQIFCKEDGKVICWVCELSQEHQGHQTFRINEVVKECQEKLQVALQRLIKEDQEAEKLEDDIRQERTAW K**xxxx**IERQKILKGFNEMRVILDNEEQRELQKLEEGEVNVLDNLAAATDQLVQQRQDASTLISDLQRRLTGSSVEMLQDVIDVMKR SESWTLKKPKSVSKKLKSVFRVPDLSGMLQVLKELTDVQYYWVDVMLNPGSATSNVAISVDQRQVKTVRTCTFKNSNPCDFSAF GVFGCQYFSSGKYYWEVDVSGKIAWILGVHSKISSLNKRKSSGFAFDPSVNYSKVYSRYRPQYGYWVIGLQNTCEYNAFEDSSSS DPKVLTLFMAV**L**P**VVL**G**FS**xxxxxxxxxxxxxxxxxxxxxxxxxxxxxxxxxxxxxxxxxxxxxxxxxxxx	442
AM040752	824	**xxxxxxxxxxxxxxxxxxxxxxxxxxxxxxxxxxxxxxxxxxxxxxxxxxxxxxxxxxxxxxxxxxxxxxxxxxxxxxxxxxxxxxxxxxxxxxx** **xxxxxxxxxxxxxxxxxxxxxxxxxxxxxxxxxxxxxxxxxxxxxxxxxxxxxxxxxxxxxxxxxxxxxxxxxxxxxxxxxxxxxxxxxxxxxxx** **xxxxxxxxxxxxxxxxxxxxxxxxxxxxxxxxxxx**QRQDASTLISDLQRRLRGSSVEMLQDVIDVMKRSESWTLKKPKSVSKKLKSVF RVPDLSGMLQVLKELTDVQYYWVDVMLNPGSATSNVAISVDQRQVKTVRTCTFKNSNPCDFSAFGVFGCQYFSSGKYYWEVDV SGKIAWILGVHSKISSLNKRKSSGFAFDPSVNYSKVYSRYRPQYGYWVIGLQNTCEYNAFEDSSSSDPKVLTLFMAVPPC**C**IGVFL DYEAGIVSFFNVTNHGALIYKFSGCRFSRPAYPYFNPWNCLVPMTVCPPSS	273

3.2 Expression, purification and refolding of TRIM22-(His)$_6$ protein

3.2.1 The TRIM22 protein is expressed as an insoluble protein in BL21(DE3) bacterial cells

In order to investigate the regulation of TRIM22 at the protein level, we required specific antibodies against the protein. These are not commercially available. Initally, a 24 aa antigenic peptide (KISSLNKRKSSGFAFDPSVNYSKV) (residues 375 – 398 of the SPRY domain) was commercially synthesized, conjugated to keyhole-limpet hemocyanin and used as an immunogen for antibody generation. However, specific antibodies were not raised. Therefore, subsequently, recombinant TRIM22 was expressed and used as an immunogen to generate specific antibodies. The TRIM22 coding sequence for the full-length 498 aa TRIM22 protein was cloned into the pET-24b(+) vector, upstream of the coding sequence for the six histidine (His) repeats [(His)$_6$]. Colonies were verified by enzyme digestion and sequencing. The pET-24b(+) vector containing the desired TRIM22 sequence in-frame with the His tag was chemically transformed into BL21(DE3) cells. A single colony was amplified and induced with 1 mM IPTG in its logarithmic growth phase. After a 4 hr induction at 30ºC, the cells were pelleted, sonicated well and the insoluble fraction separated from the soluble fraction by centrifugation. Aliquots of the total protein and the different fractions were subjected to SDS-PAGE and Coomassie blue staining. **Figure 3.2A** shows the expression of the TRIM22-(His)$_6$ protein in the insoluble fraction. The induced protein had a molecular weight of around 55 - 60 kDa. This tallied with TRIM22's calculated molecular mass of 56.9 kDa (prediction made by the Compute pI/MW tool hosted at http://www.expasy.ch/tools/pi_tool.html).

The induced protein band was excised and sent to the Proteomics Core Facility for sequencing. In this facility, the protein was reduced, alkylated and digested by trypsin before combined MS and MS/MS sequencing. **Figure 3.2B** shows the abundant peptides that could be detected and the positions that these peptides matched to on the TRIM22 protein sequence. An automated search using the Mascot search engine revealed the peptides belonged to TRIM22.

As the induced protein was in the insoluble phase, its theoretical hydrophobicity was determined. The Kyte-Doolittle hydrophobicity scale is a widely applied scale for delineating the hydrophobic character of a protein (Kyte and Doolittle, 1982). Regions with values above 0 are hydrophobic in character. A Kyte and Doolittle hydropathicity plot of the TRIM22 protein revealed that there were hydrophobic regions within the protein, particularly towards the C-terminal end (**Figure 3.3**). A Grand Average of Hydropathicity (GRAVY) score of -0.367 was obtained using the ProtPram tool (http://www.expasy.org/tools/protparam.html). The GRAVY value is calculated by adding the hydropathy value for each residue and dividing by the length of the protein sequence

As the GRAVY score was negative, indicating that the protein is likely to be more hydrophilic than hydrophobic, we attempted to improve the solubility of the induced TRIM22-$(His)_6$ protein. Induction was carried out at a lower temperature of 16ºC for 16 hr. However, this did not improve solubility. A subsequent experiment showed that TRIM22-$(His)_6$ was found in the insoluble fraction as early as half an hour after induction (**Figure 3.4**).

A

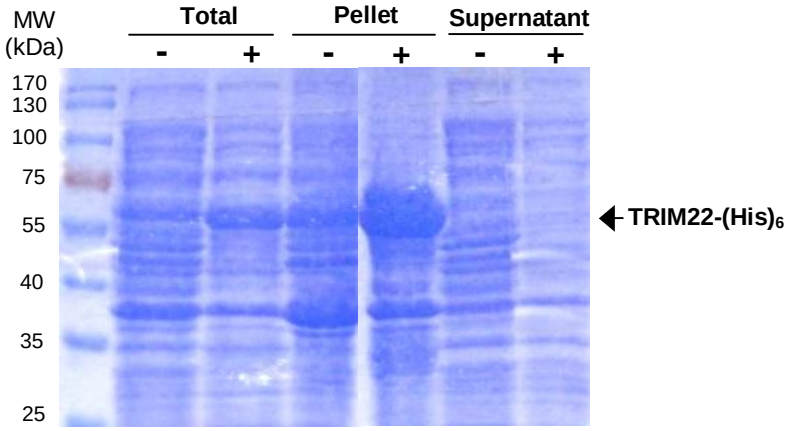

B

MDFSVKVDIEKEVTCPICLELLTEPLSLDCGHSFCQACITAKIKESVIISRGESSCPVCQTRFQPGNLRPNRHLANIVERVKE
VKMSPQEGQKRDVCEHHGKKLQIFCKEDGKVICWVCELSQEHQGHQTFRINEVVKECQEKLQVALQRLIKEDQEAEKLED
DIRQERTAWKNYIQIERQKILKGFNEMRVILDNEEQRELQK**LEEGEVNVLDNLAAATDQLVQQR**QDASTLISDLQRRLRGS
SVEMLQDVIDVMKRSESWTLKKPKSVSKKLKSVFRVPDLSGMLQVLK**ELTDVQYYWVDVMLNPGSATSNVAISVDQR**QV
KTVRTCTFKNSNPCDFSAFGVFGCQYFSSGKYYWEVDVSGKIAWILGVHSKISSLNKRKSSGFAFDPSVNYSKVYSRYRP
QYGYWVIGLQNTCEYNAFEDSSSSDPKVLTLFMAVPPCRIGVFLDYEAGIVSFFNVTNHGALIYKFSGCRFSRPAYPYFNP
WNCLVPMTVCPPSS

Figure 3.2 Bacterial expression of TRIM22-(His)$_6$ and confirmation of its identity.
(A) Uninduced (—) and IPTG-induced (+) cells cultured at 30ºC for 4 h were lysed and sonicated. The insoluble fraction (pellet) was separated from the soluble fraction (supernatant) by centrifugation for 30 min at 18,000 rpm. The total protein (total) and both fractions were analyzed by SDS-PAGE followed by Coomassie blue staining. The induced protein was observed at around the expected size of around 55 - 60 kDa, predominantly in the insoluble fraction. Result is representative of three independent experiments. **(B)** The induced protein band was excised and sent for identity verification by mass spectrometry at the Proteomics Core Facility (NTU/SBS). The abundant peptides that mapped to the TRIM22 protein sequence have been highlighted and underlined.

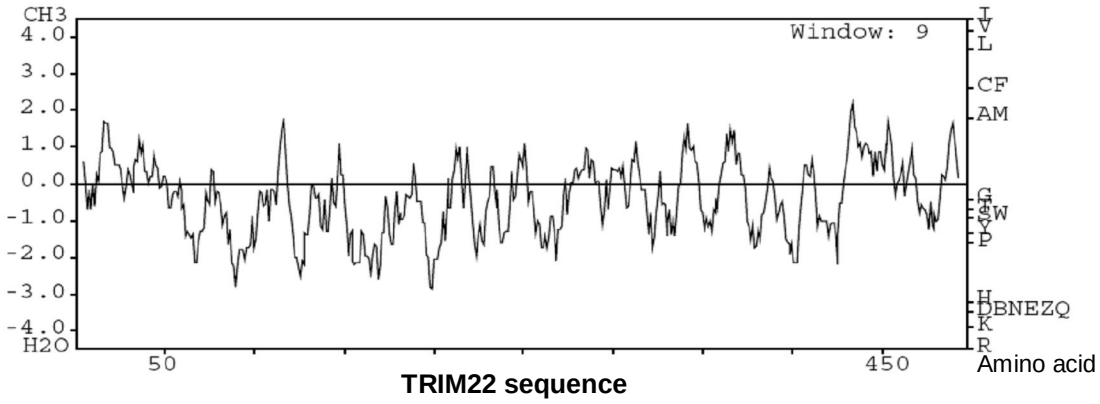

Figure 3.3 Kyte and Doolittle hydrophobicity plot of TRIM22.
The 498 aa TRIM22 protein sequence was queried using the Kyte and Doolittle scale at http://www.vivo.colostate.edu/molkit/hydropathy/index.html. Hydrophobic regions achieve a positive value and hydrophilic regions a negative value. On the axis on the right, amino acids have been plotted at their hydrophobicity value.

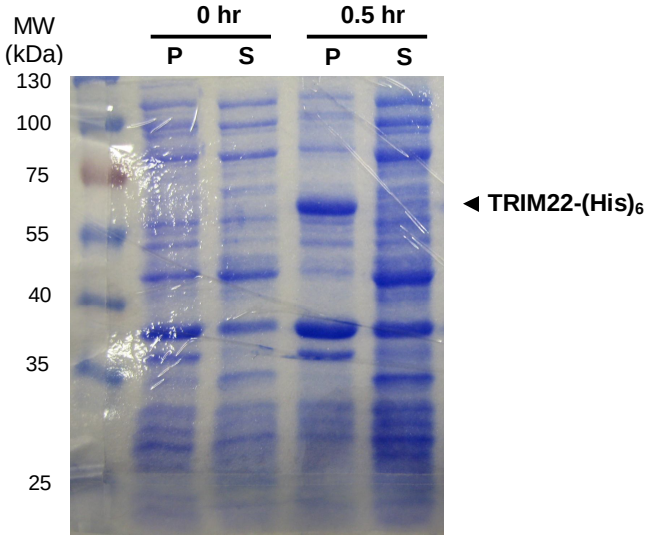

Figure 3.4 Solubility of TRIM22-$(His)_6$ at 16ºC after induction for different periods.
Cells cultured at 16ºC for 0 (i.e. uninduced), 0.5, 1 and 1.5 hr were lysed and sonicated. The insoluble fraction (P) was separated from the soluble fraction (S) by centrifugation for 30 min at 18,000 rpm. Both fractions for each of the four time-points were analyzed by SDS-PAGE followed by Coomassie blue staining. The induced protein was observed at the expected size of around 55 - 60 kDa. Result is representative of two independent experiments.

Before further efforts were taken to enhance the solubility of the induced protein, the protein sequence was scanned to determine the numbers of cysteine residues present within the sequence. Cysteine residues form strong disulphide bonds. The random formation of these bonds can lead to protein misfolding, which can be a source of protein insolubiliy (Idicula-Thomas and Balaji, 2007). TRIM22 has 20 cysteine residues along the length of its protein sequence (**Figure 3.5**). Although this is an even number indicating that intermolecular disulphide linkages are not a certainty, the abundance of cysteine residues suggests that the chances of unnatural/random disulphide bond formation and hence protein misfolding is high.

In a bacterial expression system, the high level of expression of recombinant proteins can lead to the formation of insoluble aggregates known as inclusion bodies (Idicula-Thomas and Balaji, 2007). Inclusion bodies store the recombinant protein, protecting it from degradation. Thus, more of the protein can be expressed in a stable form. As the TRIM22-$(His)_6$ protein was completely insoluble within half an hour after induction at 16ºC, its insolubility was exploited and protein expression maximized by induction for 4 hr at 30ºC. After solubilization of inclusion bodies using the strong denaturant 8 M urea, TRIM22-$(His)_6$ was purified under denaturing conditions.

3.2.2 Purification of TRIM22-$(His)_6$ under denaturing conditions and refolding

All buffers used in the purification of TRIM22-$(His)_6$ contained 8 M urea. Under denaturing conditions, the His tag in the recombinant protein is likely to be fully exposed,

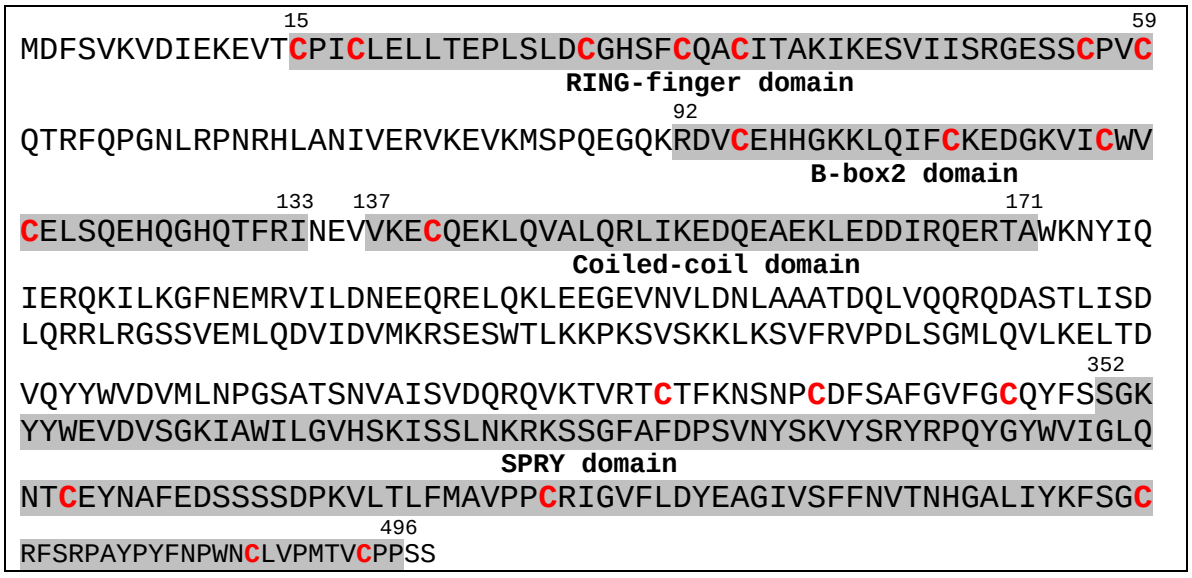

Figure 3.5 Amino acid sequence of the TRIM22 protein.
There are four identifiable domains within the TRIM22 protein – the RING-finger domain, B-box2 domain, Coiled-coil domain and the SPRY domain. The cysteine (**C**) residues are highlighted in red. The predicted molecular weight of the TRIM22 is 56.9 kDa. Theoretical isoelectric point (pI) is 7.97.

thus improving binding of the protein to the Ni-NTA matrix. In turn, this would reduce non-specific binding and improve the efficiency of the purification. Denatured TRIM22-$(His)_6$ was passed through a charged Ni-NTA column that was pre-equilibrated with 8 M urea buffer. However, not all of the protein bound to the Ni-NTA beads and a significant amount passed unbound through the column (flow-through fraction) (**Figure 3.6A**). This may have been due to the high expression level of the protein and possible saturation of the binding sites. Alternatively, the protein may not have been completely denatured in 8 M urea buffer. The column with bound protein was washed with 8 M urea buffer of pH 6.3 to remove non-specifically bound protein. This wash step led to the removal of some TRIM22-$(His)_6$. In 8 M urea buffer of pH 4.5, more than 90% of the protein eluted consisted of TRIM22-$(His)_6$ (**Figure 3.6A**). The identity of expressed protein and the protein in the eluted fraction was verified by Western blotting using an anti-His antibody (**Figure 3.6B**).

TRIM22-$(His)_6$ in the 8 M urea elution buffer was concentrated to 6000 µg/ml using a Centricon column of 10,000 MW cut-off. The protein was subsequently refolded in 50 µl pulses in cold buffer containing 0.5 M L-arginine and 0.5 mM cysteine as anti-aggregation agents. No turbidity was noted indicating TRIM22-$(His)_6$ did not aggregate to a noticeable extent in the refolding buffer. The buffer containing soluble TRIM22-$(His)_6$ protein was centrifuged to remove aggregates and concentrated. Protein concentration was adjusted to 1000 µg/ml and the protein snap-frozen as 300 µl aliquots.

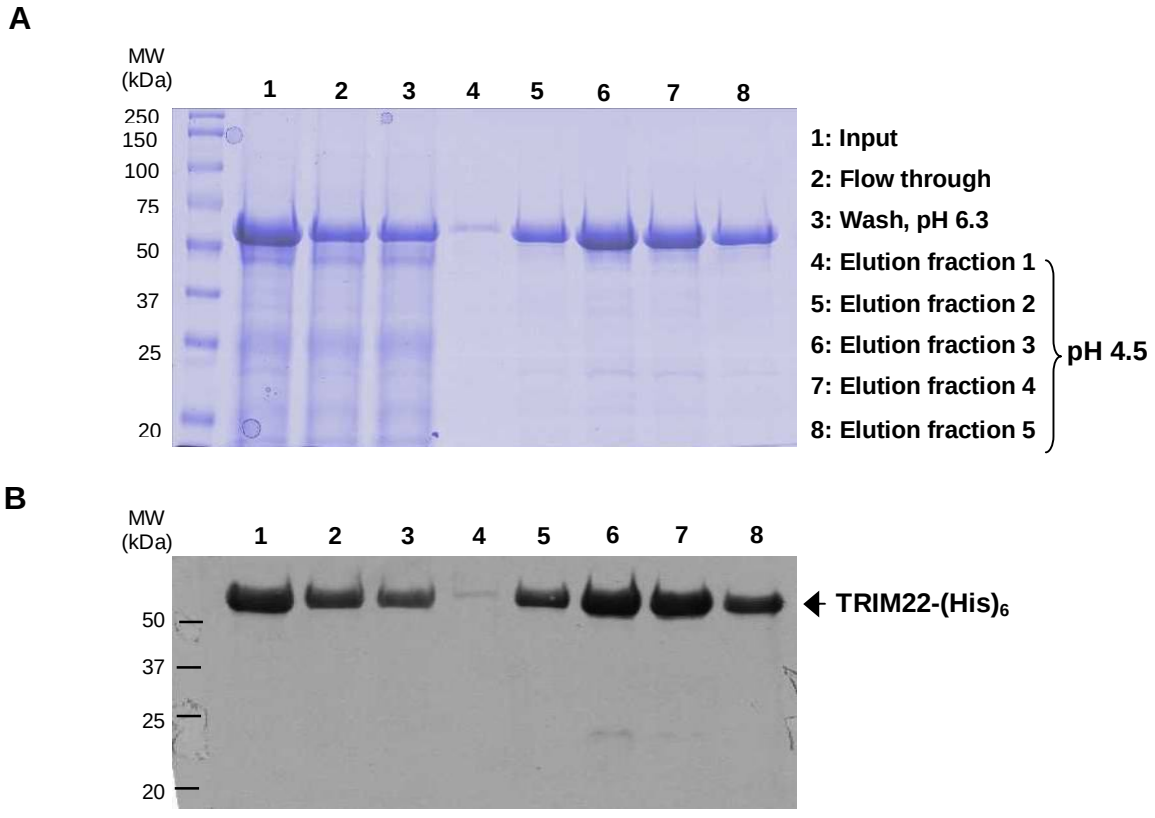

Figure 3.6 Purification of denatured TRIM22-$(His)_6$ using Ni-NTA agarose.
IPTG-induced cells cultured at 30ºC for 4 hr were lysed and sonicated and the insoluble fraction denatured in Tris-phosphate buffer containing 8 M urea buffer, pH 8.0, before incubation with Ni-NTA beads. Column was washed with the same buffer of pH 6.3 before elution in buffer of pH 4.5. **(A)** Coomassie blue-stained gel of different fractions of the TRIM22-$(His)_6$ purification process. **(B)** Duplicate samples were analyzed by Western blotting using the anti-His antibody to determine the proportion of His-tagged protein bound to the beads and the amount of protein eluted. Results are representative of at least two independent experiments.

3.3. Generation of mouse TRIM22 polyclonal antibodies using TRIM22-(His)$_6$

3.3.1 Test of sera from four mice

Mice were handled following the guidelines on the Care and Use of Animals for Scientific Purposes (2004) set by National Advisory Committee for Laboratory Animal Research (NACLAR) in Singapore. Four albino Balb/c mice were immunized with purified and refolded TRIM22-(His)$_6$ protein. Freund's Complete Adjuvant was used in the primary immunization and Freund's Incomplete Adjuvant in subsequent boosters. After boosters, 100 µl of blood was collected from tail veins of mice and sera monitored for specificity by Western blotting analysis using ethanol- and progesterone-treated ABC28 lysates as samples.

Shown in **Figure 3.7A** are results from the final bleeds of four mice (1 - 4). Blots containing resolved proteins were probed simultaneously for the housekeeping protein GAPDH since both the anti-TRIM22 and anti-GAPDH antibodies gave clean blots (**Figure 3.7B**). Sera from all four mice detected the antigen (results not shown) and an up-regulated product of around 50 – 60 kDa in the progesterone-treated cell lysate. Mouse 2 sera showed the greatest specificity as the high intensity band observed in the progesterone-treated sample was absent in the ethanol-treated sample. Sera from mice 3 and 4 detected less intense bands in the progesterone-treated sample, but these bands were still evidently up-regulated. Sera from mouse 1, unlike sera from the other 3 mice, also detected a band in the ethanol-treated sample although this band was less intense than that detected in the progesterone-treated sample. The specificity of mouse 2 sera is evident in **Figure 3.7B**, which shows only a greatly up-regulated band at 50 - 60 kDa in

the progesterone-treated lysate, corresponding to TRIM22. Besides this bright band, there were two other very faint bands at around 70 - 75 kDa and 250 kDa which were not regulated by progesterone. As sera from mouse 2 was able to detect a progesterone-induced increase in a 50 - 60 kDa protein to the greatest extent, this sera was used as a polyclonal antibody (anti-TRIM22) to detect TRIM22 in subsequent experiments.

3.3.2 Determining specificity of the TRIM22 polyclonal antibody

In order to further verify the specificity of the TRIM22 polyclonal antibody from mouse 2, siRNA knockdown experiments were conducted. The ability of pre-designed siRNA against TRIM22 to knockdown TRIM22 transcript levels was analyzed in ABC28 cells treated with progesterone. **Figure 3.8A** shows the levels of TRIM22 transcript in progesterone-treated TRIM22 siRNA-transfected cells relative to levels in progesterone-treated control siRNA-transfected cells. At the 24-hr time-point, TRIM22 siRNA 6 and 7 were both able to dramatically reduce TRIM22 levels in progesterone-treated cells by 8 fold and 3.5 fold respectively. As the *TRIM34*, *TRIM6*, and *TRIM5* genes have high sequence similarity to *TRIM22* and their transcripts could be detected reliably by real-time PCR (with basal Ct values less than 30; melting curves shown in **Appendices Figure A1**), the effect of TRIM22 siRNA on the levels of these transcripts was investigated. TRIM34, TRIM6 and TRIM5 transcript levels were not reduced by more than 2-fold by TRIM22 siRNA (**Figure 3.8A**). At the high concentration of TRIM22 siRNA 6 used (80 nM), the TRIM5 transcript was reduced by 2-fold. To minimize the non-specific effect of siRNAs, 10 nM siRNAs were used in subsequent studies.

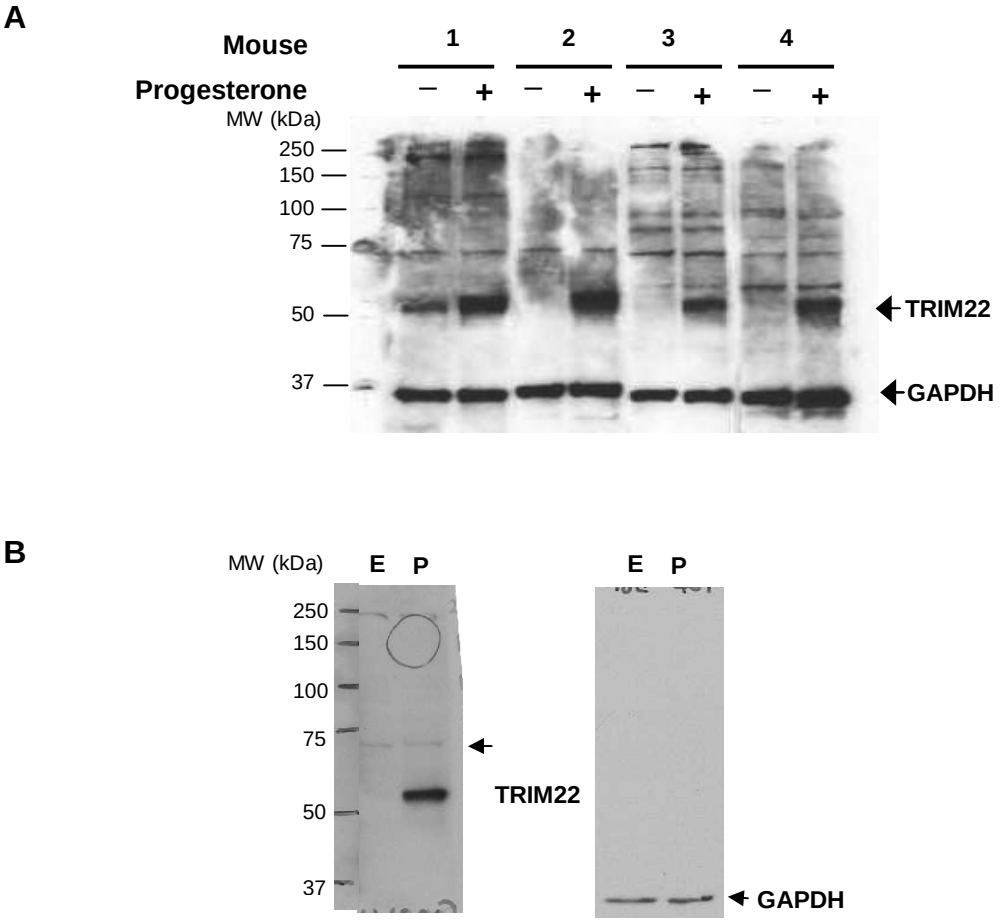

Figure 3.7 Specificity of polyclonal TRIM22 antibody raised in mice.
(A) Sera from immunized mice detect a progesterone-regulated protein product. Four mice immunized with refolded full-length TRIM22 protein were bled from tail veins 7 - 10 days after boosters to determine their ability to detect an up-regulated protein product of about 50 - 60 kDa in lysate from ABC28 cells treated with 0.1% ethanol (—) or 100 nM progesterone (+) for 48 hr. Same batch of lysate was used. Blots for the final bleeds are shown. Mouse 2 serum was used at a 1:1000 dilution while sera from mice 1, 3, and 4 were used at a 1:500 dilution. After an overnight incubation with mouse sera, blots were washed briefly before incubation with anti-GAPDH antibody to simultaneously detect levels of the housekeeping protein (37 kDa) as a loading control. **(B)** Mouse 2 serum was used to first detect TRIM22 in ethanol (E)- and progesterone (P)-treated cell lysates, with blot stripped and then re-probed with anti-GAPDH antibody to show specificity of the anti-TRIM22 antibody. Results are representative of at least three independent experiments.

Having confirmed that the siRNA sequences do indeed reduce TRIM22 transcript levels in a specific manner, the level of the up-regulated protein product in siRNA transfected cells was investigated at the 48-hr time point. All three TRIM22 siRNAs greatly reduced the up-regulated protein product to near-basal levels. Consistent with real-time PCR data, TRIM22 siRNA 6 was the most effective sequence leading to a 98% reduction in the levels of the TRIM22 protein. During the analysis of a few other TRIM transcripts, it was evident that progesterone was also able to induce a 3-fold up-regulation of the TRIM7 transcript. TRIM7 has four transcript variants, the longest of which is GINP1, encoding a 551 aa protein with a predicted molecular weight of 56.6 kDa (Skurat et al., 2002). However, TRIM22 siRNA did not inhibit the expression of the TRIM7 transcript (3.1 and 3.2 fold up-regulation in TRIM22 siRNA 6 and 7 transfected cells treated with progesterone). If the TRIM7 isoform GNIP1 was also up-regulated by progesterone at the protein level and the polyclonal antibody did cross-react with GNIP1, then levels of protein product in TRIM22 siRNA-transfected cells would not be at basal levels. The observation that the up-regulated protein product was completely inhibited by TRIM22 siRNA 6 is evidence that the polyclonal TRIM22 antibody from mouse 2 is largely specific for TRIM22, at least at the 50 - 60 kDa range.

Close examination of the Western blotting result obtained using the TRIM22 antibody consistently revealed the presence of a 75 kDa band (marked with an asterisk, **Figure 3.8B**). This band was also up-regulated slightly by progesterone but was not reduced by TRIM22 siRNA. As TRIM22 belongs to a large family of proteins that share conserved residues, particularly at their N-termini, it is possible that the polyclonal antibody

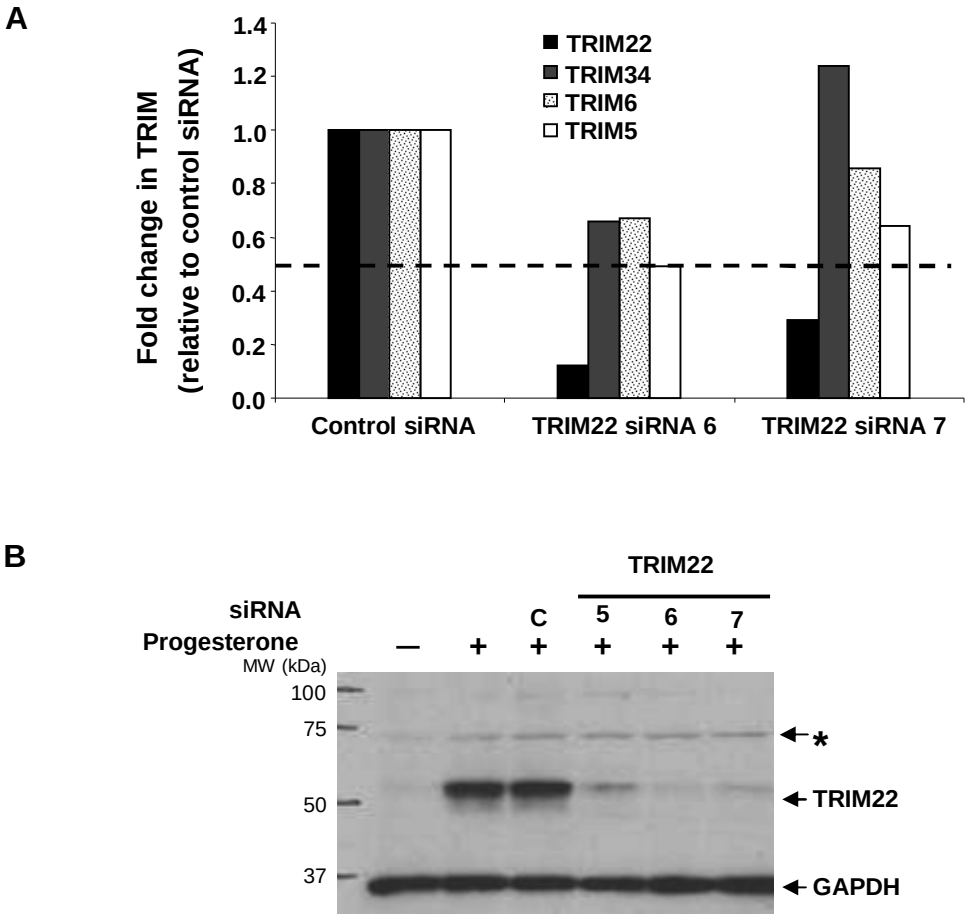

Figure 3.8 The 50 – 60 kDa band detected by the polyclonal TRIM22 antibody is greatly reduced after TRIM22 silencing.

(A) The specificity of TRIM22 siRNAs 6 and 7 was first investigated by determining the extent to which the TRIM22 transcript was silenced. ABC28 cells were transfected with 80 nM control siRNA (C) or TRIM22 siRNAs (6 and 7) for 8 hr before treatment with 100 nM progesterone. Level of the TRIM22 transcript 24 hr after progesterone treatment, relative to progesterone-treated control siRNA and after normalization with the housekeeper 36B4, was analyzed by real-time PCR using specific primers. The transcript levels of TRIM34, TRIM6 and TRIM5 were also analyzed to check for knockdown these TRIM22 paralogs. The broken line indicates the 2-fold cut-off. **(B)** Knockdown of TRIM22 by three different siRNAs (5, 6, and 7) at the protein level was investigated by Western blotting using polyclonal TRIM22 antibody from mouse 2. Blots were probed with anti-GAPDH antibody before indirect chemiluminescence analysis. The asterisk (*) denotes the position of a faint band that is not affected by TRIM22 siRNAs. **(A, B)** Results are representative of two independent experiments.

generated against the full-length TRIM22 protein recognized a conserved motif also found in at least one other TRIM protein. This may have led to the detection of a second TRIM protein. At the transcript level, the other TRIMs that have close sequence similarity to TRIM22 (TRIM34, TRIM6, TRIM5) are not up-regulated by progesterone (result not shown). Besides, these proteins have similar molecular weights to TRIM22 and therefore are unlikely to be responsible for the 75 kDa progesterone-regulated band. As one other TRIM, TRIM7, is increased upon progesterone treatment, it would be of interest to determine which other TRIM transcripts and proteins are up-regulated by progesterone. In the context of this study however, we have shown that the greatly up-regulated band at 50 - 60 kDa detected by this antibody does belong to TRIM22.

3.4. Endogenous TRIM22 levels in different cell lines

Having confirmed that the polyclonal antibody against TRIM22 is indeed specific for the TRIM22 protein, it was used to investigate endogenous TRIM22 levels in different cell lines. We investigated the tumorigenic human MECs, MCF7, T47D, and ABC28 and the non-tumorigenic MECs, MCF10A and MCF12A. The human endometrial cancer cell line HeLa was also investigated. The MCF10A and MCF12A cell lines had obviously greater TRIM22 levels compared to the tumorigenic MEC lines (**Figure 3.9A**). Of the three breast cancer cell lines, ABC28 cells had more endogenous TRIM22 protein than MCF7 or T47D cells [this was also verified at the transcript level (result not shown)]. To further investigate the identity of the dense band in MCF12A cells and to confirm that it was indeed TRIM22, MCF12A cells were transfected with TRIM22 siRNA 5, 6 or 7.

Silencing TRIM22 in these cells greatly reduced the levels of the 50 – 60 kDa band (**Figure 3.9B)**.

3.5. Regulation of endogenous TRIM22 by progesterone and IFN

3.5.1 Progesterone enhances TRIM22 protein levels in breast cancer cells

As shown in **Figure 3.8B**, the identity of the progesterone-induced protein in ABC28 cells was verified. To investigate if progesterone could enhance TRIM22 protein levels in a dose and time-dependent manner, ABC28 cells were treated with 0.1% ethanol (vehicle control) or 1 nM, 10 nM and 100 nM progesterone for 24 or 48 hr. 1 nM progesterone was adequate to enhance TRIM22 protein levels within 24 hr (**Figure 3.10A**). This effect persisted for at least 48 hr. In T47D cells however, a 100 nM progesterone dose was only able to enhance TRIM22 protein levels at the 24-hr time point. At 48 hr, the increase was not obvious (**Figure 3.10B**).

3.5.2 IFNs β and γ enhance TRIM22 protein levels in HeLa and MCF7 cells

TRIM22 was identified initially as an IFN-inducible gene in HeLa and human lymphoblastoid Daudi cells (Tissot and Mechti, 1995). The authors reported the ability of the type 1 IFNs α and β and the type 2 IFNγ to greatly enhance the TRIM22 transcript by 8 hr in these cells. In this study, the regulation of the TRIM22 protein by IFNβ and IFNγ was tested in HeLa cells and MCF7 cells. In HeLa cells, the TRIM22 protein was increased by both IFN β and γ at the 16-hr time-point and dramatically at the 24-hr time-point (**Figure 3.11A**). IFNβ's effects were more pronounced than IFNγ's at both time-points.

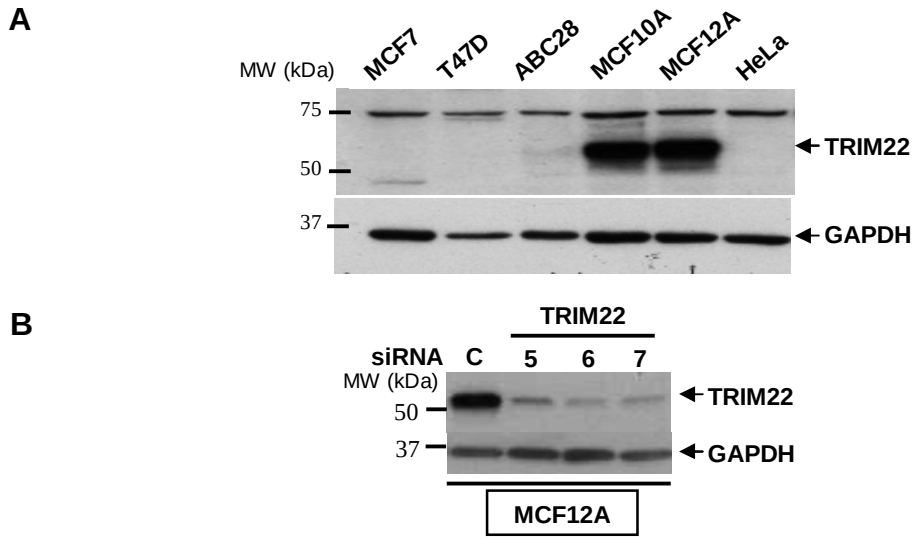

Figure 3.9 Normal mammary cells express large amounts of the TRIM22 protein.
(A) 30 μg of whole cell lysates from MCF7, T47D, ABC28, MCF10A and MCF12A cells were subjected to Western blotting and probed with anti-TRIM22 and anti-GAPDH antibodies before indirect chemiluminescence analysis. **(B)** MCF12A cells were transfected with 10 nM control siRNA (C) or TRIM22 siRNA 5, 6, or 7 for 48 hr and lysate analyzed as in **(A)**. **(A, B)** Results are representative of two independent experiments.

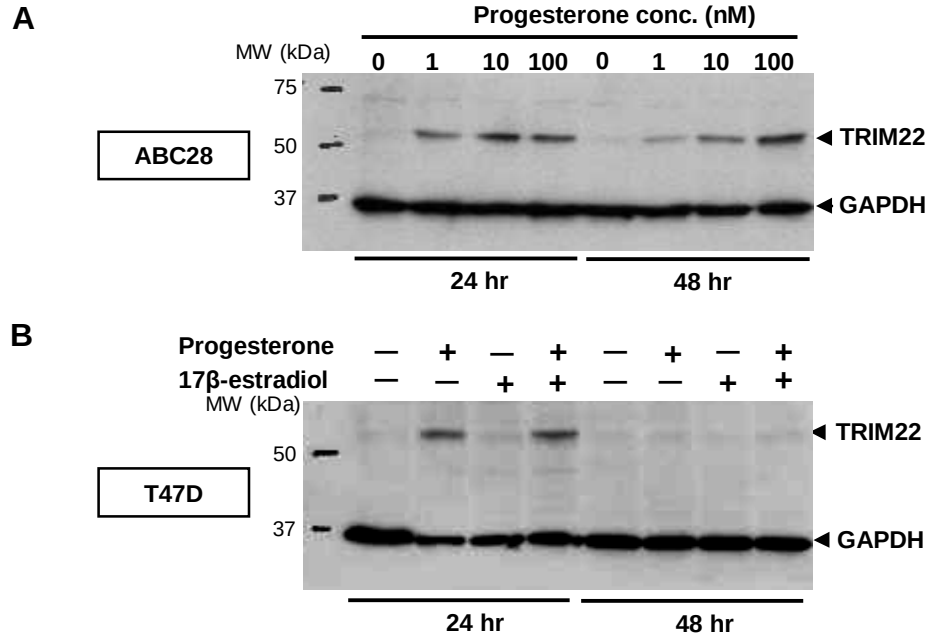

Figure 3.10 Progesterone enhances TRIM22 protein levels in both ABC28 and T47D cells.
(A) ABC28 cells were treated with ethanol (0) or 1, 10 and 100 nM progesterone for 24 or 48 hr. **(B)** T47D cells were treated with 100 nM progesterone and/or 1nM 17β-estradiol for 24 or 48 hr. 25 μg of whole cell lysates were subjected to Western blotting and probed sequentially with anti-TRIM22 and anti-GAPDH antibodies before indirect chemiluminescence analysis. **(A, B)** Results are representative of three independent experiments.

Interestingly, a 250 IU/ml IFNγ dose showed a more evident increase than the 500 IU/ml IFNγ dose. This observation was reproducible. Like in HeLa cells, IFNγ was also able to enhance TRIM22 protein levels in MCF7 cells at both 250 and 500 IU/ml (**Figure 3.11B**). The up-regulated TRIM22 protein product in IFNγ-treated HeLa cells could also be reduced to basal levels by TRIM22 siRNA 5, 6, and 7 (**Figure 3.11C**). A 10 nM concentration was just as effective as the 50 nM concentration for all three siRNAs. Like that observed in MCF12A and progesterone-treated ABC28 cells, TRIM22 siRNA 6 and 7 were more effective than TRIM22 siRNA 5 in reducing the TRIM22 protein product.

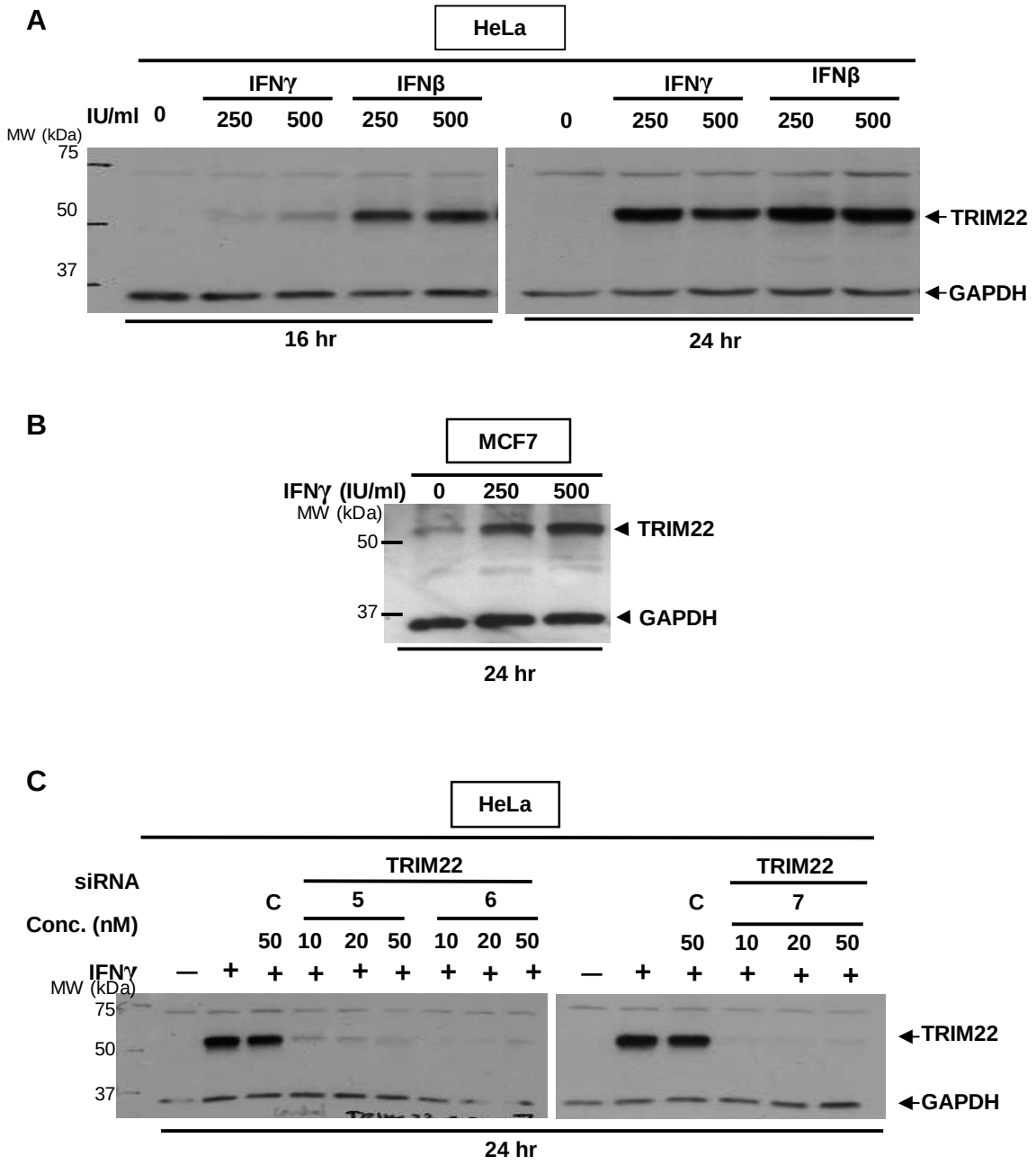

Figure 3.11 IFNs γ and β enhance TRIM22 protein levels in HeLa and MCF7 cells.
(A) HeLa cells and **(B)** MCF7 cells were left untreated (0 IU/ml) or treated with 250 or 500 IU/ml of IFN γ or β for 16 or 24 hr. 30 μg of whole cell lysates were subjected to Western blotting and probed sequentially with anti-TRIM22 and anti-GAPDH antibodies before indirect chemiluminescence analysis. **(C)** The identity of the IFNγ-regulated band in HeLa cells was also confirmed by silencing experiments that showed that all the three TRIM22 siRNAs were able to reduce the protein product to near-basal levels. **(A – C)** Results are representative of three independent experiments.

3.6 Localization of TRIM22 in mammalian cells

3.6.1 The 1497 bp TRIM22 coding sequence codes for the expression of a nuclear protein

The localization of overexpressed GFP-tagged TRIM22, as cytoplasmic speckles with some nuclear localization, has been reported (Reymond et al., 2001; Li et al., 2006). However, Reymond et al. used the shorter form of the TRIM22 coding sequence (encoded by the sequence in the NCBI entry NM_006074.2) (**Table 3.1**). There are also no studies reporting the location of the endogenous TRIM22 protein. Our experiments had shown that ABC28, T47D and HeLa cells express the longer form of the TRIM22 transcript that codes for a 498 aa protein (**Figures 3.1D, E**). Therefore, the 1497 bp TRIM22 coding sequence was cloned into the pEGFP-N1 vector to investigate the localization of TRIM22.

In all of the cell lines investigated, TRIM22-EGFP localized as distinct NB in cells expressing low to moderate levels of the exogenous protein (**Figure 3.12**). To exclude the possibility that the large GFP tag on the C-terminal of TRIM22 modified the conformation and/or the localization of the protein, the TRIM22 coding sequence was also cloned into the pEYFP-C1 and the pXJ-FLAG vectors such that the protein would have the EYFP or FLAG tags respectively on its N-terminus. TRIM22 localized as distinct NB regardless of tag size or its location (**Figure 3.12A**). The localization of TRIM22-EGFP as NB was also observed in T47D, HeLa, and COS-7 cells (**Figure 3.12B**). Besides localizing as distinct bodies, TRIM22 also localized as a nucleoplasmic protein in some FLAG-TRIM22 transfected cells (**Figure 3.12C)**.

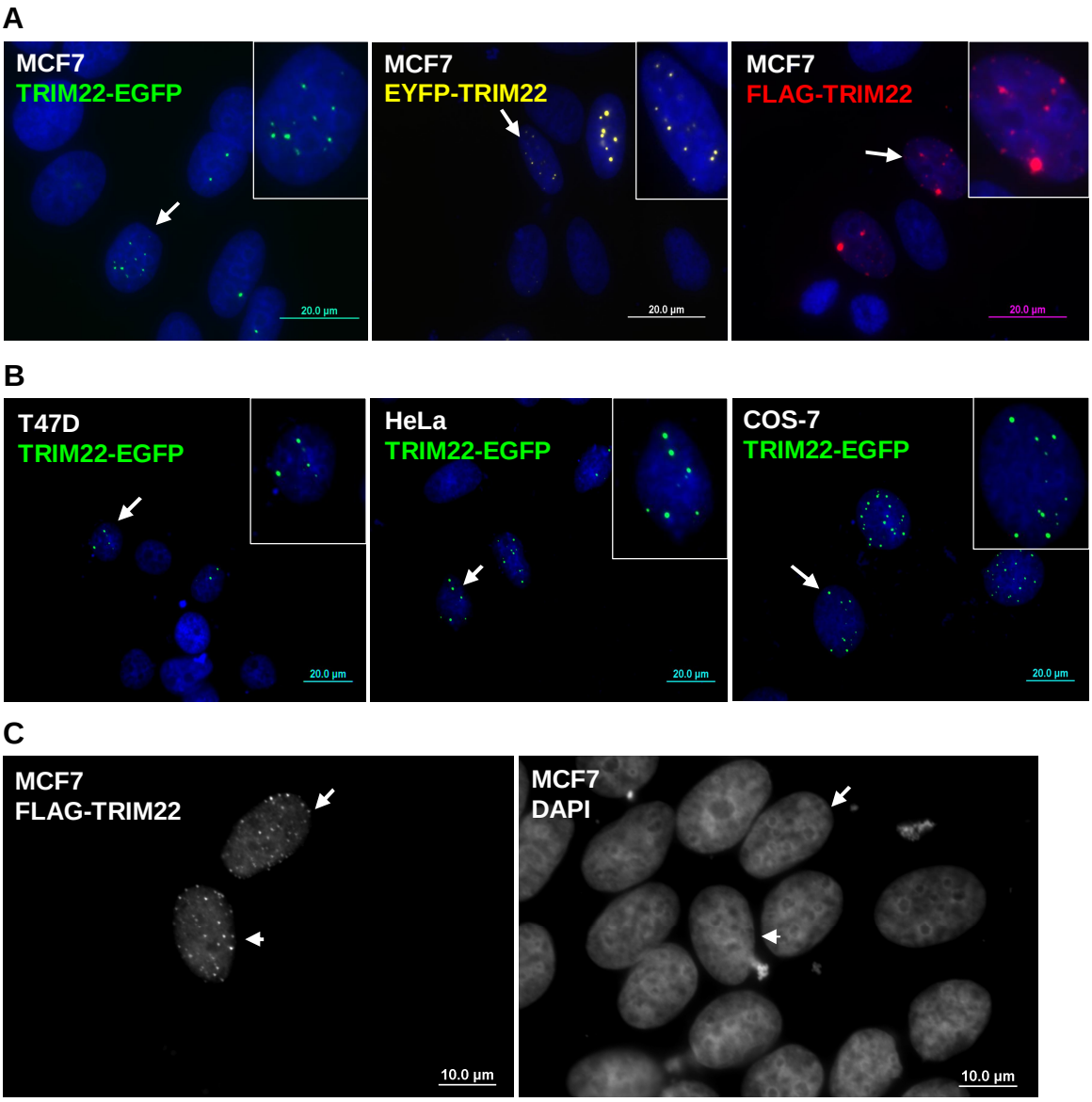

Figure 3.12 TRIM22 forms nuclear bodies.
(A) MCF7 cells stably expressing TRIM22-EGFP, or transiently (24 - 48 hr) expressing EYFP-TRIM22 (yellow) or FLAG-TRIM22 (red) were investigated. FLAG-TRIM22 cells were immunostained with mouse anti-FLAG antibody. **(B)** TRIM22-EGFP also exists as distinct nuclear bodies in T47D, HeLa and COS-7 cells transiently expressing TRIM22-EGFP. All cells in **(A)** and **(B)** were counterstained with DAPI (blue) and visualized by fluorescence microscopy at a 60X magnification. Bars, 20 µm. Insets show representative cells (arrows) enlarged 2X. **(C)** Color has not been added to highlight the nucleoplasmic staining in FLAG-TRIM22 transfected MCF7 cells expressing lower levels of the protein (identified with arrows in both panels). Bars, 10 µm. **(A – C)** Results are representative of at least three independent experiments.

3.6.2 Endogenous TRIM22 localizes as a nuclear protein in two different forms

In Western blotting, the mouse polyclonal antibody against TRIM22 detects specific TRIM22 protein. This antibody was also used to study the cellular localization of the endogenous TRIM22 protein, which has not been reported before. In MCF12A cells, TRIM22 localized as a nucleoplasmic protein with obvious NB. This staining pattern was not observed in cells immunostained with the same dilution of pre-immune mouse serum (**Figure 3.12A**). Likewise, in ABC28 cells, endogenous TRIM22 assumed a speckled pattern, besides forming distinct NB. Both nucleoplasmic staining and NBs were increased by progesterone treatment. More interestingly, TRIM22 NB in progesterone-treated ABC28 cells were frequently present as a cluster of bodies within nucleoli, which were marked by the location of the nucleolar protein fibrillarin (green) (ABC28 48P panels**, Figure 3.13B**). Distinct NB could not be detected in T47D cells regardless of whether they were treated with progesterone (**Figure 3.13C**). However, there was an increase in nucleoplasmic staining intensity in T47D cells treated with 100 nM progesterone for 24 hr. Consistent with Western blotting results, this increase was no longer evident at the 48-hr timepoint (result not shown).

The TRIM22 antibody could also detect distinct NB in HeLa and MCF7 cells (**Figure 3.13D**). While the numbers of NB did not increase in an obvious manner in IFNγ-treated cells, an increase in nucleoplasmic staining intensity in both HeLa and MCF7 cells was noted. In untreated cells, distinct NB were present in some cells, with the antibody also picking up nucleoplasmic staining in other cells (**Figure 3.13D**). We also noted that IFNγ induced some cytoplasmic staining in MCF7 cells.

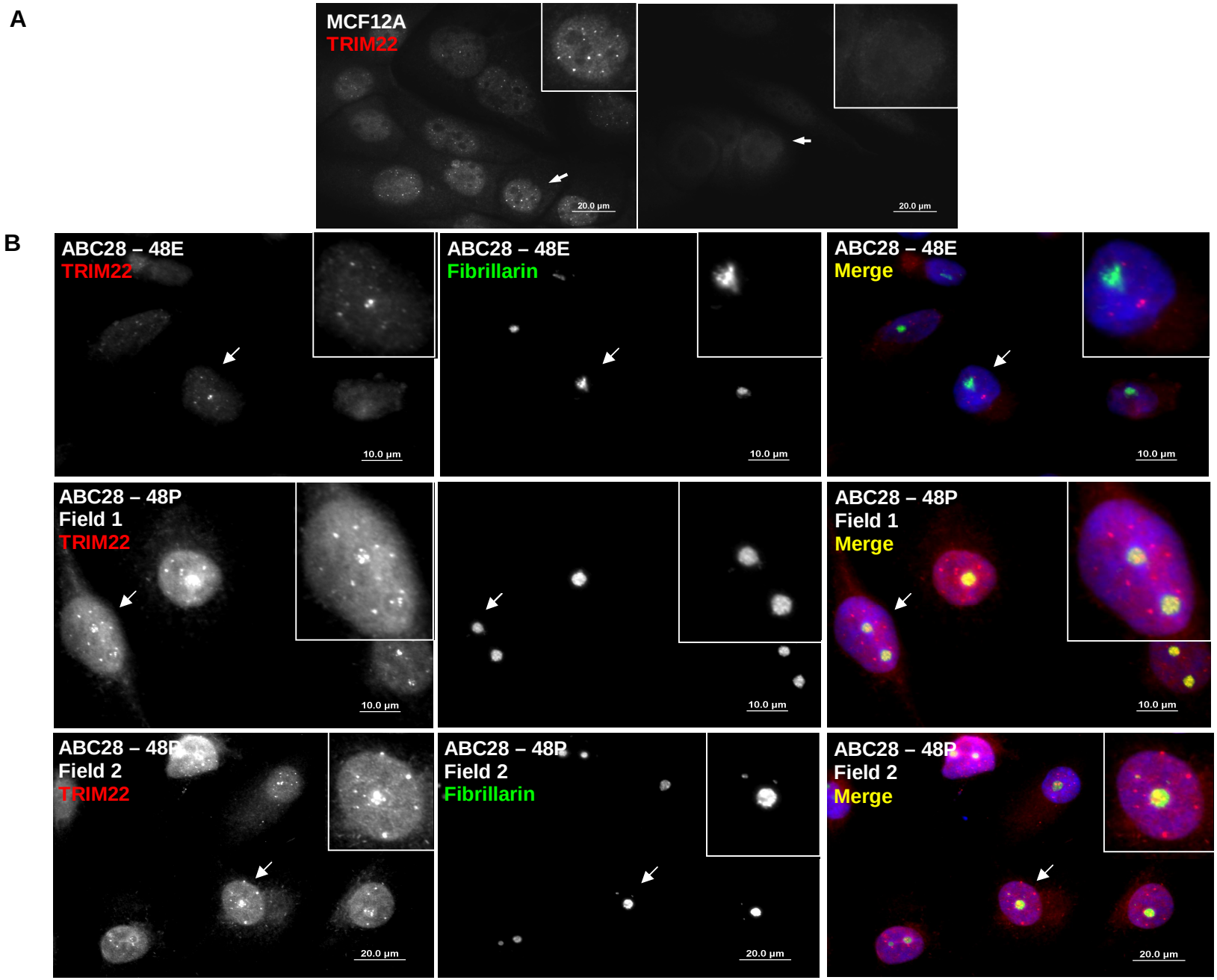
A
MCF12A
TRIM22
20.0 µm
20.0 µm
B
ABC28 – 48E
TRIM22
10.0 µm
ABC28 – 48E
Fibrillarin
10.0 µm
ABC28 – 48E
Merge
10.0 µm
ABC28 – 48P
Field 1
TRIM22
10.0 µm
10.0 µm
ABC28 – 48P
Field 1
Merge
10.0 µm
ABC28 – 48P
Field 2
TRIM22
20.0 µm
ABC28 – 48P
Field 2
Fibrillarin
20.0 µm
ABC28 – 48P
Field 2
Merge
20.0 µm

C

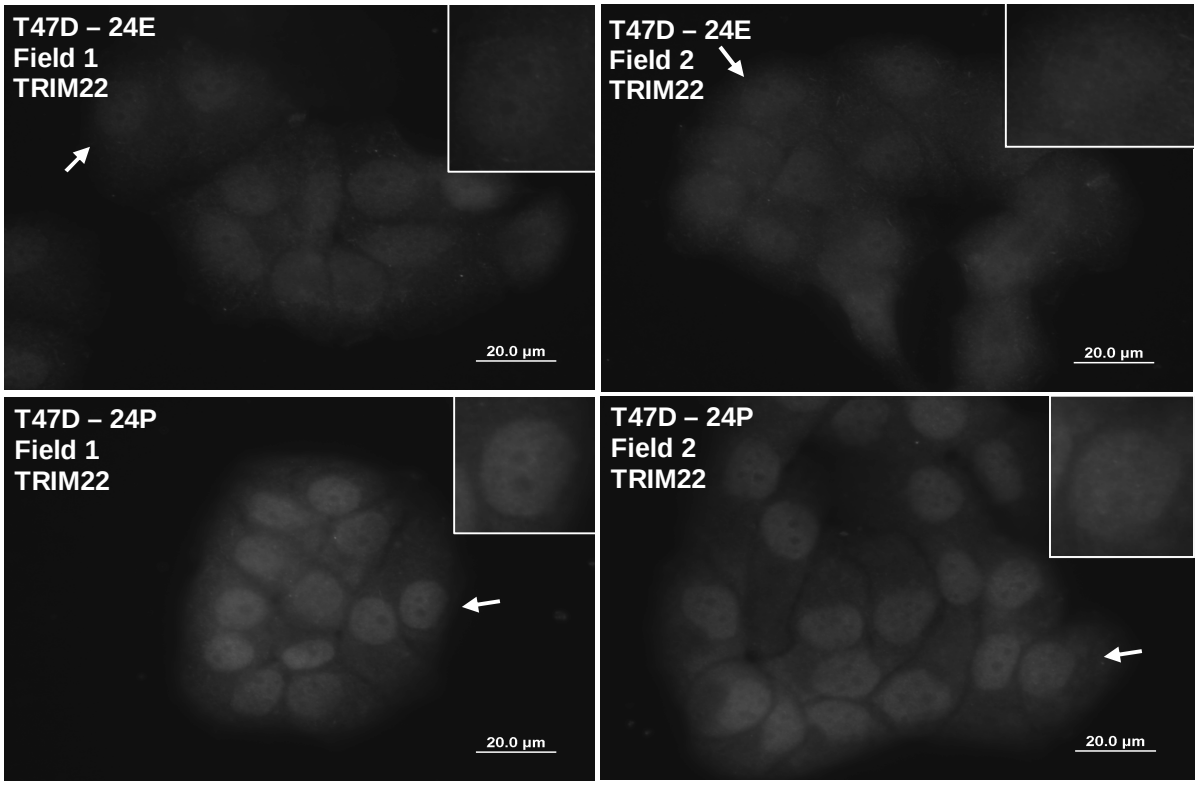
T47D – 24E
Field 1
TRIM22
20.0 µm
T47D – 24E
Field 2
TRIM22
20.0 µm
T47D – 24P
Field 1
TRIM22
20.0 µm
T47D – 24P
Field 2
TRIM22
20.0 µm

D

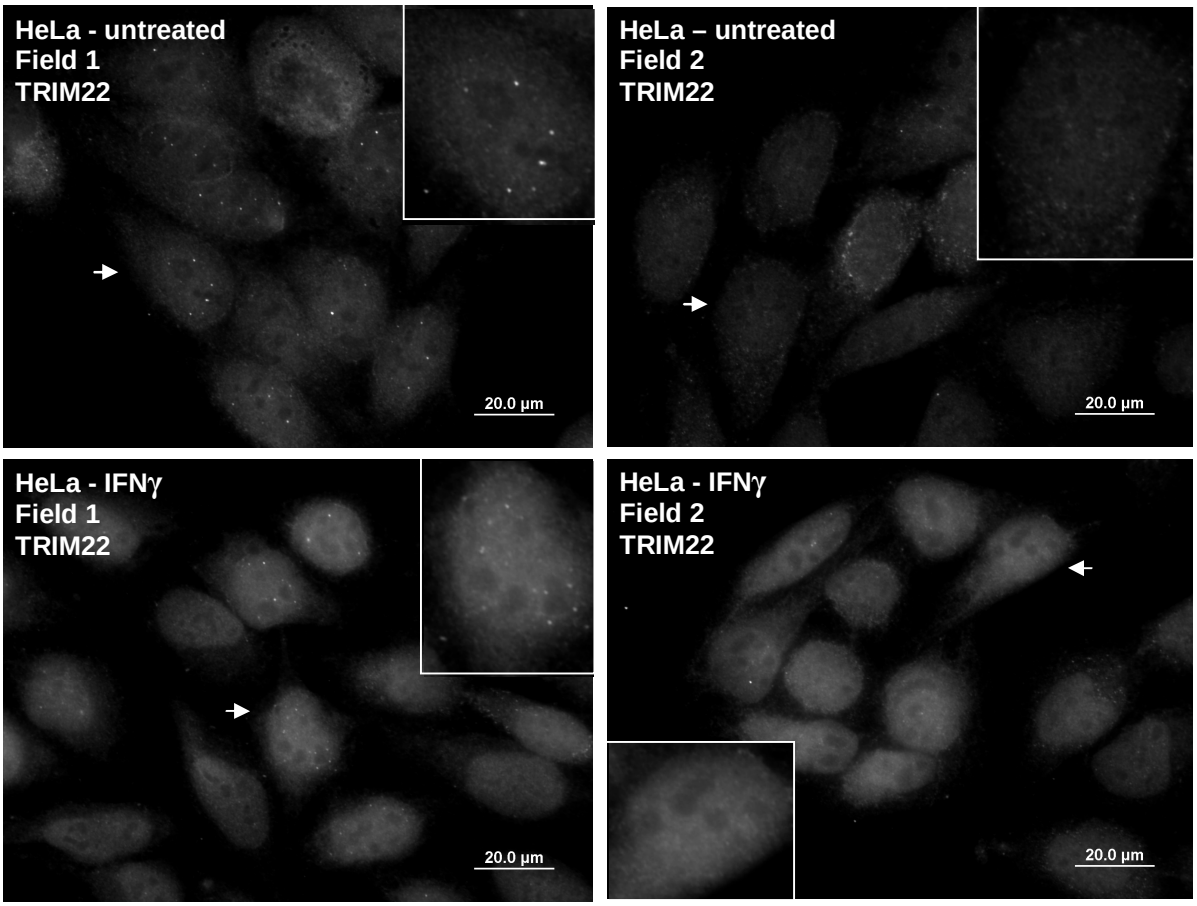
HeLa - untreated
Field 1
TRIM22
20.0 µm
HeLa – untreated
Field 2
TRIM22
20.0 µm
HeLa - IFNγ
Field 1
TRIM22
20.0 µm
HeLa - IFNγ
Field 2
TRIM22
20.0 µm

D - continuation

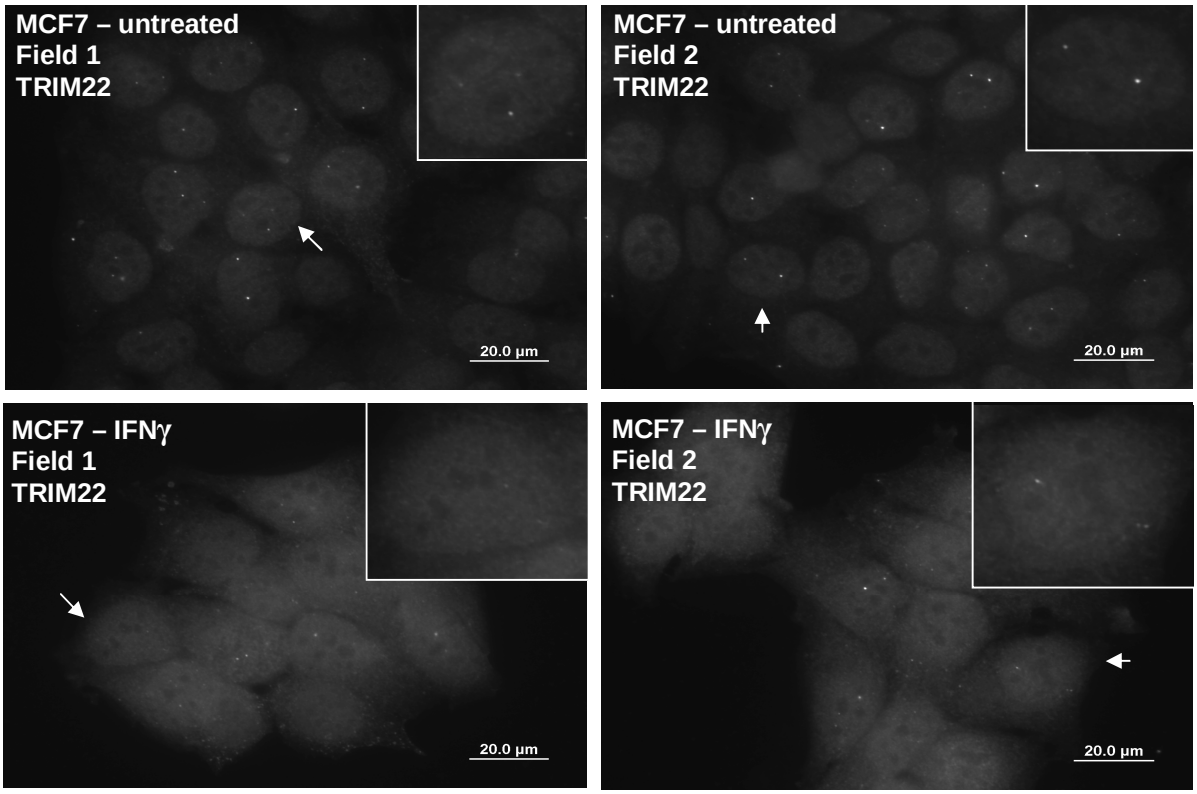

Figure 3.13 Endogenous TRIM22 is a nuclear protein that forms distinct nuclear and nucleolar bodies.
(A) Endogenous TRIM22 localizes as a nucleoplasmic protein and as nuclear bodies in MCF12A cells (left panel). MCF12A cells were also immunostained with the same dilution of pre-immune mouse serum as a control (right panel). **(B)** Endogenous TRIM22 forms nuclear and nucleolar bodies in progesterone-treated cells. ABC28 cells treated with ethanol (E) or 10 nM progesterone (P) for 48 hr were immunostained to detect TRIM22 (red) and fibrillarin (green) as a nucleolar marker. Cells were counterstained with DAPI (blue). Merged images are presented showing colocalizations (yellow). **(C)** TRIM22 only localizes as a nucleoplasmic protein in T47D cells. T47D cells treated with ethanol (E) or 100 nM progesterone (P) for 24 hr were immunostained with the anti-TRIM22 antibody. **(D)** HeLa and MCF7 cells left untreated or treated with IFNγ (250 IU/ml) for 24 hr were immunostained as in **(C)**. **(A - D)** All cells were visualized by fluorescence microscopy at a 60X or 96X magnification and images of the same cell type were taken with the same exposure times and camera gain/offset. Bars, 10 or 20 µm. Insets show representative cells (arrows) enlarged 2X. Results are representative of two independent experiments.

To check if the nuclear and nucleolar bodies detected in ABC28 cells by the antibody are indeed TRIM22 bodies, two experiments were performed. In the first experiment, ABC28 cells treated with 10 nM progesterone and transiently expressing FLAG-TRIM22 were immunostained with mouse anti-TRIM22 and rabbit anti-FLAG antibodies (**Figure 3.14A**). We anticipated that the TRIM22 antibody would bind to both endogenous TRIM22 and FLAG-TRIM22 and the anti-FLAG antibody would only bind to the FLAG-TRIM22. If the antibody did detect endogenous TRIM22, then a green signal would be largely absent and that there would be a predominant yellow signal reflecting FLAG-TRIM22 bodies or heterogeneous bodies comprised of both endogenous TRIM22 and FLAG-TRIM22. If the endogenous protein was not TRIM22, then TRIM22 antibody would not bind to FLAG-TRIM22 resulting in distinct green and red bodies. As expected, in the majority of cells transfected with FLAG-TRIM22, there was a high degree of overlay between FLAG-TRIM22 (green) and endogenous TRIM22 (red), resulting in a predominant yellow signal. Therefore, the TRIM22 antibody and FLAG antibody detected the same protein in these cells. As expected, there was also some red signal, perhaps due to the inability of FLAG-TRIM22 to penetrate the dense bodies formed by endogenous TRIM22 as soon as it was expressed. These observations allow us to conclude that the NB detected by the anti-TRIM22 antibody are indeed TRIM22 NB. The aggregation of endogenous TRIM22 with FLAG-TRIM22 was also observed within nucleoli (field 2; **Figure 3.14A**).

In the second experiment, the staining pattern of the TRIM22 antibody in control siRNA and TRIM22 siRNA transfected cells was compared. **Figure 3.14B** shows representative

images of 10 nM progesterone-treated ABC28 cells that were untransfected, transfected with control siRNA or with TRIM22 siRNA 6 or 7 and then immunostained with the TRIM22 antibody. The numbers of cells having nuclear and/or nucleolar bodies were also quantitated (**Figure 3.14C**). There was an obvious reduction in the nucleoplasmic staining and some reduction in the intensity of the NB observed with the TRIM22 siRNA transfected cells compared to the control siRNA transfected cells (**Figure 3.14B**). Compared to the control siRNA-transfected cells, of which around 50% had nucleolar bodies, only 7 – 12% of TRIM22 siRNA 6 and 7 transfected cells had nucleolar TRIM22 bodies (**Figure 3.14C**). On the other hand, the numbers of TRIM22 siRNA-transfected cells having NB identified by the TRIM22 antibody were not reduced (**Figure 3.14C**). Since we have shown that the TRIM22 siRNA used in this study is very effective in reducing the levels of the TRIM22 protein (**Figure 3.9B**), the NB that remained may be the pre-existing TRIM22 protein. Indeed, Li et al. (2006) found FLAG-TRIM22 to be a very stable protein whose levels were unaffected by a 7-hr cycloheximide treatment. However, the reduction in intensity of the NB in the TRIM22 siRNA-transfected samples in **Figure 3.14B** suggests these are TRIM22 bodies. The observations that 1) FLAG-TRIM22 could be detected with the TRIM22 antibody and possibly aggregated with the nuclear and nucleolar bodies identified by the TRIM22 antibody and that 2) there was an obvious reduction in nucleolar bodies and nucleoplasmic staining with a slight reduction in intensity of NB in TRIM22 siRNA transfected cells confirm that endogenous TRIM22 exists as nuclear and nucleolar bodies.

A

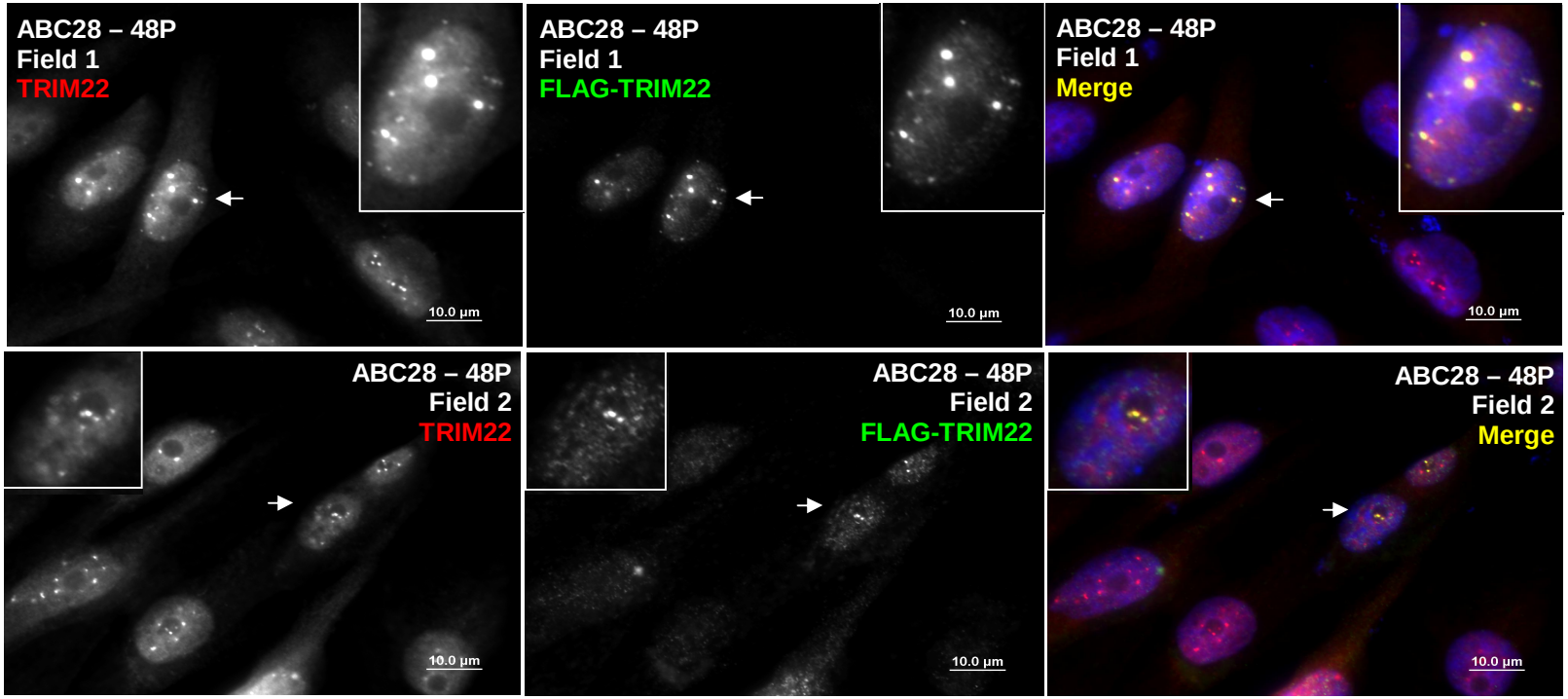
ABC28 – 48P
Field 1
TRIM22
10.0 µm
ABC28 – 48P
Field 1
FLAG-TRIM22
10.0 µm
ABC28 – 48P
Field 1
Merge
10.0 µm
ABC28 – 48P
Field 2
TRIM22
10.0 µm
ABC28 – 48P
Field 2
FLAG-TRIM22
10.0 µm
ABC28 – 48P
Field 2
Merge
10.0 µm

B

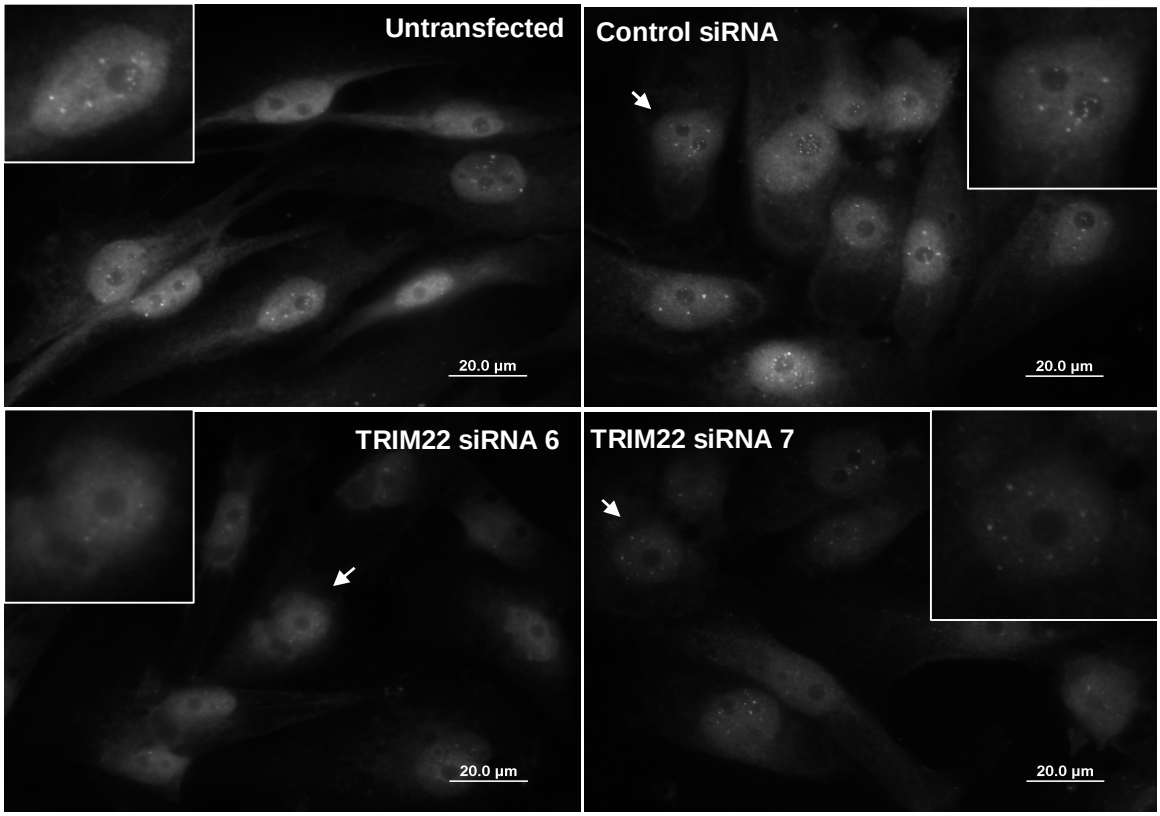
Untransfected
Control siRNA
TRIM22 siRNA 6
TRIM22 siRNA 7
20.0 µm
20.0 µm
20.0 µm
20.0 µm

C

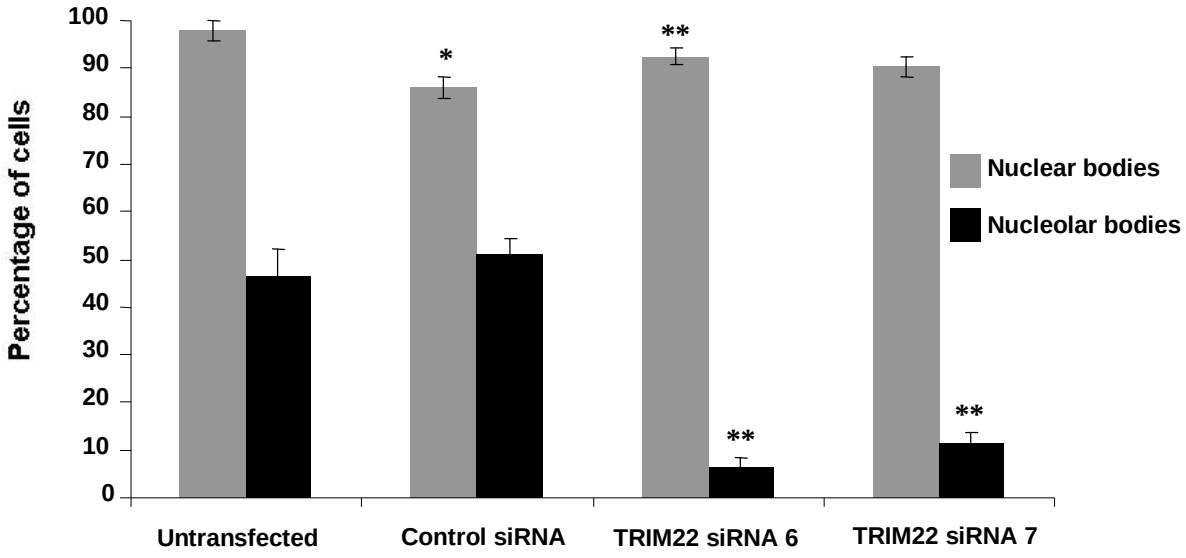
Percentage of cells
100
90
80
70
60
50
40
30
20
10
0
*
**
**
**
Nuclear bodies
Nucleolar bodies
Untransfected
Control siRNA
TRIM22 siRNA 6
TRIM22 siRNA 7

Figure 3.14 Nucleolar bodies, but not nuclear bodies, are greatly reduced upon TRIM22 knockdown

(A) Endogenous nuclear bodies detected with the anti-TRIM22 antibody colocalize with overexpressed TRIM22 nuclear bodies. ABC28 cells treated with progesterone (10 nM) and simultaneously transfected with FLAG-TRIM22 were immunostained with mouse anti-TRIM22 and rabbit anti-FLAG antibodies to detect endogenous (red) and overexpressed (green) TRIM22. Cells were visualized by fluorescence microscopy at a 96X magnification. Bars, 10 μm. **(B)** ABC28 cells were left untransfected or transfected with control siRNA or TRIM22 siRNA 6 or 7 (10 nM) before treatment with 10 nM progesterone for 48 hr. Cells were immunostained with anti-TRIM22 antibody and then visualized by fluorescence microscopy at 60X magnification. Images were taken with the same exposure times, camera gain, and offsets. Bars, 20 μm. Result is representative of two independent experiments. (**A, B)** Insets show representative cells (arrow) enlarged 2X. **(C)** Numbers of ABC28 cells expressing nuclear and nucleolar TRIM22 bodies were quantitated in two independent experiments (untransfected, n = 145; control siRNA, n = 263; TRIM22 siRNA 6, n = 213; TRIM22 siRNA 7, n = 209). Percentage of cells having nuclear and nucleolar TRIM22 bodies presented. Error bars reflect standard error of the mean (SEM). **P<0.05,* versus untransfected; ***P<0.05,* versus control siRNA.

3.7 TRIM22 localization varies in a cell state-dependent manner

3.7.1 Growth inhibition reduces numbers of TRIM22 NB while growth stimulation enhances numbers of TRIM22 NB.

In initial studies of TRIM22 localization, there appeared to be vast differences in the numbers and sizes of the NB formed by TRIM22-EGFP. Was this due to cells expressing different levels of the protein or was this an inherent property of the protein to aggregate and disperse depending on the state of the cell? To answer these questions, MCF7 cells, which express the least TRIM22 transcript (result not shown) and very low levels of the TRIM22 protein (**Figure 3.9**) were stably transfected with the TRIM22-pEGFP-N1 construct to generate MCF7-TRIM22-EGFP cells. These cells were then sorted to obtain a high percentage of cells with moderate fluorescence.

MCF7 or MCF7-TRIM22-EGFP cells were subjected to growth inhibition and growth stimulation protocols in order to investigate the size and numbers of the TRIM22 bodies in these cells. MCF7 cells were growth inhibited by exposure to low quantities of methotrexate (an inhibitor of DNA, RNA and protein synthesis resulting in a S phase block). To test the effects of growth inhibition by serum starvation, MCF7-TRIM22-EGFP cells were serum starved for 72 hr (to achieve a G0/G1 phase block). To stimulate cell growth, MCF7-TRIM22-EGFP cells were treated with serum after a 24-hr serum-starvation period.

In an asynchronous population, MCF7 or MCF7-TRIM22-EGFP cells typically expressed one to four TRIM22 bodies (10% serum control panel in **Figure 3.15A** and 10% serum

panel in **Figure 3.15C**). Growth inhibition by methotrexate treatment led to a dispersal of TRIM22 NB such that the endogenous protein assumed a more diffuse distribution (**Figure 3.15A**). On the other hand, serum starvation reduced the numbers of TRIM22-EGFP bodies to one or two per cell (0% serum (72 hr) panel in **Figure 3.15B**). Apart from a reduction in the numbers of bodies per cell, the TRIM22-EGFP bodies in serum-starved cells were not much brighter than those in the serum-treated cell population (**Figure 3.15B**). Of note, cells treated with serum for 24 or 72 hr [10% serum (24 hr) panel in **Figure 3.15C** and 10% serum control (72 hr) in **Figure 3.15B**] had a much greater incidence of multiple, dispersed bodies compared to the serum-starved population (0% serum control (24 hr) in **Figure 3.15C** and 0% serum (72 hr) in **Figure 3.15B**). These observations suggest that TRIM22 bodies undergo dynamic changes in distribution within nuclei and that their distribution correlates with cell state.

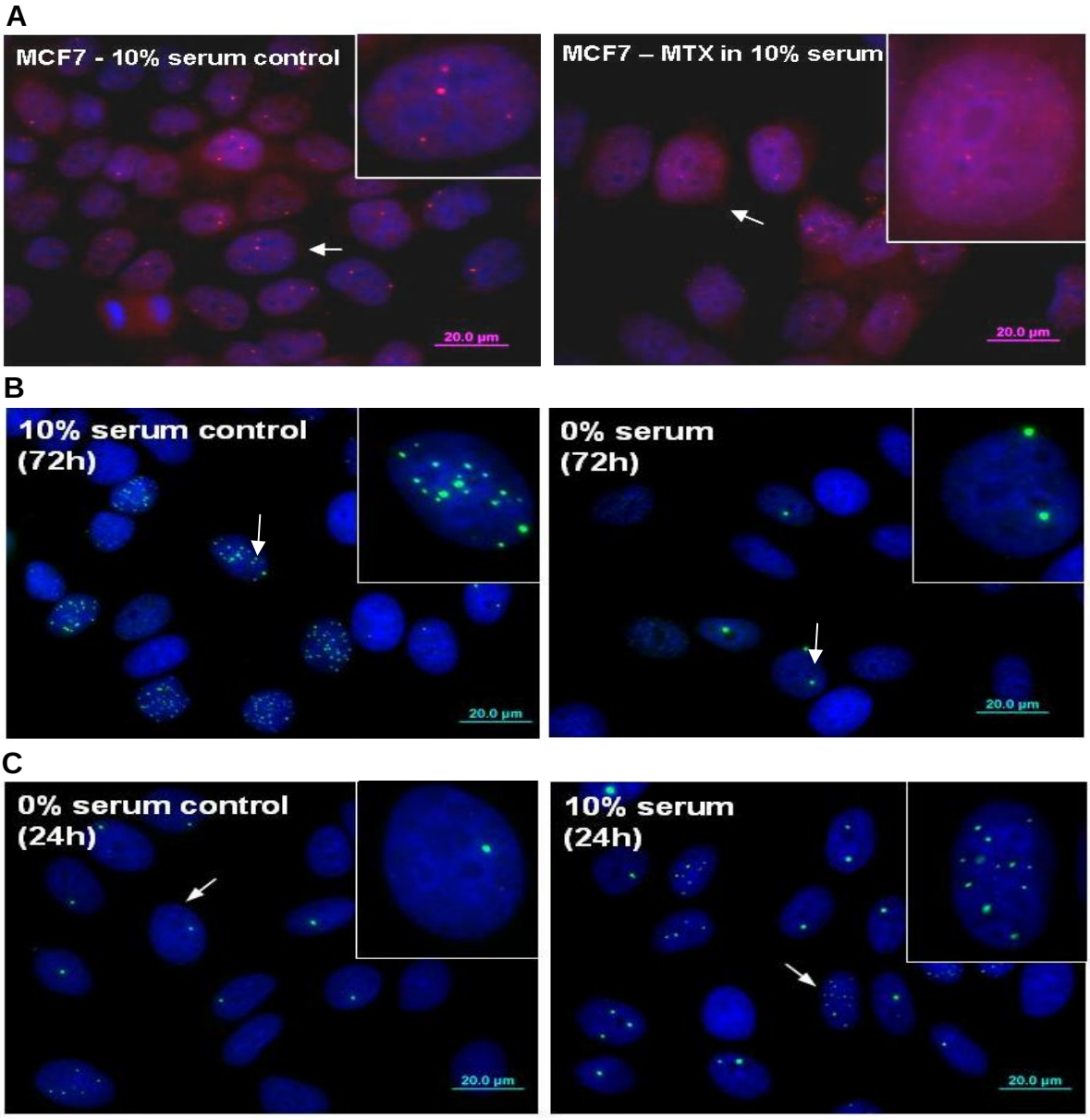

Figure 3.15 TRIM22 bodies undergo dynamic changes in size and numbers in response to methotrexate treatment, serum deprivation and serum treatment.
(A) Methotrexate treatment induces a dispersion of TRIM22 NB. MCF7 cells were plated in normal growth media (containing 10% FCS) and 48 hr later, left untreated (10% serum control) or were treated with methotrexate (10 µM; MTX in 10% serum). 48 hr later, cells were immunostained with anti-TRIM22 antibody, counterstained with DAPI and visualized by fluorescence microscopy at a 60X magnification. Bars, 20 µm. Images were taken with the same exposure time and camera gain/offset. **(B)** Serum deprivation reduces the number of TRIM22-EGFP bodies. MCF7 cells stably expressing TRIM22-EGFP (MCF7-TRIM22-EGFP) were cultured in 10% serum-containing media (10% serum control) or in serum-free media (0% serum) for 72 hr. **(C)** Serum treatment increases the number of TRIM22-EGFP bodies. MCF7-TRIM22-EGFP cells were serum starved for 72 hr before being cultured in serum-free media (0% serum control) or in 10% serum-containing media (10% serum) for 24 hr. **(B, C)** Cells were stained with DAPI and visualized by fluorescence microscopy at a 60X magnification. Bars, 20 µm. Insets for all panels show representative cells (arrows) enlarged 2.5X. **(A – C)** Results are representative of two independent experiments.

3.7.2 Cell cycle distribution of TRIM22-EGFP in HeLa cells

The changes in numbers and sizes of TRIM22-EGFP bodies in response to growth inhibition and stimulation suggested that these bodies exhibit cell-cycle dependent changes. To investigate if the distribution of TRIM22-EGFP would vary at different stages of the cell cycle, cells were synchronized using the double thymidine block method. Thymidine block is achieved by adding excessive amounts of the deoxyribonucleoside thymidine to block DNA replication and thereby arrest cells at the G1/S border. However, this protocol is only effective in cells without an intact p53 apoptotic response. Releasing the cells from the thymidine block would then allow the G1 phase cells to move in a highly synchronous fashion through the cell cycle.

HeLa cells lack a functional p53 response and are known for their ease of synchronization by the double thymidine block method. Therefore, HeLa cells stably expressing low to moderate levels of TRIM22-EGFP (HeLa-TRIM22-EGFP) were generated by transfecting HeLa cells with TRIM22-pEGFP-N1, selecting fluorescent cells in G418 media and then sorting cells to enrich for TRIM22-EGFP cells. These cells were grown to a subconfluent density (60%) in normal growth media, subjected to a 16-hr thymidine (2.5 mM) block, a 12-hr release period and another 16-hr thymidine (2.5 mM) block before cell cycle analysis. Cells were subsequently analysed by flow cytometry. A relatively high percentage of cells in the G0/G1 (72.2% at 14 hr post-release), S (68.9 – 70.8% at 3 - 5 hr post release), and G2/M (66.4% at 8 hr post-release) phases could be reproducibly achieved after releasing these cells from the double thymidine block (**Figure 3.16A**).

Using a duplicate set of cells grown on coverslips, the numbers, sizes and distribution of TRIM22-EGFP bodies could be determined in these cells at fixed time points after removal of the double thymidine block. It appeared that cells at the G1/S boundary displayed regular TRIM22-EGFP bodies (0 hr, **Figure 3.16B**). When allowed to progress into the S-phase of the cycle, TRIM22-EGFP assumed a speckled pattern in the vast majority of these cells observed (3 and 5 hr, **Figure 3.16B**). The speckled pattern was also observed in cells that had a distinct nuclear boundary in the G2/M population. During M phase, when DNA condenses and segregates, TRIM22-EGFP became completely diffused (7 hr, **Figure 3.16B**). The diffused localization of TRIM22-EGFP was also observed in cells in telophase (Panel * in 8 hr, **Figure 3.16B**). Regular multiple TRIM22 bodies were evident in cells undergoing cytokinesis (Panel ** in 14 hr, **Figure 3.16B**) and were present after the cells entered G0/G1 phase (14 hr, **Figure 3.16B**). Interestingly, TRIM22-EGFP bodies appeared to be localized frequently within and next to nucleoli in cells that had entered the G0/G1 phase (14 hr, **Figure 3.16B**). The changes observed in the distribution of TRIM22-EGFP in different phases of the cell cycle are unlikely to be due to changes in level of TRIM22-EGFP expression levels as Western blotting analysis showed that TRIM22-EGFP protein levels was relatively constant during different phases of cell cycle (**Figure 3.16C**).

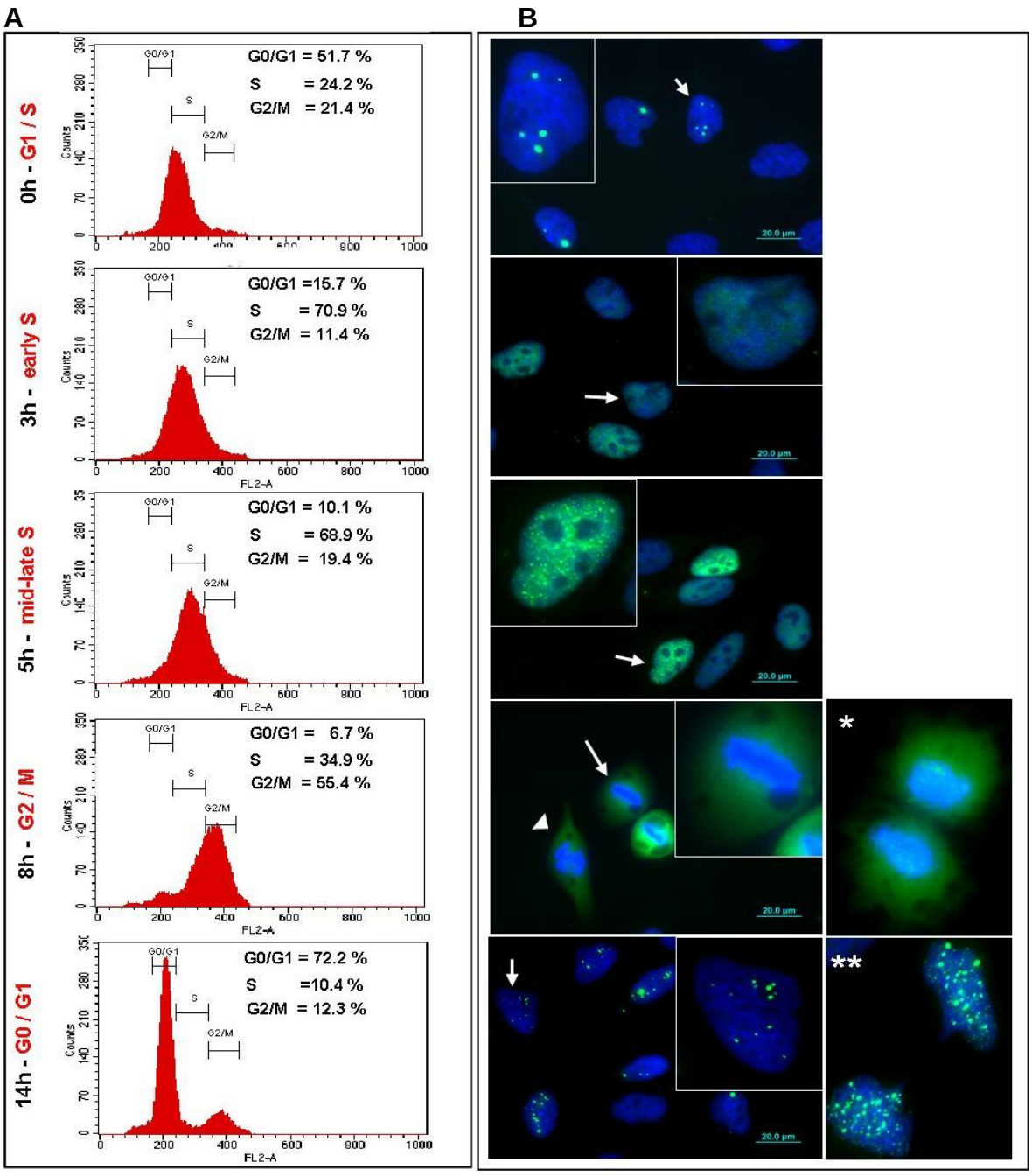
A
B
0h - G1 / S
G0/G1 = 51.7 %
S = 24.2 %
G2/M = 21.4 %
3h - early S
G0/G1 =15.7 %
S = 70.9 %
G2/M = 11.4 %
5h - mid-late S
G0/G1 = 10.1 %
S = 68.9 %
G2/M = 19.4 %
8h - G2 / M
G0/G1 = 6.7 %
S = 34.9 %
G2/M = 55.4 %
14h - G0 / G1
G0/G1 = 72.2 %
S =10.4 %
G2/M = 12.3 %
Counts
FL2-A
20.0 µm
*
**

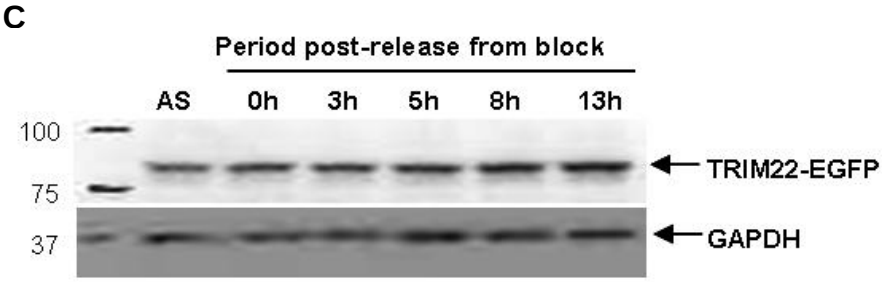
C
Period post-release from block
AS
0h
3h
5h
8h
13h
100
75
37
TRIM22-EGFP
GAPDH

Figure 3.16 Dynamics of TRIM22 bodies during the cell cycle.
(A) HeLa cells stably expressing TRIM22-EGFP were synchronized by the double thymidine block and cell cycle distribution at different time points after synchronization was analyzed by flow cytometry. Percentages of cells in each phase of the cycle are indicated. **(B)** TRIM22-EGFP bodies (0 hr) progressively assumed a speckled pattern (3 – 5 hr) and ultimately as a diffuse protein (8 hr and panel *) when progressing through the S and G2/M phases. Distinct bodies that reform after during cytokinesis (panel **) localize to nucleoli in the G0/G1 phase (14 hr). Samples synchronized on coverslips were DAPI stained and visualized by fluorescence microscopy at a 60X magnification. Bars, 20 μm. Insets show representative cells (arrows) enlarged 2.5X. **(C)** TRIM22-EGFP expression levels remain constant through the cell cycle. Whole cell lysates from asynchronous cells (AS) and cells collected at the different time points after synchronization were subjected to Western blotting analysis using anti-GFP and anti-GAPDH antibodies to detect TRIM22-EGFP (~ 80 kDa) and GAPDH (37 kDa; loading control) respectively. **(A – C)** Results are representative of three independent experiments.

3.8 Localization of TRIM22 deletion mutants

The Reymond et al. (2001) and Li et al. (2007) studies, which reported that TRIM22 localizes as diffuse cytoplasmic speckles with some nuclear staining, used the sequence coding for a 442 aa protein. However, there are seven nucleotide sequence entries for TRIM22 in the NCBI database, representing four different sequences in all (**Table 3.1**). Two of these sequences code for larger 498 aa proteins (termed as "full length"), whilst the remaining two are N and C-terminal truncation variants that code for 442 aa and 273 aa proteins respectively. Knowledge that the full-length TRIM22 protein localizes as distinct NB and not as cytoplasmic speckles or aggregates that was observed with the shorter variant prompted an investigation into the role of the different domains of the TRIM22 protein in modulating the localization of the protein. To this end, different N and C terminal deletion mutants of the full-length protein and a NLS-deficient mutant were cloned into the pXJ-FLAG vector (**Figure 3.17**). The mutants produced proteins of expected sizes when analyzed by Western blotting (**Figure 3.18**). The constructs were transfected into MCF7 cells, which were immunostained with the anti-FLAG antibody and co-stained with DAPI 24 - 48 hr later. The locations of the exogenous proteins were visualized by fluorescence microscopy using band pass filters (**Figure 3.19**). To exclude artifacts resulting from excessive overexpression, all images shown in **Figure 3.19** are of cells with relatively low levels of FLAG-tagged TRIM22 and mutants.

Deletion construct	Protein map	Regions absent	Predicted MW (kDa)
TRIM22	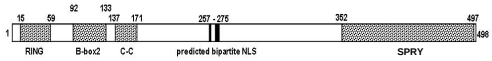	--	58.8
TRIM22-SPRYΔ4	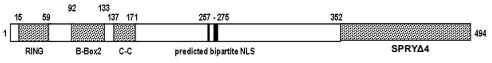	4 aa in SPRY	58.3
TRIM22-SPRYΔ5	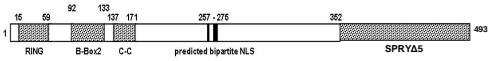	5 aa in SPRY	58.2
TRIM22-SPRYΔ9	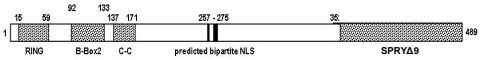	9 aa in SPRY	57.8
TRIM22-SPRYΔ14	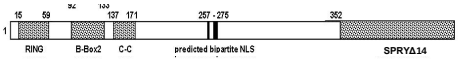	14 aa in SPRY	57.2
TRIM22-SPRYΔ19	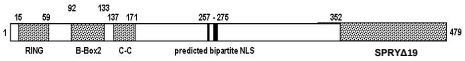	19 aa in SPRY	56.5
TRIM22-SPRYΔ29	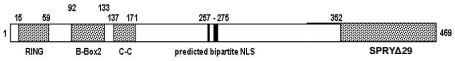	29 aa in SPRY	55.4
TRIM22-ΔSPRY	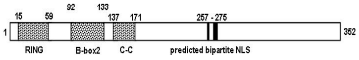	SPRY	41.5
TRIM22-ΔSPRY/CC	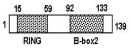	CC, SPRY	17.0
TRIM22-ΔSPRY/CC/B2		B-box2, CC, SPRY	8.7
TRIM22-ΔRING	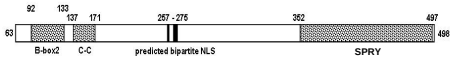	RING	51.1
TRIM22-ΔRING/B2	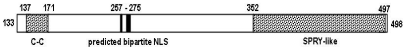	RING, B-box2	43.0
TRIM22-ΔRING/B2/CC	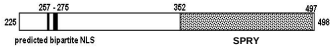	RING, B-box2, CC, 53 aa	38.4
TRIM22-ΔRING/B2/CC/182		RING, B-box2, CC, 182 aa	17.7
TRIM22-ΔNLS		Predicted bipartite NLS	57.0

Figure 3.17 TRIM22 deletion mutants generated to investigate the contribution of the different domains to TRIM22 nuclear localization.

Different C- and N-terminal deletion mutants of the full-length TRIM22 protein and an NLS-deficient mutant were cloned into the pXJ-FLAG vector. The maps of these mutants and their predicted sizes (including the FLAG tag) are shown above.

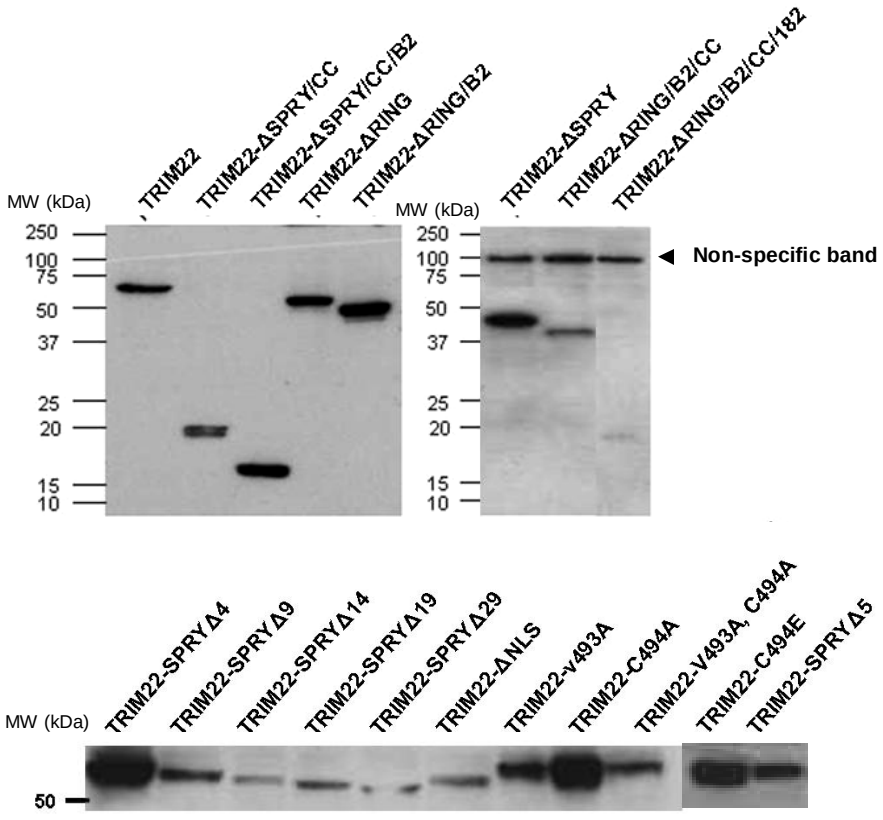

Figure 3.18 TRIM22 mutant constructs code for proteins of predicted sizes.
Western blotting analysis of TRIM22 deletion and point mutants. Whole cell lysates were collected from MCF7 or HeLa cells expressing the different mutants. 10 – 40 µg of lysates were subjected to SDS-PAGE and Western blotting using the anti-FLAG antibody. A non-specific band at around 100 kDa is always detected with this antibody.

3.8.1 The putative bipartite NLS is unlikely to be the motif solely responsible for nuclear localization of TRIM22

Tissot and Mechti predicted the presence of a bipartite NLS (KRSESWTLKKPKSVSKKLK) from residues 257 – 275 of the TRIM22 sequence when they first cloned the *TRIM22* gene (Tissot and Mechti, 1995). As the contribution of this motif to the nuclear localization of TRIM22 has not been reported before, the localization of a NLS-deficient TRIM22 mutant (TRIM22-ΔNLS) was first investigated. Deletion of the putative NLS motif resulted in a 57 kDa protein that was localized in both the nucleus and the cytoplasm in a diffuse fashion (**Figure 3.19**). The observation that this mutant was still able to enter the nucleus suggested that the bipartite NLS may not be the only motif responsible for the nuclear localization of TRIM22.

3.8.2 The SPRY domain contributes to nuclear localization of TRIM22

To identify other motifs responsible for the nuclear localization of TRIM22, the protein was sequentially truncated from the N-terminus. Deletion of the RING domain (TRIM22-ΔRING) abolished the formation of distinct bodies but the protein was still primarily localized in the nucleus (**Figure 3.19**). Further deletion of B-box2 domain from TRIM22-ΔRING mutant (TRIM22-ΔRING/B2) led to the formation of a ring around the nucleus in cells expressing larger amounts of the protein (**Figure 3.19**). Nonetheless, in cells expressing low levels of the protein, a large proportion of the protein was still localized in the nucleus. Therefore, the sequence required for nuclear localization is unlikely to be in the RING or B-box2 domains.

The other major domain that varies amongst the different TRIM proteins and is of considerably interest to the localization and function of these proteins is the C-terminal SPRY domain. To investigate the role of this domain to TRIM22's localization, 29 aa from the 145 aa SPRY domain (TRIM22-SPRYΔ29) was deleted from the C-terminal end. This was adequate to abolish TRIM22's nuclear localization, with exclusive presence as a diffuse cytoplasmic protein (**Figure 3.19**). Therefore, the last 29 aa of the SPRY domain are likely to contain the residues important for the nuclear localization of TRIM22. To investigate if the SPRY domain alone was adequate for nuclear localization, the TRIM22-ΔRING/B2/CC/182 mutant encoding just the SPRY domain was generated. This mutant formed cytoplasmic aggregates. Although the size of the aggregates may have prevented the mutant protein from entering the nucleus, the absence of this mutant from the nucleus suggests that residues in both the bipartite NLS motif and the last 29 aa of the SPRY domain may be required for the nuclear localization of TRIM22. This postulation is further supported by the evidence that all deletion mutants with intact SPRY domains and NLS motifs (TRIM22-ΔRING, TRIM22-ΔRING/B2, TRIM22-ΔRING/B2/CC) were localized predominantly in the nucleus. Given the small molecular sizes of the TRIM22-ΔSPRY/CC and TRIM22-ΔSPRY/CC/B2 mutants (17 kDa and 8.7 kDa, respectively), it was not surprising to find them located diffusely in both the cytoplasm and the nucleus (**Figures 3.17, 3.19**).

3.8.3 Residues 480 - 494 of the TRIM22 protein are important for its nuclear localization

Having shown that removing the last 29 aa of the SPRY domain abrogated TRIM22's nuclear localization, we were keen to identify a minimal stretch within these 29 residues. Deleting the last 4 aa (TRIM22-SPRYΔ4; residues 495 – 498) did not alter the localization of TRIM22 as distinct NB (**Figure 3.20**). However, deleting the last 5 aa (TRIM22-SPRYΔ5; residues 494 - 498) resulted in the mutant localizing in both the nucleus and cytoplasm as a diffuse protein. Therefore, nuclear localization was compromised. Deleting 9 (TRIM22-SPRYΔ9; residues 490 – 498) or 14 aa (TRIM22-SPRYΔ14; residues 485 – 498) further compromised nuclear localization with increasingly greater cytoplasmic localization. Deleting 19 aa (TRIM22-SPRYΔ19; residues 480 – 498) abrogated nuclear localization with the protein localizing exclusively in the cytoplasm as a diffuse protein (**Figure 3.20**). These observations provide evidence that residues 480 - 494 are all likely to be important for the optimal folding of TRIM22 and its localization within the nucleus. This is in contrast to the N-terminal end of the protein, which when deleted (resulting in TRIM22-ΔRING), does not compromise nuclear localization.

3.8.4 Residues V493 and C494 are critical for the formation of regular TRIM22 bodies

Using the specific TRIM22 antibody, it was clear that the endogenous protein also exists as distinct NB, with a dramatic localization of these bodies within nucleoli in progesterone-treated cells. The formation of distinct bodies may therefore have a

functional significance. In the search for the determinants of TRIM22 nuclear localization, it emerged that deleting the RING domain greatly abrogated TRIM22 body formation. Absence of the cysteine residue at position 494 also clearly abrogated NB formation (TRIM22-SPRYΔ5, **Figure 3.20**). To investigate if a disulphide bond formed between this cysteine residue and another cysteine residue in the protein was critical for NB formation, we mutated C494 to either an alanine residue (TRIM22-C494A) or a glutamic acid residue (TRIM22-C494E). Both point mutants continued to localize as NB (**Figure 3.21**). Therefore, C494 is critical for NB formation not because of a disulphide bond. Rather, it is the spatial positioning of the residue that is critical for this process.

Unlike TRIM22, TRIM6 and TRIM5α exist as cytoplasmic speckles (Reymond et al., 2001). The localization of TRIM34 is not known. Alignment of the human TRIM22 protein with its closest paralogs TRIM34, TRIM6, and TRIM5α showed that the valine residue at position 493 (V493) in TRIM22 is the only residue within the last 9 aa stretch that set it apart from its paralogs, all of which have a leucine (L) residue in place of the valine (V) (**Figure 3.21A**). However, mutating V493 to a leucine residue (TRIM22-V493L) did not change the localization of TRIM22 as NB and bodies looked very similar to those formed by wild-type TRIM22 (**Figure 3.21B**). In contrast, mutating V493 to an alanine residue (TRIM22-V493A) disrupted the formation of regular bodies, resulting in a hollow-ring phenomenon in as many as 75% of bodies observed (**Figure 3.21B**). Although some TRIM22 NB also appeared ring-shaped in some cases (as in **Figure 3.15B, C)**, the frequency of these was much less and the ring-shaped bodies much smaller than those formed by TRIM22-V493A.

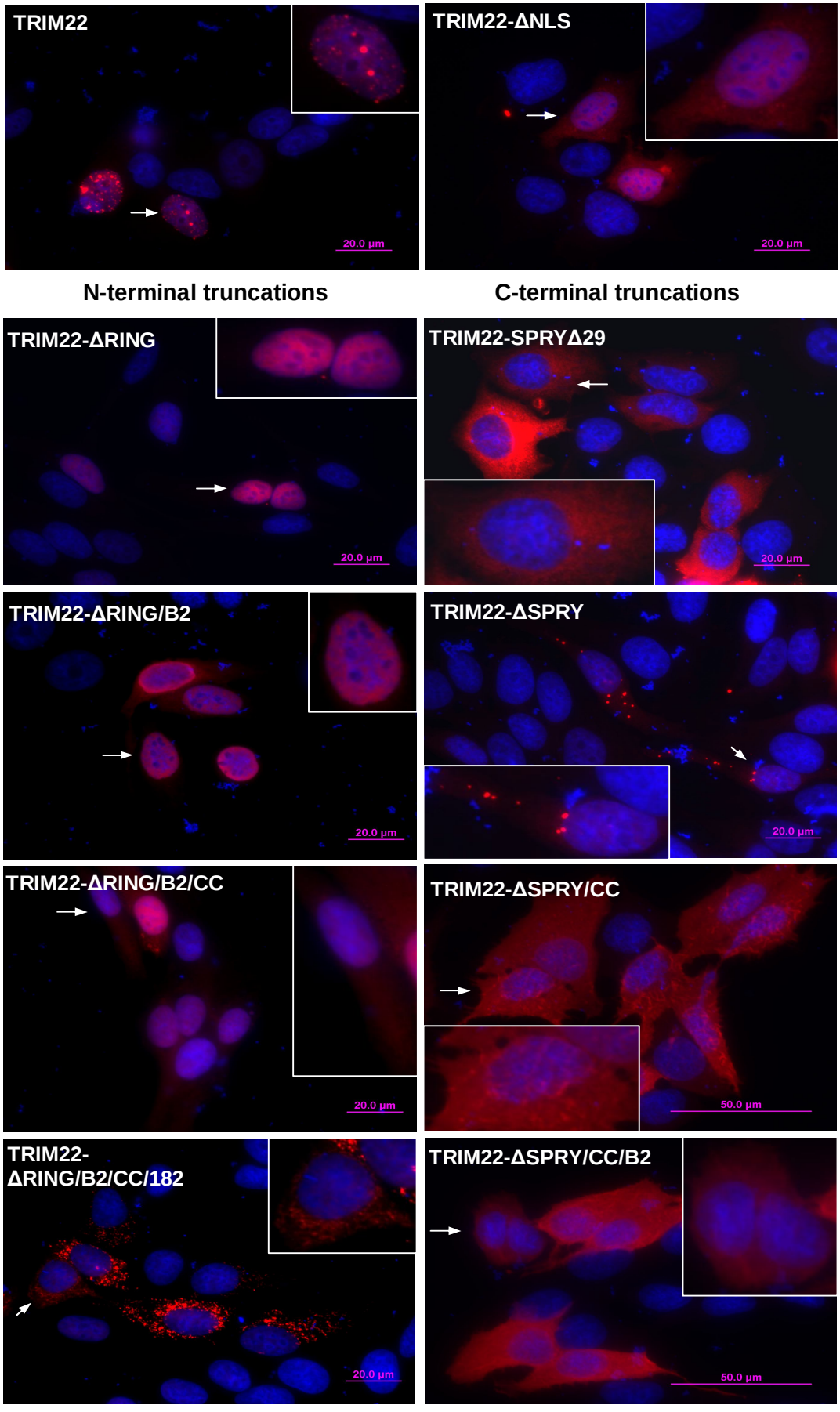
TRIM22
20.0 µm
TRIM22-ΔNLS
20.0 µm
N-terminal truncations
C-terminal truncations
TRIM22-ΔRING
20.0 µm
TRIM22-SPRYΔ29
20.0 µm
TRIM22-ΔRING/B2
20.0 µm
TRIM22-ΔSPRY
20.0 µm
TRIM22-ΔRING/B2/CC
20.0 µm
TRIM22-ΔSPRY/CC
50.0 µm
TRIM22-
ΔRING/B2/CC/182
20.0 µm
TRIM22-ΔSPRY/CC/B2
50.0 µm

Figure 3.19 Localization of TRIM22 deletion mutants.
Localization of various TRIM22 deletion mutants. MCF7 cells expressing the different deletion mutants were immunostained with anti-FLAG antibody and counterstained with DAPI. Cells were imaged at a 60X magnification. Bars, 20 µm or 50 µm. Insets show representative cells (arrows) enlarged 2X. Results are representative of at least two independent experiments.

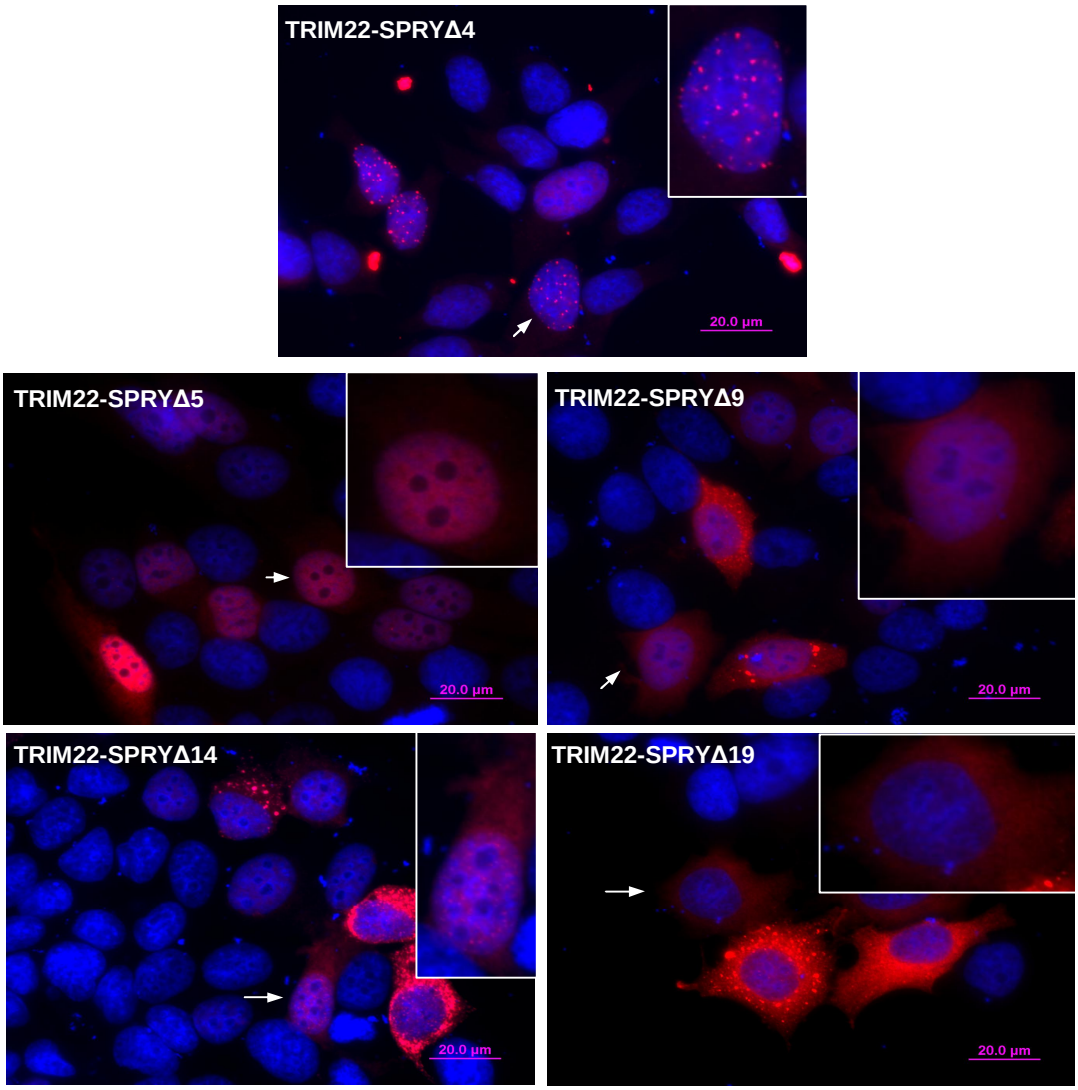

Figure 3.20 Residues 480 – 494 in the SPRY domain are required for formation of TRIM22 nuclear bodies and nuclear localization.
Localization of TRIM22 mutants lacking 4, 5, 9, 14 and 19 aa of the SPRY domain. MCF7 cells expressing the different deletion mutants were immunostained with anti-FLAG antibody and counterstained with DAPI. Cells were imaged at a 60X magnification. Bars, 20 µm. Insets show representative cells (arrows) enlarged 2X. Results are representative of at least two independent experiments.

As both valine and leucine are hydrophobic amino acids, the replacement of valine with leucine may have been inadequate to disrupt the structure of the protein, which was achieved when valine was replaced with the small amino acid alanine. We also noted that when both V493 and C494 residues were mutated to alanine residues (TRIM22-V493A,C494A) the propensity to form regular bodies was reduced. The propensity to form regular bodies was judged by comparing the intensity of the NB to the intensity of the nucleoplasmic fluorescence. As shown in **Figure 3.21C**, it can be seen that the wild-type TRIM22 protein, TRIM22-V493L, and TRIM22-C494A mutant proteins were able to form bodies with weak nucleoplasmic staining. At the same exposure, however, the TRIM22-V493A,C494A double mutant had a higher nucleoplasmic fluorescence. Collectively, our results show that V493 and C494 in the SPRY domain of TRIM22 are important for the proper folding of TRIM22 and resultant body formation.

3.8.5 TRIM22 aggregation is due to the exposure of a self-interaction motif on the surface

Li et al. (2007a) showed that FLAG-TRIM22, like TRIM34, TRIM6 and TRIM5α exists as trimers in HeLa cells. Our observations of distinct TRIM22-EGFP NB also suggest that TRIM22 forms multimers with itself. These findings are in line with the presence of the CC motif, found to be responsible for TRIM protein dimerization or multimerization, in TRIM22. In this study, to investigate TRIM22 self-interaction, MCF7 cells were transiently transfected with TRIM22-EGFP and subjected to live-cell imaging over a 20 hr period. Imaging revealed that the TRIM22-EGFP bodies were expressed in the

A

TRIM22	479	YPYFNPWNCLVPMT**VC**PPSS	498
TRIM34	469	YPYFNPWNCPAPMTLCPPSS	488
TRIM6	497	CPYFNP C NCVIPMTLRRPSS	516
TRIM5α	474	FPYLNPR KCGVPMTLCSPSS	493

B

TRIM22	479	YPYFNPWNCLVPMT**VC**PPSS	498
TRIM22-C494A	479	YPYFNPWNCLVPMTV**A**PPSS	498
TRIM22-C494E	479	YPYFNPWNCLVPMTV**E**PPSS	498
TRIM22-V493L	479	YPYFNPWNCLVPMT**L**CPPSS	498
TRIM22-V493A	479	YPYFNPWNCLVPMT**A**CPPSS	498
TRIM22-V493A, C494A	479	YPYFNPWNCLVPMT**AA**PPSS	498

C

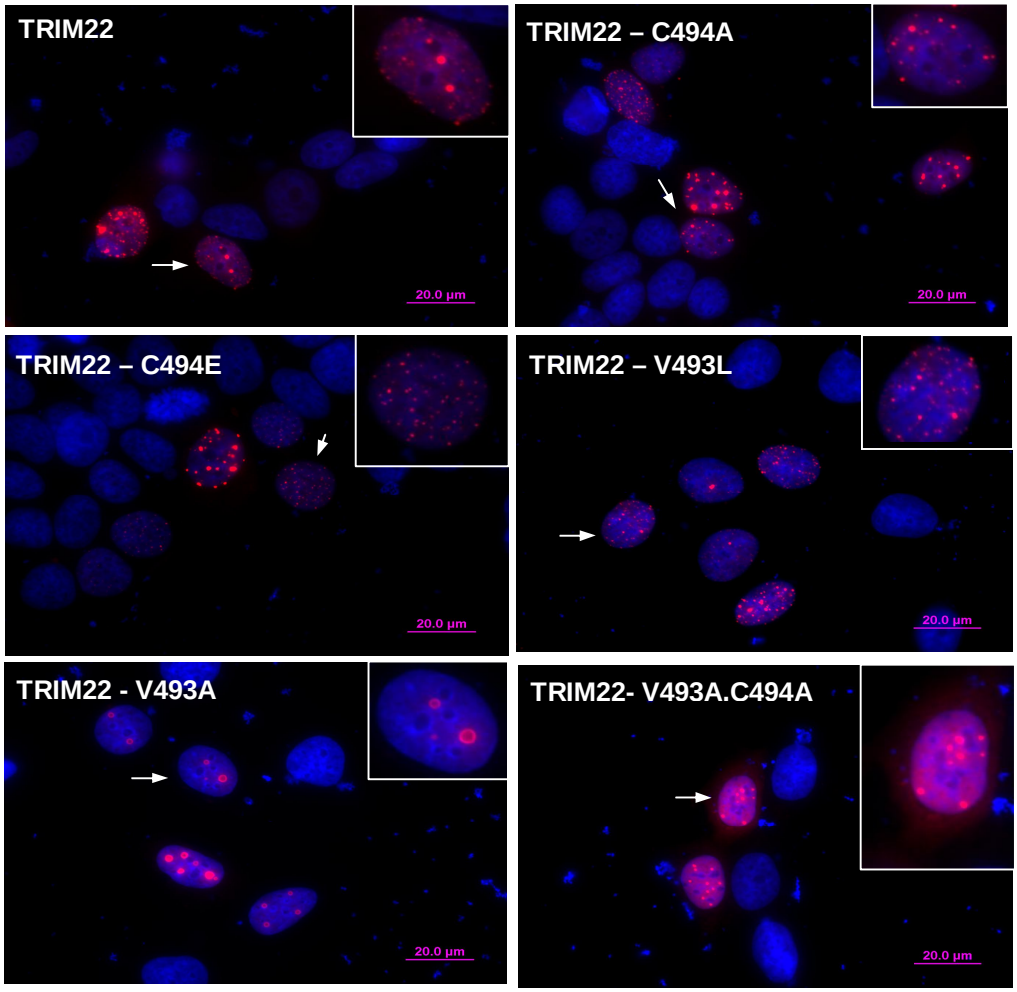

Figure 3.21 A hydrophobic residue in position 493 and a residue in position 494 are important for proper nuclear body formation.
(A) Alignment of the last 20 residues of human TRIM22 with TRIM34, TRIM6 and TRIM5α. **(B)** Sequences of the C494A, C494E, V493L, V493A, and V493A,C494A point mutants of TRIM22. **(C)** Localization of the five TRIM22 point mutants. MCF7 cells expressing either the wild-type TRIM22 protein or one of these mutants were immunostained with anti-FLAG antibody and counterstained with DAPI. Cells were imaged at a 60X magnification. Bars, 20 µm. Insets show representative cells (arrows) enlarged 2X. Results are representative of at least two independent experiments.

cytoplasm as a diffuse protein (evident at the 120 min time point) but quickly aggregated to form bodies (evident at the 240 min time point, **Figure 3.22A**). The bodies became more densely packed during the 480 – 840 min period but failed to aggregate into one large body during the period of analysis.

As shown in **Figure 3.17**, TRIM22 has four recognized domains (RING, B-box2, CC, and SPRY). All four domains have been found to mediate protein-protein interactions in other TRIM proteins. To identify the domain that is likely to be involved in TRIM22 self-interaction, TRIM22-EGFP was co-expressed with FLAG-TRIM22 deletion mutants in MCF7 cells, which were immunostained with the anti-FLAG antibody 24 hr post-transfection. The mutants selected for co-expression analyses were TRIM22-ΔRING (lacking the RING domain), TRIM22-ΔSPRY (lacking the SPRY domain), and TRIM22-ΔRING/B2/CC/182 (lacking the RING, B-box2 and CC domains; only the SPRY domain present). The localization of these mutants in the presence of TRIM22-EGFP allowed us to 1) determine the contribution of the RING and SPRY domains to TRIM22 self-interaction and 2) the location of the self-interaction motif in the TRIM22 body.

TRIM22-ΔRING localizes as a nucleoplasmic protein when expressed alone (**Figure 3.19**). Besides retaining its nucleoplasmic localization, TRIM22-ΔRING also surrounded the distinct TRIM22-EGFP bodies and formed an obvious ring around these bodies (TRIM22-ΔRING panel, **Figure 3.22B**). Compared to the TRIM22-EGFP bodies observed thus far, the TRIM22-EGFP bodies in the presence of TRIM22-ΔRING were less compact. TRIM22-ΔSPRY, an exclusively extranuclear protein when present alone,

was found in close association with TRIM22-EGFP and frequently within the nucleus (TRIM22-ΔSPRY panel, **Figure 3.22B**). In addition, in these cells, TRIM22-EGFP, a nuclear protein, was frequently found outside the nucleus in combination with TRIM22-ΔSPRY (see magnified cell and cell marked with an arrowhead, **Figure 3.22B**). In contrast, TRIM22-ΔRING/B2/CC/182 remained as an extranuclear protein and did not alter the nuclear localization of TRIM22-EGFP (TRIM22-ΔRING/B2/CC/182 panel, **Figure 3.22B**). These observations allow us to conclude that 1) the RING and SPRY domains are not necessary for TRIM22 self-interaction and 2) TRIM22 aggregates possibly due to the exposure of a self-interaction motif on the surface of the body.

3.9 Cellular proteins that interact with TRIM22

3.9.1 TRIM22 bodies are found adjacent to Cajal bodies

The localization of TRIM22 as nuclear and nucleolar bodies shown by overexpression studies was confirmed by immunofluorescence results using a specific TRIM22 antibody. As the TRIM22 protein formed regular bodies similar in appearance to Cajal bodies (CB), the localization of TRIM22 relative to the signature CB protein p80-coilin was investigated in MCF7 cells. MCF7 cells stably expressing TRIM22-EGFP were immunostained to detect endogenous p80-coilin. TRIM22-EGFP bodies colocalized partially with endogenous p80-coilin (**Figure 3.23A**). Using the mouse anti-TRIM22 and rabbit anti-p80-coilin antibodies to detect endogenous proteins, it was evident that endogenous TRIM22 also colocalized partially with endogenous p80-coilin in MCF7 cells (**Figure 3.23B**). Even though all fluorescence microscopy images in this study were taken without altering the plane in focus, an additional Z-stack analysis using laser

A

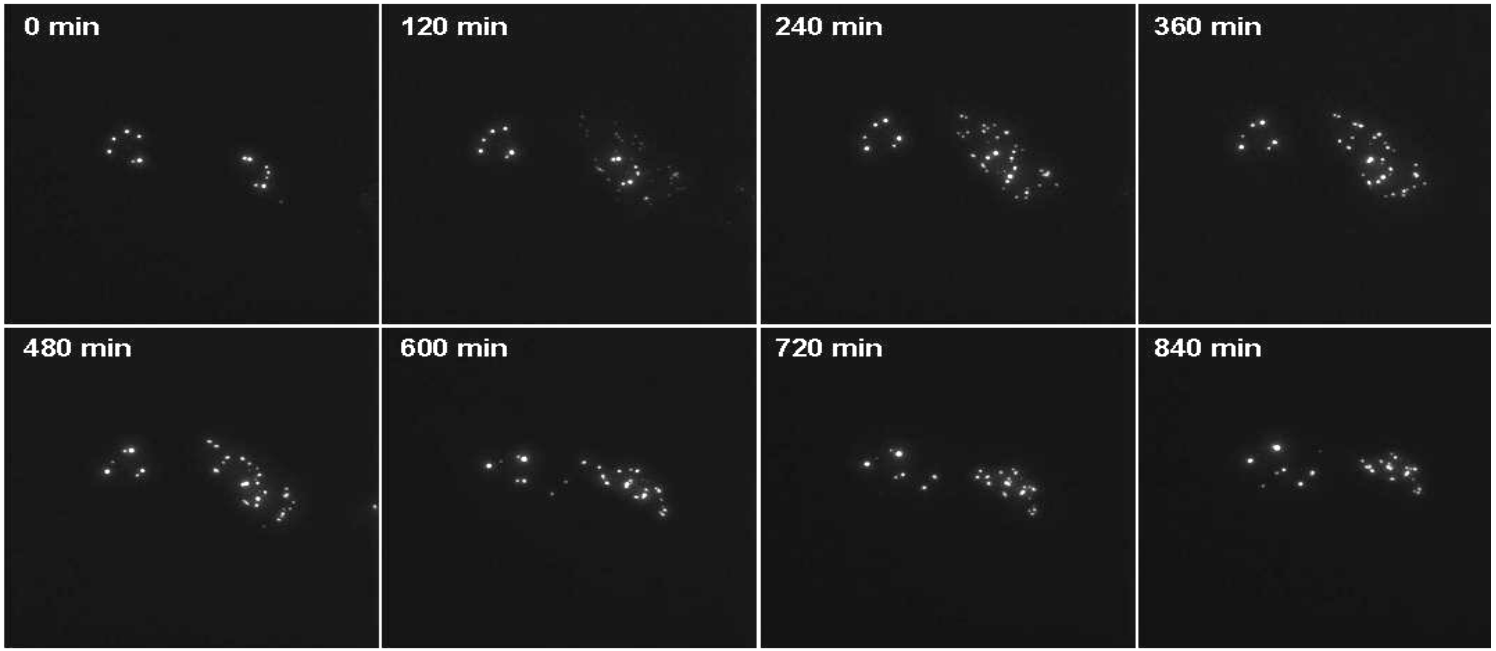

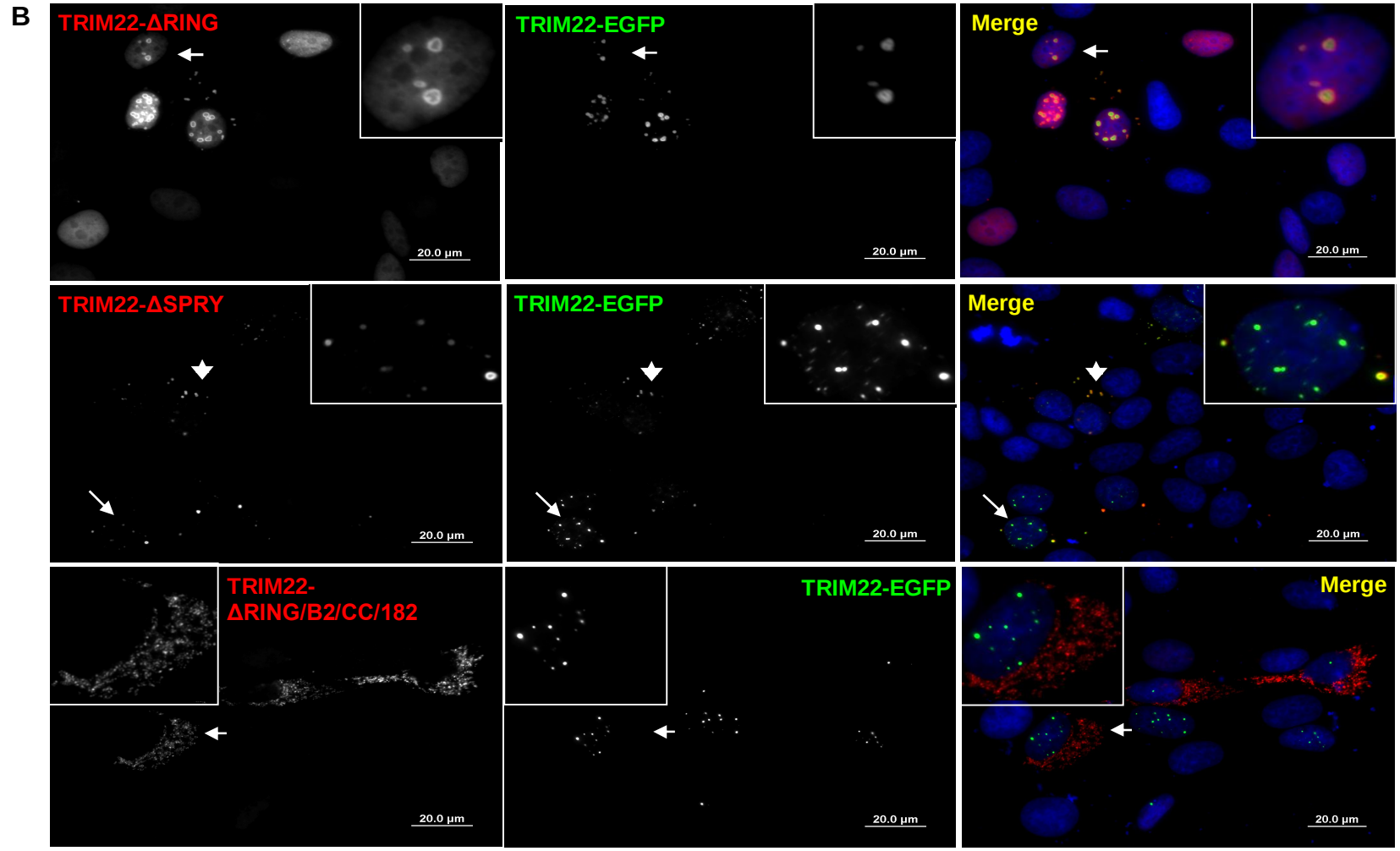

Figure 3.22 TRIM22 aggregation is due to exposure of a self-interaction motif on the surface of the body.
(A) Live cell imaging was performed on MCF7 cells transiently expressing TRIM22-EGFP. Images obtained at 120 min intervals at a 60X magnification are shown. **(B)** TRIM22-EGFP was co-expressed with TRIM22-ΔRING, TRIM22-ΔSPRY or TRIM22-ΔRING/B2/CC/182 in MCF7 cells. 24 hr post-transfection, cells were immunostained with anti-FLAG antibody and counterstained with DAPI. Localizations of TRIM22-EGFP (green) and TRIM22 deletion mutants (red) were visualized by fluorescence microscopy at a 60X magnification. Bars, 20 µm. Insets show representative cells (arrows) enlarged 3X (TRIM22-ΔRING and TRIM22-ΔSPRY panels) or 2X (TRIM22-ΔRING/B2/CC/182 panel). Arrowheads in TRIM22-ΔSPRY panels show extranuclear localization of TRIM22-EGFP with TRIM22-ΔSPRY.

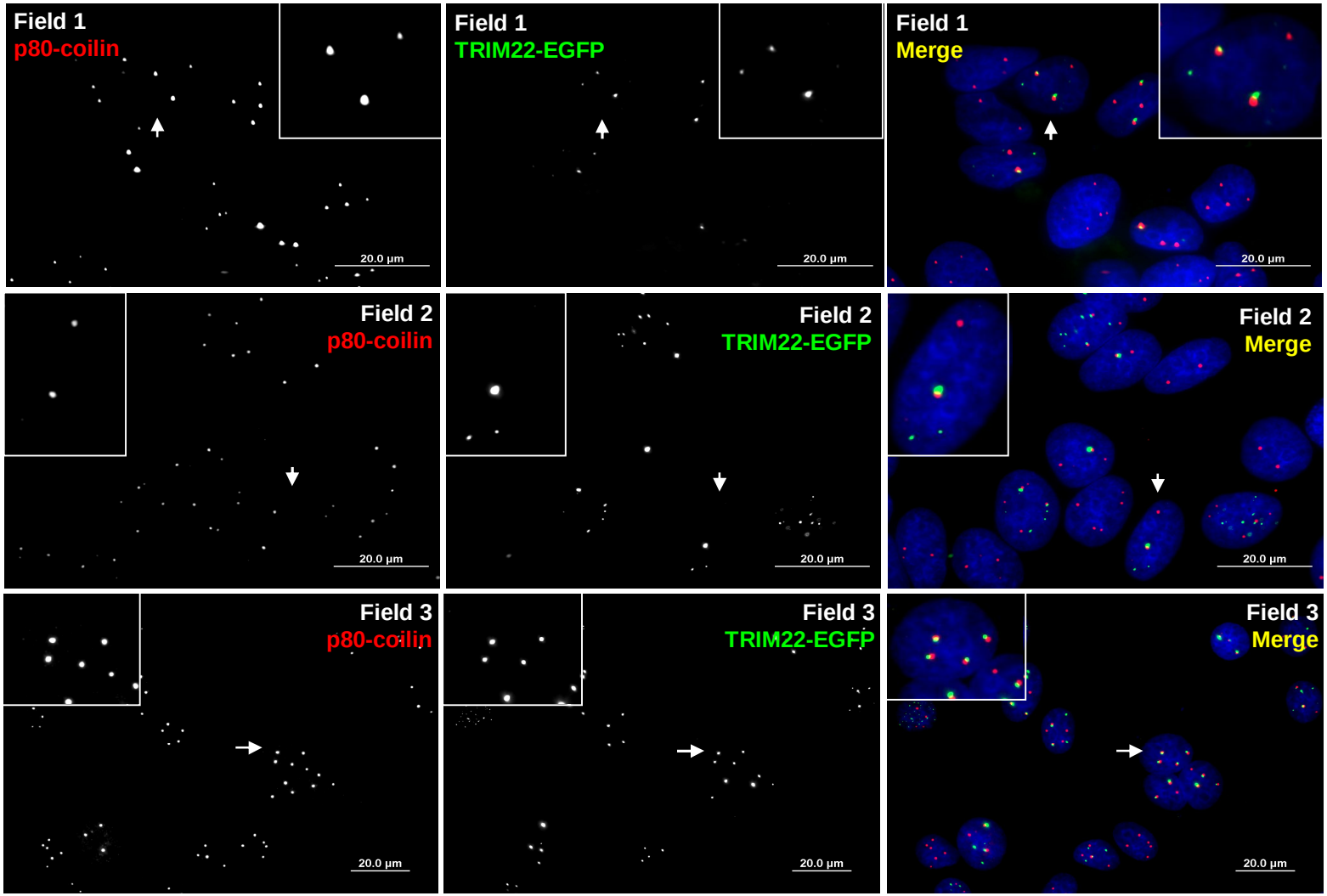
Field 1
p80-coilin
20.0 µm
Field 1
TRIM22-EGFP
20.0 µm
Field 1
Merge
20.0 µm
Field 2
p80-coilin
20.0 µm
Field 2
TRIM22-EGFP
20.0 µm
Field 2
Merge
20.0 µm
Field 3
p80-coilin
20.0 µm
Field 3
TRIM22-EGFP
20.0 µm
Field 3
Merge
20.0 µm

B

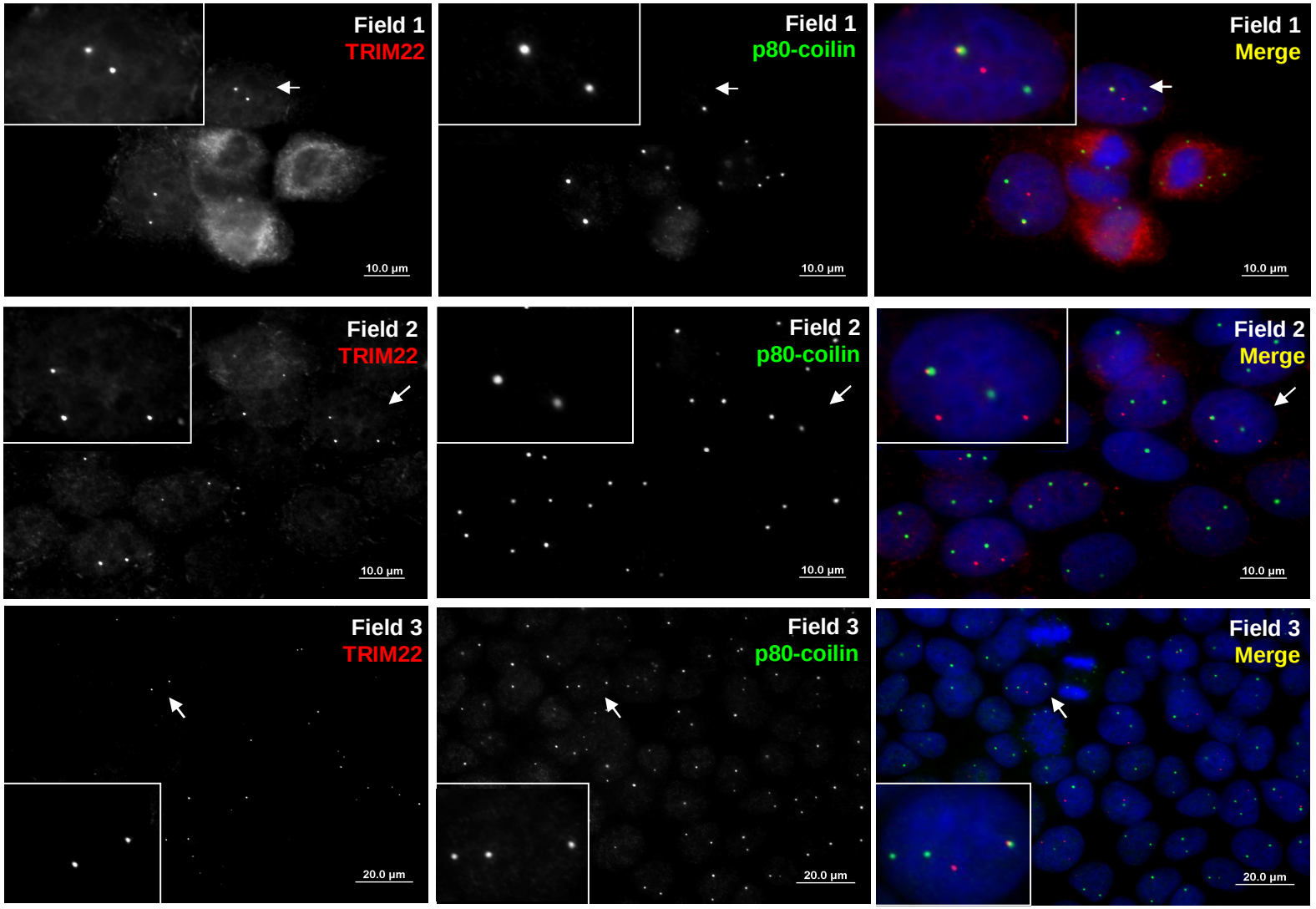
Field 1
TRIM22
10.0 µm
Field 1
p80-coilin
10.0 µm
Field 1
Merge
10.0 µm
Field 2
TRIM22
10.0 µm
Field 2
p80-coilin
10.0 µm
Field 2
Merge
10.0 µm
Field 3
TRIM22
20.0 µm
Field 3
p80-coilin
20.0 µm
Field 3
Merge
20.0 µm

C

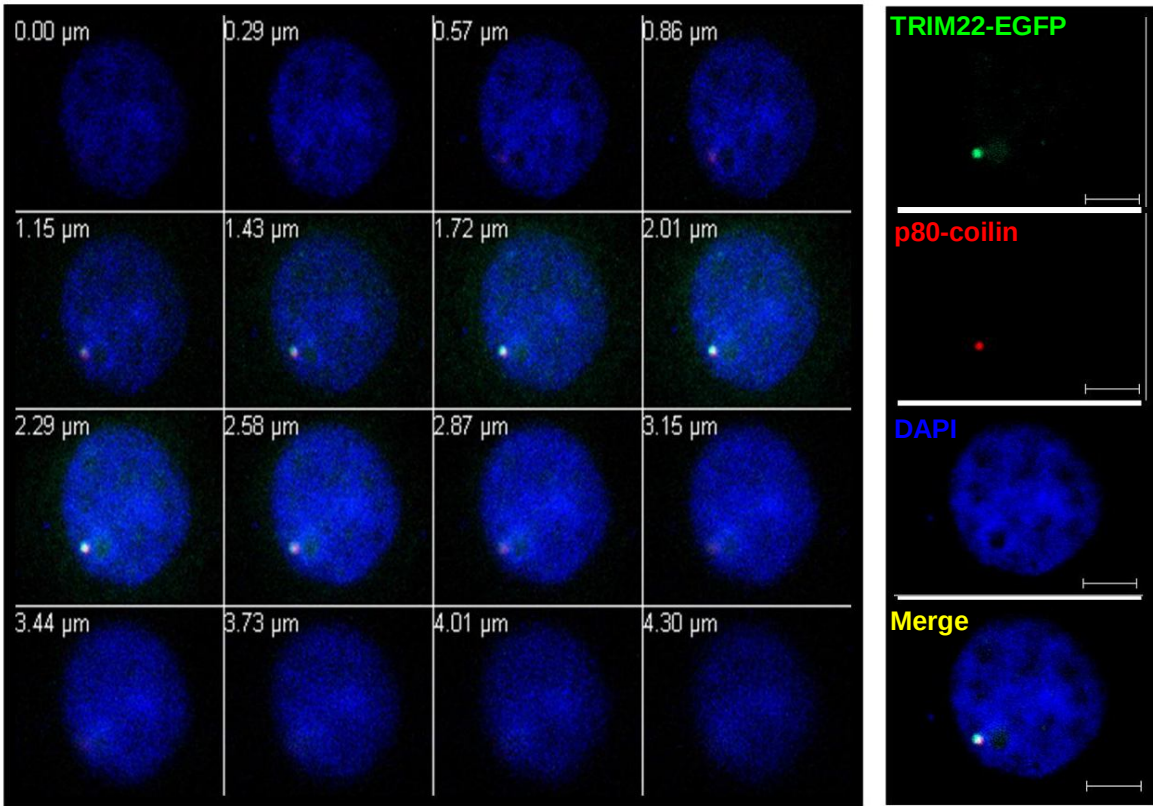

Figure 3.23 TRIM22 nuclear bodies colocalize partially with Cajal bodies in MCF7 cells.

(A) TRIM22-EGFP bodies overlap partially with endogenous CBs. MCF7 cells stably expressing TRIM22-EGFP (green) were immunostained with anti-p80-coilin antibody to detect endogenous CBs (red). Insets show representative cells (arrows) enlarged 2X. **(B)** Endogenous TRIM22 NB (red) overlap partially with CBs (green) (arrows). MCF7 cells were immunostained with rabbit anti-p80-coilin and mouse anti-TRIM22 antibodies. Insets show representative cells (arrows) enlarged 2X (fields 1, 2) or 3X (field 3). **(A, B)** All cells were counterstained with DAPI (blue) and visualized by fluorescence microscopy at 60X or 96X magnifications. Bars, 10 or 20 µm. Results are representative of at least two independent experiments.
(C) TRIM22-EGFP bodies are found in the same plane as CBs. MCF7 cells expressing TRIM22-EGFP were immunostained with anti-p80-coilin antibodies and analyzed by laser scanning confocal microscopy. A representative nucleus is shown. Z-stacks were obtained at 0.29 µm sections for a total of 4.3 µm. Merged images at different sections are shown in the left panel and individual images obtained at mid-section are shown in the right panel. Bars, 5 µm.

scanning confocal microscopy was conducted so as to confirm the colocalization of the two bodies. MCF7 cells expressing TRIM22-EGFP and immunostained for p80-coilin were imaged at 0.29 μm sections for a total of 4.3 μm. As the TRIM22-EGFP body appeared in the same sections as the CB, it can be concluded that TRIM22-EGFP bodies are found in the same plane as CBs (**Figure 3.23C**).

Like in MCF7 cells, bodies formed by endogenous p80-coilin and TRIM22 also colocalized in progesterone-treated ABC28 cells (**Figure 3.24**). Notably, in almost all progesterone-treated ABC28 cells observed, TRIM22 also appeared to colocalize with p80-coilin within extranuclear strand-like structures (arrows in ABC28 48P panels, **Figure 3.24**). Cytoplasmic p80-coilin strands were not observed in untreated control cells (ABC28-untreated panel, **Figure 3.24**).

3.9.2 TRIM22 is not a resident protein of Cajal bodies

Interestingly, the adjacency noted between endogenous CBs and TRIM22 (either endogenous or ectopically expressed) was not found in all cells. In some cells, all the CBs were found associated, whilst in others, only some or none of the CBs were found associated with TRIM22 NB (**Figure 3.23**). As the number of CBs present in a cell is cell-cycle dependent and CBs are absent in mitotic cells (Andrade et al., 1993), the association of TRIM22-EGFP NB with CBs was also analyzed in cells expressing different numbers of CBs. In MCF7 cells, 144 (35%) of the 415 endogenous CBs counted were found either adjacent to or colocalized with TRIM22-EGFP NB. When cells with multiple dispersed TRIM22 NB were not considered (as this may have been due to high

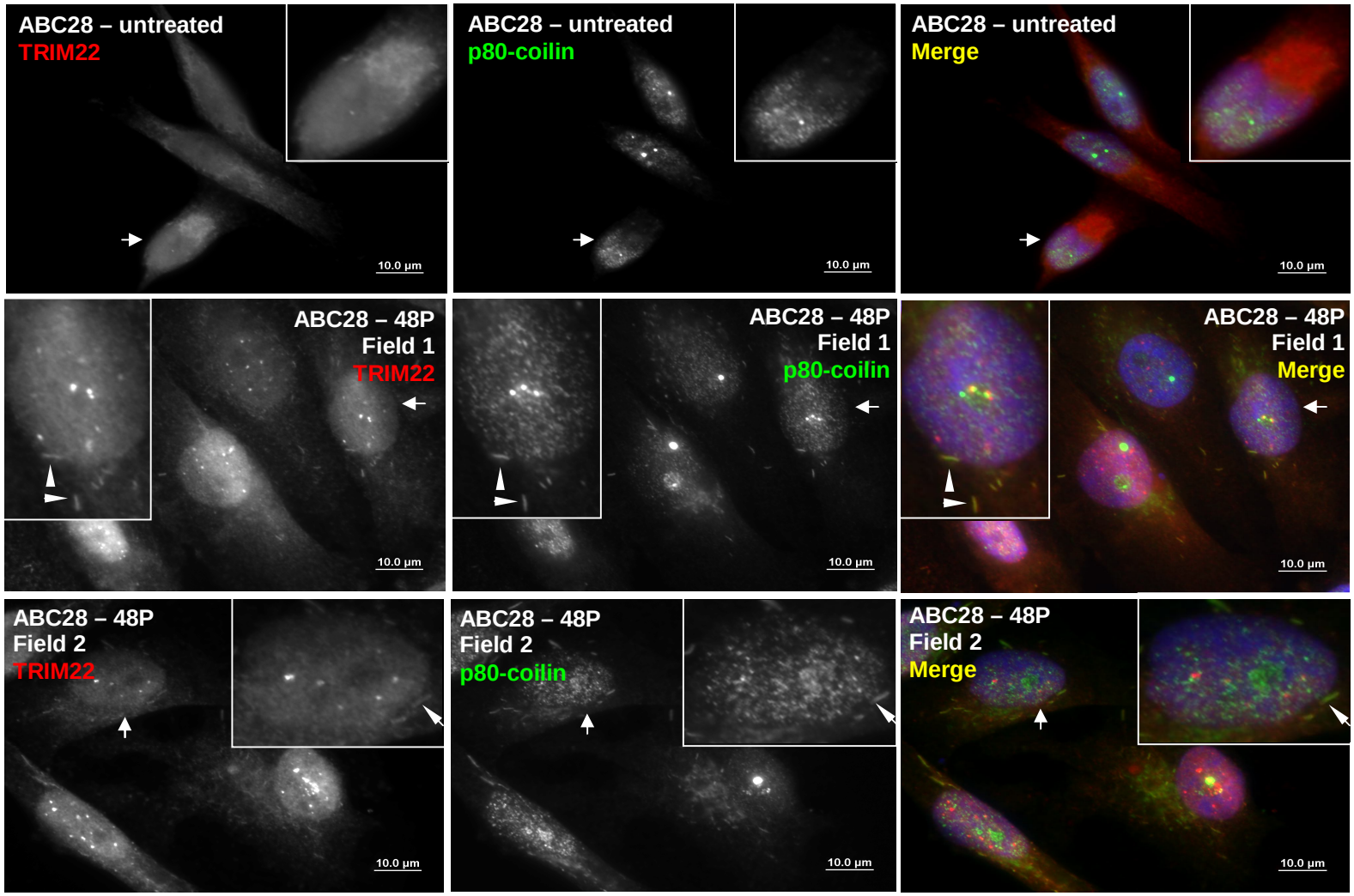

Figure 3.24 TRIM22 nuclear bodies colocalize partially with Cajal bodies in ABC28 cells.
Untreated and progesterone-treated ABC28 cells were immunostained with mouse anti-TRIM22 and rabbit anti-p80-coilin antibodies. Endogenous TRIM22 NB (red) overlap partially with CBs (green) (arrows in ABC28 – 48P Field 1 panel). TRIM22 (red) and p80-coilin (green) also colocalize in strand-like structures in the cytoplasm (arrows in ABC28 – 48P magnified panels). All cells were counterstained with DAPI (blue) and visualized by fluorescence microscopy at a 96X magnification. Bars, 10 µm. Insets show representative cells (arrows) enlarged 2X. Results are representative of at least two independent experiments.

expression of TRIM22-EGFP), all CBs colocalized with TRIM22 NB in 23 (18%) of the 130 cells analyzed.

There was no obvious correlation between the numbers of CBs within the cell and the extent of its adjacency/colocalization with TRIM22 NB. The observation that CBs are associated with TRIM22 NB (sometimes in a 1:1 relationship) in only some cells and not others suggests that TRIM22 is not a resident protein of CBs like p80-coilin, but is likely to be a dynamic protein which may associate with CBs at certain stages of the cell cycle rather than constitutively. Such a cell-cycle dependent association between NB, such as between CBs and cleavage bodies, has been reported (Li et al., 2006).

3.9.3 TRIM22 interacts with p80-coilin

The absence of a complete colocalization of TRIM22 NB with CBs in MCF7 and ABC28 cells prompted an investigation into whether p80-coilin does interact physically with TRIM22 NB and, if so, the regions responsible for this interaction. Coimmunoprecipitation experiments were performed in MCF7 cells co-expressing p80-coilin-EGFP and FLAG-TRIM22 (TRIM22) or its deletion mutants (TRIM22-ΔSPRY, TRIM22-ΔSPRY/CC, TRIM22-ΔRING, TRIM22-ΔRING/B2, and TRIM22-ΔRING/B2/CC/182). p80-coilin-EGFP coimmunoprecipitated with TRIM22 (second lane, **Figure 3.25**). p80-coilin-EGFP also coimmunoprecipitated with all the deletion mutants, but to different extents. The low level of p80-coilin-EGFP pull-down with TRIM22-ΔRING/B2/CC/182 could be due to the low expression level of this mutant. Conversely, the expression level of TRIM22-ΔSPRY/CC was comparable to that of the

other well-expressed mutants such as TRIM22-ΔRING/B2 and greater than TRIM22-ΔSPRY, yet it too pulled-down much less p80-coilin-EGFP compared to TRIM22-ΔSPRY. Therefore, the region of TRIM22 from residues 139 - 352 is likely to contain the residues important for interaction with p80-coilin. Furthermore, TRIM22-ΔRING and TRIM22-ΔRING/B2 interacted to the same extent as full-length TRIM22, suggesting that the RING and B-box2 domains are most likely not the domains responsible for interaction of TRIM22 with p80-coilin, even though these domains are known for being involved in protein-protein interactions (**Figure 3.25**). Reverse co-immunoprecipitation experiments, wherein p80-coilin-EGFP is immunoprecipitated and then the presence of FLAG-TRIM22 is detected, would provide additional support for the interaction of TRIM22 with p80-coilin.

3.9.4 TRIM22 associates and interacts with B23/nucleophosmin

The mechanism of protein localization within nucleoli is generally not well understood, Studies with other nucleolar proteins such as ARF and C23/nucleolin point to interaction with B23 as a prerequisite for nucleolar localization (Colombo et al., 2005; Enomoto et al., 2006; Li et al., 1996). As endogenous TRIM22 NB appeared to be localized within nucleoli in progesterone-treated ABC28 cells and TRIM22-EGFP NB were frequently noted next to nucleoli in MCF7 cells, the association of B23 with TRIM22 was investigated. In MCF7 cells expressing low to moderate levels of TRIM22-EGFP, the staining of endogenous B23 was absent in the regions where TRIM22 NB were present (**Figure 3.26A**). TRIM22 NB may have obstructed the access of B23 antibodies, or TRIM22 NB displaced B23 in the region while making its way from the nucleolus to the

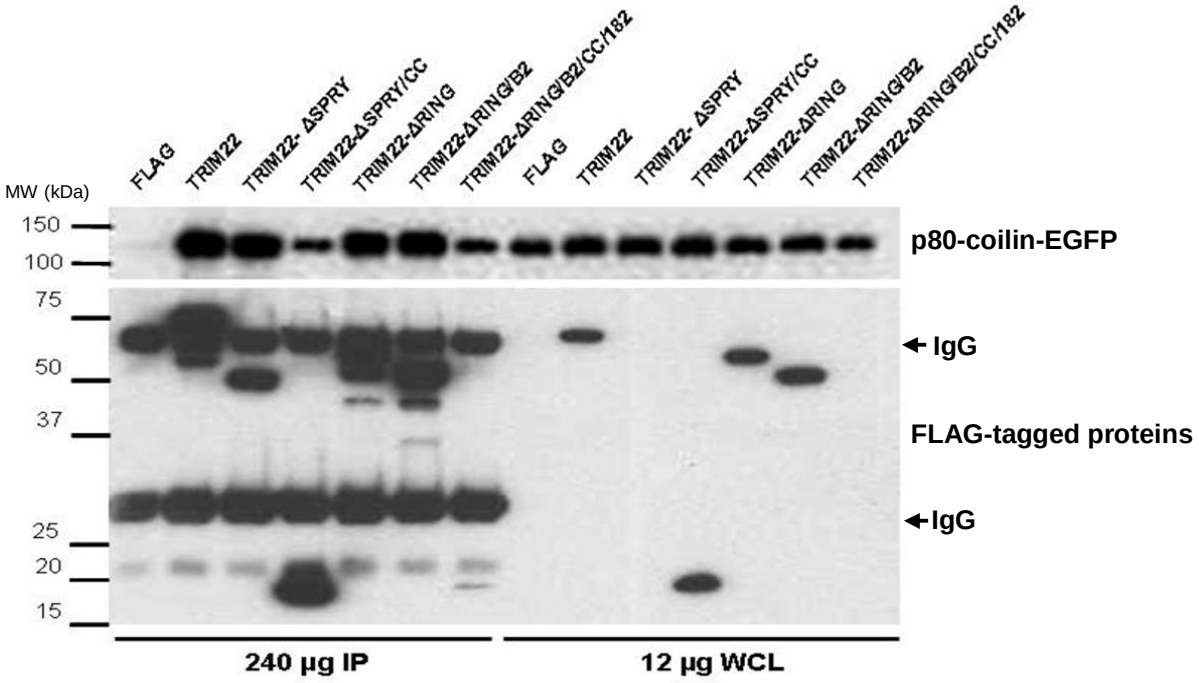

Figure 3.25 TRIM22 interacts with p80-coilin.
MCF7 cells were cotransfected with p80-coilin-EGFP and either pXJ-FLAG (FLAG), FLAG-tagged TRIM22 or FLAG-tagged TRIM22 deletion mutants. FLAG-tagged proteins were immunoprecipitated from 240 µg of whole cell lysates (WCL) using anti-FLAG M2 affinity beads. 12 µg of WCL were electrophoresed alongside the immunoprecipitated proteins. Blots were probed with anti-GFP antibody to detect p80-coilin-EGFP (105 kDa), then stripped and probed with anti-FLAG antibody to detect FLAG-TRIM22 and deletion mutants. The TRIM22-ΔSPRY and TRIM22-ΔRING/B2/CC/182 mutants could be detected when immunoprecipitated (evident in the IP lanes) but failed to be detected in lanes containing only 12 µg of WCL due to poorer expression of these mutants compared to the other mutants. Results are representative of two independent experiments.

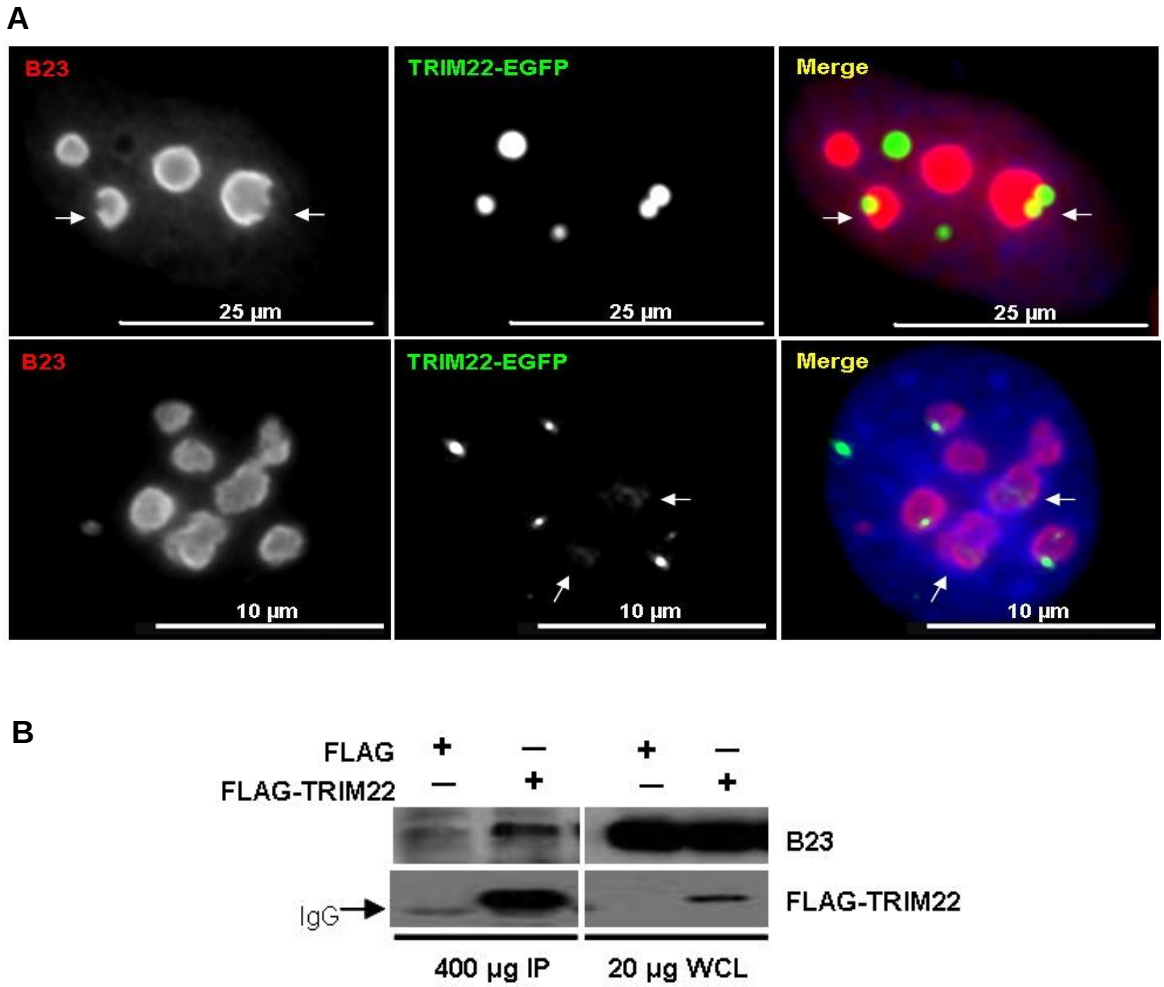

Figure 3.26 TRIM22 interacts with B23.
(A) TRIM22 bodies displace B23 in the granular layer of the nucleolus. MCF7 cells stably expressing TRIM22-EGFP (green) were immunostained with anti-B23 antibody, counterstained with DAPI (blue) and then visualized by fluorescence microscopy at a 96X magnification. Bars, 10 or 25 µm. The B23 ring (red) is disrupted where TRIM22 bodies are present (first panel). TRIM22-EGFP bodies disperse slightly within nucleoli of MCF7-TRIM22-EGFP cells (second panel). **(B)** TRIM22 physically interacts with endogenous B23. Whole cell lysates (WCL) from MCF7 cells transfected with pXJ-FLAG (FLAG) or FLAG-TRIM22 were subjected to immunoprecipitation using anti-FLAG M2 affinity beads (400 µg IP). Immunoprecipitated proteins were analyzed by Western blotting alongside 20 µg WCL. Endogenous B23 (36 kDa) and FLAG-TRIM22 (~ 57 kDa) were detected sequentially. **(A, B)** Results are representative of three independent experiments.

nucleoplasm. Alternatively, it is possible that TRIM22 NB are biochemically different entities and that TRIM22 associates with further molecules besides B23 *en route* to the nucleolus. The presence of TRIM22 as NB in the granular region of the nucleolus but as a dispersed protein within the nucleolus in some cells supports the idea that the TRIM22 NB may require disintegration for entry into the nucleolus (second panel in **Figure 3.26A**). Coimmunoprecipitation experiments showed that endogenous B23 immunoprecipitated with FLAG-TRIM22 (**Figure 3.26B**). The results tallied with the immunofluorescence data in that only a fraction of the nucleolar and nucleoplasmic B23 colocalized with TRIM22. The interaction of TRIM22 with B23, which should be confirmed with reverse co-immunoprecipitation experiments, may be a means for TRIM22 to find its way into the nucleolus.

3.10 TRIM22's role in the cell

3.10.1 TRIM22 overexpression inhibits the growth of MCF7 cells

The first functional study of TRIM22 was done in leukemic U-937 cells, in which it was found that overexpressing the TRIM22 protein led to reduced clonogenic growth (Obad et al., 2004). As the authors also found that TRIM22 was a p53 target gene and p53 induces differentiation in leukemic cells, they postulated that TRIM22 may be a mediator of p53's differentiative effects in leukemic cells. In this study, to investigate the role of TRIM22 in mammalian cells, particularly in breast cancer cells, an overexpression study was performed. The MEC line MCF7 was utilized since MCF7 cells had very low levels of the TRIM22 protein (**Figure 3.9**). The 1497 bp TRIM22 coding sequence was cloned into pcDNA3.1Hyg to generate the TRIM22-pcDNA3.1Hyg construct. This construct,

which resulted in low to moderate levels of TRIM22 at the expected size in MCF7 cells (data not shown), was stably transfected into MCF7 cells to overexpress the TRIM22 protein without a tag. The pcDNA3.1Hyg vector-transfected MCF7 cells were used as a control. In two independent assays, after selection of hygromycin-resistant cells for 3 - 4 weeks, there were much fewer colonies observed in the dishes transfected with TRIM22-pcDNA3.1Hyg compared to the vector-transfected control dishes (**Figure 3.27A**). To determine at which stage of the cell cycle the TRIM22-expressing cells were halted, MCF7 cells transiently transfected with EGFP or TRIM22-EGFP were sorted to obtain relatively pure transfected cell populations and then analyzed by flow cytometry. Cell cycle analysis revealed a greater proportion of TRIM22-EGFP-expressing cells in the G0/G1 phase (13.9% more) with concomitant reductions in the percentage of cells in the S and G2/M phases compared to the EGFP-expressing cell population (**Figure 3.27B**)**.** These results are consistent with the previous finding of clonogenic growth inhibition in leukemic cells when TRIM22 was overexpressed (Obad et al., 2004).

3.10.2 Silencing TRIM22 enhances cell cycle progression in the normal mammary epithelial cell line MCF12A

The overexpression of a protein, particularly a nuclear and nucleolar protein such as TRIM22 can result in non-specific death of cells due to toxicity in the presence of large amounts of the protein. To further investigate if TRIM22 does indeed have growth inhibitory properties, MCF12A cells that express large amounts of the TRIM22 protein were transfected with 10 nM TRIM22 siRNA for 72 hr and the percentage of cells in different phases of the cell cycle analyzed. As shown in **Figure 3.28**, silencing TRIM22

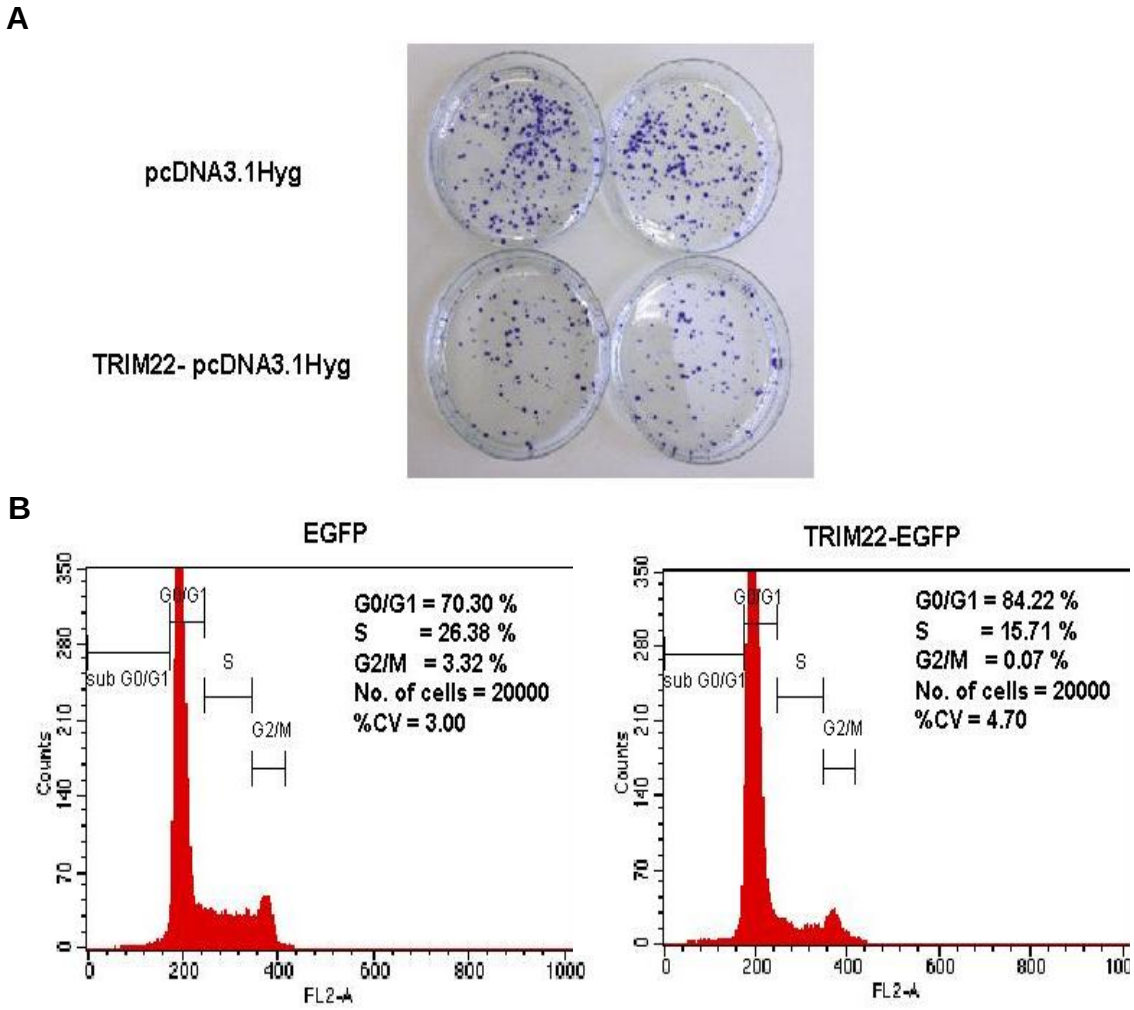

Figure 3.27 Overexpression of TRIM22 in MCF7 cells results in a reduction in colony numbers and G0/G1 cell cycle arrest.

(A) MCF7 cells were transfected with pcDNA3.1Hyg (vector-transfected control) or TRIM22-pcDNA3.1Hyg and maintained in hygromycin (200 µg/ml) containing growth media. 3 - 4 weeks post-transfection, cells were washed and stained with crystal violet. Result is representative of two independent experiments. **(B)** MCF7 cells were transfected with EGFP or TRIM22-EGFP and fluorescent cells sorted 48 hr later in a cell sorter. Fluorescent cells were subjected to propidium iodide staining and cell cycle analysis. Results are presented as cell numbers (counts) versus intensity of propidium iodide (FL2-A). Inset shows the Modfit analyses of the percentage of cells in the G0/G1, S, and G2/M phases of the cell cycle.

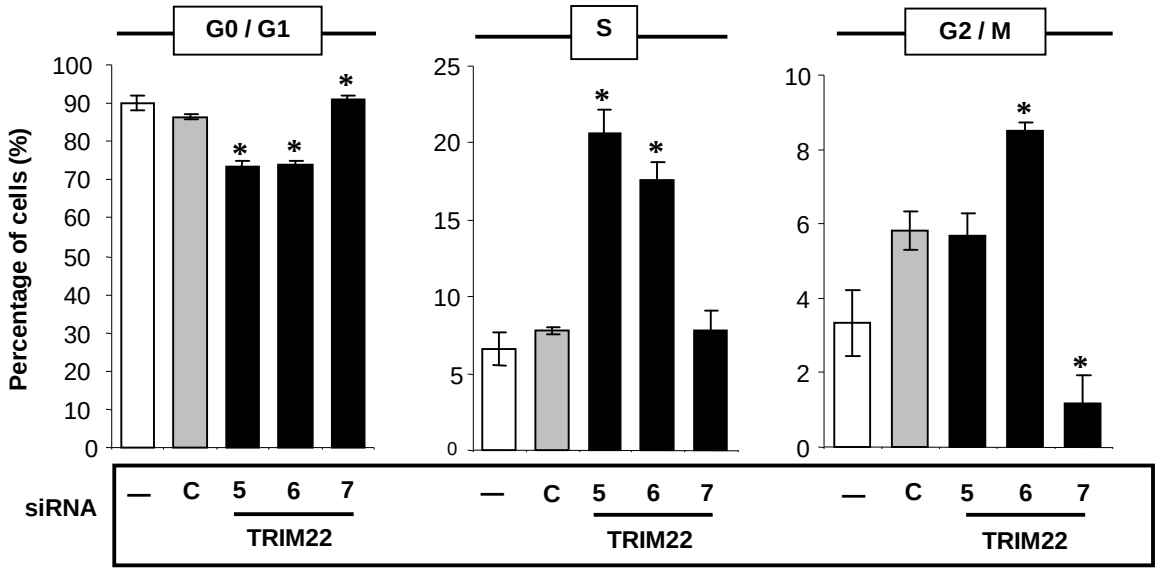

Figure 3.28 Silencing TRIM22 enhances cell cycle progression in the non-tumorigenic mammary epithelial cell line MCF12A

MCF12A cells were left untransfected or transfected with 10 nM control (C) or TRIM22 siRNAs 5, 6, or 7. 72 hr later, cells were harvested and analyzed by flow cytometry to determine percentage of cells in each phase of the cell cycle. 10,000 cells were analyzed for each set and the samples run in quadriplicate. Error bars reflect SEM. Results are representative of two independent experiments at 72 hr and another at 48 hr (*$P<0.05$, versus C).

with TRIM22 siRNAs 5 and 6 enhanced the percentage of cells in the S phase of the cell cycle by at least 10% and with concomitant reductions in the percentage of cells in the G0/G1 phase. Unlike the other two siRNAs, TRIM22 siRNA 7 slightly enhanced the percentage of cells in the G0/G1 phase with little change in the S phase fraction but a much lower G2/M phase fraction.

3.10.3 Silencing TRIM22 does not reverse the progesterone-induced G0/G1 cell cycle arrest in ABC28 cells

The ABC28 cell line, unlike the normal MEC line MCF12A, was derived from the metastatic and tumorigenic cell line MDA-MB-231. To test if TRIM22 likewise exhibits growth-inhibitory properties in ABC28 cells, a gene silencing experiment was also performed in these cells after treatment with progesterone. The ability of progesterone, an inducer of TRIM22, to induce G0/G1 arrest in ABC28 cells has been reported previously (Lin et al., 1999). Would reducing TRIM22 levels reverse this growth-inhibition noted in the presence of progesterone? To answer this question, ABC28 cells were transfected with 10 nM control siRNA or TRIM22 siRNA 5, 6, or 7. 8 hr later, cells were treated with 10 nM progesterone for 48 hr and analyzed by flow cytometry.

Figure 3.29 shows the percentage of cells in the G0/G1, S, and G2/M phases of the cell cycle for each sample. Lin et al. reported a dose-dependent increase in the percentage of progesterone-treated ABC28 cells in the G0/G1 phase compared to ethanol-treated controls (Lin et al., 1999). In the current study, 10 nM progesterone was capable of increasing the numbers of cells in the G0/G1 phase by 6.9% relative to the ethanol-

treated controls (**Figure 3.29**). Relative to the control siRNA transfected cell population, all three TRIM22 siRNA-transfected cell populations had greater numbers of cells in the G0/G1 phase (3.5 – 10% increase). TRIM22 siRNA 7 was the most effective and TRIM22 siRNA 5 the least effective in enhancing cell numbers in the G0/G1 phase (**Figure 3.29**). This increase in G0/G1 arrest was associated with fewer numbers of cells in the S and G2/M phases, indicating that silencing TRIM22 further enhanced the G0/G1 arrest induced by progesterone. Therefore, TRIM22 may not mediate progesterone's growth-inhibitory properties in breast cancer cells.

3.10.4 Downstream targets of TRIM22 in ABC28 and HeLa cells

The idea that TRIM22 may not inhibit growth in breast cancer cells prompted a gene expression analysis in ABC28 and HeLa cells to identify the downstream targets of TRIM22. Cells transfected with control or TRIM22 siRNA 6 or 7 were treated with progesterone or IFNγ for 48 hr before RNA extraction. The integrity of RNA samples were checked by electrophoresis on a 1% TBE gel containing ethidium bromide before further manipulation. The intensity of the 28S RNA species was two times greater than that of the 18S species for all samples (representative samples shown in **Figure 3.30**). Together with an $Abs_{260\ nm}/Abs_{280\ nm}$ ratio of at least 1.9, this indicated that the extracted RNA was of good quality. RNA samples were prepared for hybridization to Illumina Sentrix® BeadChip arrays as described in **section 2.19.1**. After hybridization, arrays were scanned using the BeadArray Reader. The data output was analyzed to identify genes that were differentially regulated by at least 2 fold in both the TRIM22 siRNA samples compared to the control siRNA sample for each cell line.

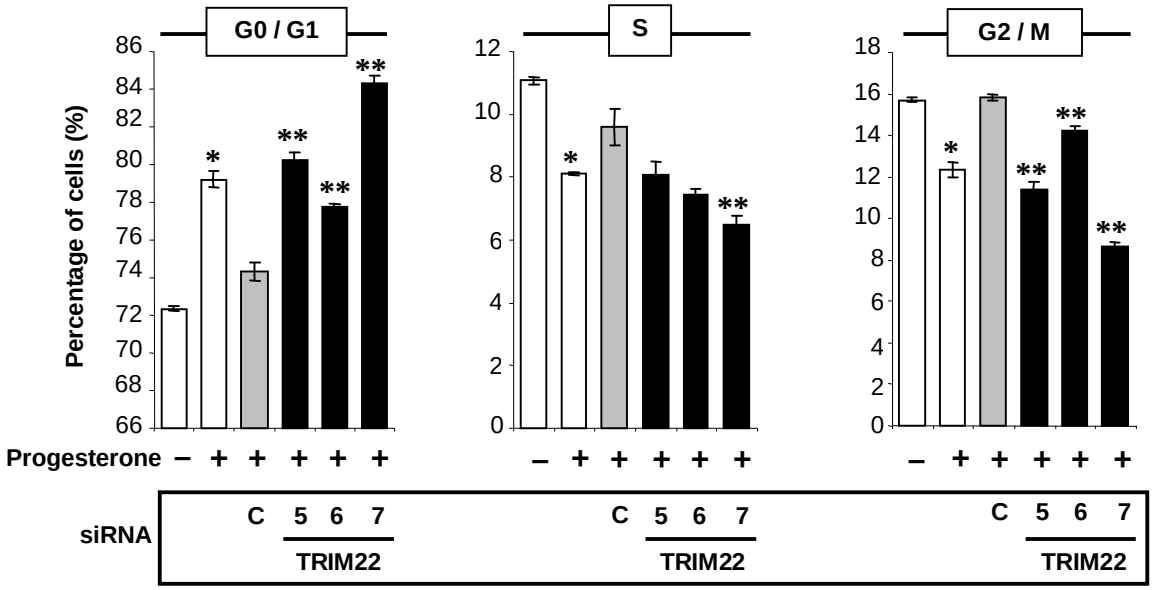

Figure 3.29 Silencing TRIM22 does not reverse the progesterone-induced GO/G1 arrest of ABC28 cells

ABC28 cells were treated with ethanol (─) or 10 nM progesterone after transfecting with 10 nM control or TRIM22 siRNAs 5, 6, or 7. 48 hr later, cells were harvested and analyzed by flow cytometry to determine percentage of cells in each phase of the cell cycle. 20,000 cells were analyzed for each set and the samples run in triplicate. Error bars reflect SEM. Results are representative of three independent experiments (**P<0.05*, versus ─; ***P<0.05*, versus C).

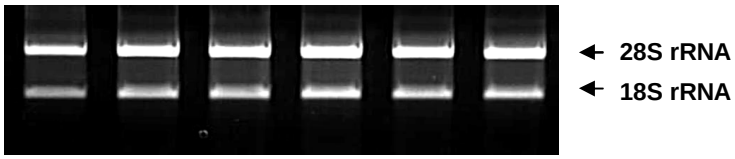

Figure 3.30 Integrity of RNA used in gene expression analysis.

Representative gel showing integrity of RNA extracted from ABC28 and HeLa cells that was eventually used for gene expression analysis. RNA was quantitated and 0.5 µg resolved on a 1% TBE gel. The 28S and 18S bands are marked. All RNA samples had $Abs_{260\ nm}/Abs_{280\ nm}$ of at least 1.9.

Table 3.2 lists the genes that were differentially regulated by at least 2 fold after TRIM22 silencing in ABC28 cells and HeLa cells. As expected, TRIM22 was down-regulated in both cell lines in the presence of TRIM22 siRNA, with the silencing being more effective in HeLa cells. 10 genes found to be regulated in either one or both cell lines were also analyzed by real-time PCR using specific primers (values indicated for the tested genes in the "RT-PCR" column; melting curves for the primers used in **Appendices Figure A1**). 9 of these genes in ABC28 cells and 8 of these genes in HeLa cells were validated.

Of the 14 genes found to be differentially regulated in ABC28 cells, 4 were up-regulated and 9 were down-regulated. Of the 37 genes found to be differentially regulated in HeLa cells, 12 were up-regulated and 25 were down-regulated. Notably, STEAP3, CSS2, CLDN1, and TMEM2 were regulated by at least 2 fold in both cell lines. On the other hand, some were unique to each cell type (such as E2F7, ATF3, MAPK3 and LSM14a in ABC28 cells and BNIP3L, ADAMTS8, and RAFTLIN in HeLa cells). These genes may reflect a signal-specific role for TRIM22.

21% of regulated genes in ABC28 cells and 19% of regulated genes in HeLa cells are membrane proteins. Transmembrane protein 2 (TMEM2) was previously identified by Leo et al. to be up-regulated by progesterone by 3-fold (Leo et al., 2005). In this study, knockdown of TRIM22 led to down-regulation of TMEM2 by at least 2-fold in progesterone-treated ABC28 cells. This is consistent with the ability of progesterone to enhance TRIM22 levels. TMEM2 was down-regulated in HeLa cells to a greater extent consistent with the greater knockdown efficiency of TRIM22 in these cells (**Table 3.2**).

Although not much is known about TMEM2 apart from its plausible role in auditory loss (Scott et al., 2000), our results suggest that TMEM2 is a downstream target of TRIM22.

STEAP3, up-regulated in both cell lines upon TRIM22 silencing, is a direct p53-target gene. In the absence of TRIM22 siRNA, IFNγ also enhanced STEAP3 levels (by about 4.5 fold) in HeLa cells unlike progesterone, which did not enhance STEAP3 levels in ABC28 cells. STEAP3 was found to enhance apoptosis (Passer et al., 2003). The increase in STEAP3 levels is consistent with the greater growth G0/G1 arrest observed in TRIM22 siRNA-transfected ABC28 cells in cell cycle analyses (**Figure 3.29**). The regulation of STEAP3 at the protein level could not be studied due to the unavailability of a good antibody.

Of the regulated genes, the expression of CLDN1 (Claudin-1) and ATF3 (Activating Transcription Factor 3) was investigated at the protein level. Claudin-1 is a structural tight junction (TJ) protein which regulates epithelial barrier function. It also serves as a mode of cell-to-cell adhesion in epithelial and endothelial cells. ATF3 is member of the mammalian activation transcription factor/CREB protein family of transcription factors. The regulation of ATF3 was specific to ABC28 cells, where TRIM22 siRNA reduced ATF3 transcript levels by at least 2 fold.

Figure 3.31 shows the protein levels of TRIM22, Claudin-1, ATF3 and the housekeeper GAPDH in TRIM22 siRNA-transfected samples compared to the control siRNA transfected samples in ABC28 and HeLa cells. The increase in TRIM22 levels upon IFNγ

Table 3.2 Genes differentially regulated in ABC28 and HeLa cells after TRIM22 silencing.

Cells were transfected with 10 nM control or TRIM22 siRNA 6 or 7 for 8 hr, then treated for 48 hr with 10 nM progesterone (ABC28) or 250 IU/ml IFNγ (HeLa). RNA was extracted, mRNA amplified and hybridized to Illumina BeadChip Arrays. Results from array read-outs were analyzed by the GeneSpring GX software. Genes regulated by at least 2 fold in the microarray (MA) analysis have been tabulated. Ten genes were validated by real-time PCR (RT-PCR) using specific primers. Highlighted genes were regulated in both ABC28 and HeLa cells.

ABC28			**siRNA 6**	**siRNA 7**
Public ID number	**Gene Symbol**	**MA**	**RT-PCR**	
NM_006074	TRIM22	-2.3	-5.6	-3.3
Cell cycle, growth and apoptosis regulators				
NM_203394	E2F7	-3.0	-2.0	-3.3
NM_002155	HSPA6	-2.6		
NM_005345	HSP72	-2.2		
NM_015578	LSM14a	2.2	2.8	2.8
NM_018234	**STEAP3**	**2.5**	**2.0**	**3.9**
Signal transduction				
NM_016103	SARA2	2.2	2.0	2.0
NM_002746	MAPK3	2.5	2.3	2.5
Cytokines and chemokines				
NM_181339	IL-24	-2.2		
Genes involved in metabolism				
NM_024536	**CSS2**	**2.0**	**2.7**	**3.9**
Membrane proteins				
NM_006691	XLKD1	-2.4		
NM_021101	**CLDN1**	**-2.0**	**-2.1**	**-3.0**
NM_013390	**TMEM2**	**-2.0**	**-2.6**	**-1.9**
Transcription factors				
NM_001030287	ATF3	-2.0	-2.4	-2.6

HeLa			**siRNA 6**	**siRNA 7**
Public ID number	**Gene Symbol**	**MA**	**RT-PCR**	
NM_006074	TRIM22	-3.6	-8.3	-10.0
Cell cycle, growth and apoptosis regulators				
NM_001013398	IBP3	-3.8		
NM_004331	BNIP3L	-2.3	-3.2	-2.3
NM_005156	ROD1	2.4		
NM_018234	**STEAP3**	**3.3**	**3.8**	**2.9**
Signal transduction				
NM_006240	PPEF1	-3.5		
NM_033120	NKD2	-2.9		
NM_138689	PPP1R14B	2.2		
NM_003405	YWHAH	2.8		
Cell adhesion, motility, angiogenesis				
NM_007037	ADAMTS8	-4.2	-9.1	-3.2
NM_001145	ANG	-2.1		
NM_001627	ALCAM	3.0		
Genes involved in metabolism				
NM_018192	LEPREL1	-3.5		
NM_012434	SLC17A5	-2.0		
NM_175856	CSS3	2.4		
NM_024536	**CSS2**	**2.6**	**2.3**	**2.3**
NM_002133	HMOX1	3.9		
Genes related to neural function				
NM_020783	SYT4	-3.6		
NM_000304	PMP22	-2.0		

HeLa			**siRNA 6**	**siRNA 7**
Public ID number	**Gene Symbol**	**MA**	**RT-PCR**	
Membrane proteins				
NM_021101	**CLDN1**	**-**	**-3.6**	**-12.5**
NM_015150	RAFTLIN	-4.9	-3.9	-2.0
NM_013390	**TMEM2**	**-3.5**	**-7.2**	**-4.2**
NM_173833	SCARA5	-2.9		
NM_174959	SVOPL	-2.9		
NM_001024847	TGFBR2	-2.7		
NM_004616	TM4SF3	-2.5		
Transcription factors				
NM_001030287	ATF3	-	-2.4	***-1.6***
NM_080473	GATA5	-2.8		
Genes with unknown functions				
NM_031476	CRISPLD2	-3.4		
NM_144973	FLJ41648	-3.4		
NM_080833	C20orf121	-3.2		
NM_020299	AKR1B10	-2.9		
NM_173553	TRIML2	-2.8		
NM_174983	C19orf28	-2.6		
NM_138720	HIST1H2BD	-2.3		
NM_024096	XTP3TPA	2.1		
NM_024625	ZC3HAV1	2.5		
NM_052853	ADCK2	2.6		
NM_017918	FLJ20647	4.0		

treatment was more obvious than the increase induced by progesterone treatment. Despite this, both ATF3 and Claudin-1 were up-regulated by progesterone in ABC28 cells but not by IFNγ in HeLa cells. This points to a previously unknown effect of progesterone on the regulation of these proteins.

In the presence of TRIM22 siRNA, Claudin-1 was down-regulated in both cell lines while ATF3 was exclusively down-regulated in ABC28 cells (**Figure 3.31**). This is consistent with the gene expression analysis results where ATF3 was down-regulated by both TRIM22 siRNA in ABC28 cells but not in HeLa cells. Interestingly, the differential regulation of CLDN1 in HeLa cells upon TRIM22 silencing missed detection by microarray analysis. However, real-time PCR analyses showed that Claudin-1 transcript levels were reduced in both ABC28 and HeLa cells and this was confirmed at the protein level.

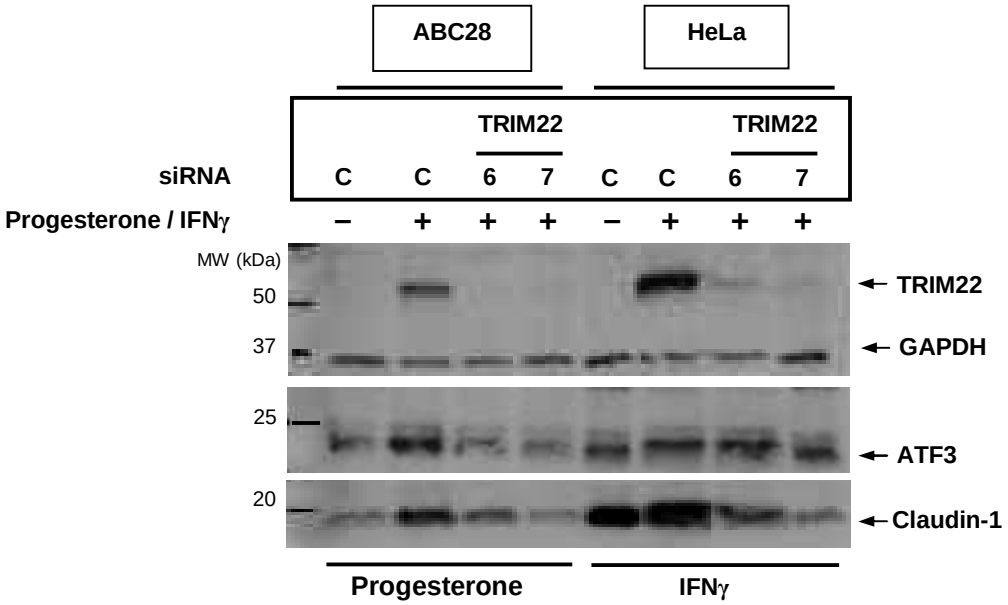

Figure 3.31 Silencing TRIM22 reduces Claudin-1 protein levels in both ABC28 and HeLa cells but reduces ATF3 levels in only ABC28 cells.

ABC28 cells were treated with ethanol (–) or 10 nM progesterone after transfecting with control (C) or TRIM22 siRNA (10 nM). HeLa cells were left untreated (–) or treated with 250 IU/ml IFNγ after transfecting with control (C) or TRIM22 siRNAs 6 or 7 (10 nM). 48 hr later, cells were harvested and lysates analyzed by Western blotting using anti-ATF3, anti-Claudin-1, anti-TRIM22 and anti-GAPDH antibodies. Results are representative of three independent experiments.

CHAPTER 4

DISCUSSION

There is intensive research being conducted in the area of TRIM family proteins because of their recognized antiviral activities. Compared to some TRIM proteins like TRIM5α and TRIM19/PML, TRIM22 has been fairly understudied. Our interest in TRIM22 stems from the finding that the TRIM22 transcript was greatly up-regulated in progesterone-treated breast cancer cells. In order to understand the relevance of TRIM22 to breast cancer, we first needed to evaluate the location of the endogenous protein, which has not been reported before. Using a specific antibody against TRIM22 and different TRIM22 specific siRNA, we show for the first time that TRIM22 is a predominantly nuclear protein that localizes as NB and as a nucleoplasmic protein. In contrast to progesterone which increases both forms, IFNγ stimulates a dispersal of TRIM22 bodies, a situation typically observed in the S phase, and this is coincident with when antiviral activity, such as in the suppression of viral gene expression, is likely to be most relevant. A notable finding in this study is that TRIM22 is associated with growth inhibition in MECs.

4.1 TRIM22 is a dynamically regulated nuclear protein

Previous studies in cells ectopically expressing TRIM22 have reported a predominant cytoplasmic localization for the protein. An important finding of this study is that, like PML, endogenous TRIM22 can exist as a nucleoplasmic protein as well as distinct NB, irrespective of cell type. The TRIM22 NB is not merely a static aggregate of a sticky protein since it underwent dynamic changes in response to cell state. The NB is also not the result of large amounts of protein since IFNγ-treated HeLa cells expressed much greater levels of the TRIM22 protein but it did not localize as evidently to NB in these cells as in progesterone-treated ABC28 cells. Notably, progesterone also induced the

nucleolar localization of TRIM22 NB. Our findings with TRIM22 parallel findings with other NB such as CBs and SMN foci/gems, which also undergo dynamic changes during the cell cycle (Platani et al., 2000; Sleeman et al., 2003).

4.1.1 Nucleolar TRIM22

4.1.1.1 Evidence for the nucleolar localization of TRIM22

The presence of progesterone-induced TRIM22 NB within nucleoli is consistent with the ability of TRIM22 to interact, either directly or indirectly, with B23, a major component of the granular layer of the nucleolus. The nucleolar localization of other well-described nucleolar proteins ARF and C23/nucleolin also requires their physical interaction with B23 (Colombo et al., 2005; Enomoto et al., 2006; Li et al., 1996). The mediocre pull-down of B23 by TRIM22 in MCF7 cells is not surprising since only a very small fraction of TRIM22 NB were observed to be present within the granular layer of the nucleolus at any given point in these cells and immunofluorescence studies showed a displacement of B23 in positions where TRIM22 NB were present. The displacement of B23 may be due to the inability of the TRIM22 molecules within the TRIM22 body to interact with B23, allowing only those present in the exterior of the protein to interact. Clearly, further studies, including the identification of a minimal motif required for interaction of TRIM22 with B23 and confocal and/or electron microscopy, are required to lend further support to the postulation that TRIM22 is a nucleolar protein.

4.1.1.2 Nucleolar localization signals

Nucleolar localization signals (NoLS) have been identified in several nucleolar proteins, such as nucleolin, ARF, MDM2, and p80-coilin, to be critical for nucleolar localization. The NoLS sequence is typically rich in arginine (R) and lysine (K) residues, much like the NLS. The motif responsible for the nucleolar localization of ARF appears to be a cluster of basic amino acids while that of MDM2 and p80-coilin have been specified to be KKLKKRNK and KKNKRKNK, respectively (Hebert and Matera, 2000; Lohrum et al., 2000; Weber et al., 1999). In this study, we have shown that the putative central bipartite NLS identified previously (KRSESWTLKKPKSVSKKLK) is, by itself, inadequate to induce the nuclear localization of TRIM22 since the NLS-deficient mutant continues to localize within the nucleus to some extent and C-terminal deletion mutants (lacking as few as 19 aa) having this motif do not localize within the nucleus. As this region is also rich in arginine and lysine residues, its contribution to nucleolar localization should be investigated.

4.1.1.3 Significance of nucleolar TRIM22

Within the nucleolus, TRIM22 may be involved in conventional nucleolar processes such as ribosome biogenesis and rDNA gene regulation similar to other nuclear proteins that can regulate nucleolar processes despite not being constitutively resident within the nucleolus (MacCallum and Hall, 2000). Observations with ARF, ER and p80-coilin offer other possibilities. ARF primarily functions as a tumor suppressor since, by sequestering and inactivating the p53-degrader MDM2, it stabilizes p53. Despite some evidence that nucleolar ARF may negatively regulate rDNA transcription and bind MDM2,

sequestering it away from nucleoplasmic p53, there is evidence implicating the nucleolus as a storage compartment for ARF, and perhaps other proteins (Ayrault et al., 2006; Weber et al., 1999). The localization of ARF within nucleoli not only stabilizes the protein but was also found to negatively regulate its tumor suppressor function. B23, abundant in the nucleolus, inhibited the association of ARF with MDM2 and B23 knockdown led to ARF's nucleoplasmic localization coincident with greater ARF-mediated growth suppression and p53 activation (Korgaonkar et al., 2005; Moulin et al., 2008; Rodway et al., 2004). Further support for a storage role for the nucleolus comes from a study that found that ectopic GFP-tagged ER could localize within nucleoli in ER-negative cell lines but not in ER-positive cell lines (Htun et al., 1999).

In the case of p80-coilin required for CB formation, almost half of all the CBs were found to exist within the nucleolus in adult tissues but were exclusively nucleoplasmic in rapidly dividing cultured cells (Young et al., 2001). Phosphorylation has been identified to be one mechanism through which localization of p80-coilin is regulated. Treatment of cells with a CDK inhibitor (olomoucine) led to a relocalization of p80-coilin to the nucleolar periphery (Liu et al., 2000). Moreover, p80-coilin has a consensus serine residue (S_{184}PKK) that is likely to be phosphorylated by the CDK2/cyclin E complex, which is present within the CBs and is necessary for G1/S transition and S phase DNA synthesis (Carmo-Fonseca et al., 1993; Liu et al., 2000). Mimicking a constitutively dephosporylated state of p80-coilin by mutating this serine residue to an alanine residue led to p80-coilin localizing within the nucleolus (Hebert and Matera, 2000). Together, these observations suggest that, in the absence of an active CDK2/cyclin E complex,

dephosphorylated p80-coilin might associate with nucleoli. Since CBs have a variety of roles outside the nucleolus and a nucleolar role for mammalian CBs has yet to be established, nucleoli-associated p80-coilin/CBs may be dormant bodies. We have identified progesterone to be an inducer of TRIM22 nucleolar localization but the significance of this relocalization and the mechanism through which this is achieved is not clear. It is possible that TRIM22, like ARF and p80-coilin, is stored in or next to nucleoli in the G0/G1 phase awaiting distribution during the S phase of the cycle where the protein assumes a nucleoplasmic localization. Although a nucleolar role for TRIM22 cannot be dismissed, its aggregation as bodies would presumably also limit the number of functional TRIM22 protein molecules within these structures. The relative inactivity of TRIM22 in progesterone-treated ABC28 cells is supported by the finding that TRIM22, though growth inhibitory in other MECs and effectively silenced in progesterone-treated ABC28 cells, does not mediate progesterone's growth inhibitory effects in the latter.

4.1.2 Nucleoplasmic TRIM22

Barr et al. noted that IFNγ induced the TRIM22 transcript more so than those of the other TRIM proteins (Barr et al., 2008). In our experiments, IFNγ enhanced TRIM22 transcript levels by more than 100-fold. The preference for nucleoplasmic localization of large amounts of TRIM22 in IFNγ-treated cells is interesting. It is similar to the localization of PML in virus-infected cells (Everett and Chelbi-Alix, 2007) and suggests that TRIM22 may be functional when dispersed. It is also evidence that TRIM22 NB formation is a specific event that occurs not just because of large protein amounts. Further experimentation on the biochemical nature of (that is, the proteins associated with) the

nucleoplasmic and NB forms of TRIM22 is required before the functionality of the nucleoplasmic form as the antiviral form can be tested. While it is possible that nucleoplasmic TRIM22 may reflect a transitory stage in the formation of NB in IFNγ-treated cells, the rare occurance of TRIM22 NB in the numerous cells observed when TRIM22 is present in large amounts in these cells does not support this possibility. Rather, the observation that IFNγ keeps the large amounts of TRIM22 dispersed suggests the presence of other factors that may work to minimize TRIM22 NB formation.

4.1.2.1 Significance of nucleoplasmic TRIM22

A variety of cellular processes occur within the nucleoplasm. Although further proof is required, the finding that ectopically-expressed 442 aa TRIM22 inhibited transcription from the LTR of HIV-1 in reporter assays suggests TRIM22 may serve as a transcription factor within the nucleoplasm (Tissot and Mechti, 1995). A role for TRIM22 in protein degradation within nuclear proteasomes should also be considered for several reasons. Firstly, while not yet reported for TRIM22, numerous TRIM proteins have been found to induce degradation of specific substrates, typically via their RING domains and associated E3 ligase activities, as a means for regulating cell processes (Trockenbacher et al., 2001; Urano et al., 2002). Secondly, the finding that IFNγ also enhances the expression of three subunits of the 20S proteasome suggests a greater-than-normal proteasomal activity within the nucleus in the presence of IFNγ and, subsequently, TRIM22 (Aki et al., 1994; Akiyama et al., 1994; Früh et al., 1994).

A recent study showed that TRIM22, by associating with the HIV-1 Gag protein via the former's RING domain, inhibited Gag oligomerization and that this was associated with reduced HIV-1 infection (Barr et al., 2008). While Gag itself is capable of self-assembly and capsid formation *in vitro*, several host factors, such as Staufen 1, the δ subunit of the AP-3 complex, and the ATPase ABCE-1, have been found to facilitate the assembly of Gag polyproteins (Goff, 2007). Since ectopic 442 aa TRIM22 did not alter Gag levels in their study, Barr et al. proposed that TRIM22 may target a host cell factor required for Gag trafficking, if not Gag itself, to cause Gag mis-localization thereby preventing its assembly at the plasma membrane. While this is certainly a possibility, the ability of full-length 498 aa TRIM22 to degrade Gag should also be investigated since the SPRY domain in TRIM22 is the largest of the four domains, and it can have a substantial influence on the conformation, localization (as we have shown in this study), and function of the protein. Moreover, a large proportion of Gag is known to undergo rapid proteasome-mediated degradation but a human protein responsible for Gag degradation has yet to be identified (Schubert et al., 2000). Nucleoplasmic TRIM22 may also function as a growth-inhibitory protein since MCF12A cells also expressed this form of the protein.

4.2 TRIM22's SPRY domain is a critical determinant of nuclear localization and NB formation

Early in the study, we found that the endogenous TRIM22 mRNA contained the 3' end required for the expression of a 498 aa TRIM22 protein. This led to our focus on the full-length TRIM22 protein as opposed to the shorter variants. As the largest identified

domain and one that has the most variability between the different TRIM proteins, we also expected the SPRY domain (a 145 aa domain) to contain the crucial residues that set TRIM22 apart from its paralogs. Indeed, deleting the last 5 aa or 19 aa within the SPRY domain was adequate to reduce and abrogate nuclear localization, respectively. Although deleting residues within the SPRY domain could have altered the protein's actual conformation and contributed to the block in nuclear entry, larger deletion mutants such as those lacking the RING and B-box2 domains (TRIM22-ΔRING and TRIM22-ΔRING/B2) were still able to enter the nucleus. Thus, important residues in the last 19 residues of the protein may interact with those in the putative bipartite NLS to facilitate nuclear localization of TRIM22.

We also found that a hydrophobic residue in the 493rd position of the protein and the residue at position 494 are important for the localization of TRIM22 as distinct NB. Mutating V493 to the small amino acid alanine led to the formation of large rings, which were not observed as evidently when C494 was mutated to alanine or glutamic acid. Deleting C494 or mutating both V493 and C494 to alanine residues also reduced the propensity of the mutant to form NB, resulting in greater nucleoplasmic staining. There may be other residues within the N-terminal region that also contribute to NB formation since TRIM22-ΔRING could not form NB. Further studies are underway to identify the residues that dictate the formation of TRIM22 NB. The formation of bodies may serve to limit the function of the protein, since the number of molecules in contact with substrates would be reduced. Alternatively, bodies may also concentrate the protein and provide a more optimal environment for certain processes, as seen with PML bodies. Regardless,

knowing what drives body formation, the significance of these bodies and whether bodies within and outside of nucleoli have different functions are likely to improve our understanding of TRIM22's function.

4.3 A model for TRIM22 dynamics

Analysis of TRIM22 localization in different cell types expressing different levels of endogenous TRIM22 protein and the use of TRIM22 siRNA has given us some important insights regarding the final destination of TRIM22 in the cell. Both the nucleolar and nucleoplasmic forms of the protein were almost *completely* eliminated by TRIM22 siRNA, confirming that these forms were indeed TRIM22. In contrast, TRIM22 NB, though of lesser intensity compared to those in control siRNA transfected cells, were not completely abrogated by TRIM22 siRNA. It is tempting to speculate that the majority of nucleoplasmic and nucleolar TRIM22 bodies were formed with newly synthesized TRIM22 protein as a result of progesterone stimulation, while TRIM22 NB may consist of a mixture of older and newer TRIM22 protein. In order to discern the pathway that TRIM22 takes once within the nucleus, MCF7 cells stably expressing TRIM22-EGFP were subjected to live-cell imaging (results not shown). These experiments revealed that TRIM22-EGFP NB frequently attach to the nucleolar periphery. As these ectopically expressed NB were much bigger that endogenous TRIM22 NB, their size may have precluded entry into nucleoli, if the NB does not disintegrate prior to nucleolar entry. As it is also possible that the TRIM22 NB disintegrates before entering nucleoli and then reforms within the nucleolus as a biochemically distinct entity, then the absence of

appropriate signals, such as those provided by progesterone, may explain their nucleolar exclusion.

Collectively, the current findings suggest that nuclear TRIM22 may take three possible routes soon after expression: 1) In the absence of stimuli targeting their entry into the nucleolus, TRIM22 is exclusively extranucleolar, where its propensity to form NB is determined by cell state and/or its functionality, 2) TRIM22 NBs are initially formed in the nucleoli and then exported out of nucleoli, where they may disperse or localize as distinct NB, and 3) TRIM22 NBs are formed outside the nucleoli but are translocated into nucleoli or tethered next to nucleoli before subsequent translocation back out of the nucleoli to the extra-nuclear regions and/or dispersion (depicted in **Figure 3.33**). The last possibility is supported by evidence from cell synchronization experiments where TRIM22 NB formed and were present throughout the nucleus during cytokinesis, when nucleoli are forming, and were present within the nucleoli in early G0/G1 phase.

4.4 Probable functions of TRIM22

4.4.1 TRIM22 is a progesterone-regulated protein

TRIM22 was initially reported as an IFN-inducible gene. In addition to confirming the ability of IFNs β and γ to regulate the TRIM22 protein, we have shown for the first time that TRIM22 is dramatically enhanced by the female reproductive hormone progesterone. Upon analyzing TRIM22 transcript and protein levels in different MEC lines with different hormone receptor statuses and tumorigenicity, we not only noted differences in the basal levels of the TRIM22 protein but also differences in the fold-induction of

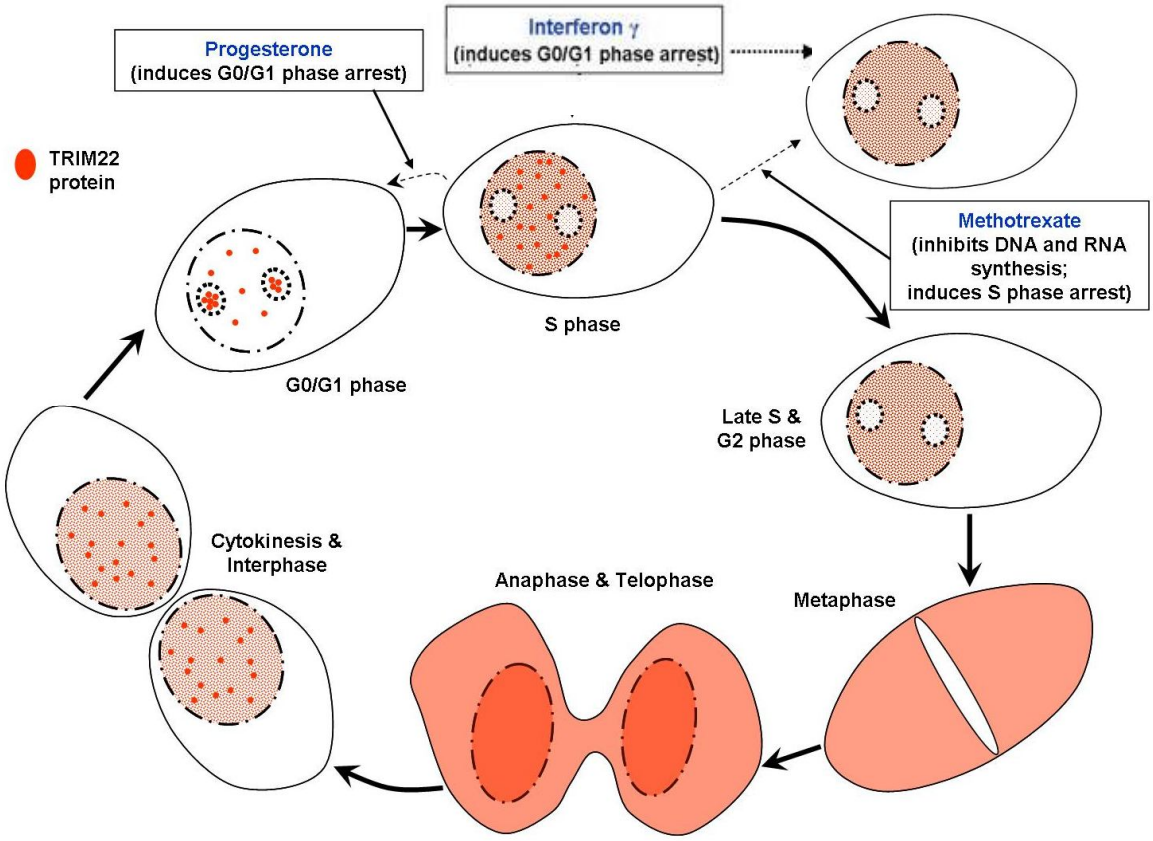

Figure 3.32 Model for TRIM22 dynamics.
The schematic summarizes the observations of TRIM22 (red) localization in cells in different phases of the cell cycle and in response to progesterone, interferon γ and methotrexate. The regular bodies present in the G0/G1 phase gradually disperse as cell progress through the S and G2/M phases. In metaphase, anaphase and telophase, TRIM22 is likely to be completely diffused. Bodies reform before the end of cytokinesis. Cells in the G0/G1 phase tend to have nucleolar TRIM22 bodies.

TRIM22 upon progesterone treatment. Thus far, two TRIM proteins have been found to be linked to estrogen signaling in MECs. TRIM25/Efp is an estrogen-regulated protein that enhances cell proliferation by modulating the levels of the cell-cycle regulator 14-3-3σ (Urano et al., 2002). TRIM27/RFP is a transcription factor and a component of PML bodies (Cao et al., 1998). By interacting with the ER repressor Scaffold attachment factor B1 (SAFB1), RFP has been implicated in modulating ER-directed gene expression (Townson et al., 2006). For the first time, we have shown that progesterone regulates the expression of a TRIM member. The finding is significant for two reasons. First, the up-regulation of TRIM22 by progesterone was of high magnitude (10 – 20 fold at the mRNA level and 4 - 10 fold at protein level) and was observed in breast cancer cell lines with both ectopic PR expression (ABC28 cells) and endogenous PR expression (T47D cells). Secondly, progesterone is critically involved in implantation, maintenance of pregnancy, and the growth and differentiation of the mammary gland. The observation that TRIM22 is the target protein of endogenous PR and is present abundantly in non-tumorigenic mammary epithelial cells suggests that TRIM22 may play a role in female reproductive function.

4.4.2 TRIM22 is a growth-inhibitory protein in mammary epithelial cells

Having confirmed the regulation of the TRIM22 protein by both progesterone and IFNs, and in view of a previous report that ectopic TRIM22 expression inhibits the growth of leukemic cells, it was of interest to investigate if TRIM22 was responsible for the growth inhibitory activity of progesterone in breast cancer cells (Obad et al., 2004). The low levels of TRIM22 in tumorigenic cells and high levels in non-tumorigenic cells allowed

us to study the effect of overexpressing and silencing TRIM22 in MCF7 and MCF12A cells, respectively. Indeed, three lines of evidence show that TRIM22 is growth-inhibitory in MEC: 1) basal TRIM22 protein levels are much higher in non-tumorigenic MEC compared to tumorigenic MEC, 2) overexpression of the protein in the MCF7 cell line (which had less endogenous TRIM22 transcript compared to the other breast cancer cell lines investigated) resulted in enhanced growth inhibition in the G0/G1 phase of the cell cycle, and 3) silencing TRIM22 using two out of the three TRIM22 siRNA in non-tumorigenic MCF12A cells enhanced the percentage of cells in the S phase of the cell cycle. These findings are consistent with TRIM22 being a target gene of the tumor suppressor p53. Interestingly, the results of a recent gene expression study in patients afflicted with the neuroblastoma Wilms' tumor support a tumor suppressor role for TRIM22. In this study, TRIM22 mRNA levels were greatly reduced in tumor tissue and this correlated with a higher incidence of tumor relapse and death, despite p53 being a positive predicator of poor prognosis in these patients (Maheswaran et al., 1995; Sredni et al., 2001; Wittmann et al., 2008).

TRIM22 inhibited growth in two types of MECs. However, in tumorigenic ABC28 cells induced to express TRIM22, silencing TRIM22 was not adequate to reverse the progesterone-induced G0/G1 arrest. This suggests that, in ABC28 cells, TRIM22 is either not active or is not involved in growth inhibition and has other functions. As TRIM22 is a downstream target of p53, the inability of TRIM22 to inhibit growth in ABC28 cells like it did in MCF7 and MCF12A cells may be related to the p53 status of these cells. MDA-MB-231 cells, from which the ABC28 cell line was derived, have a mutant p53 gene

while both the MCF7 and MCF12A cells are positive for p53 (Kenny et al., 2007). The third possibility is that the silencing TRIM22 in itself is inadequate to reverse the progesterone-induced growth arrest. This is because progesterone has been previously shown to regulate the activity of several important cell-cycle proteins. It up-regulates the expression of the CDK inhibitor $p21^{WAF1}$ and decreases the expression of cyclins A, B1 and D1, which are required for progression from the G1 to the S phase of the cell cycle (Lin et al., 2003). Whether it is an inactive TRIM22 or an inadequately active TRIM22 that is responsible for the lack of growth inhibition in progesterone-treated ABC28 cells needs to be clarified. Regardless, the under-expression of this protein in breast cancer cells with high expression in normal MECs supports a potential tumor suppressor role for TRIM22.

4.4.3 Endogenous TRIM22 may have different roles in tumorigenic cells

To gain a better understanding of the function of TRIM22 in ABC28 and HeLa cells, a gene expression analysis was conducted and results of this analysis were verified by real-time PCR. The TRIM22 siRNA sequences used for microarray analysis were both specific for TRIM22 and did not have homology with sequences for the transcripts that emerged as being down-regulated. In addition, as the TRIM22 siRNA sequences targeted different regions of the TRIM22 transcript (**Table 2.4**), genes that were truly regulated as a result of TRIM22 knockdown, and not because of non-specific knockdown effects that can occur in gene silencing studies, were identified.

4.4.4 A non-apoptotic role for TRIM22 in ABC28 cells

While the gene expression analysis did not reveal deregulations in specific pathways for the role of TRIM22 to be obvious, differential regulation of some genes supported the results of the cell-cycle analysis. For instance, the STEAP3 transcript was up-regulated after TRIM22 knockdown in both ABC28 and HeLa cells. As STEAP3 is a pro-apoptotic downstream target of p53 and STEAP3 is known to interact with other pro-apoptotic proteins like BNIP3L, STEAP3 protein levels in TRIM22 knockdown cells should be investigated once a good commercial antibody for this protein becomes available (Chen et al., 1999; Passer et al., 2003). While verifying the results of the gene expression analysis by real-time PCR, IFNγ, but not progesterone, was found to enhance STEAP3 transcript levels (results not shown). Though inconsistent with IFNγ being an enhancer of TRIM22, these results point to a possible role for TRIM22 in regulating the extent of STEAP3 induction by IFNγ.

Unlike STEAP3, some other genes like ATF3, were down-regulated specifically in only ABC28 cells. The significance of the down-regulation of ATF3 in ABC28 cells is not clear since a recent study showed that ATF3 has both apoptotic and anti-apoptotic functions depending on the aggressiveness of the cell line. ATF3 induced apoptosis in MCF10A cells but protected transformed and aggressive derivatives from stress-induced cell cycle arrest (Yin et al., 2007). The ATF3 gene was also found to be amplified in breast cancer epithelia, supporting an oncogenic role for the protein (Yin et al., 2007). The ABC28 cell line was derived from the invasive cell line MDA-MB-231 (Lin et al., 1999). Presumably therefore, the down-regulation of ATF3 protein levels upon TRIM22

silencing would reverse the protective oncogenic effect of ATF3 in these cells. Besides progesterone's effects on cell-cycle proteins, the induction of STEAP3 and inhibition of ATF3 in ABC28 cells may also explain why silencing TRIM22 did not reverse the G0/G1 arrest in breast cancer cells. The absence of ATF3 regulation in TRIM22 siRNA transfected HeLa cells suggests that ATF3 may be downstream of TRIM22 in a cell- and/or stimulus-specific manner.

4.4.5 TRIM22 is a potential mediator of progesterone's effect on Claudin-1 expression in breast cancer cells.

In this study, Claudin-1 was found to be increased by progesterone treatment and down-regulated upon TRIM22 silencing in both progesterone-treated ABC28 cells and IFNγ-treated HeLa cells. The induction of Claudin-1 by progesterone, via TRIM22, is a novel finding that may be important in elucidating progesterone's contribution to cell proliferation. Claudin-1 is an integral TJ protein that is critical for the function of TJs as barriers (Furuse et al., 1998). TJs, by forming a narrow continuous seal around both epithelial and endothelial cells, regulate the transport of solutes through the paracellular pathway. A complete absence of TJs has been associated with the development of neoplasia in epithelial cells, particularly those in the colon (Mullin et al., 2000). Proliferating MEC also have lower Claudin-1 levels compared to senescent MEC (Swisshelm et al., 1999). How Claudin-1 links to neoplasia is not clear; it has been hypothesized that the disruption of TJs in the absence of Claudin-1 may allow luminal growth factors to cross the epithelial cell and bind to growth factor receptors on the

basolateral surface of the cell or on other cell types to stimulate cell proliferation (Mullin et al., 2000).

It is also noteworthy that Claudin-1 is reduced or mis-localized in invasive breast tumors (Martinez-Estrada et al., 2006; Tokes et al., 2005). The conversion of epithelial cells to mesenchymal cells, termed an epithelial-mesenchymal transition (EMT) that have fibroblastic morphology is an important event in cancer progression, enabling cancer cells to become invasive and metastatic. EMT is regulated by the Snail superfamily of zinc-finger transcription factors which are known to repress the expression of the adherens junction protein E-cadherin and TJ proteins (Batlle et al., 2000; Bolos et al., 2003; Cano et al., 2000; Hajra et al., 2002; Ikenouchi et al., 2003). Recently, Snail and Slug were shown to directly repress Claudin-1 expression in breast cancer cells (Martinez-Estrada et al., 2006). The invasive and metastatic MDA-MB-231 cell line had lower levels of Claudin-1 and higher levels of Slug transcripts compared to the non-invasive MCF7 and T47D cell lines (Martinez-Estrada et al., 2006).

Previous studies have shown that progesterone-treated ABC28 cells are less tumorigenic in SCID mice (Lin et al., 2001). Given that silencing TRIM22 results in an inhibition of Claudin-1 at both the transcript and the protein levels and Claudin-1 is a critical component of TJs, TRIM22 may serve to enhance TJ integrity and thereby contribute to the reduced tumorigenicity observed in progesterone-treated ABC28 cells. The localization of Claudin-1 is also an important factor relevant to the function of Claudin-1 in TJ integrity. In cervical epithelial cells, for instance, Claudin-1 expression increased

during pregnancy but a large portion of these molecules were cytoplasmic and only localized to TJs when epithelial cells underwent terminal differentiation (Timmons et al., 2007). As such, it is important to test if progesterone does enhance TJ integrity and if TRIM22 is a mediator of this.

4.4.6 TRIM22's role in the cell may be linked to that of CBs

The ability of TRIM22 to interact with p80-coilin was demonstrated. Their interaction is likely to be involved in the association of TRIM22 NB with CBs within MCF7 and progesterone-treated ABC28 cells. Using a domain deletion approach, the site important for TRIM22's interaction with p80-coilin was narrowed down to a region spanning residues 139 to 352 of the protein. The CC domain, and residues flanking this domain, particularly those between the CC and the SPRY domains, may be important in the interaction of TRIM22 with p80-coilin. The observation that TRIM22 NB colocalizes only partially with the CB and that CC domains, known to mediate multimerization in other TRIM proteins, is likely to be exposed on the surface of the TRIM22 NB supports the contribution of TRIM22's CC domain to its association with CBs. However, whether it is the CC domain *per se* that is required for interaction with p80-coilin or if it is the CC-dependent multimerization of TRIM22 that is required for interaction needs to be ascertained.

As TRIM22 NB associate with CBs, unlike our observations with PML bodies which did not occur adjacent to TRIM22 NB (data not shown), TRIM22 NB and CBs may be functionally related. However, since CBs were not associated with TRIM22 NB in all

cells, TRIM22 NB may associate only transiently with CBs at certain stages of the cell cycle. A transient interaction between TRIM22 NB and CBs is supported by striking differences in their dynamics during the S phase. Like TRIM22 NB, CBs also disappear during metaphase and reform in the G0/G1 phase, with cells in mid-to-late G1 phase having multiple CBs (Andrade et al., 1993). However, late in the cell cycle as cells progress through the S and G2 phases, CBs are larger and fewer in number. Considering this, the probability of observing an association between TRIM22 NB and CBs would be greatest in the early G0/G1 phase. Although there was no obvious difference in the association between these two nuclear structures at any particular phase in synchronized HeLa cells stably expressing TRIM22-EGFP (results not shown), TRIM22 bodies were observed to be in close association with CBs at the periphery of the nucleolus in some progesterone-treated ABC28 cells. Thus, these bodies do associate early in interphase. There was also an obvious colocalization between p80-coilin and TRIM22 in cytoplasmic strand-like structures. CBs are important in the biogenesis of snRNP and snoRNP, which are crucial for splicing reactions. From the literature, it is also evident that CBs are important for several cell proliferation processes such as histone biosynthesis. Since we have observed that TRIM22 is growth-inhibitory and that TRIM22 bodies are associated with CBs within nuclei and the cytoplasm, it would be worthwhile investigating if the presence of TRIM22 NB impinges on CB activity to exert its growth-inhibitory effect in MECs, and if so, how it does this.

4.5 Future studies

In the present study, using specific antibodies generated against the TRIM22 protein, we have made novel observations regarding the regulation and localization of basal and induced TRIM22 protein within the nucleus of the mammalian cell. Importantly, progesterone was identified as a novel regulator and p80-coilin as an interactor of TRIM22. Through gene overexpression and silencing studies, TRIM22 was also found to be growth inhibitory in MECs. The microarray analyses in progesterone and IFNγ-treated cells have also allowed enabled the identification of several TRIM22 targets.

One of the more notable findings in this study is that TRIM22 is a progesterone-regulated protein and an increase in the TRIM22 transcript levels is obvious within 3 hr of treatment. Thus, TRIM22 is likely to be a direct target of progesterone. One way to test this is to analyze the TRIM22 promoter for possible PRE(s) and then test these sequences for their ability to bind to PR using chromatin immunoprecipitation assays and/or reporter assays. A preliminary bioinformatics search of the TRIM22 promoter has been conducted, revealing several PRE half-sites within the first 500 bases upstream of the transcriptional start site. It is also possible that a functional PRE is absent but that activated PR may bind to other transcription factors to induce TRIM22 expression. An extension of this study would be to determine which PR isoform mediates progesterone's effect on TRIM22 levels. PR-B is the more transcriptionally active isoform in normal MECs. However, as elucidated to in **section 1.3.2**, the ratio of isoform expression shifts from an approximately equal PR-A:PR-B expression to a predominant PR-A expression in tumors. Thus, it may be relevant to investigate TRIM22 levels in cell lines expressing

solely PR-A or PR-B. Along the same lines, it would be of interest to determine why TRIM22 protein levels are low in breast cancer cells. The progression of a normal cell into a tumorigenic state has been reported to involve an aberrant methylation of several cancer genes. For instance, the promoters of the *BRAC1* and $p16^{INK4\alpha}$ tumor suppressor genes were found to be hypermethylated in breast cancer samples (Esteller et al., 2001). Likewise, is the distinctly poor expression of TRIM22 in breast cancer cells due to promoter hypermethylation?

While we have shown that the formation of distinct TRIM22 NB requires the presence of the SPRY domain, the observation that TRIM22 induced in IFNγ-treated HeLa and MCF7 cells fails to form NB suggests there may be other molecules regulating the formation of TRIM22 NB. Sumoylation has been identified as a mechanism by which PML forms NB and preliminary experiments in our laboratory have revealed that TRIM22 is a sumoylated protein. We are in the process of determining if sumoylation (or the lack thereof) is involved in TRIM22 NB formation, the residues in TRIM22 that are sumoylated and how progesterone and IFNs affect these processes.

Besides identifying a minimal motif important for the interaction of TRIM22 with the nucleolar protein B23, the intranuclear dynamics of TRIM22 should also be investigated to determine if the TRIM22 NB itself gains access into the nucleolus or if it disassembles prior to entry into the nucleolus (and thereafter re-assembling into distinct bodies). If nucleolar entry is signal-specific and the signal is identified, then the live cell imaging of stimulated cells expressing TRIM22 tagged to photoactivatable GFP (PA-GFP) can be

used to monitor the intracellular mobility of fluorescently tagged TRIM22. The complementary imaging techniques Fluorescent recovery after photobleaching (FRAP) and Fluorescence loss in photobleaching (FLIP) can also be used to investigate the residence time for TRIM22 within the nucleolus and hence how fast nucleolar TRIM22 exchanges with its nucleoplasmic fraction. Such techniques have shed light on the dynamics of other nucleolar proteins (Phair and Misteli, 2000).

As discussed earlier, the inability of TRIM22 to inhibit growth of ABC28 cells may be due to a mutation in the p53 gene in these cells. To test this possibility, the effect of silencing TRIM22 in the presence of apoptotic inducers that cause DNA damage and work via the p53 pathway, can be investigated in MCF7 cells and the normal mammary epithelial cells MCF10A and MCF12A. Such apoptotic inducers include UV radiation, adriamycin, camptothecin, and cisplatin (Amundson et al., 2005). If indeed TRIM22 is involved in growth inhibition via the p53 pathway, then silencing the protein may perturb the apoptotic response one way or other in these cells. The findings from these studies would guide further studies on the roles of TRIM22 in p53 pathways.

Expression analysis has identified a number of molecules downstream of TRIM22 in ABC28 and HeLa cells. An expression analysis in MCF12A and/or MCF10A cells would provide additional information, particularly regarding which genes are involved in TRIM22's growth inhibitory effects. This is currently being pursued in the laboratory. Further experiments with transcriptional and translational inhibitors are also required to investigate if the genes regulated in ABC28 and HeLa cells are direct downstream targets

of TRIM22 or if they are indirectly regulated. Moreover, the other targets such as STEAP3, E2F7, and TMEM2 should also be validated at the protein level. These will help in delineating TRIM22's signaling pathway(s) within the cell.

The inability to express TRIM22 as a soluble protein in its native form has also been an impediment to *in vitro* studies, such as structure determination, that require the use of recombinant protein folded accurately. Circular dichroism spectroscopy of refolded TRIM22-$(His)_6$ used in this study revealed that it had a secondary structure that was not similar to its theoretical secondary structure (results not shown). Thus, its use as a pure recombinant protein was limited to immunization for the purpose of antibody generation. The refolding of TRIM22 into its natural form is likely to be challenging given the presence of numerous cysteine residues within the protein. It is important to determine the conditions that promote the folding of TRIM22 into a structure that is consistent with at least its theoretical/predicted secondary structure. Alternatively, changing the expression host may solve the problem. The expression of the 21-cysteine residue containing protein Muskelin was recently reported (Kiedzierska et al., 2008). By using the Rosetta gami (DE3) strain of *E. coli*, which has mutations enabling the bacterium to maintain reducing conditions within its cytoplasm, the investigators were able to express Muskelin in its native form. This protein was good enough for crystallization. Using the Rosetta gami (DE3) strain of bacteria might facilitate the expression of TRIM22 in its native form.

NB are dynamic heterogeneous structures and TRIM22 NB, like CBs and PML bodies, may contain other proteins and/or associate with other nuclear structures. We have shown using coimmunoprecipitation and immunofluorescence analyses that TRIM22 interacts with the CB signature protein p80-coilin. To confirm this interaction, *in vitro* binding assays can be performed using *in vitro* translated TRIM22 or pure TRIM22 expressed as a fusion to GST. Since we have observed an association between CBs and TRIM22 NB, in order to understand the function of TRIM22, the association of TRIM22 with structures and proteins that CBs are known to interact with should also be investigated. p80-coilin within CBs interacts with SMN, and CBs associate with various gene loci such as the histone and U2 snRNA gene loci, besides NB formed by other proteins (Frey and Matera, 2001; Hebert et al., 2001; Li et al., 2006). TRIM22's association with histone loci and U2 snRNA can be tested using antibodies against Lsm11 and U2 snRNP, respectively, while its association with components of the snRNP complex and other NB can be tested using antibodies against proteins known to exist within these structures. If an association is found, interactions between proteins in these complexes and TRIM22 can then be investigated using conventional co-immunoprecipitation, *in vitro* binding assays and immunofluorescence analyses.

4.6 Conclusion

In this study, using a variety of molecular and cellular approaches and a specific polyclonal TRIM22 antibody, we have shown that TRIM22 is a progesterone- and IFN-inducible nuclear protein that can localize as both a diffuse nucleoplasmic protein and as distinct NB. Importantly, the results of this study suggest TRIM22 is growth inhibitory in

MECs, supporting a tumor suppressor role for TRIM22 in these cells. We have identified a number of TRIM22 targets such as Claudin-1 and STEAP3 that may be relevant in elucidating TRIM22's function. TRIM22 is a worthwhile pursuit because there is increasing evidence that it provides innate immunity against HIV-1, the retrovirus that causes the lethal disease AIDS. Understanding the mechanisms behind TRIM22's antiviral activity may provide further avenues for the design of HIV-1 therapeutics. Our investigation into the localization of the endogenous protein and its functions in MECs is an important step required for the realization of this goal.

REFERENCES

Aasland, R., Gibson, T.J., and Stewart, A.F. (1995). The PHD finger: implications for chromatin-mediated transcriptional regulation. *Trends Biochem Sci* **20**, 56-59.

Achsel, T., Brahms, H., Kastner, B., Bachi, A., Wilm, M., and Luhrmann, R. (1999). A doughnut-shaped heteromer of human Sm-like proteins binds to the 3'-end of U6 snRNA, thereby facilitating U4/U6 duplex formation in vitro. *EMBO J* **18**, 5789-5802.

Aki, M., Shimbara, N., Takashina, M., Akiyama, K., Kagawa, S., Tamura, T., Tanahashi, N., Yoshimura, T., Tanaka, K., and Ichihara, A. (1994). Interferon-gamma induces different subunit organizations and functional diversity of proteasomes. *J Biochem **115***, 257-269.

Akiyama, K., Kagawa, S., Tamura, T., Shimbara, N., Takashina, M., Kristensen, P., Hendil, K.B., Tanaka, K., and Ichihara, A. (1994). Replacement of proteasome subunits X and Y by LMP7 and LMP2 induced by interferon-gamma for acquirement of the functional diversity responsible for antigen processing. *FEBS Lett* **343**, 85-88.

Albor, A., El-Hizawi, S., Horn, E.J., Laederich, M., Frosk, P., Wrogemann, K., and Kulesz-Martin, M. (2006). The interaction of Piasy with Trim32, an E3-ubiquitin ligase mutated in limb-girdle muscular dystrophy type 2H, promotes Piasy degradation and regulates UVB-induced keratinocyte apoptosis through NFkappaB. *J Biol Chem* **281**, 25850-25866.

Alcalay, M., Tomassoni, L., Colombo, E., Stoldt, S., Grignani, F., Fagioli, M., Szekely, L., Helin, K., and Pelicci, P.G. (1998). The promyelocytic leukemia gene product (PML) forms stable complexes with the retinoblastoma protein. *Mol Cell Biol* **18**, 1084-1093.

Amundson, S.A., Do, K.T., Vinikoor, L., Koch-Paiz, C.A., Bittner, M.L., Trent, J.M., Meltzer, P., and Fornace, A.J., Jr. (2005). Stress-specific signatures: expression profiling of p53 wild-type and -null human cells. *Oncogene* **24**, 4572-4579.

Andersen, J.S., Lyon, C.E., Fox, A.H., Leung, A.K., Lam, Y.W., Steen, H., Mann, M., and Lamond, A.I. (2002). Directed proteomic analysis of the human nucleolus. *Curr Biol* **12**, 1-11.

Andrade, L.E., Tan, E.M., and Chan, E.K. (1993). Immunocytochemical analysis of the coiled body in the cell cycle and during cell proliferation. *Proc Natl Acad Sci U S A* **90**, 1947-1951.

Arama, E., Dickman, D., Kimchie, Z., Shearn, A., and Lev, Z. (2000). Mutations in the beta-propeller domain of the Drosophila brain tumor (brat) protein induce neoplasm in the larval brain. *Oncogene* **19**, 3706-3716.

Aranda, A., and Pascual, A. (2001). Nuclear hormone receptors and gene expression. *Physiol Rev* **81**, 1269-1304.

Arnett-Mansfield, R.L., deFazio, A., Wain, G.V., Jaworski, R.C., Byth, K., Mote, P.A., and Clarke, C.L. (2001). Relative expression of progesterone receptors A and B in endometrioid cancers of the endometrium. *Cancer Res* **61**, 4576-4582.

Aupperlee, M.D., and Haslam, S.Z. (2007). Differential hormonal regulation and function of progesterone receptor isoforms in normal adult mouse mammary gland. *Endocrinology* **148**, 2290-2300.

Aupperlee, M.D., Smith, K.T., Kariagina, A., and Haslam, S.Z. (2005). Progesterone receptor isoforms A and B: temporal and spatial differences in expression during murine mammary gland development. *Endocrinology* **146**, 3577-3588.

Avela, K., Lipsanen-Nyman, M., Idanheimo, N., Seemanova, E., Rosengren, S., Makela, T.P., Perheentupa, J., Chapelle, A.D., and Lehesjoki, A.E. (2000). Gene encoding a new RING-B-box-Coiled-coil protein is mutated in mulibrey nanism. *Nat Genet* **25**, 298-301.

Ayrault, O., Andrique, L., Fauvin, D., Eymin, B., Gazzeri, S., and Seite, P. (2006). Human tumor suppressor p14ARF negatively regulates rRNA transcription and inhibits UBF1 transcription factor phosphorylation. *Oncogene* **25**, 7577-7586.

Bachand, F., Boisvert, F.M., Cote, J., Richard, S., and Autexier, C. (2002). The product of the survival of motor neuron (SMN) gene is a human telomerase-associated protein. *Mol Biol Cell* **13**, 3192-3202.

Balint, I., Muller, A., Nagy, A., and Kovacs, G. (2004). Cloning and characterisation of the RBCC728/TRIM36 zinc-binding protein from the tumor suppressor gene region at chromosome 5q22.3. *Gene* **332**, 45-50.

Barcaroli, D., Bongiorno-Borbone, L., Terrinoni, A., Hofmann, T.G., Rossi, M., Knight, R.A., Matera, A.G., Melino, G., and De Laurenzi, V. (2006a). FLASH is required for histone transcription and S-phase progression. Proc Natl Acad Sci U S A *103*, 14808-14812.

Barcaroli, D., Dinsdale, D., Neale, M.H., Bongiorno-Borbone, L., Ranalli, M., Munarriz, E., Sayan, A.E., McWilliam, J.M., Smith, T.M., Fava, E., et al. (2006b). FLASH is an essential component of Cajal bodies. *Proc Natl Acad Sci U S A* **103**, 14802-14807.

Barr, S.D., Smiley, J.R., and Bushman, F.D. (2008). The interferon response inhibits HIV particle production by induction of TRIM22. *PLoS Pathog* **4**, e1000007.

Batlle, E., Sancho, E., Franci, C., Dominguez, D., Monfar, M., Baulida, J., and Garcia De Herreros, A. (2000). The transcription factor snail is a repressor of E-cadherin gene expression in epithelial tumour cells. *Nat Cell Biol* **2**, 84-89.

Batra, S., and Iosif, S. (1985). Progesterone receptors in human vaginal tissue. *Am J Obstet Gynecol* **153**, 524-528.

Beato, M., Chalepakis, G., Schauer, M., and Slater, E.P. (1989). DNA regulatory elements for steroid hormones. *J Steroid Biochem* **32**, 737-747.

Beenders, B., Jones, P.L., and Bellini, M. (2007). The Tripartite Motif (TRIM) of Nuclear Factor 7 is required for its association with transcriptional units. *Mol Cell Biol* **27**, 2615-2624.

Beer, H.D., Munding, C., Dubois, N., Mamie, C., Hohl, D., and Werner, S. (2002). The estrogen-responsive B box protein: a novel regulator of keratinocyte differentiation. *J Biol Chem* **277**, 20740-20749.

Bell, M., Schreiner, S., Damianov, A., Reddy, R., and Bindereif, A. (2002). p110, a novel human U6 snRNP protein and U4/U6 snRNP recycling factor. *EMBO J* **21**, 2724-2735.

Bentel, J.M., Birrell, S.N., Pickering, M.A., Holds, D.J., Horsfall, D.J., and Tilley, W.D. (1999). Androgen receptor agonist activity of the synthetic progestin, medroxyprogesterone acetate, in human breast cancer cells. *Mol Cell Endocrinol* **154**, 11-20.

Bernardi, R., and Pandolfi, P.P. (2007). Structure, dynamics and functions of promyelocytic leukaemia nuclear bodies. *Nat Rev Mol Cell Biol* **8**, 1006-1016.

Berti, C., Messali, S., Ballabio, A., Reymond, A., and Meroni, G. (2002). TRIM9 is specifically expressed in the embryonic and adult nervous system. *Mech Dev* **113**, 159-162.

Birrell, S.N., Hall, R.E., and Tilley, W.D. (1998). Role of the androgen receptor in human breast cancer. *J Mammary Gland Biol Neoplasia* **3**, 95-103.

Bloch, D.B., de la Monte, S.M., Guigaouri, P., Filippov, A., and Bloch, K.D. (1996). Identification and characterization of a leukocyte-specific component of the nuclear body. *J Biol Chem* **271**, 29198-29204.

Bodine, S.C., Latres, E., Baumhueter, S., Lai, V.K., Nunez, L., Clarke, B.A., Poueymirou, W.T., Panaro, F.J., Na, E., Dharmarajan, K., et al. (2001). Identification of ubiquitin ligases required for skeletal muscle atrophy. *Science* **294**, 1704-1708.

Bohmann, K., Ferreira, J.A., and Lamond, A.I. (1995). Mutational analysis of p80 coilin indicates a functional interaction between coiled bodies and the nucleolus. *J Cell Biol* **131**, 817-831.

Boisvert, F.M., Hendzel, M.J., and Bazett-Jones, D.P. (2000). Promyelocytic leukemia (PML) nuclear bodies are protein structures that do not accumulate RNA. *J Cell Biol* **148**, 283-292.

Bolos, V., Peinado, H., Perez-Moreno, M.A., Fraga, M.F., Esteller, M., and Cano, A. (2003). The transcription factor Slug represses E-cadherin expression and induces epithelial to mesenchymal transitions: a comparison with Snail and E47 repressors. *J Cell Sci* **116**, 499-511.

Boonyaratanakornkit, V., Scott, M.P., Ribon, V., Sherman, L., Anderson, S.M., Maller, J.L., Miller, W.T., and Edwards, D.P. (2001). Progesterone receptor contains a proline-rich motif that directly interacts with SH3 domains and activates c-Src family tyrosine kinases. *Mol Cell* **8**, 269-280.

Borden, K.L., Boddy, M.N., Lally, J., O'Reilly, N.J., Martin, S., Howe, K., Solomon, E., and Freemont, P.S. (1995). The solution structure of the RING finger domain from the acute promyelocytic leukaemia proto-oncoprotein PML. *EMBO J* **14**, 1532-1541.

Borden, K.L., CampbellDwyer, E.J., and Salvato, M.S. (1997). The promyelocytic leukemia protein PML has a pro-apoptotic activity mediated through its RING domain. *FEBS Lett* **418**, 30-34.

Borden, K.L., Lally, J.M., Martin, S.R., O'Reilly, N.J., Solomon, E., and Freemont, P.S. (1996). In vivo and in vitro characterization of the B1 and B2 zinc-binding domains from the acute promyelocytic leukemia protooncoprotein PML. *Proc Natl Acad Sci U S A* **93**, 1601-1606.

Borden, K.L., Martin, S.R., O'Reilly, N.J., Lally, J.M., Reddy, B.A., Etkin, L.D., and Freemont, P.S. (1993). Characterisation of a novel cysteine/histidine-rich metal binding domain from Xenopus nuclear factor XNF7. *FEBS Lett* **335**, 255-260.

Bouazzaoui, A., Kreutz, M., Eisert, V., Dinauer, N., Heinzelmann, A., Hallenberger, S., Strayle, J., Walker, R., Rubsamen-Waigmann, H., Andreesen, R., et al. (2006). Stimulated trans-acting factor of 50 kDa (Staf50) inhibits HIV-1 replication in human monocyte-derived macrophages. *Virology* **356**, 79-94.

Boulon, S., Verheggen, C., Jady, B.E., Girard, C., Pescia, C., Paul, C., Ospina, J.K., Kiss, T., Matera, A.G., Bordonne, R., et al. (2004). PHAX and CRM1 are required sequentially to transport U3 snoRNA to nucleoli. *Mol Cell* **16**, 777-787.

Boutou, E., Matsas, R., and Mamalaki, A. (2001). Isolation of a mouse brain cDNA expressed in developing neuroblasts and mature neurons. *Brain Res Mol Brain Res* **86**, 153-167.

Brzoska, P.M., Chen, H., Zhu, Y., Levin, N.A., Disatnik, M.H., Mochly-Rosen, D., Murnane, J.P., and Christman, M.F. (1995). The product of the ataxia-telangiectasia group D complementing gene, ATDC, interacts with a protein kinase C substrate and inhibitor. *Proc Natl Acad Sci U S A* **92**, 7824-7828.

Buchner, G., Montini, E., Andolfi, G., Quaderi, N., Cainarca, S., Messali, S., Bassi, M.T., Ballabio, A., Meroni, G., and Franco, B. (1999). MID2, a homologue of the Opitz syndrome gene MID1: similarities in subcellular localization and differences in expression during development. *Hum Mol Genet* **8**, 1397-1407.

Cainarca, S., Messali, S., Ballabio, A., and Meroni, G. (1999). Functional characterization of the Opitz syndrome gene product (midin): evidence for homodimerization and association with microtubules throughout the cell cycle. *Hum Mol Genet* **8**, 1387-1396.

Callan, H.G., and Gall, J.G. (1991). Association of RNA with the B and C snurposomes of Xenopus oocyte nuclei. *Chromosoma* **101**, 69-82.

Cameron, D.A., Keen, J.C., Dixon, J.M., Bellamy, C., Hanby, A., Anderson, T.J., and Miller, W.R. (2000). Effective tamoxifen therapy of breast cancer involves both antiproliferative and pro-apoptotic changes. *Eur J Cancer* **36**, 845-851.

Campbell, E.M., Perez, O., Anderson, J.L., and Hope, T.J. (2008). Visualization of a proteasome-independent intermediate during restriction of HIV-1 by rhesus TRIM5alpha. *J Cell Biol* **180**, 549-561.

Cano, A., Perez-Moreno, M.A., Rodrigo, I., Locascio, A., Blanco, M.J., del Barrio, M.G., Portillo, F., and Nieto, M.A. (2000). The transcription factor snail controls epithelial-mesenchymal transitions by repressing E-cadherin expression. *Nat Cell Biol* **2**, 76-83.

Cao, T., Borden, K.L., Freemont, P.S., and Etkin, L.D. (1997). Involvement of the rfp tripartite motif in protein-protein interactions and subcellular distribution. *J Cell Sci* **110 (Pt 14)**, 1563-1571.

Cao, T., Duprez, E., Borden, K.L., Freemont, P.S., and Etkin, L.D. (1998). Ret finger protein is a normal component of PML nuclear bodies and interacts directly with PML. *J Cell Sci* **111 (Pt 10)**, 1319-1329.

Carmo-Fonseca, M., Ferreira, J., and Lamond, A.I. (1993). Assembly of snRNP-containing coiled bodies is regulated in interphase and mitosis--evidence that the coiled body is a kinetic nuclear structure. *J Cell Biol* **120**, 841-852.

Casey, G. (1997). The BRCA1 and BRCA2 breast cancer genes. *Curr Opin Oncol* **9**, 88-93.

Castro-Rivera, E., Samudio, I., and Safe, S. (2001). Estrogen regulation of cyclin D1 gene expression in ZR-75 breast cancer cells involves multiple enhancer elements. *J Biol Chem* **276**, 30853-30861.

Cato, A.C., Miksicek, R., Schutz, G., Arnemann, J., and Beato, M. (1986). The hormone regulatory element of mouse mammary tumour virus mediates progesterone induction. *EMBO J* **5**, 2237-2240.

Centner, T., Yano, J., Kimura, E., McElhinny, A.S., Pelin, K., Witt, C.C., Bang, M.L., Trombitas, K., Granzier, H., Gregorio, C.C., et al. (2001). Identification of muscle specific ring finger proteins as potential regulators of the titin kinase domain. *J Mol Biol* **306**, 717-726.

Chae, J.J., Wood, G., Masters, S.L., Richard, K., Park, G., Smith, B.J., and Kastner, D.L. (2006). The B30.2 domain of pyrin, the familial Mediterranean fever protein, interacts directly with caspase-1 to modulate IL-1beta production. *Proc Natl Acad Sci U S A* **103**, 9982-9987.

Chang, R., Xu, X., and Li, M.D. (2002). Molecular cloning, mapping and characterization of a novel mouse RING finger gene, Mrf1. *Gene* **291**, 241-249.

Chatterji, U., Bobardt, M.D., Gaskill, P., Sheeter, D., Fox, H., and Gallay, P.A. (2006). Trim5alpha accelerates degradation of cytosolic capsid associated with productive HIV-1 entry. *J Biol Chem* **281**, 37025-33

Chelbi-Alix, M.K., Pelicano, L., Quignon, F., Koken, M.H., Venturini, L., Stadler, M., Pavlovic, J., Degos, L., and de The, H. (1995). Induction of the PML protein by interferons in normal and APL cells. *Leukemia* **9**, 2027-2033.

Chelbi-Alix, M.K., Quignon, F., Pelicano, L., Koken, M.H., and de The, H. (1998). Resistance to virus infection conferred by the interferon-induced promyelocytic leukemia protein. *J Virol* **72**, 1043-1051.

Chen, D., Gould, C., Garza, R., Gao, T., Hampton, R.Y., and Newton, A.C. (2007). Amplitude control of protein kinase C by RINCK, a novel E3 ubiquitin ligase. *J Biol Chem* **282**, 33776-33787.

Chen, G., Cizeau, J., Vande Velde, C., Park, J.H., Bozek, G., Bolton, J., Shi, L., Dubik, D., and Greenberg, A. (1999). Nix and Nip3 form a subfamily of pro-apoptotic mitochondrial proteins. *J Biol Chem* **274**, 7-10.

Chen, H., Lin, R.J., Schiltz, R.L., Chakravarti, D., Nash, A., Nagy, L., Privalsky, M.L., Nakatani, Y., and Evans, R.M. (1997). Nuclear receptor coactivator ACTR is a novel histone acetyltransferase and forms a multimeric activation complex with P/CAF and CBP/p300. *Cell* **90**, 569-580.

Chen, J.D., and Evans, R.M. (1995). A transcriptional co-repressor that interacts with nuclear hormone receptors. *Nature* **377**, 454-457.

Cioce, M., and Lamond, A.I. (2005). Cajal bodies: a long history of discovery. *Annu Rev Cell Dev Biol* **21**, 105-131.

Clarke, C.L., and Sutherland, R.L. (1990). Progestin regulation of cellular proliferation. *Endocr Rev* **11**, 266-301.

Clarke, R.B. (2004). Human breast cell proliferation and its relationship to steroid receptor expression. *Climacteric* **7**, 129-137.

Colombo, E., Bonetti, P., Lazzerini Denchi, E., Martinelli, P., Zamponi, R., Marine, J.C., Helin, K., Falini, B., and Pelicci, P.G. (2005). Nucleophosmin is required for DNA integrity and p19Arf protein stability. *Mol Cell Biol* **25**, 8874-8886.

Condon, J.C., Hardy, D.B., Kovaric, K., and Mendelson, C.R. (2006). Up-regulation of the progesterone receptor (PR)-C isoform in laboring myometrium by activation of nuclear factor-kappaB may contribute to the onset of labor through inhibition of PR function. *Mol Endocrinol* **20**, 764-775.

Conneely, O.M., Maxwell, B.L., Toft, D.O., Schrader, W.T., and O'Malley, B.W. (1987). The A and B forms of the chicken progesterone receptor arise by alternate initiation of translation of a unique mRNA. *Biochem Biophys Res Commun* **149**, 493-501.

Couse, J.F., and Korach, K.S. (1999). Estrogen receptor null mice: what have we learned and where will they lead us? *Endocr Rev* **20**, 358-417.

Desterro, J.M., Rodriguez, M.S., and Hay, R.T. (1998). SUMO-1 modification of IkappaBalpha inhibits NF-kappaB activation. *Mol Cell* **2**, 233-239.

Dho, S.H., and Kwon, K.S. (2003). The Ret finger protein induces apoptosis via its RING finger-B box-coiled-coil motif. *J Biol Chem* **278**, 31902-31908.

Djavani, M., Rodas, J., Lukashevich, I.S., Horejsh, D., Pandolfi, P.P., Borden, K.L., and Salvato, M.S. (2001). Role of the promyelocytic leukemia protein PML in the interferon sensitivity of lymphocytic choriomeningitis virus. *J Virol* **75**, 6204-6208.

Doucas, V., Tini, M., Egan, D.A., and Evans, R.M. (1999). Modulation of CREB binding protein function by the promyelocytic (PML) oncoprotein suggests a role for nuclear bodies in hormone signaling. *Proc Natl Acad Sci U S A* **96**, 2627-2632.

Dundr, M., Hebert, M.D., Karpova, T.S., Stanek, D., Xu, H., Shpargel, K.B., Meier, U.T., Neugebauer, K.M., Matera, A.G., and Misteli, T. (2004). In vivo kinetics of Cajal body components. *J Cell Biol* **164**, 831-842.

Dupont, S., Zacchigna, L., Cordenonsi, M., Soligo, S., Adorno, M., Rugge, M., and Piccolo, S. (2005). Germ-layer specification and control of cell growth by Ectodermin, a Smad4 ubiquitin ligase. *Cell* **121**, 87-99.

Dyck, J.A., Maul, G.G., Miller, W.H., Jr., Chen, J.D., Kakizuka, A., and Evans, R.M. (1994). A novel macromolecular structure is a target of the promyelocyte-retinoic acid receptor oncoprotein. *Cell* **76**, 333-343.

El-Husseini, A.E., and Vincent, S.R. (1999). Cloning and characterization of a novel RING finger protein that interacts with class V myosins. *J Biol Chem* **274**, 19771-19777.

Enmark, E., and Gustafsson, J.A. (1999). Oestrogen receptors - an overview. *J Intern Med* **246**, 133-138.

Enomoto, T., Lindstrom, M.S., Jin, A., Ke, H., and Zhang, Y. (2006). Essential role of the B23/NPM core domain in regulating ARF binding and B23 stability. *J Biol Chem* **281**, 18463-18472.

Esteller, M., Corn, P.G., Baylin, S.B., and Herman, J.G. (2001). A gene hypermethylation profile of human cancer. *Cancer Res* **61**, 3225-3229.

Everett, R.D., and Chelbi-Alix, M.K. (2007). PML and PML nuclear bodies: implications in antiviral defence. *Biochimie* **89**, 819-830.

Everett, R.D., Rechter, S., Papior, P., Tavalai, N., Stamminger, T., and Orr, A. (2006). PML contributes to a cellular mechanism of repression of herpes simplex virus type 1 infection that is inactivated by ICP0. *J Virol* **80**, 7995-8005.

Fagioli, M., Alcalay, M., Tomassoni, L., Ferrucci, P.F., Mencarelli, A., Riganelli, D., Grignani, F., Pozzan, T., Nicoletti, I., and Pelicci, P.G. (1998). Cooperation between the RING + B1-B2 and coiled-coil domains of PML is necessary for its effects on cell survival. *Oncogene* **16**, 2905-2913.

Feng, Y., Manka, D., Wagner, K.U., and Khan, S.A. (2007). Estrogen receptor-alpha expression in the mammary epithelium is required for ductal and alveolar morphogenesis in mice. *Proc Natl Acad Sci U S A* **104**, 14718-14723.

Fogal, V., Gostissa, M., Sandy, P., Zacchi, P., Sternsdorf, T., Jensen, K., Pandolfi, P.P., Will, H., Schneider, C., and Del Sal, G. (2000). Regulation of p53 activity in nuclear bodies by a specific PML isoform. *EMBO J* **19**, 6185-6195.

Fox, A.H., Lam, Y.W., Leung, A.K., Lyon, C.E., Andersen, J., Mann, M., and Lamond, A.I. (2002). Paraspeckles: a novel nuclear domain. *Curr Biol* **12**, 13-25.

Frank, D.J., and Roth, M.B. (1998). ncl-1 is required for the regulation of cell size and ribosomal RNA synthesis in Caenorhabditis elegans. *J Cell Biol* **140**, 1321-1329.

Freeman, B.C., and Yamamoto, K.R. (2002). Disassembly of transcriptional regulatory complexes by molecular chaperones. *Science* **296**, 2232-2235.

Frey, M.R., and Matera, A.G. (1995). Coiled bodies contain U7 small nuclear RNA and associate with specific DNA sequences in interphase human cells. *Proc Natl Acad Sci U S A* **92**, 5915-5919.

Frey, M.R., and Matera, A.G. (2001). RNA-mediated interaction of Cajal bodies and U2 snRNA genes. *J Cell Biol* **154**, 499-509.

Fridell, R.A., Harding, L.S., Bogerd, H.P., and Cullen, B.R. (1995). Identification of a novel human zinc finger protein that specifically interacts with the activation domain of lentiviral Tat proteins. *Virology* **209**, 347-357.

Fruh, K., Gossen, M., Wang, K., Bujard, H., Peterson, P.A., and Yang, Y. (1994). Displacement of housekeeping proteasome subunits by MHC-encoded LMPs: a newly discovered mechanism for modulating the multicatalytic proteinase complex. *EMBO J* **13**, 3236-3244.

Furuse, M., Sasaki, H., Fujimoto, K., and Tsukita, S. (1998). A single gene product, claudin-1 or -2, reconstitutes tight junction strands and recruits occludin in fibroblasts. *J Cell Biol* **143**, 391-401.

Gack, M.U., Shin, Y.C., Joo, C.H., Urano, T., Liang, C., Sun, L., Takeuchi, O., Akira, S., Chen, Z., Inoue, S., et al. (2007). TRIM25 RING-finger E3 ubiquitin ligase is essential for RIG-I-mediated antiviral activity. *Nature* **446**, 916-920.

Gao, G., Guo, X., and Goff, S.P. (2002). Inhibition of retroviral RNA production by ZAP, a CCCH-type zinc finger protein. *Science* **297**, 1703-1706.

Gee, A.C., and Katzenellenbogen, J.A. (2001). Probing conformational changes in the estrogen receptor: evidence for a partially unfolded intermediate facilitating ligand binding and release. *Mol Endocrinol* **15**, 421-428.

Gee, J.M., Robertson, J.F., Ellis, I.O., and Nicholson, R.I. (2001). Phosphorylation of ERK1/2 mitogen-activated protein kinase is associated with poor response to anti-hormonal therapy and decreased patient survival in clinical breast cancer. *Int J Cancer* **95**, 247-254.

Geiss-Friedlander, R., and Melchior, F. (2007). Concepts in sumoylation: a decade on. *Nat Rev Mol Cell Biol* **8**, 947-956.

Glass, C.K. (1994). Differential recognition of target genes by nuclear receptor monomers, dimers, and heterodimers. *Endocr Rev* **15**, 391-407.

Goff, S.P. (2007). Host factors exploited by retroviruses. *Nat Rev Microbiol* **5**, 253-263.

Gongora, C., Tissot, C., Cerdan, C., and Mechti, N. (2000). The interferon-inducible Staf50 gene is downregulated during T cell costimulation by CD2 and CD28. *J Interferon Cytokine Res* **20**, 955-961.

Graham, J.D., Yeates, C., Balleine, R.L., Harvey, S.S., Milliken, J.S., Bilous, A.M., and Clarke, C.L. (1995). Characterization of progesterone receptor A and B expression in human breast cancer. *Cancer Res* **55**, 5063-5068.

Gregorio, C.C., Perry, C.N., and McElhinny, A.S. (2005). Functional properties of the titin/connectin-associated proteins, the muscle-specific RING finger proteins (MURFs), in striated muscle. *J Muscle Res Cell Motil* **26**, 389-400.

Grey, A.B., Stapleton, J.P., Evans, M.C., and Reid, I.R. (1995a). The effect of the anti-estrogen tamoxifen on cardiovascular risk factors in normal postmenopausal women. *J Clin Endocrinol Metab* **80**, 3191-3195.

Grey, A.B., Stapleton, J.P., Evans, M.C., Tatnell, M.A., Ames, R.W., and Reid, I.R. (1995b). The effect of the antiestrogen tamoxifen on bone mineral density in normal late postmenopausal women. *Am J Med* **99**, 636-641.

Groshong, S.D., Owen, G.I., Grimison, B., Schauer, I.E., Todd, M.C., Langan, T.A., Sclafani, R.A., Lange, C.A., and Horwitz, K.B. (1997). Biphasic regulation of breast cancer cell growth by progesterone: role of the cyclin-dependent kinase inhibitors, p21 and p27(Kip1). *Mol Endocrinol* **11**, 1593-1607.

Gubitz, A.K., Feng, W., and Dreyfuss, G. (2004). The SMN complex. *Exp Cell Res* **296**, 51-56.

Guiochon-Mantel, A., Savouret, J.F., Quignon, F., Delabre, K., Milgrom, E., and De The, H. (1995). Effect of PML and PML-RAR on the transactivation properties and subcellular distribution of steroid hormone receptors. *Mol Endocrinol* **9**, 1791-1803.

Hajra, K.M., Chen, D.Y., and Fearon, E.R. (2002). The SLUG zinc-finger protein represses E-cadherin in breast cancer. *Cancer Res* **62**, 1613-1618.

Harada, H., Harada, Y., O'Brien, D.P., Rice, D.S., Naeve, C.W., and Downing, J.R. (1999). HERF1, a novel hematopoiesis-specific RING finger protein, is required for terminal differentiation of erythroid cells. *Mol Cell Biol* **19**, 3808-3815.

Harris, R.S., Petersen-Mahrt, S.K., and Neuberger, M.S. (2002). RNA editing enzyme APOBEC1 and some of its homologs can act as DNA mutators. *Mol Cell* **10**, 1247-1253.

Hasegawa, N., Iwashita, T., Asai, N., Murakami, H., Iwata, Y., Isomura, T., Goto, H., Hayakawa, T., and Takahashi, M. (1996). A RING finger motif regulates transforming activity of the rfp/ret fusion gene. *Biochem Biophys Res Commun* **225**, 627-631.

Haslam, S.Z., and Woodward, T.L. (2003). Host microenvironment in breast cancer development: epithelial-cell-stromal-cell interactions and steroid hormone action in normal and cancerous mammary gland. *Breast Cancer Res* **5**, 208-215.

Hatziioannou, T., Cowan, S., and Bieniasz, P.D. (2004a). Capsid-dependent and -independent postentry restriction of primate lentivirus tropism in rodent cells. *J Virol* **78**, 1006-1011.

Hatziioannou, T., Cowan, S., Goff, S.P., Bieniasz, P.D., and Towers, G.J. (2003). Restriction of multiple divergent retroviruses by Lv1 and Ref1. *EMBO J* **22**, 385-394.

Hatziioannou, T., Perez-Caballero, D., Yang, A., Cowan, S., and Bieniasz, P.D. (2004b). Retrovirus resistance factors Ref1 and Lv1 are species-specific variants of TRIM5alpha. *Proc Natl Acad Sci U S A* **101**, 10774-10779.

Hebert, M.D., and Matera, A.G. (2000). Self-association of coilin reveals a common theme in nuclear body localization. *Mol Biol Cell* **11**, 4159-4171.

Hebert, M.D., Szymczyk, P.W., Shpargel, K.B., and Matera, A.G. (2001). Coilin forms the bridge between Cajal bodies and SMN, the spinal muscular atrophy protein. *Genes Dev* **15**, 2720-2729.

Heery, D.M., Kalkhoven, E., Hoare, S., and Parker, M.G. (1997). A signature motif in transcriptional co-activators mediates binding to nuclear receptors. *Nature* **387**, 733-736.

Heinzel, T., Lavinsky, R.M., Mullen, T.M., Soderstrom, M., Laherty, C.D., Torchia, J., Yang, W.M., Brard, G., Ngo, S.D., Davie, J.R., et al. (1997). A complex containing N-CoR, mSin3 and histone deacetylase mediates transcriptional repression. *Nature* **387**, 43-48.

Heuser, M., van der Kuip, H., Falini, B., Peschel, C., Huber, C., and Fischer, T. (1998). Induction of the pro-myelocytic leukaemia gene by type I and type II interferons. *Mediators Inflamm* **7**, 319-325.

Hewitt, S.C., and Korach, K.S. (2000). Progesterone action and responses in the alphaERKO mouse. *Steroids* **65**, 551-557.

Hirose, S., Nishizumi, H., and Sakano, H. (2003). Pub, a novel PU.1 binding protein, regulates the transcriptional activity of PU.1. *Biochem Biophys Res Commun* **311**, 351-360.

Hoffmann, J., and Sommer, A. (2005). Steroid hormone receptors as targets for the therapy of breast and prostate cancer--recent advances, mechanisms of resistance, and new approaches. *J Steroid Biochem Mol Biol* **93**, 191-200.

Hong, S.H., and Privalsky, M.L. (2000). The SMRT corepressor is regulated by a MEK-1 kinase pathway: inhibition of corepressor function is associated with SMRT phosphorylation and nuclear export. *Mol Cell Biol* **20**, 6612-6625.

Hopfner, K.P., Brandstetter, H., Karcher, A., Kopetzki, E., Huber, R., Engh, R.A., and Bode, W. (1997). Converting blood coagulation factor IXa into factor Xa: dramatic increase in amidolytic activity identifies important active site determinants. *EMBO J* **16**, 6626-6635.

Horlein, A.J., Naar, A.M., Heinzel, T., Torchia, J., Gloss, B., Kurokawa, R., Ryan, A., Kamei, Y., Soderstrom, M., Glass, C.K., et al. (1995). Ligand-independent repression by the thyroid hormone receptor mediated by a nuclear receptor co-repressor. *Nature* **377**, 397-404.

Horn, E.J., Albor, A., Liu, Y., El-Hizawi, S., Vanderbeek, G.E., Babcock, M., Bowden, G.T., Hennings, H., Lozano, G., Weinberg, W.C., et al. (2004). RING protein Trim32 associated with skin carcinogenesis has anti-apoptotic and E3-ubiquitin ligase properties. *Carcinogenesis* **25**, 157-167.

Htun, H., Holth, L.T., Walker, D., Davie, J.R., and Hager, G.L. (1999). Direct visualization of the human estrogen receptor alpha reveals a role for ligand in the nuclear distribution of the receptor. *Mol Biol Cell* **10**, 471-486.

Hu, X., and Lazar, M.A. (1999). The CoRNR motif controls the recruitment of corepressors by nuclear hormone receptors. *Nature* **402**, 93-96.

Huang, E.Y., Zhang, J., Miska, E.A., Guenther, M.G., Kouzarides, T., and Lazar, M.A. (2000). Nuclear receptor corepressors partner with class II histone deacetylases in a Sin3-independent repression pathway. *Genes Dev* **14**, 45-54.

Hunter, T. (2007). The age of crosstalk: phosphorylation, ubiquitination, and beyond. *Mol Cell* **28**, 730-738.

Idicula-Thomas, S., and Balaji, P.V. (2007). Protein aggregation: a perspective from amyloid and inclusion–body formation. *Curr Sci* **92**, 758-767

Ikenouchi, J., Matsuda, M., Furuse, M., and Tsukita, S. (2003). Regulation of tight junctions during the epithelium-mesenchyme transition: direct repression of the gene expression of claudins/occludin by Snail. *J Cell Sci* **116**, 1959-1967.

Imai, Y., Kimura, T., Murakami, A., Yajima, N., Sakamaki, K., and Yonehara, S. (1999). The CED-4-homologous protein FLASH is involved in Fas-mediated activation of caspase-8 during apoptosis. *Nature* **398**, 777-785.

Inui, S., Sanjo, H., Maeda, K., Yamamoto, H., Miyamoto, E., and Sakaguchi, N. (1998). Ig receptor binding protein 1 (alpha4) is associated with a rapamycin-sensitive signal transduction in lymphocytes through direct binding to the catalytic subunit of protein phosphatase 2A. *Blood* **92**, 539-546.

Ishov, A.M., Sotnikov, A.G., Negorev, D., Vladimirova, O.V., Neff, N., Kamitani, T., Yeh, E.T., Strauss, J.F., 3rd, and Maul, G.G. (1999). PML is critical for ND10 formation and recruits the PML-interacting protein daxx to this nuclear structure when modified by SUMO-1. *J Cell Biol* **147**, 221-234.

Izmailova, E., Bertley, F.M., Huang, Q., Makori, N., Miller, C.J., Young, R.A., and Aldovini, A. (2003). HIV-1 Tat reprograms immature dendritic cells to express chemoattractants for activated T cells and macrophages. *Nat Med* **9**, 191-197.

Jacobsen, B.M., Richer, J.K., Sartorius, C.A., and Horwitz, K.B. (2003). Expression profiling of human breast cancers and gene regulation by progesterone receptors. *J Mammary Gland Biol Neoplasia* **8**, 257-268.

Jacobsen, B.M., Schittone, S.A., Richer, J.K., and Horwitz, K.B. (2005). Progesterone-independent effects of human progesterone receptors (PRs) in estrogen receptor-positive breast cancer: PR isoform-specific gene regulation and tumor biology. *Mol Endocrinol* **19**, 574-587.

Jady, B.E., Bertrand, E., and Kiss, T. (2004). Human telomerase RNA and box H/ACA scaRNAs share a common Cajal body-specific localization signal. *J Cell Biol* **164**, 647-652.

Javanbakht, H., Yuan, W., Yeung, D.F., Song, B., Diaz-Griffero, F., Li, Y., Li, X., Stremlau, M., and Sodroski, J. (2006). Characterization of TRIM5alpha trimerization and its contribution to human immunodeficiency virus capsid binding. *Virology* **353**, 234-246.

Jensen, K., Shiels, C., and Freemont, P.S. (2001). PML protein isoforms and the RBCC/TRIM motif. *Oncogene* **20**, 7223-7233.

Jordan, P., Cunha, C., and Carmo-Fonseca, M. (1997). The cdk7-cyclin H-MAT1 complex associated with TFIIH is localized in coiled bodies. *Mol Biol Cell* **8**, 1207-1217.

Jordan, V.C., and Dowse, L.J. (1976). Tamoxifen as an anti-tumour agent: effect on oestrogen binding. *J Endocrinol* **68**, 297-303.

Kallijarvi, J., Avela, K., Lipsanen-Nyman, M., Ulmanen, I., and Lehesjoki, A.E. (2002). The TRIM37 gene encodes a peroxisomal RING-B-box-coiled-coil protein: classification of mulibrey nanism as a new peroxisomal disorder. *Am J Hum Genet* **70**, 1215-1228.

Kapanadze, B., Kashuba, V., Baranova, A., Rasool, O., van Everdink, W., Liu, Y., Syomov, A., Corcoran, M., Poltaraus, A., Brodyansky, V., et al. (1998). A cosmid and cDNA fine physical map of a human chromosome 13q14 region frequently lost in B-cell chronic lymphocytic leukemia and identification of a new putative tumor suppressor gene, Leu5. *FEBS Lett* **426**, 266-270.

Kariagina, A., Aupperlee, M.D., and Haslam, S.Z. (2007). Progesterone receptor isoforms and proliferation in the rat mammary gland during development. *Endocrinology* **148**, 2723-2736.

Kastner, P., Krust, A., Turcotte, B., Stropp, U., Tora, L., Gronemeyer, H., and Chambon, P. (1990). Two distinct estrogen-regulated promoters generate transcripts encoding the two functionally different human progesterone receptor forms A and B. *EMBO J* **9**, 1603-1614.

Kastner, P., Perez, A., Lutz, Y., Rochette-Egly, C., Gaub, M.P., Durand, B., Lanotte, M., Berger, R., and Chambon, P. (1992). Structure, localization and transcriptional properties of two classes of retinoic acid receptor alpha fusion proteins in acute promyelocytic leukemia (APL): structural similarities with a new family of oncoproteins. *EMBO J* **11**, 629-642.

Kato, J., Onouchi, T., and Okinaga, S. (1978). Hypothalamic and hypophysial progesterone receptors: estrogen-priming effect, differential localization, 5alpha-dihydroprogesterone binding, and nuclear receptors. *J Steroid Biochem* **9**, 419-427.

Katze, M.G., He, Y., and Gale, M., Jr. (2002). Viruses and interferon: a fight for supremacy. *Nat Rev Immunol* **2**, 675-687.

Kawashima, H., Takano, H., Sugita, S., Takahara, Y., Sugimura, K., and Nakatani, T. (2003). A novel steroid receptor co-activator protein (SRAP) as an alternative form of steroid receptor RNA-activator gene: expression in prostate cancer cells and enhancement of androgen receptor activity. *Biochem J* **369**, 163-171.

Kenny, P.A., Lee, G.Y., Myers, C.A., Neve, R.M., Semeiks, J.R., Spellman, P.T., Lorenz, K., Lee, E.H., Barcellos-Hoff, M.H., Petersen, O.W., et al. (2007). The morphologies of breast cancer cell lines in three-dimensional assays correlate with their profiles of gene expression. *Mol Oncol* **1**, 84-96.

Keydar, I., Chen, L., Karby, S., Weiss, F.R., Delarea, J., Radu, M., Chaitcik, S., Brenner, H.J. (1979). Establishment and characterization of a cell line of human breast carcinoma origin. *Eur J Cancer* **15**, 659-670.

Khetchoumian, K., Teletin, M., Mark, M., Lerouge, T., Cervino, M., Oulad-Abdelghani, M., Chambon, P., and Losson, R. (2004). TIF1delta, a novel HP1-interacting member of the transcriptional intermediary factor 1 (TIF1) family expressed by elongating spermatids. *J Biol Chem* **279**, 48329-48341.

Khetchoumian, K., Teletin, M., Tisserand, J., Mark, M., Herquel, B., Ignat, M., Zucman-Rossi, J., Cammas, F., Lerouge, T., Thibault, C., et al. (2007). Loss of Trim24 (Tif1alpha) gene function confers oncogenic activity to retinoic acid receptor alpha. *Nat Genet* **39**, 1500-1506.

Kiedzierska, A., Czepczynska, H., Smietana, K., and Otlewski, J. (2008). Expression, purification and crystallization of cysteine-rich human protein muskelin in Escherichia coli. *Protein Expr Purif* **60**, 82-88

Kim, H.J., Kim, J.H., and Lee, J.W. (1998). Steroid receptor coactivator-1 interacts with serum response factor and coactivates serum response element-mediated transactivations. *J Biol Chem* **273**, 28564-28567.

Kim, S.H., Ryabov, E.V., Kalinina, N.O., Rakitina, D.V., Gillespie, T., MacFarlane, S., Haupt, S., Brown, J.W., and Taliansky, M. (2007). Cajal bodies and the nucleolus are required for a plant virus systemic infection. *EMBO J* **26**, 2169-2179.

Kim, S.S., Chen, Y.M., O'Leary, E., Witzgall, R., Vidal, M., and Bonventre, J.V. (1996). A novel member of the RING finger family, KRIP-1, associates with the KRAB-A transcriptional repressor domain of zinc finger proteins. *Proc Natl Acad Sci U S A* **93**, 15299-15304.

Kimura, F., Suzu, S., Nakamura, Y., Nakata, Y., Yamada, M., Kuwada, N., Matsumura, T., Yamashita, T., Ikeda, T., Sato, K., et al. (2003). Cloning and characterization of a novel RING-B-box-coiled-coil protein with apoptotic function. *J Biol Chem* **278**, 25046-25054.

Klijn, J.G., Setyono-Han, B., and Foekens, J.A. (2000). Progesterone antagonists and progesterone receptor modulators in the treatment of breast cancer. *Steroids* **65**, 825-830.

Klinge, C.M. (2001). Estrogen receptor interaction with estrogen response elements. *Nucleic Acids Res* **29**, 2905-2919.

Ko, L.J., and Prives, C. (1996). p53: puzzle and paradigm. *Genes Dev* **10**, 1054-1072.

Korgaonkar, C., Hagen, J., Tompkins, V., Frazier, A.A., Allamargot, C., Quelle, F.W., and Quelle, D.E. (2005). Nucleophosmin (B23) targets ARF to nucleoli and inhibits its function. *Mol Cell Biol* **25**, 1258-1271.

Kosano, H., Stensgard, B., Charlesworth, M.C., McMahon, N., and Toft, D. (1998). The assembly of progesterone receptor-hsp90 complexes using purified proteins. *J Biol Chem* **273**, 32973-32979.

Kousteni, S., Bellido, T., Plotkin, L.I., O'Brien, C.A., Bodenner, D.L., Han, L., Han, K., DiGregorio, G.B., Katzenellenbogen, J.A., Katzenellenbogen, B.S., et al. (2001). Nongenotropic, sex-nonspecific signaling through the estrogen or androgen receptors: dissociation from transcriptional activity. *Cell* **104**, 719-730.

Kozak, C.A., and Chakraborti, A. (1996). Single amino acid changes in the murine leukemia virus capsid protein gene define the target of Fv1 resistance. *Virology* **225**, 300-305.

Kraus, W.L., Montano, M.M., and Katzenellenbogen, B.S. (1993). Cloning of the rat progesterone receptor gene 5'-region and identification of two functionally distinct promoters. *Mol Endocrinol* **7**, 1603-1616.

Krutzfeldt, M., Ellis, M., Weekes, D.B., Bull, J.J., Eilers, M., Vivanco, M.D., Sellers, W.R., and Mittnacht, S. (2005). Selective ablation of retinoblastoma protein function by the RET finger protein. *Mol Cell* **18**, 213-224.

Kuenen-Boumeester, V., Van der Kwast, T.H., Claassen, C.C., Look, M.P., Liem, G.S., Klijn, J.G., and Henzen-Logmans, S.C. (1996). The clinical significance of androgen receptors in breast cancer and their relation to histological and cell biological parameters. *Eur J Cancer* **32A**, 1560-1565.

Kyte, J., and Doolittle, R.F. (1982). A simple method for displaying the hydropathic character of a protein. *J Mol Biol* **157**, 105-132.

Lalonde, J.P., Lim, R., Ingley, E., Tilbrook, P.A., Thompson, M.J., McCulloch, R., Beaumont, J.G., Wicking, C., Eyre, H.J., Sutherland, G.R., et al. (2004). HLS5, a novel RBCC (ring finger, B box, coiled-coil) family member isolated from a hemopoietic lineage switch, is a candidate tumor suppressor. *J Biol Chem* **279**, 8181-8189.

Lamond, A.I., and Spector, D.L. (2003). Nuclear speckles: a model for nuclear organelles. *Nat Rev Mol Cell Biol* **4**, 605-612.

LaMorte, V.J., Dyck, J.A., Ochs, R.L., and Evans, R.M. (1998). Localization of nascent RNA and CREB binding protein with the PML-containing nuclear body. *Proc Natl Acad Sci U S A* **95**, 4991-4996.

Lanz, R.B., McKenna, N.J., Onate, S.A., Albrecht, U., Wong, J., Tsai, S.Y., Tsai, M.J., and O'Malley, B.W. (1999). A steroid receptor coactivator, SRA, functions as an RNA and is present in an SRC-1 complex. *Cell* **97**, 17-27.

Lavau, C., Marchio, A., Fagioli, M., Jansen, J., Falini, B., Lebon, P., Grosveld, F., Pandolfi, P.P., Pelicci, P.G., and Dejean, A. (1995). The acute promyelocytic leukaemia-associated PML gene is induced by interferon. *Oncogene* **11**, 871-876.

Laz, E.V., Holloway, M.G., Chen, C.S., and Waxman, D.J. (2007). Characterization of three growth hormone-responsive transcription factors preferentially expressed in adult female liver. *Endocrinology* **148**, 3327-3337.

Le Douarin, B., Nielsen, A.L., Garnier, J.M., Ichinose, H., Jeanmougin, F., Losson, R., and Chambon, P. (1996). A possible involvement of TIF1 alpha and TIF1 beta in the epigenetic control of transcription by nuclear receptors. *EMBO J* **15**, 6701-6715.

Lea, O.A., Kvinnsland, S., and Thorsen, T. (1989). Improved measurement of androgen receptors in human breast cancer. *Cancer Res* **49**, 7162-7167.

Leavitt, W.W., Chen, T.J., and Allen, T.C. (1977). Regulation of progesterone receptor formation by estrogen action. *Ann N Y Acad Sci* **286**, 210-225.

Leavitt, W.W., Toft, D.O., Strott, C.A., and O'Malley, B.W. (1974). A specific progesterone receptor in the hamster uterus: physiologic properties and regulation during the estrous cycle. *Endocrinology* **94**, 1041-1053.

Lee, S.K., Kim, H.J., Kim, J.W., and Lee, J.W. (1999). Steroid receptor coactivator-1 and its family members differentially regulate transactivation by the tumor suppressor protein p53. *Mol Endocrinol* **13**, 1924-1933.

Lee, S.K., Kim, J.H., Lee, Y.C., Cheong, J., and Lee, J.W. (2000). Silencing mediator of retinoic acid and thyroid hormone receptors, as a novel transcriptional corepressor molecule of activating protein-1, nuclear factor-kappaB, and serum response factor. *J Biol Chem* **275**, 12470-12474.

Lefebvre, S., Burglen, L., Reboullet, S., Clermont, O., Burlet, P., Viollet, L., Benichou, B., Cruaud, C., Millasseau, P., Zeviani, M., et al. (1995). Identification and characterization of a spinal muscular atrophy-determining gene. *Cell* **80**, 155-165.

Leo, J.C., Wang, S.M., Guo, C.H., Aw, S.E., Zhao, Y., Li, J.M., Hui, K.M., and Lin, V.C. (2005). Gene regulation profile reveals consistent anticancer properties of progesterone in hormone-independent breast cancer cells transfected with progesterone receptor. *Int J Cancer* **117**, 561-568.

Lerner, M., Corcoran, M., Cepeda, D., Nielsen, M.L., Zubarev, R., Ponten, F., Uhlen, M., Hober, S., Grander, D., and Sangfelt, O. (2007). The RBCC gene RFP2 (Leu5) encodes a novel transmembrane E3 ubiquitin ligase involved in ERAD. *Mol Biol Cell* **18**, 1670-1682.

Li, J., O'Malley, B.W., and Wong, J. (2000). p300 requires its histone acetyltransferase activity and SRC-1 interaction domain to facilitate thyroid hormone receptor activation in chromatin. *Mol Cell Biol* **20**, 2031-2042.

Li, L., Roy, K., Katyal, S., Sun, X., Bleoo, S., and Godbout, R. (2006). Dynamic nature of cleavage bodies and their spatial relationship to DDX1 bodies, Cajal bodies, and gems. *Mol Biol Cell* **17**, 1126-1140.

Li, X., Gold, B., O'HUigin, C., Diaz-Griffero, F., Song, B., Si, Z., Li, Y., Yuan, W., Stremlau, M., Mische, C., et al. (2007a). Unique features of TRIM5alpha among closely related human TRIM family members. *Virology* **360**, 419-433.

Li, X., Song, B., Xiang, S.H., and Sodroski, J. (2007b). Functional interplay between the B-box 2 and the B30.2(SPRY) domains of TRIM5alpha. *Virology* **366**, 234-244.

Li, Y., Chin, L.S., Weigel, C., and Li, L. (2001). Spring, a novel RING finger protein that regulates synaptic vesicle exocytosis. *J Biol Chem* **276**, 40824-40833.

Li, Y.P., Busch, R.K., Valdez, B.C., and Busch, H. (1996). C23 interacts with B23, a putative nucleolar-localization-signal-binding protein. *Eur J Biochem* **237**, 153-158.

Lin, V.C., Eng, A.S., Hen, N.E., Ng, E.H., and Chowdhury, S.H. (2001). Effect of progesterone on the invasive properties and tumor growth of progesterone receptor-transfected breast cancer cells MDA-MB-231. *Clin Cancer Res* **7**, 2880-2886.

Lin, V.C., Ng, E.H., Aw, S.E., Tan, M.G., and Bay, B.H. (2000). Progesterone induces focal adhesion in breast cancer cells MDA-MB-231 transfected with progesterone receptor complementary DNA. *Mol Endocrinol* **14**, 348-358.

Lin, V.C., Ng, E.H., Aw, S.E., Tan, M.G., Ng, E.H., Chan, V.S., and Ho, G.H. (1999). Progestins inhibit the growth of MDA-MB-231 cells transfected with progesterone receptor complementary DNA. *Clin Cancer Res* **5**, 395-403.

Lin, V.C., Woon, C.T., Aw, S.E., and Guo, C. (2003). Distinct molecular pathways mediate progesterone-induced growth inhibition and focal adhesion. *Endocrinology* **144**, 5650-5657.

Liu, J., Hebert, M.D., Ye, Y., Templeton, D.J., Kung, H., and Matera, A.G. (2000). Cell cycle-dependent localization of the CDK2-cyclin E complex in Cajal (coiled) bodies. *J Cell Sci* **113 (Pt 9)**, 1543-1552.

Liu, J., Prickett, T.D., Elliott, E., Meroni, G., and Brautigan, D.L. (2001). Phosphorylation and microtubule association of the Opitz syndrome protein mid-1 is regulated by protein phosphatase 2A via binding to the regulatory subunit alpha 4. *Proc Natl Acad Sci U S A* **98**, 6650-6655.

Liu, Z., Wong, J., Tsai, S.Y., Tsai, M.J., and O'Malley, B.W. (1999). Steroid receptor coactivator-1 (SRC-1) enhances ligand-dependent and receptor-dependent cell-free transcription of chromatin. *Proc Natl Acad Sci U S A* **96**, 9485-9490.

Lohrum, M.A., Ashcroft, M., Kubbutat, M.H., and Vousden, K.H. (2000). Identification of a cryptic nucleolar-localization signal in MDM2. *Nat Cell Biol* **2**, 179-181.

Lupas, A. (1996). Coiled coils: new structures and new functions. *Trends Biochem Sci* **21**, 375-382.

Lydon, J.P., DeMayo, F.J., Funk, C.R., Mani, S.K., Hughes, A.R., Montgomery, C.A., Jr., Shyamala, G., Conneely, O.M., and O'Malley, B.W. (1995). Mice lacking progesterone receptor exhibit pleiotropic reproductive abnormalities. *Genes Dev* **9**, 2266-2278.

MacCallum, D.E., and Hall, P.A. (2000). The location of pKi67 in the outer dense fibrillary compartment of the nucleolus points to a role in ribosome biogenesis during the cell division cycle. *J Pathol* **190**, 537-544.

MacLusky, N.J., and McEwen, B.S. (1980). Progestin receptors in the developing rat brain and pituitary. *Brain Res* **189**, 262-268.

Maheswaran, S., Englert, C., Bennett, P., Heinrich, G., and Haber, D.A. (1995). The WT1 gene product stabilizes p53 and inhibits p53-mediated apoptosis. *Genes Dev* **9**, 2143-2156.

Manabe, R., Whitmore, L., Weiss, J.M., and Horwitz, A.R. (2002). Identification of a novel microtubule-associated protein that regulates microtubule organization and cytokinesis by using a GFP-screening strategy. *Curr Biol* **12**, 1946-1951.

Mani, S.K., Allen, J.M., Clark, J.H., Blaustein, J.D., and O'Malley, B.W. (1994). Convergent pathways for steroid hormone- and neurotransmitter-induced rat sexual behavior. *Science* **265**, 1246-1249.

Mansfield, E., Chae, J.J., Komarow, H.D., Brotz, T.M., Frucht, D.M., Aksentijevich, I., and Kastner, D.L. (2001). The familial Mediterranean fever protein, pyrin, associates with microtubules and colocalizes with actin filaments. *Blood* **98**, 851-859.

Marcand, S., Brevet, V., Mann, C., and Gilson, E. (2000). Cell cycle restriction of telomere elongation. *Curr Biol* **10**, 487-490.

Martinez-Estrada, O.M., Culleres, A., Soriano, F.X., Peinado, H., Bolos, V., Martinez, F.O., Reina, M., Cano, A., Fabre, M., and Vilaro, S. (2006). The transcription factors Slug and Snail act as repressors of Claudin-1 expression in epithelial cells. *Biochem J* **394**, 449-457.

Massenet, S., Pellizzoni, L., Paushkin, S., Mattaj, I.W., and Dreyfuss, G. (2002). The SMN complex is associated with snRNPs throughout their cytoplasmic assembly pathway. *Mol Cell Biol* **22**, 6533-6541.

Massiah, M.A., Matts, J.A., Short, K.M., Simmons, B.N., Singireddy, S., Yi, Z., and Cox, T.C. (2007). Solution structure of the MID1 B-box2 CHC(D/C)C(2)H(2) zinc-binding domain: insights into an evolutionarily conserved RING fold. *J Mol Biol* **369**, 1-10.

Massiah, M.A., Simmons, B.N., Short, K.M., and Cox, T.C. (2006). Solution structure of the RBCC/TRIM B-box1 domain of human MID1: B-box with a RING. *J Mol Biol* **358**, 532-545.

Matera, A.G. (1999). Nuclear bodies: multifaceted subdomains of the interchromatin space. *Trends Cell Biol* **9**, 302-309.

McGowan, E.M., Saad, S., Bendall, L.J., Bradstock, K.F., and Clarke, C.L. (2004). Effect of progesterone receptor a predominance on breast cancer cell migration into bone marrow fibroblasts. *Breast Cancer Res Treat* **83**, 211-220.

Meiering, C.D., and Linial, M.L. (2003). The promyelocytic leukemia protein does not mediate foamy virus latency in vitro. *J Virol* **77**, 2207-2213.

Meroni, G., and Diez-Roux, G. (2005). TRIM/RBCC, a novel class of 'single protein RING finger' E3 ubiquitin ligases. *Bioessays* **27**, 1147-1157.

Migliaccio, A., Piccolo, D., Castoria, G., Di Domenico, M., Bilancio, A., Lombardi, M., Gong, W., Beato, M., and Auricchio, F. (1998). Activation of the Src/p21ras/Erk pathway by progesterone receptor via cross-talk with estrogen receptor. *EMBO J* **17**, 2008-2018.

Milovic-Holm, K., Krieghoff, E., Jensen, K., Will, H., and Hofmann, T.G. (2007). FLASH links the CD95 signaling pathway to the cell nucleus and nuclear bodies. *EMBO J* **26**, 391-401.

Miyamoto, K., Nakamura, N., Kashiwagi, M., Honda, S., Kato, A., Hasegawa, S., Takei, Y., and Hirose, S. (2002). RING finger, B-box, and coiled-coil (RBCC) protein expression in branchial epithelial cells of Japanese eel, Anguilla japonica. *Eur J Biochem* **269**, 6152-6161.

Moosmann, P., Georgiev, O., Le Douarin, B., Bourquin, J.P., and Schaffner, W. (1996). Transcriptional repression by RING finger protein TIF1 beta that interacts with the KRAB repressor domain of KOX1. *Nucleic Acids Res* **24**, 4859-4867.

Morimoto, R.I. (2002). Dynamic remodeling of transcription complexes by molecular chaperones. *Cell* **110**, 281-284.

Mote, P.A., Balleine, R.L., McGowan, E.M., and Clarke, C.L. (1999). Colocalization of progesterone receptors A and B by dual immunofluorescent histochemistry in human endometrium during the menstrual cycle. *J Clin Endocrinol Metab* **84**, 2963-2971.

Mote, P.A., Bartow, S., Tran, N., and Clarke, C.L. (2002). Loss of co-ordinate expression of progesterone receptors A and B is an early event in breast carcinogenesis. *Breast Cancer Res Treat* **72**, 163-172.

Moulin, S., Llanos, S., Kim, S.H., and Peters, G. (2008). Binding to nucleophosmin determines the localization of human and chicken ARF but not its impact on p53. *Oncogene* **27**, 2382-2389.

Mu, Z.M., Chin, K.V., Liu, J.H., Lozano, G., and Chang, K.S. (1994). PML, a growth suppressor disrupted in acute promyelocytic leukemia. *Mol Cell Biol* **14**, 6858-6867.

Mulac-Jericevic, B., Mullinax, R.A., DeMayo, F.J., Lydon, J.P., and Conneely, O.M. (2000). Subgroup of reproductive functions of progesterone mediated by progesterone receptor-B isoform. *Science* **289**, 1751-1754.

Muller, S., and Dejean, A. (1999). Viral immediate-early proteins abrogate the modification by SUMO-1 of PML and Sp100 proteins, correlating with nuclear body disruption. *J Virol* **73**, 5137-5143.

Muller, S., Matunis, M.J., and Dejean, A. (1998). Conjugation with the ubiquitin-related modifier SUMO-1 regulates the partitioning of PML within the nucleus. *EMBO J* **17**, 61-70.

Mullin, J.M., Laughlin, K.V., Ginanni, N., Marano, C.W., Clarke, H.M., and Peralta Soler, A. (2000). Increased tight junction permeability can result from protein kinase C activation/translocation and act as a tumor promotional event in epithelial cancers. *Ann N Y Acad Sci* **915**, 231-236.

Murata, K., Wu, J., and Brautigan, D.L. (1997). B cell receptor-associated protein alpha4 displays rapamycin-sensitive binding directly to the catalytic subunit of protein phosphatase 2A. *Proc Natl Acad Sci U S A* **94**, 10624-10629.

Musgrove, E.A., Swarbrick, A., Lee, C.S., Cornish, A.L., and Sutherland, R.L. (1998). Mechanisms of cyclin-dependent kinase inactivation by progestins. *Mol Cell Biol* **18**, 1812-1825.

Nagai, M.A., Da Ros, N., Neto, M.M., de Faria Junior, S.R., Brentani, M.M., Hirata, R., Jr., and Neves, E.J. (2004). Gene expression profiles in breast tumors regarding the presence or absence of estrogen and progesterone receptors. *Int J Cancer* **111**, 892-899.

Nagy, L., Kao, H.Y., Chakravarti, D., Lin, R.J., Hassig, C.A., Ayer, D.E., Schreiber, S.L., and Evans, R.M. (1997). Nuclear receptor repression mediated by a complex containing SMRT, mSin3A, and histone deacetylase. *Cell* **89**, 373-380.

Narayanan, A., Speckmann, W., Terns, R., and Terns, M.P. (1999). Role of the box C/D motif in localization of small nucleolar RNAs to coiled bodies and nucleoli. *Mol Biol Cell* **10**, 2131-2147.

Narayanan, U., Achsel, T., Luhrmann, R., and Matera, A.G. (2004). Coupled in vitro import of U snRNPs and SMN, the spinal muscular atrophy protein. *Mol Cell* **16**, 223-234.

Narayanan, U., Ospina, J.K., Frey, M.R., Hebert, M.D., and Matera, A.G. (2002). SMN, the spinal muscular atrophy protein, forms a pre-import snRNP complex with snurportin1 and importin beta. *Hum Mol Genet* **11**, 1785-1795.

Nardulli, A.M., Greene, G.L., O'Malley, B.W., and Katzenellenbogen, B.S. (1988). Regulation of progesterone receptor messenger ribonucleic acid and protein levels in MCF-7 cells by estradiol: analysis of estrogen's effect on progesterone receptor synthesis and degradation. *Endocrinology* **122**, 935-944.

Nelson, C.C., Hendy, S.C., Shukin, R.J., Cheng, H., Bruchovsky, N., Koop, B.F., and Rennie, P.S. (1999). Determinants of DNA sequence specificity of the androgen, progesterone, and glucocorticoid receptors: evidence for differential steroid receptor response elements. *Mol Endocrinol* **13**, 2090-2107.

Nervi, C., Ferrara, F.F., Fanelli, M., Rippo, M.R., Tomassini, B., Ferrucci, P.F., Ruthardt, M., Gelmetti, V., Gambacorti-Passerini, C., Diverio, D., et al. (1998). Caspases mediate retinoic acid-induced degradation of the acute promyelocytic leukemia PML/RARalpha fusion protein. *Blood* **92**, 2244-2251.

Niikura, T., Hashimoto, Y., Tajima, H., Ishizaka, M., Yamagishi, Y., Kawasumi, M., Nawa, M., Terashita, K., Aiso, S., and Nishimoto, I. (2003). A tripartite motif protein TRIM11 binds and destabilizes Humanin, a neuroprotective peptide against Alzheimer's disease-relevant insults. *Eur J Neurosci* **17**, 1150-1158.

Nisole, S., Stoye, J.P., and Saib, A. (2005). TRIM family proteins: retroviral restriction and antiviral defence. *Nat Rev Microbiol* **3**, 799-808.

Notredame, C., Higgins, D.G., and Heringa, J. (2000). T-Coffee: A novel method for fast and accurate multiple sequence alignment. *J Mol Biol* **302**, 205-217.

Obad, S. (2007). TRIM22/Staf50 - A Novel Target Gene of the Tumor Suppressor p53. In Division of Hematology and Transfusion Medicine, Faculty of Medicine (Lund, Sweden, Lund University), pp. 65.

Obad, S., Brunnstrom, H., Vallon-Christersson, J., Borg, A., Drott, K., and Gullberg, U. (2004). Staf50 is a novel p53 target gene conferring reduced clonogenic growth of leukemic U-937 cells. *Oncogene* **23**, 4050-4059.

Obad, S., Olofsson, T., Mechti, N., Gullberg, U., and Drott, K. (2007a). Expression of the IFN-inducible p53-target gene TRIM22 is down-regulated during erythroid differentiation of human bone marrow. *Leuk Res* **31**, 995-1001

Obad, S., Olofsson, T., Mechti, N., Gullberg, U., and Drott, K. (2007b). Regulation of the interferon-inducible p53 target gene TRIM22 (Staf50) in human T lymphocyte activation. *J Interferon Cytokine Res* **27**, 857-864.

Ogawa, S., Goto, W., Orimo, A., Hosoi, T., Ouchi, Y., Muramatsu, M., and Inoue, S. (1998). Molecular cloning of a novel RING finger-B box-coiled coil (RBCC) protein, terf, expressed in the testis. *Biochem Biophys Res Commun* **251**, 515-519.

Ogawa, S., Saito, T., Matsuda, Y., Seki, N., Hayashi, A., Orimo, A., Hosoi, T., Ouchi, Y., Muramatsu, M., Hori, T., et al. (2000). Chromosome mapping of RNF16 and rnf16, human, mouse and rat genes coding for testis RING finger protein (terf), a member of the RING finger family. *Cytogenet Cell Genet* **89**, 56-58.

Ohkawa, N., Kokura, K., Matsu-Ura, T., Obinata, T., Konishi, Y., and Tamura, T.A. (2001). Molecular cloning and characterization of neural activity-related RING finger protein (NARF): a new member of the RBCC family is a candidate for the partner of myosin V. *J Neurochem* **78**, 75-87.

Ohkura, S., Yap, M.W., Sheldon, T., and Stoye, J.P. (2006). All three variable regions of the TRIM5alpha B30.2 domain can contribute to the specificity of retrovirus restriction. *J Virol* **80**, 8554-8565.

Onate, S.A., Boonyaratanakornkit, V., Spencer, T.E., Tsai, S.Y., Tsai, M.J., Edwards, D.P., and O'Malley, B.W. (1998). The steroid receptor coactivator-1 contains multiple receptor interacting and activation domains that cooperatively enhance the activation function 1 (AF1) and AF2 domains of steroid receptors. *J Biol Chem* **273**, 12101-12108.

Orimo, A., Tominaga, N., Yoshimura, K., Yamauchi, Y., Nomura, M., Sato, M., Nogi, Y., Suzuki, M., Suzuki, H., Ikeda, K., et al. (2000a). Molecular cloning of ring finger protein 21 (RNF21)/interferon-responsive finger protein (ifp1), which possesses two RING-B box-coiled coil domains in tandem. *Genomics* **69**, 143-149.

Orimo, A., Yamagishi, T., Tominaga, N., Yamauchi, Y., Hishinuma, T., Okada, K., Suzuki, M., Sato, M., Nogi, Y., Suzuki, H., et al. (2000b). Molecular cloning of testis-abundant finger Protein/Ring finger protein 23 (RNF23), a novel RING-B box-coiled coil-B30.2 protein on the class I region of the human MHC. *Biochem Biophys Res Commun* **276**, 45-51.

Papin, S., Duquesnoy, P., Cazeneuve, C., Pantel, J., Coppey-Moisan, M., Dargemont, C., and Amselem, S. (2000). Alternative splicing at the MEFV locus involved in familial Mediterranean fever regulates translocation of the marenostrin/pyrin protein to the nucleus. *Hum Mol Genet* **9**, 3001-3009.

Passer, B.J., Nancy-Portebois, V., Amzallag, N., Prieur, S., Cans, C., Roborel de Climens, A., Fiucci, G., Bouvard, V., Tuynder, M., Susini, L., et al. (2003). The p53-inducible TSAP6 gene product regulates apoptosis and the cell cycle and interacts with Nix and the Myt1 kinase. *Proc Natl Acad Sci U S A* **100**, 2284-2289.

Patarca, R., Freeman, G.J., Schwartz, J., Singh, R.P., Kong, Q.T., Murphy, E., Anderson, Y., Sheng, F.Y., Singh, P., Johnson, K.A., et al. (1988). rpt-1, an intracellular protein from helper/inducer T cells that regulates gene expression of interleukin 2 receptor and human immunodeficiency virus type 1. *Proc Natl Acad Sci U S A* **85**, 2733-2737.

Pearson, M., Carbone, R., Sebastiani, C., Cioce, M., Fagioli, M., Saito, S., Higashimoto, Y., Appella, E., Minucci, S., Pandolfi, P.P., et al. (2000). PML regulates p53 acetylation and premature senescence induced by oncogenic Ras. *Nature* **406**, 207-210.

Pederson, T., and Robbins, E. (1971). A method for improving synchrony in the G2 phase of the cell cycle. *J Cell Biol* **49**, 942-945.

Peng, H., Begg, G.E., Schultz, D.C., Friedman, J.R., Jensen, D.E., Speicher, D.W., and Rauscher, F.J., 3rd (2000). Reconstitution of the KRAB-KAP-1 repressor complex: a model system for defining the molecular anatomy of RING-B box-coiled-coil domain-mediated protein-protein interactions. *J Mol Biol* **295**, 1139-1162.

Perissi, V., Staszewski, L.M., McInerney, E.M., Kurokawa, R., Krones, A., Rose, D.W., Lambert, M.H., Milburn, M.V., Glass, C.K., and Rosenfeld, M.G. (1999). Molecular determinants of nuclear receptor-corepressor interaction. *Genes Dev* **13**, 3198-3208.

Perron, M.J., Stremlau, M., Song, B., Ulm, W., Mulligan, R.C., and Sodroski, J. (2004). TRIM5alpha mediates the postentry block to N-tropic murine leukemia viruses in human cells. *Proc Natl Acad Sci U S A* **101**, 11827-11832.

Pettersson, K., Delaunay, F., and Gustafsson, J.A. (2000). Estrogen receptor beta acts as a dominant regulator of estrogen signaling. *Oncogene* **19**, 4970-4978.

Pettersson, K., Grandien, K., Kuiper, G.G., and Gustafsson, J.A. (1997). Mouse estrogen receptor beta forms estrogen response element-binding heterodimers with estrogen receptor alpha. *Mol Endocrinol* **11**, 1486-1496.

Petz, L.N., and Nardulli, A.M. (2000). Sp1 binding sites and an estrogen response element half-site are involved in regulation of the human progesterone receptor A promoter. *Mol Endocrinol* **14**, 972-985.

Petz, L.N., Ziegler, Y.S., Loven, M.A., and Nardulli, A.M. (2002). Estrogen receptor alpha and activating protein-1 mediate estrogen responsiveness of the progesterone receptor gene in MCF-7 breast cancer cells. *Endocrinology* **143**, 4583-4591.

Phair, R.D., and Misteli, T. (2000). High mobility of proteins in the mammalian cell nucleus. *Nature* **404**, 604-609.

Platani, M., Goldberg, I., Swedlow, J.R., and Lamond, A.I. (2000). In vivo analysis of Cajal body movement, separation, and joining in live human cells. *J Cell Biol* **151**, 1561-1574.

Pluta, A.F., Earnshaw, W.C., and Goldberg, I.G. (1998). Interphase-specific association of intrinsic centromere protein CENP-C with HDaxx, a death domain-binding protein implicated in Fas-mediated cell death. *J Cell Sci* **111 (Pt 14)**, 2029-2041.

Quignon, F., De Bels, F., Koken, M., Feunteun, J., Ameisen, J.C., and de The, H. (1998). PML induces a novel caspase-independent death process. *Nat Genet* **20**, 259-265.

Rajsbaum, R., Stoye, J.P., and O'Garra, A. (2008). Type I interferon-dependent and -independent expression of tripartite motif proteins in immune cells. *Eur J Immunol* **38**, 619-630.

Read, L.D., Snider, C.E., Miller, J.S., Greene, G.L., and Katzenellenbogen, B.S. (1988). Ligand-modulated regulation of progesterone receptor messenger ribonucleic acid and protein in human breast cancer cell lines. *Mol Endocrinol* **2**, 263-271.

Regad, T., Saib, A., Lallemand-Breitenbach, V., Pandolfi, P.P., de The, H., and Chelbi-Alix, M.K. (2001). PML mediates the interferon-induced antiviral state against a complex retrovirus via its association with the viral transactivator. *EMBO J* **20**, 3495-3505.

Renne, R., Barry, C., Dittmer, D., Compitello, N., Brown, P.O., and Ganem, D. (2001). Modulation of cellular and viral gene expression by the latency-associated nuclear antigen of Kaposi's sarcoma-associated herpesvirus. *J Virol* **75**, 458-468.

Reymond, A., Meroni, G., Fantozzi, A., Merla, G., Cairo, S., Luzi, L., Riganelli, D., Zanaria, E., Messali, S., Cainarca, S., et al. (2001). The tripartite motif family identifies cell compartments. *Embo J* **20**, 2140-2151.

Rhodes, D.A., Ihrke, G., Reinicke, A.T., Malcherek, G., Towey, M., Isenberg, D.A., and Trowsdale, J. (2002). The 52 000 MW Ro/SS-A autoantigen in Sjogren's syndrome/systemic lupus erythematosus (Ro52) is an interferon-gamma inducible tripartite motif protein associated with membrane proximal structures. *Immunology* **106**, 246-256.

Rhodes, D.A., and Trowsdale, J. (2007). TRIM21 is a trimeric protein that binds IgG Fc via the B30.2 domain. *Mol Immunol* **44**, 2406-2414.

Richer, J.K., Jacobsen, B.M., Manning, N.G., Abel, M.G., Wolf, D.M., and Horwitz, K.B. (2002). Differential gene regulation by the two progesterone receptor isoforms in human breast cancer cells. *J Biol Chem* **277**, 5209-5218.

Roberts, J.D., Jr., Chiche, J.D., Kolpa, E.M., Bloch, D.B., and Bloch, K.D. (2007). cGMP-dependent protein kinase I interacts with TRIM39R, a novel Rpp21 domain-containing TRIM protein. *Am J Physiol Lung Cell Mol Physiol* **293**, L903-912.

Robyr, D., Wolffe, A.P., and Wahli, W. (2000). Nuclear hormone receptor coregulators in action: diversity for shared tasks. *Mol Endocrinol* **14**, 329-347.

Rodway, H., Llanos, S., Rowe, J., and Peters, G. (2004). Stability of nucleolar versus non-nucleolar forms of human p14(ARF). *Oncogene* **23**, 6186-6192.

Rossouw, J.E., Anderson, G.L., Prentice, R.L., LaCroix, A.Z., Kooperberg, C., Stefanick, M.L., Jackson, R.D., Beresford, S.A., Howard, B.V., Johnson, K.C., et al. (2002). Risks and benefits of estrogen plus progestin in healthy postmenopausal women: principal results From the Women's Health Initiative randomized controlled trial. *Jama* **288**, 321-333.

Rowley, J.D., Golomb, H.M., Vardiman, J., Fukuhara, S., Dougherty, C., and Potter, D. (1977). Further evidence for a non-random chromosomal abnormality in acute promyelocytic leukemia. *Int J Cancer* **20**, 869-872.

Ruan, W., Monaco, M.E., and Kleinberg, D.L. (2005). Progesterone stimulates mammary gland ductal morphogenesis by synergizing with and enhancing insulin-like growth factor-I action. *Endocrinology* **146**, 1170-1178.

Sabbah, M., Courilleau, D., Mester, J., and Redeuilh, G. (1999). Estrogen induction of the cyclin D1 promoter: involvement of a cAMP response-like element. *Proc Natl Acad Sci U S A* **96**, 11217-11222.

Saitoh, M., Ohmichi, M., Takahashi, K., Kawagoe, J., Ohta, T., Doshida, M., Takahashi, T., Igarashi, H., Mori-Abe, A., Du, B., et al. (2005). Medroxyprogesterone acetate induces cell proliferation through

up-regulation of cyclin D1 expression via phosphatidylinositol 3-kinase/Akt/nuclear factor-kappaB cascade in human breast cancer cells. *Endocrinology* **146**, 4917-4925.

Santen, R.J. (2003). Risk of breast cancer with progestins: critical assessment of current data. *Steroids* **68**, 953-964.

Sartorius, C.A., Groshong, S.D., Miller, L.A., Powell, R.L., Tung, L., Takimoto, G.S., and Horwitz, K.B. (1994a). New T47D breast cancer cell lines for the independent study of progesterone B- and A-receptors: only antiprogestin-occupied B-receptors are switched to transcriptional agonists by cAMP. *Cancer Res* **54**, 3868-3877.

Sartorius, C.A., Melville, M.Y., Hovland, A.R., Tung, L., Takimoto, G.S., and Horwitz, K.B. (1994b). A third transactivation function (AF3) of human progesterone receptors located in the unique N-terminal segment of the B-isoform. *Mol Endocrinol* **8**, 1347-1360.

Sawyer, S.L., Emerman, M., and Malik, H.S. (2007). Discordant Evolution of the Adjacent Antiretroviral Genes TRIM22 and TRIM5 in Mammals. *PLoS Pathog* **3**, e197.

Sawyer, S.L., Wu, L.I., Emerman, M., and Malik, H.S. (2005). Positive selection of primate TRIM5alpha identifies a critical species-specific retroviral restriction domain. *Proc Natl Acad Sci U S A* **102**, 2832-2837.

Scherl, A., Coute, Y., Deon, C., Calle, A., Kindbeiter, K., Sanchez, J.C., Greco, A., Hochstrasser, D., and Diaz, J.J. (2002). Functional proteomic analysis of human nucleolus. *Mol Biol Cell* **13**, 4100-4109.

Schubert, U., Anton, L.C., Gibbs, J., Norbury, C.C., Yewdell, J.W., and Bennink, J.R. (2000). Rapid degradation of a large fraction of newly synthesized proteins by proteasomes. *Nature* **404**, 770-774.

Schul, W., Groenhout, B., Koberna, K., Takagaki, Y., Jenny, A., Manders, E.M., Raska, I., van Driel, R., and de Jong, L. (1996). The RNA 3' cleavage factors CstF 64 kDa and CPSF 100 kDa are concentrated in nuclear domains closely associated with coiled bodies and newly synthesized RNA. *EMBO J* **15**, 2883-2892.

Schul, W., van Der Kraan, I., Matera, A.G., van Driel, R., and de Jong, L. (1999). Nuclear domains enriched in RNA 3'-processing factors associate with coiled bodies and histone genes in a cell cycle-dependent manner. *Mol Biol Cell* **10**, 3815-3824.

Schwartz, D.C., and Hochstrasser, M. (2003). A superfamily of protein tags: ubiquitin, SUMO and related modifiers. *Trends Biochem Sci* **28**, 321-328.

Schweiger, S., Foerster, J., Lehmann, T., Suckow, V., Muller, Y.A., Walter, G., Davies, T., Porter, H., van Bokhoven, H., Lunt, P.W., et al. (1999). The Opitz syndrome gene product, MID1, associates with microtubules. *Proc Natl Acad Sci U S A* **96**, 2794-2799.

Scott, D.A., Drury, S., Sundstrom, R.A., Bishop, J., Swiderski, R.E., Carmi, R., Ramesh, A., Elbedour, K., Srikumari Srisailapathy, C.R., Keats, B.J., et al. (2000). Refining the DFNB7-DFNB11 deafness locus using intragenic polymorphisms in a novel gene, TMEM2. *Gene* **246**, 265-274.

Shang, Y., and Brown, M. (2002). Molecular determinants for the tissue specificity of SERMs. *Science* **295**, 2465-2468.

Shen, T.H., Lin, H.K., Scaglioni, P.P., Yung, T.M., and Pandolfi, P.P. (2006). The mechanisms of PML-nuclear body formation. *Mol Cell* **24**, 331-339.

Shiama, N. (1997). The p300/CBP family: integrating signals with transcription factors and chromatin. *Trends Cell Biol* **7**, 230-236.

Shimono, Y., Murakami, H., Hasegawa, Y., and Takahashi, M. (2000). RET finger protein is a transcriptional repressor and interacts with enhancer of polycomb that has dual transcriptional functions. *J Biol Chem* **275**, 39411-39419.

Shopland, L.S., Byron, M., Stein, J.L., Lian, J.B., Stein, G.S., and Lawrence, J.B. (2001). Replication-dependent histone gene expression is related to Cajal body (CB) association but does not require sustained CB contact. *Mol Biol Cell* **12**, 565-576.

Short, K.M., and Cox, T.C. (2006). Subclassification of the RBCC/TRIM superfamily reveals a novel motif necessary for microtubule binding. *J Biol Chem* **281**, 8970-8980.

Short, K.M., Hopwood, B., Yi, Z., and Cox, T.C. (2002). MID1 and MID2 homo- and heterodimerise to tether the rapamycin-sensitive PP2A regulatory subunit, alpha 4, to microtubules: implications for the clinical variability of X-linked Opitz GBBB syndrome and other developmental disorders. *BMC Cell Biol* **3**, 1.

Shupnik, M.A. (2004). Crosstalk between steroid receptors and the c-Src-receptor tyrosine kinase pathways: implications for cell proliferation. *Oncogene* **23**, 7979-7989.

Shyu, H.W., Hsu, S.H., Hsieh-Li, H.M., and Li, H. (2003). Forced expression of RNF36 induces cell apoptosis. *Exp Cell Res* **287**, 301-313.

Sirri, V., Urcuqui-Inchima, S., Roussel, P., and Hernandez-Verdun, D. (2008). Nucleolus: the fascinating nuclear body. *Histochem Cell Biol* **129**, 13-31.

Skildum, A., Faivre, E., and Lange, C.A. (2005). Progesterone receptors induce cell cycle progression via activation of mitogen-activated protein kinases. *Mol Endocrinol* **19**, 327-339.

Skurat, A.V., Dietrich, A.D., Zhai, L., and Roach, P.J. (2002). GNIP, a novel protein that binds and activates glycogenin, the self-glucosylating initiator of glycogen biosynthesis. *J Biol Chem* **277**, 19331-19338.

Slack, F.J., Basson, M., Liu, Z., Ambros, V., Horvitz, H.R., and Ruvkun, G. (2000). The lin-41 RBCC gene acts in the C. elegans heterochronic pathway between the let-7 regulatory RNA and the LIN-29 transcription factor. *Mol Cell* **5**, 659-669.

Sleeman, J.E., Trinkle-Mulcahy, L., Prescott, A.R., Ogg, S.C., and Lamond, A.I. (2003). Cajal body proteins SMN and Coilin show differential dynamic behaviour in vivo. *J Cell Sci* **116**, 2039-2050.

Sluyser, M. (1994). Hormone resistance in cancer: the role of abnormal steroid receptors. *Crit Rev Oncog* **5**, 539-554.

Spencer, J.A., Eliazer, S., Ilaria, R.L., Jr., Richardson, J.A., and Olson, E.N. (2000). Regulation of microtubule dynamics and myogenic differentiation by MURF, a striated muscle RING-finger protein. *J Cell Biol* **150**, 771-784.

Spencer, T.E., Jenster, G., Burcin, M.M., Allis, C.D., Zhou, J., Mizzen, C.A., McKenna, N.J., Onate, S.A., Tsai, S.Y., Tsai, M.J., et al. (1997). Steroid receptor coactivator-1 is a histone acetyltransferase. *Nature* **389**, 194-198.

Sredni, S.T., de Camargo, B., Lopes, L.F., Teixeira, R., and Simpson, A. (2001). Immunohistochemical detection of p53 protein expression as a prognostic indicator in Wilms tumor. *Med Pediatr Oncol* **37**, 455-458.

Stadler, M., Chelbi-Alix, M.K., Koken, M.H., Venturini, L., Lee, C., Saib, A., Quignon, F., Pelicano, L., Guillemin, M.C., Schindler, C., et al. (1995). Transcriptional induction of the PML growth suppressor gene by interferons is mediated through an ISRE and a GAS element. *Oncogene* **11**, 2565-2573.

Stanek, D., and Neugebauer, K.M. (2006). The Cajal body: a meeting place for spliceosomal snRNPs in the nuclear maze. *Chromosoma* **115**, 343-354.

Stoye, J.P. (1998). Fv1, the mouse retrovirus resistance gene. *Rev Sci Tech* **17**, 269-277.

Stremlau, M., Owens, C.M., Perron, M.J., Kiessling, M., Autissier, P., and Sodroski, J. (2004). The cytoplasmic body component TRIM5alpha restricts HIV-1 infection in Old World monkeys. *Nature* **427**, 848-853.

Stremlau, M., Perron, M., Welikala, S., and Sodroski, J. (2005). Species-specific variation in the B30.2(SPRY) domain of TRIM5alpha determines the potency of human immunodeficiency virus restriction. *J Virol* **79**, 3139-3145.

Su, C., Gao, G., Schneider, S., Helt, C., Weiss, C., O'Reilly, M.A., Bohmann, D., and Zhao, J. (2004). DNA damage induces downregulation of histone gene expression through the G1 checkpoint pathway. *EMBO J* **23**, 1133-1143.

Sumida, T., Itahana, Y., Hamakawa, H., and Desprez, P.Y. (2004). Reduction of human metastatic breast cancer cell aggressiveness on introduction of either form A or B of the progesterone receptor and then treatment with progestins. *Cancer Res* **64**, 7886-7892.

Sutherland, R.L., Hall, R.E., Pang, G.Y., Musgrove, E.A., and Clarke, C.L. (1988). Effect of medroxyprogesterone acetate on proliferation and cell cycle kinetics of human mammary carcinoma cells. *Cancer Res* **48**, 5084-5091.

Swisshelm, K., Machl, A., Planitzer, S., Robertson, R., Kubbies, M., and Hosier, S. (1999). SEMP1, a senescence-associated cDNA isolated from human mammary epithelial cells, is a member of an epithelial membrane protein superfamily. *Gene* **226**, 285-295.

Takahashi, M., and Cooper, G.M. (1987). ret transforming gene encodes a fusion protein homologous to tyrosine kinases. *Mol Cell Biol* **7**, 1378-1385.

Takahashi, M., Inaguma, Y., Hiai, H., and Hirose, F. (1988). Developmentally regulated expression of a human "finger"-containing gene encoded by the 5' half of the ret transforming gene. *Mol Cell Biol* **8**, 1853-1856.

Tanaka, M., Fukuda, Y., Mashima, K., and Hanai, R. (2005). Intracellular localization and domain organization of human TRIM41 proteins. *Mol Biol Rep* **32**, 87-93.

Terner, C. (1977). Progesterone and progestins in the male reproductive system. *Ann N Y Acad Sci* **286**, 313-320.

Thiry, M., and Lafontaine, D.L. (2005). Birth of a nucleolus: the evolution of nucleolar compartments. *Trends Cell Biol* **15**, 194-199.

Timmons, B.C., Mitchell, S.M., Gilpin, C., and Mahendroo, M.S. (2007). Dynamic changes in the cervical epithelial tight junction complex and differentiation occur during cervical ripening and parturition. *Endocrinology* **148**, 1278-1287.

Tissot, C., and Mechti, N. (1995). Molecular cloning of a new interferon-induced factor that represses human immunodeficiency virus type 1 long terminal repeat expression. *J Biol Chem* **270**, 14891-14898.

Tissot, C., Taviaux, S.A., Diriong, S., and Mechti, N. (1996). Localization of Staf50, a member of the Ring finger family, to 11p15 by fluorescence in situ hybridization. *Genomics* **34**, 151-153.

Tokes, A.M., Kulka, J., Paku, S., Szik, A., Paska, C., Novak, P.K., Szilak, L., Kiss, A., Bogi, K., and Schaff, Z. (2005). Claudin-1, -3 and -4 proteins and mRNA expression in benign and malignant breast lesions: a research study. *Breast Cancer Res* **7**, R296-305.

Toniato, E., Chen, X.P., Losman, J., Flati, V., Donahue, L., and Rothman, P. (2002). TRIM8/GERP RING finger protein interacts with SOCS-1. *J Biol Chem* **277**, 37315-37322.

Torok, M., and Etkin, L.D. (2001). Two B or not two B? Overview of the rapidly expanding B-box family of proteins. *Differentiation* **67**, 63-71.

Torii, S., Egan, D.A., Evans, R.A., and Reed, J.C. (1999). Human Daxx regulates Fas-induced apoptosis from nuclear PML oncogenic domains (PODs). *EMBO J* **18**, 6037-6049.

Towers, G., Bock, M., Martin, S., Takeuchi, Y., Stoye, J.P., and Danos, O. (2000). A conserved mechanism of retrovirus restriction in mammals. *Proc Natl Acad Sci U S A* **97**, 12295-12299.

Townson, S.M., Kang, K., Lee, A.V., and Oesterreich, S. (2006). Novel role of the RET finger protein in estrogen receptor-mediated transcription in MCF-7 cells. *Biochem Biophys Res Commun* **349**, 540-548.

Tremblay, A., Tremblay, G.B., Labrie, F., and Giguere, V. (1999). Ligand-independent recruitment of SRC-1 to estrogen receptor beta through phosphorylation of activation function AF-1. *Mol Cell* **3**, 513-519.

Trockenbacher, A., Suckow, V., Foerster, J., Winter, J., Krauss, S., Ropers, H.H., Schneider, R., and Schweiger, S. (2001). MID1, mutated in Opitz syndrome, encodes an ubiquitin ligase that targets phosphatase 2A for degradation. *Nat Genet* **29**, 287-294.

Uchil, P.D., Quinlan, B.D., Chan, W.T., Luna, J.M., and Mothes, W. (2008). TRIM E3 Ligases Interfere with Early and Late Stages of the Retroviral Life Cycle. *PLoS Pathog* **4**, e16.

Urano, T., Saito, T., Tsukui, T., Fujita, M., Hosoi, T., Muramatsu, M., Ouchi, Y., and Inoue, S. (2002). Efp targets 14-3-3 sigma for proteolysis and promotes breast tumour growth. *Nature* **417**, 871-875.

Vandeputte, D.A., Meije, C.B., van Dartel, M., Leenstra, S., H, I.J.-K., Das, P.K., Troost, D., Bosch, D.A., Baas, F., and Hulsebos, T.J. (2001). GOA, a novel gene encoding a ring finger B-box coiled-coil protein, is overexpressed in astrocytoma. *Biochem Biophys Res Commun* **286**, 574-579.

Venturini, L., You, J., Stadler, M., Galien, R., Lallemand, V., Koken, M.H., Mattei, M.G., Ganser, A., Chambon, P., Losson, R., et al. (1999). TIF1gamma, a novel member of the transcriptional intermediary factor 1 family. *Oncogene* **18**, 1209-1217.

Verhagen, A.M., Coulson, E.J., and Vaux, D.L. (2001). Inhibitor of apoptosis proteins and their relatives: IAPs and other BIRPs. *Genome Biol* **2**, REVIEWS3009.

Vincent, S.R., Kwasnicka, D.A., and Fretier, P. (2000). A novel RING finger-B box-coiled-coil protein, GERP. *Biochem Biophys Res Commun* **279**, 482-486.

Vitale, N., Moss, J., and Vaughan, M. (1996). ARD1, a 64-kDa bifunctional protein containing an 18-kDa GTP-binding ADP-ribosylation factor domain and a 46-kDa GTPase-activating domain. *Proc Natl Acad Sci U S A* **93**, 1941-1944.

Vitale, N., Pacheco-Rodriguez, G., Ferrans, V.J., Riemenschneider, W., Moss, J., and Vaughan, M. (2000). Specific functional interaction of human cytohesin-1 and ADP-ribosylation factor domain protein (ARD1). *J Biol Chem* **275**, 21331-21339.

Voegel, J.J., Heine, M.J., Tini, M., Vivat, V., Chambon, P., and Gronemeyer, H. (1998). The coactivator TIF2 contains three nuclear receptor-binding motifs and mediates transactivation through CBP binding-dependent and -independent pathways. *EMBO J* **17**, 507-519.

Wada, K., and Kamitani, T. (2006). Autoantigen Ro52 is an E3 ubiquitin ligase. *Biochem Biophys Res Commun* **339**, 415-421.

Wan, Y., and Nordeen, S.K. (2002). Overlapping but distinct gene regulation profiles by glucocorticoids and progestins in human breast cancer cells. *Mol Endocrinol* **16**, 1204-1214.

Wang, Y., Li, Y., Qi, X., Yuan, W., Ai, J., Zhu, C., Cao, L., Yang, H., Liu, F., Wu, X., et al. (2004). TRIM45, a novel human RBCC/TRIM protein, inhibits transcriptional activities of ElK-1 and AP-1. *Biochem Biophys Res Commun* **323**, 9-16.

Wang, Z.G., Ruggero, D., Ronchetti, S., Zhong, S., Gaboli, M., Rivi, R., and Pandolfi, P.P. (1998). PML is essential for multiple apoptotic pathways. *Nat Genet* **20**, 266-272.

Warrell, R.P., Jr., Frankel, S.R., Miller, W.H., Jr., Scheinberg, D.A., Itri, L.M., Hittelman, W.N., Vyas, R., Andreeff, M., Tafuri, A., Jakubowski, A., et al. (1991). Differentiation therapy of acute promyelocytic leukemia with tretinoin (all-trans-retinoic acid). *N Engl J Med* **324**, 1385-1393.

Weber, J.D., Taylor, L.J., Roussel, M.F., Sherr, C.J., and Bar-Sagi, D. (1999). Nucleolar Arf sequesters Mdm2 and activates p53. *Nat Cell Biol* **1**, 20-26.

Wei, L.L., Hawkins, P., Baker, C., Norris, B., Sheridan, P.L., and Quinn, P.G. (1996). An amino-terminal truncated progesterone receptor isoform, PRc, enhances progestin-induced transcriptional activity. *Mol Endocrinol* **10**, 1379-1387.

Wei, L.L., Krett, N.L., Francis, M.D., Gordon, D.F., Wood, W.M., O'Malley, B.W., and Horwitz, K.B. (1988). Multiple human progesterone receptor messenger ribonucleic acids and their autoregulation by progestin agonists and antagonists in breast cancer cells. *Mol Endocrinol* **2**, 62-72.

Wei, L.L., Norris, B.M., and Baker, C.J. (1997). An N-terminally truncated third progesterone receptor protein, PR(C), forms heterodimers with PR(B) but interferes in PR(B)-DNA binding. *J Steroid Biochem Mol Biol* **62**, 287-297.

Weinberg, R.A. (1995). The retinoblastoma protein and cell cycle control. *Cell* **81**, 323-330.

Wilson, G.R., Cramer, A., Welman, A., Knox, F., Swindell, R., Kawakatsu, H., Clarke, R.B., Dive, C., and Bundred, N.J. (2006). Activated c-SRC in ductal carcinoma in situ correlates with high tumour grade, high proliferation and HER2 positivity. *Br J Cancer* **95**, 1410-1414.

Wittmann, S., Wunder, C., Zirn, B., Furtwangler, R., Wegert, J., Graf, N., and Gessler, M. (2008). New prognostic markers revealed by evaluation of genes correlated with clinical parameters in Wilms tumors. *Genes Chromosomes Cancer* **47**, 386-395.

Woo, J.S., Imm, J.H., Min, C.K., Kim, K.J., Cha, S.S., and Oh, B.H. (2006). Structural and functional insights into the B30.2/SPRY domain. *EMBO J* **25**, 1353-1363.

Yamauchi, K., Wada, K., Tanji, K., Tanaka, M., and Kamitani, T. (2008). Ubiquitination of E3 ubiquitin ligase TRIM5alpha and its potential role. *FEBS J*. **275**, 1540-1555

Yang, Y.L., and Li, X.M. (2000). The IAP family: endogenous caspase inhibitors with multiple biological activities. *Cell Res* **10**, 169-177.

Yao, S., Liu, M.S., Masters, S.L., Zhang, J.G., Babon, J.J., Nicola, N.A., Nicholson, S.E., and Norton, R.S. (2006). Dynamics of the SPRY domain-containing SOCS box protein 2: flexibility of key functional loops. *Protein Sci* **15**, 2761-2772.

Yap, M.W., Nisole, S., Lynch, C., and Stoye, J.P. (2004). Trim5alpha protein restricts both HIV-1 and murine leukemia virus. *Proc Natl Acad Sci U S A* **101**, 10786-10791.

Ye, X., Wei, Y., Nalepa, G., and Harper, J.W. (2003). The cyclin E/Cdk2 substrate p220(NPAT) is required for S-phase entry, histone gene expression, and Cajal body maintenance in human somatic cells. *Mol Cell Biol* **23**, 8586-8600.

Yin, X., Dewille, J.W., and Hai, T. (2007). A potential dichotomous role of ATF3, an adaptive-response gene, in cancer development. *Oncogene* **27**, 2118-27

Yondola, M.A., and Hearing, P. (2007). The Adenovirus E4 ORF3 Protein Binds and Reorganizes the TRIM Family Member Transcriptional Intermediary Factor 1 Alpha. *J Virol* **81**, 4264-71

Yoshikawa, T., Seki, N., Azuma, T., Masuho, Y., Muramatsu, M., Miyajima, N., and Saito, T. (2000). Isolation of a cDNA for a novel human RING finger protein gene, RNF18, by the virtual transcribed sequence (VTS) approach(1). *Biochim Biophys Acta* **1493**, 349-355.

Young, P.J., Le, T.T., Dunckley, M., Nguyen, T.M., Burghes, A.H., and Morris, G.E. (2001). Nuclear gems and Cajal (coiled) bodies in fetal tissues: nucleolar distribution of the spinal muscular atrophy protein, SMN. *Exp Cell Res* **265**, 252-261.

Zhang, F., Hatziioannou, T., Perez-Caballero, D., Derse, D., and Bieniasz, P.D. (2006). Antiretroviral potential of human tripartite motif-5 and related proteins. *Virology* **353**, 396-409.

Zhang, H., Yang, B., Pomerantz, R.J., Zhang, C., Arunachalam, S.C., and Gao, L. (2003). The cytidine deaminase CEM15 induces hypermutation in newly synthesized HIV-1 DNA. *Nature* **424**, 94-98.

Zhang, J., Das, S.C., Kotalik, C., Pattnaik, A.K., and Zhang, L. (2004). The latent membrane protein 1 of Epstein-Barr virus establishes an antiviral state via induction of interferon-stimulated genes. *J Biol Chem* **279**, 46335-46342.

Zhang, J., Guenther, M.G., Carthew, R.W., and Lazar, M.A. (1998). Proteasomal regulation of nuclear receptor corepressor-mediated repression. *Genes Dev* **12**, 1775-1780.

Zhao, J., Dynlacht, B., Imai, T., Hori, T., and Harlow, E. (1998). Expression of NPAT, a novel substrate of cyclin E-CDK2, promotes S-phase entry. *Genes Dev* **12**, 456-461.

Zhao, J., Kennedy, B.K., Lawrence, B.D., Barbie, D.A., Matera, A.G., Fletcher, J.A., and Harlow, E. (2000). NPAT links cyclin E-Cdk2 to the regulation of replication-dependent histone gene transcription. *Genes Dev* **14**, 2283-2297.

Zhong, S., Hu, P., Ye, T.Z., Stan, R., Ellis, N.A., and Pandolfi, P.P. (1999). A role for PML and the nuclear body in genomic stability. *Oncogene* **18**, 7941-7947.

Zhong, S., Muller, S., Ronchetti, S., Freemont, P.S., Dejean, A., and Pandolfi, P.P. (2000a). Role of SUMO-1-modified PML in nuclear body formation. *Blood* **95**, 2748-2752.

Zhong, S., Salomoni, P., and Pandolfi, P.P. (2000b). The transcriptional role of PML and the nuclear body. *Nat Cell Biol* **2**, E85-90.

Zhong, S., Salomoni, P., Ronchetti, S., Guo, A., Ruggero, D., and Pandolfi, P.P. (2000c). Promyelocytic leukemia protein (PML) and Daxx participate in a novel nuclear pathway for apoptosis. *J Exp Med* **191**, 631-640.

Zhu, Y., Tomlinson, R.L., Lukowiak, A.A., Terns, R.M., and Terns, M.P. (2004). Telomerase RNA accumulates in Cajal bodies in human cancer cells. *Mol Biol Cell* **15**, 81-90.

Zou, W., Wang, J., and Zhang, D.E. (2007). Negative regulation of ISG15 E3 ligase EFP through its autoISGylation. *Biochem Biophys Res Commun* **354**, 321-327.

Zou, W., and Zhang, D.E. (2006). The interferon-inducible ubiquitin-protein isopeptide ligase (E3) EFP also functions as an ISG15 E3 ligase. *J Biol Chem* **281**, 3989-3994.

Zwijsen, R.M., Buckle, R.S., Hijmans, E.M., Loomans, C.J., and Bernards, R. (1998). Ligand-independent recruitment of steroid receptor coactivators to estrogen receptor by cyclin D1. *Genes Dev* **12**, 3488-3498.

Zwijsen, R.M., Wientjens, E., Klompmaker, R., van der Sman, J., Bernards, R., and Michalides, R.J. (1997). CDK-independent activation of estrogen receptor by cyclin D1. *Cell* **88**, 405-415.

APPENDICES

FIGURES

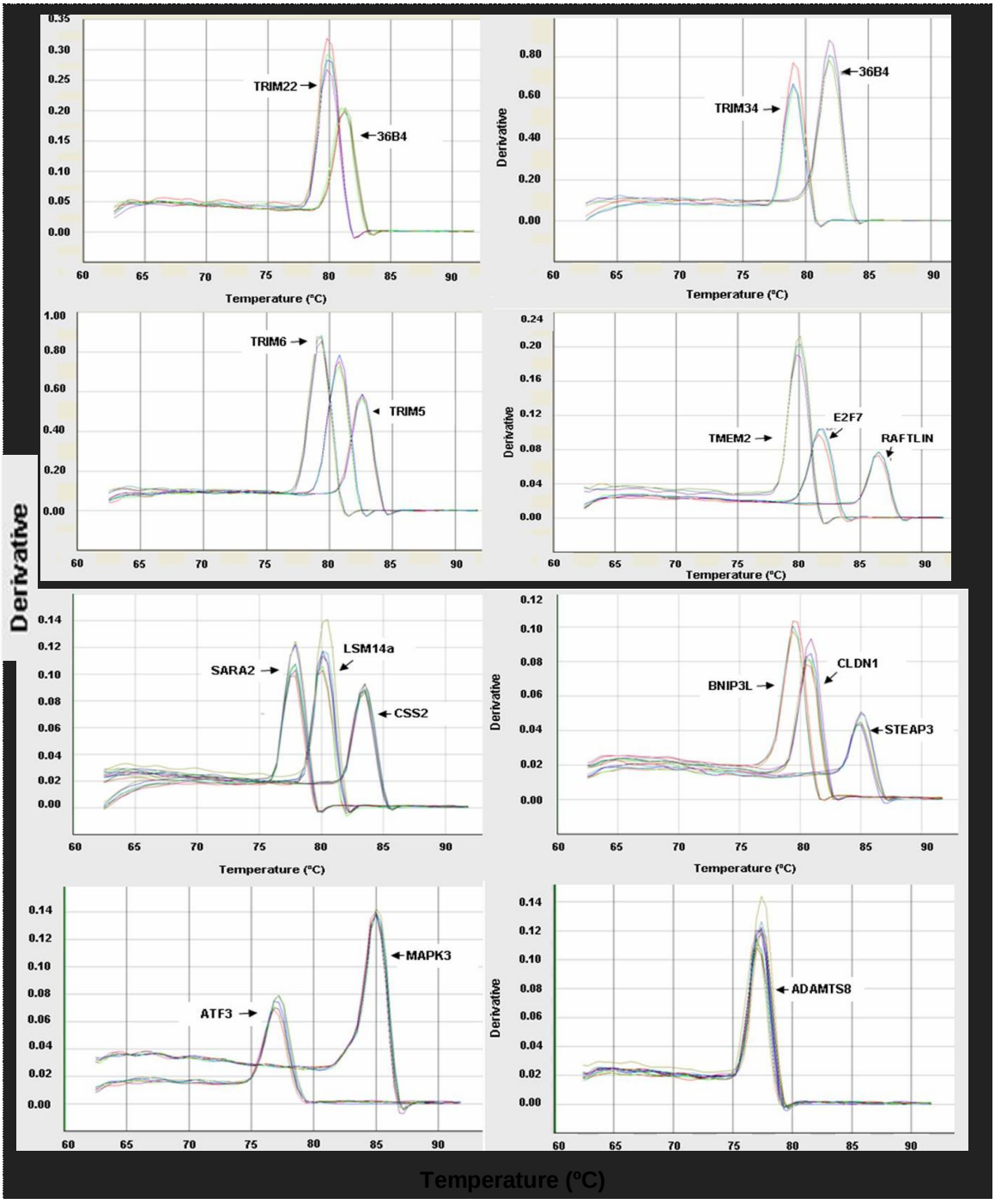

Figure A1 Melting curves for real-time PCR products

Melting curves (dissociation curves) for TRIM22, TRIM34, 36B4, TRIM6, TRIM5, TMEM2, E2F7, RAFTLIN, SARA2, LSM14a, CSS2, BNIP3L, CLDN1, STEAP3, ATF3, MAPK3, and ADAMTS8 PCR products were generated after real-time PCR amplification. One peak represents one single, specific product.

LIST OF BUFFERS AND RECIPES

Luria-Bertani (LB) broth / agar

Bacto-tryptone	10 g/L
Yeast extract	5 g/L
NaCl	5 g/L
+ agar (for LB agar)	15 g/L
ddH2O	

1X PBS

NaCl	9.000 g/L
$Na_2HPO_4 \cdot 7H_2O$	0.795 g/L
KH_2PO_4	0.144 g/L
ddH_2O	

1X DPBS (pH 7.4)

KCl	0.200 g/L
NaCl	8.000 g/L
Na_2HPO_4	1.150 g/L
KH_2PO_4	0.200 g/L
ddH_2O	

Cell lysis buffer

NaF	100 mM
HEPES (pH 7.5)	50 mM
NaCl	150 mM
PMSF	1 mM
Sodium vanadate	1 mM
Pepstatin A	5 µg/ml
Leupeptin	5 µg/ml
Aprotinin	2 µg/ml
Triton-X-100	1 %
ddH_2O	

5X Sample buffer for immunoblotting

Tris-HCl (pH 6.8)	0.625 M
SDS	10%
Glycerol	50%
β-mercapthoethanol	5%
Bromophenol Blue	Pinch
ddH_2O	

1X TBS buffer for washing M2-FLAG agarose beads

Tris-HCl (pH 7.4)	50 mM
NaCl	150 mM
ddH_2O	

1X Running buffer for immunoblotting

Tris Base	6.000 g/L
Glycine	28.800 g/L
SDS	1.000 g/L
ddH_2O	

1X Transfer buffer for immunoblotting

Tris Base	3.030 g/L
Glycine	14.410 g/L
Methanol	10% (v/v)
ddH_2O	

1X Wash buffer for Immunoblotting (TBST)

Tris-HCl (pH 7.5)	10 mM
NaCl	100 mM
TWEEN 20	0.1 %
ddH_2O	

Stripping buffer for immunoblotting

Tris-HCl (pH 6.8)	62.5 mM
SDS	2%
β-mercapthoethanol	0.8%
ddH_2O	

1X Tris-Borate-EDTA buffer (TBE) (pH 8.35)

Tris Base	90 mM
Boric Acid	50 mM
EDTA	2 mM
ddH_2O	

1X Propidium Iodide – Vindelov's cocktail

Tris-HCl (pH 8.8)	10 mM
NaCl	10 mM
Propidium Iodide	50 mg/L
RNase A	10 mg/L
Nonidet P40 (NP-40)	0.1 %
ddH_2O	

1X Tris-Phosphate buffer (pH 8.0)

Tris-HCl	10 mM
NaH_2PO_4	100 mM
ddH_2O	

8 M Urea lysis / wash / elution buffers

Tris Base	1.2 g/L
$NaH_2PO_4.H_2O$	13.8 g/L
Urea	480.5 g/L
ddH_2O	
pH adjusted with NaOH or HCl to	pH 8.0 / pH 6.3 / pH 4.5

Pulse refolding buffer, pH 7.5

Tris Base	50 mM
$CaCl_2$	20 mM
EDTA	5 mM
L-arginine	0.5 M
L-cysteine	0.5 mM
ddH_2O	